

HIGH RESOLUTION PHOTON INELASTIC SCATTERING

ON  $^{56}\text{Fe}$  AND  $^{48}\text{Ti}$

by

William Kent Wells

Department of Physics  
Duke University

Date: \_\_\_\_\_

Approved:

\_\_\_\_\_  
E. G. Bilpuch, Supervisor

\_\_\_\_\_

\_\_\_\_\_

\_\_\_\_\_

\_\_\_\_\_

A dissertation submitted in partial fulfillment of  
the requirements for the degree of Doctor of  
Philosophy in the Department of Physics  
in the Graduate School of Arts and  
Sciences of Duke University

1978

ABSTRACT

(Physics)

HIGH RESOLUTION PROTON INELASTIC SCATTERING

ON  $^{56}\text{Fe}$  AND  $^{48}\text{Ti}$

by

William Kent Wells

Department of Physics  
Duke University -

Date: \_\_\_\_\_

Approved:

\_\_\_\_\_  
E. G. Bilpuch, Supervisor

\_\_\_\_\_  
\_\_\_\_\_  
\_\_\_\_\_  
\_\_\_\_\_

An abstract of a dissertation submitted in partial fulfillment of the requirements for the degree of Doctor of Philosophy in the Department of Physics in the Graduate School of Duke University

1978

# HIGH RESOLUTION INELASTIC SCATTERING

ON  $^{56}\text{Fe}$  AND  $^{48}\text{Ti}$

by

William Kent Wells

Inelastic proton decay from p-wave resonances in  $^{49}\text{V}$  and  $^{57}\text{Co}$  were studied using the high resolution proton beam from the Triangle Universities Nuclear Laboratory's 3 MV Van de Graaff accelerator. The inelastically scattered proton and de-excitation gamma-ray angular distributions were measured at four angles for one hundred and twenty resonances in  $^{49}\text{V}$  and thirty-six resonances in  $^{57}\text{Co}$ . The results of the two singles measurements unambiguously determine the spin of the compound nuclear state for each resonance. The magnitudes and relative phase of the two inelastic decay channel amplitudes were measured for  $3/2^-$  resonances.

Inelastic spectroscopic factors were determined for three isobaric analogue states in  $^{57}\text{Co}$  and for two isobaric analogue states in  $^{49}\text{V}$ . The strength functions for the elastic and inelastic scattering channels were calculated from the average spacing and reduced width data.

A sequence of 72  $3/2^-$  resonances in  $^{49}\text{V}$  was used to

test the statistical hypotheses for width distributions in the orthogonal ensemble. Evidence is presented for non-statistical behavior indicative of two doorway states in 497.

## ACKNOWLEDGEMENTS

I would like to thank my research advisor, Dr. E. G. Bilpuch, for his support during my graduate career at Duke, especially during my first year. I am very grateful to Dr. G. E. Mitchell for his help and encouragement during all stages of my work at Triangle Universities Nuclear Laboratories, and particularly for his help in the preparation of this dissertation.

Many thanks go to C. E. Westerfeldt, K. B. Sales, J. E. Chandler, W. A. Watson, and B. H. Chou (the high resolution crew) for their invaluable help during the many hours required to take the data presented in this dissertation. The patient help and teaching of Dr. D. A. Outlaw early in my graduate career was a very important part of my graduate education. His good humored assistance shortened many long nights in the Laboratory.

The TUNL electronics shop has been a great help in keeping the equipment used in this experiment in working condition. I want to especially thank Mr. Sidney Edwards for his help and advice with the electronics used in the new Homogenizer. Also the fine work of the machine shop, under the direction of Mr. A. W. Lovette, is greatly appreciated.

To my parents a long overdue thank you for their encouragement and financial support during my graduate

career. And to Lisa, I give my love. Her patience and help have been indispensable.

This work was supported in part by the United States Department of Energy. Some of the analysis was performed at the Triangle Universities Computation Center, which is supported in part by the National Science Foundation.

## TABLE OF CONTENTS

ABSTRACT	ii
ACKNOWLEDGEMENTS	v
LIST OF FIGURES	ix
LIST OF TABLES	xiii
1. INTRODUCTION	2
2. METHOD	10
2.1 General Considerations	10
2.2 General Angular Correlation Formulas	13
2.3 Distribution Equations for Isolated $3/2^-$ Resonances	17
2.4 Amplitude Mixing Ratios	25
3. EQUIPMENT AND EXPERIMENTAL PROCEDURES	37
3.1 3 MV Van de Graaff Accelerator	37
3.2 Targets	41
3.3 Scattering Chambers and Detectors	42
3.4 Counting Electronics	46
3.5 Experimental Procedures	53
4. DATA AND PRELIMINARY ANALYSIS	62
4.1 Elastic Scattering Experiments	62
4.2 Resonance Parameters	65
5. WIDTH DISTRIBUTIONS	81
5.1 General Theoretical Background	81
5.2 Probability Distributions for Mixing Ratios	93
5.3 Inelastic decay of Isobaric Analogue States	105

	viii
5.4 Reduced Width Fluctuations	123
6. SUMMARY	152
APPENDIX A	155
A.1 Introduction	155
A.2 Model of the TUNL Homogenizer as a Position Regulator	156
A.3 Homogenizer Component Description	167
A.4 Feedback Analysis	179
A.5 Conclusions and Recommendations	187
APPENDIX B	189
APPENDIX C	222
BIBLIOGRAPHY	271
BIOGRAPHY	275



## LIST OF FIGURES

1.1	Sample Resonance Shapes for Isolated s-, p-, and d-wave Resonances as a Function of Scattering Angle.	5
2.1	Energy Levels and Schematic Diagram of the Reaction Studied with Angular Momentum Coupling Schemes.	12
2.2	Coulomb Penetrabilities for $l=0,1,2,3$ for $^{52}\text{Cr}$ .	21
2.3	$a_2$ Versus $\varphi$ in the Channel Spin Representation.	31
2.4	$a_2$ Versus $\varphi$ in the Total Angular Momentum Representation.	33
2.5	$a_2$ Versus $\varphi$ in the Total Angular Momentum Representation with $l'=3$ Amplitude Admixtures.	35
3.1	The Floor Plan of the 3 MV Van de Graaff Accelerator Laboratory.	39
3.2	Schematic Diagram of the Charged Particle Scattering Chamber and its Associated Collimator Assembly.	44
3.3	Schematic Diagram of the Gamma-Ray Scattering Chamber and Associated Collimator Assembly.	48
3.4	Schematic Diagram of the Charged Particle and Gamma-Ray Detection Electronics.	50

3.5	Charged Particle Spectrum from a Resonance Excited via the $^{56}\text{Fe}(p,p')^{56}\text{Fe}$ Reaction at 3.01 MeV.	55
3.6	De-Excitation Gamma-Ray Spectrum from a Resonance Excited via the $^{56}\text{Fe}(p,p')^{56}\text{Fe}$ Reaction at 3.01 MeV.	57
4.1	Differential Cross Section of Proton Elastic Scattering at 160 Degrees on $^{56}\text{Fe}$ .	64
4.2	Differential Cross Section of Proton Elastic and Inelastic Scattering on $^{48}\text{T}$ at 160 Degrees.	67
4.3	$\varphi$ versus $E_p$ in the Channel Spin Representation for $^{56}\text{Fe}$ .	72
4.4	$\varphi$ versus $E_p$ in the Total Angular Momentum Representation for $^{48}\text{Ti}$ .	74
4.5	Plot of Total Inelastic Reduced Widths versus $E_p$ .	78
4.6	Elastic and Inelastic Reduced Widths versus $E_p$ .	80
5.1	Geometrical Relationships Between Reduced Width Amplitudes and Mixing Parameters.	95
5.2	Distribution Function for Mixing Ratios.	100
5.3	Distribution Function for $\varphi$ .	102
5.4	Effects of Intermediate Structure on the Distribution of $\varphi$ .	104

5.5	The Fine Structure Distribution for $^{48}\text{Ti}(p,p)^{48}\text{Ti}$ .	108
5.6	The Fine Structure Distribution for $^{48}\text{Ti}(p,p')^{48}\text{Ti}$ .	110
5.7	The Fine Structure Distribution for $^{48}\text{Ti}(p,p')^{48}\text{Ti}$ in the $s'=3/2$ Channel.	113
5.8	The Fine Structure Distribution for $^{48}\text{Ti}(p,p')^{48}\text{Ti}$ in the $s'=5/2$ Channel.	115
5.9	$\delta'_{s=3/2}$ $\delta'_{s=5/2}$ versus Proton Bombarding Energy.	117
5.10	Off-Diagonal Strength Function in the Channel Spin Representation.	119
5.11	The Distribution of Elastic and Inelastic Partial Reduced Widths.	126
5.12	The Distribution of Inelastic Reduced Widths in the $j'=1/2$ and $j'=3/2$ Channels.	128
5.13	The Distribution of Inelastic Reduced Widths in the $s'=3/2$ and $s'=5/2$ Channels.	130
5.14	The $\chi^2$ Distribution for $\nu$ Degrees of Freedom.	133
5.15	Distribution of $\phi$ for Inelastic Decay from $3/2^-$ Resonances in $^{57}\text{Co}$ in the Channel Spin Representation.	136
5.16	Distribution of $\phi$ for Inelastic Decay from $3/2^-$ Resonances in $^{49}\text{V}$ in the Channel Spin Representation.	139

5.17	Distribution of Sum of Squares Statistic for Different Number of Bins.	141
5.18	$\sum_i \chi_{ci} \chi_{ci}$ versus $E_p$ for Inelastic Decay from $3/2^-$ Resonances in $^{49}\text{V}$ in both Channel Spin and Total Angular Momentum Representations.	144
5.19	$\phi'$ in the Total Angular Momentum Representation versus $E_p$ for Inelastic Decay from $3/2^-$ Resonances in $^{49}\text{V}$ .	149
5.20	$\sum_i \chi_{ci} \chi_{ci}$ versus $E_p$ for Inelastic Decay from $3/2^-$ Resonances in $^{57}\text{Co}$ .	151
A.1	Schematic Diagram of Cylindrical Electrostatic Analyzer.	159
A.2	Diagram of the Analyzer Image Slits.	165
A.3	Block Diagram of Homogenizer Circuitry.	169
A.4	Schematic Diagram of Inverter, Summing, and Buffer Amplifiers.	172
A.5	High Voltage Amplifier Schematic Diagram.	176
A.6	Magnetic Controller Schematic Diagram.	178
A.7	Block Diagram of the Control Systems in the 3 MV Laboratory.	182

## LIST OF TABLES

5.1	Inelastic Spectroscopic Factors	121
5.2	P-wave Strength Functions	123
5.3	Degrees of Freedom	134
5.4	Linear Correlation Coefficients Between Channels	145
5.5	Linear Correlation Coefficients Between Channels	146
	RESONANCE PARAMETERS	189
B.1		190
B.2		192
B.3		196
B.4		197
B.5		198
B.6		203
B.7		215
B.8		219

"By God! How many provinces did he name! How many nations did he enumerate, giving to each, with wonderful speed, its peculiar attributes, so absorbed and wrapped up was he in all that he had read in his lying books! Sancho Panza hung on his words without uttering one. Now and then he turned his head to see whether he could perceive the knights and giants his master named. Seeing none, he said at last: 'Master, I'll commend to the Devil any man, giant or knight of all those you mentioned who is actually here. At least I do not see them. Perhaps all may be enchantment like last night's specters.'

'Why do you say that?' said Don Quixote. 'Do you not hear the neighing of the horses, the blaring of the trumpets, and the rattle of the drums?'

'I hear nothing,' answered Sancho, 'but the bleating of sheep and lambs.' And so it was, for now the two flocks were close at hand."

---- Don Quixote  
by Miguel de Cervantes Saavedra

HIGH RESOLUTION PROTON INELASTIC SCATTERING

ON  $^{56}\text{Fe}$  AND  $^{48}\text{Ti}$

## Chapter 1

### INTRODUCTION

In the past four years high resolution proton inelastic scattering experiments have been performed at Triangle Universities Nuclear Laboratory (TUNL) using a technique described by Dittrich et al. (1975). This technique permits the measurement of the ratio of inelastic decay amplitudes from isolated compound nuclear states. By measuring both the angular distributions of inelastically scattered protons and of de-excitation gamma-rays, the magnitude and relative phase (sign) of the mixing ratios can be determined.

This technique is particularly simple for the case of p-wave compound nuclear resonances formed with the addition of a proton to even-even nuclei. Angular distributions for both reaction products are isotropic for  $1/2^-$  resonances and are non-isotropic in at least one angular distribution of the reaction products for  $3/2^-$  resonances. By performing inelastic decay angular distribution measurements on known

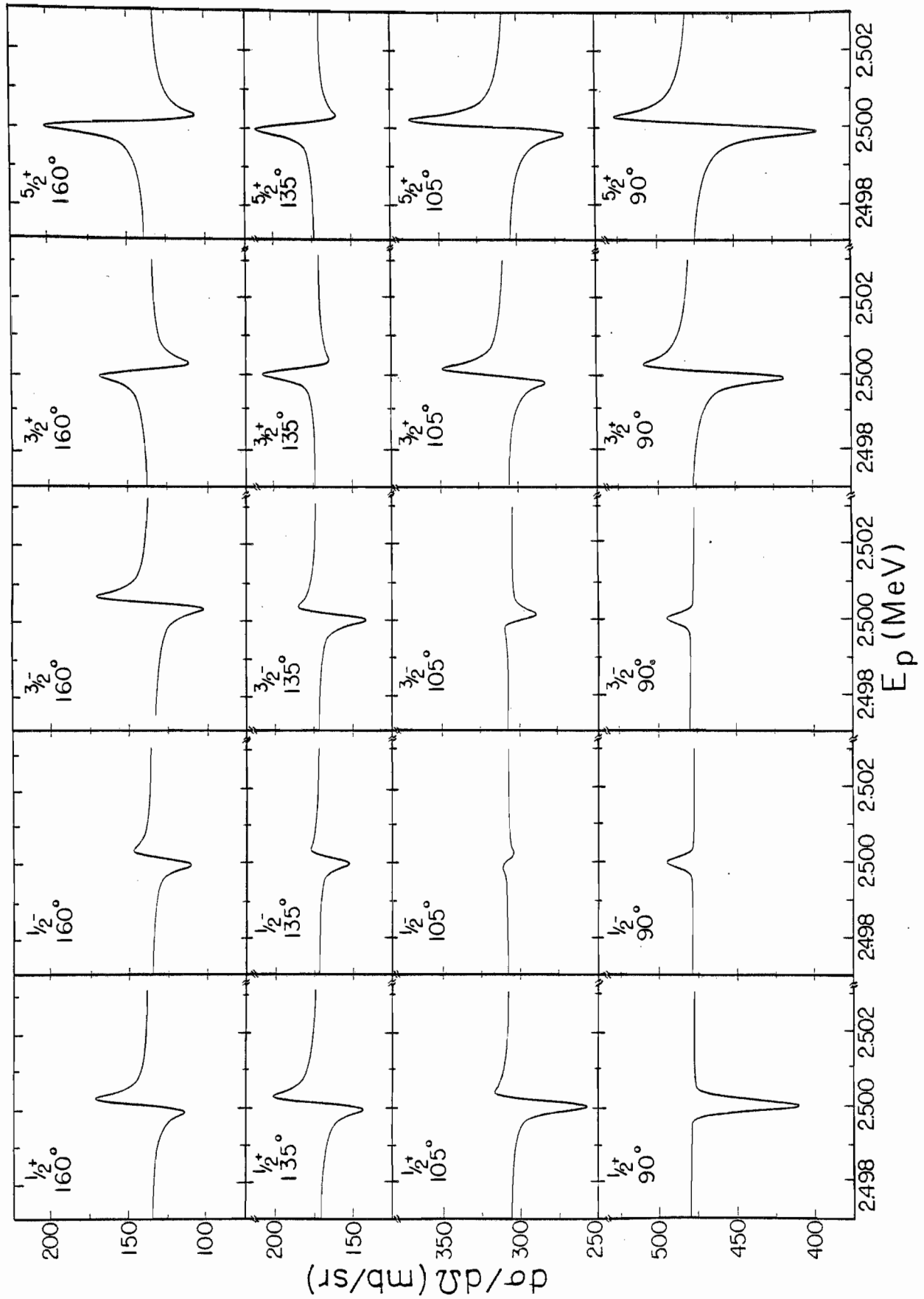


p-wave resonances, the spin of the resonance can be uniquely determined and the mixing of two decay amplitudes for  $3/2^-$  resonances measured.

High resolution proton elastic scattering experiments on doubly-even nuclei ( $26 < A < 92$ ) have been performed at TUNL during the past 12 years in the study of fragmented Isobaric Analogue States (IAS). This work is reviewed by Bilpuch et al. (1976). As the experiments became more refined and higher level densities were encountered, it became apparent that the statistical nature of level spacings and width fluctuations play an important role in the study of fragmented IAS. With this in mind, Wilson (1975) analyzed sequences of  $1/2^-$  resonances in  $^{45}\text{Sc}$  and  $1/2^+$  resonances in  $^{49}\text{V}$  using theories of Dyson (1962), Mehta (1960) and others.

The limitation to  $1/2^+$  resonances in  $^{49}\text{V}$  is due to the ambiguity arising from spin assignments for small compound nuclear resonances. Each possible incident orbital angular momentum  $\ell$  can be coupled to the intrinsic spin of the proton to form total angular momentum  $j = \ell \pm 1/2$ . Only for the case of  $\ell = 0$  does this yield a unique spin. Hypothetical resonance shapes are shown in Figure 1.1. All resonances have the same width, resonance energy, and experimental resolution, and are in the same compound nucleus,  $^{51}\text{Mn}$ . The parity of these resonances can be determined by inspection. However, except for  $\ell = 0$  resonances, the only difference in the cross section for resonances of different  $j$  and the

Figure 1.1 Sample Resonance Shapes for Isolated s-, p-, and d-wave Resonances as a Function of Scattering Angle. The resonances all have a laboratory width of  $\Gamma = \Gamma_p = 50$  eV. The resolution width was 300 eV, the hypothetical target  $^{50}\text{Cr}$ , and the bombarding energy 2.5 MeV.



same  $\ell$  is the spin statistical factor of the resonance. Therefore, for small resonances, spin assignments made from shape analysis are subject to error.

The examination of  $1/2^-$  resonances in  $^{45}\text{Sc}$  for statistical analysis of spacings is made possible by the existence of a  $1/2^-$  IAS with spreading width of 45 keV. This unusually large spreading width enhances the  $1/2^-$  background resonance widths near the analogue state, especially on the lower energy side, making spin assignments more accurate. The  $1/2^-$  resonances were also enhanced since  $^{45}\text{Sc}$  is near the maximum of the  $1/2^-$  strength function. Since IAS distort width distributions but have little effect on the spacing distributions, analysis of the spacing distributions was emphasized by Wilson (1975) in  $^{49}\text{V}$ .

With the addition of the inelastic scattering technique to the parity assignments made by elastic scattering shape analysis, reliable spin assignments can be made for  $\ell=1$  resonances. This sorting of spins from the sequence of p-wave resonances available from previously obtained elastic scattering data permits a statistical analysis of resonance parameters. Also, an opportunity exists to study in  $3/2^-$  resonances the correlation between partial width amplitudes from different reaction channels. Previous studies of channel-channel correlations using sequences of single resonances were bereft of information about the relative phase of the amplitudes in different channels. The signs of

the mixing ratios from a sequence of resonances also allows the hypothesis of random phases to be tested.

In the mass region studied at TUNL in high resolution proton elastic and inelastic scattering, the presence of fragmented p-wave IAS hinders the study of purely statistical features of the resonance spectrum. This fact does, however, allow the study of the effects of intermediate structure (via IAS) on what is hypothesized to be a background of statistically distributed resonances. The partial inelastic reduced width amplitude correlation presented by Mitchell (1978) in the  $^{44}\text{Ca}(p,p')$  reaction has been shown by Lane (1978) to be usefully described in terms of an "off diagonal strength function" or covariance matrix divided by the average level spacing, defined as

$$S_{cc'} = \frac{\sum_{\lambda} c_{c\lambda} c_{c'\lambda}}{D} = \frac{\overline{\delta_{\lambda c} \delta_{\lambda c'}}}{D}$$

where the bar denotes an average over levels  $\lambda$ ,  $D$  is the average level spacing, and  $C$  and  $C'$  are channel labels. When  $C = C'$ , the definition is the same as that for the standard strength function. Predictions made about the behavior of  $S_{cc'}$  near an IAS agree with the  $^{44}\text{Ca}(p,p')$  data extremely well. Data on  $^{46}\text{Ti}(p,p')$  by Chandler (1978) further confirm these predictions.

The interpretation of the data on IAS is a special case of a doorway state common to several channels. Definite

predictions have been given for the covariance matrix,  $\sum_{cc'}$ , by Lane (1971) and Porter (1965). If each channel in a reaction has partial reduced width amplitudes that are distributed independently as a gaussian of zero mean, then

$$\sum_{cc'} = 0.$$

There are other equivalent descriptions for this condition. For example, the running sum of  $\gamma_{\lambda c} \gamma_{\lambda c'}$  versus energy should have zero slope or the linear correlation coefficient between the sequence  $\{\gamma_{\lambda c}\}$  and  $\{\gamma_{\lambda c'}\}$  is zero. Any localized correlation or non-zero slope of the running sum of  $\gamma_{\lambda c} \gamma_{\lambda c'}$  is indicative of a common doorway state. Statistical theories can allow for small linear correlations between sets of reduced width amplitudes in different channels. The existence of a linear correlation requires that the distribution of reduced width amplitudes in one channel is a function of the amplitudes in other channels.

The experiments reported in this dissertation were measurements of inelastic decays from p-wave resonances in  $^{57}\text{Co}$  and  $^{49}\text{V}$ . The  $3/2^-$  IAS in these two nuclei are not fragmented and did not influence the background states. This apparent lack of intermediate structure favored these nuclei as subjects for study of partial width fluctuations.

In Chapter two the method by which the charged particle decay amplitude mixing ratios are calculated from experimental angular distributions is discussed. The

angular correlation formulas with two inelastic partial decay amplitudes for orbital angular momentum  $\ell' = 1$  in the exit channels are given. The possibility of a larger number of decay amplitudes is discussed and upper limits on the amplitudes from  $\ell' = 3$  are estimated. The method for eliminating systematic inclusion of resonances with  $\ell' = 3$  decay amplitudes is also discussed. Computer programs for evaluating these angular correlation formulas are listed in Appendix C.

The equipment and procedures used to accumulate the data presented in this dissertation are described in Chapter three. Detailed information on the accelerator control systems employed to obtain the high resolution proton beam is given in Appendix A.

The method for the reduction of the data and its preliminary analysis are explained in Chapter four. Appendix B contains lists of all the data used in subsequent analysis.

An introduction to the theoretical concepts underlying a statistical description of nuclear spectra is outlined in Chapter five. Using these ideas, a derivation of the distribution function for reduced width amplitudes in two channels is given. This distribution formula is then simplified to an extreme statistical model and the experimental results are discussed in terms of this model.

## Chapter 2

### METHOD

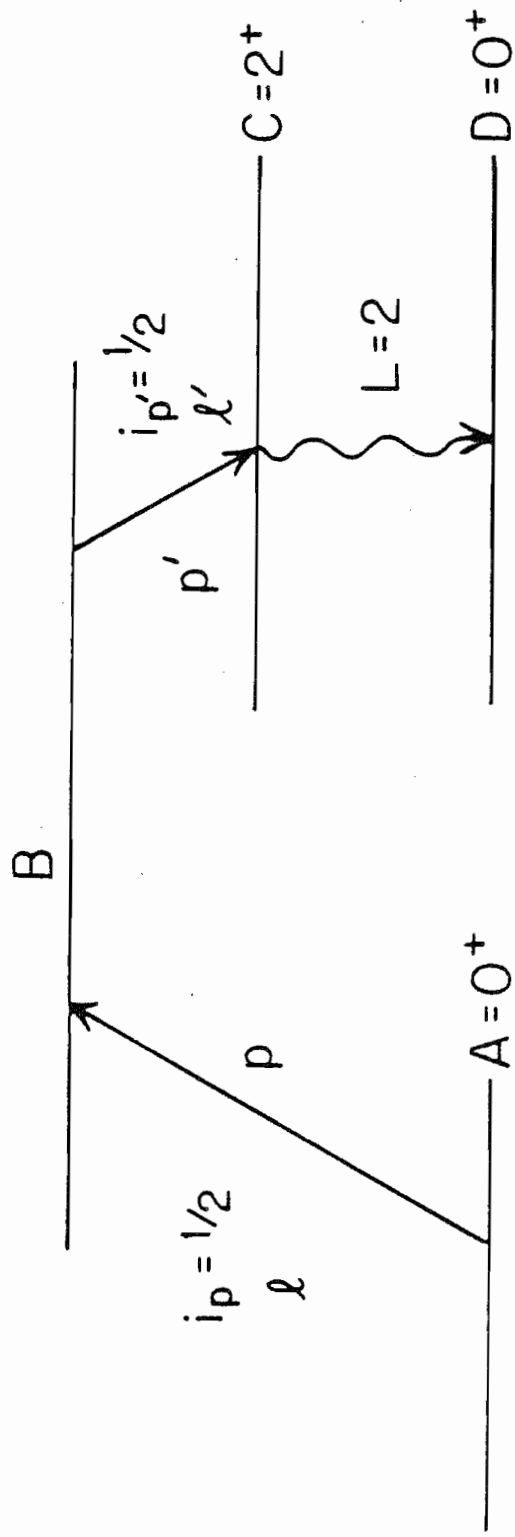
#### 2.1 General Considerations

The determination of the mixing ratios of nuclear resonance decay amplitudes with two singles measurements of reaction products was first described by Dittrich et al. (1975). The measurement of channel spin mixing ratios for neutron resonances via low energy neutron capture has been described by Chrien (1973) and Becvar (1974). This neutron capture method has been applied to only a few resonances. These measurements of mixing between particle decay amplitudes are analogous to measurements of multipole mixing ratios of electromagnetic transitions, and when compound nuclear processes predominate can provide important information.

The mixing ratio in this experiment is the ratio of the partial reduced width amplitudes for inelastic proton decay of p-wave compound nuclear states. The reaction is shown



Figure 2.1 Energy levels and Schematic Diagram of the Reaction Studied with Angular Momentum Coupling Schemes. The ground state of a  $0^+$  nucleus combines with a proton with orbital angular momentum  $l$  to form a compound nuclear state B. The state B decays by proton emission with orbital angular momentum  $l'$ . The residual nucleus is left in the first  $2^+$  excited state, which decays by gamma-ray emission. The different ways in which the various angular momenta may be coupled in the entrance and exit channels are listed in the accompanying table.



	ENTRANCE CHANNEL	EXIT CHANNEL
CHANNEL SPIN REPRESENTATION	$\vec{s} = \vec{A} + \vec{i}_p$ $\vec{B} = \vec{s} + \vec{l}$	$\vec{s}' = \vec{C} + \vec{i}_{p'}$ $\vec{B} = \vec{s}' + \vec{l}'$
TOTAL ANGULAR MOMENTUM REPRESENTATION	$\vec{j} = \vec{l} + \vec{i}_p$ $\vec{B} = \vec{A} + \vec{j}$	$\vec{j}' = \vec{l}' + \vec{i}_{p'}$ $\vec{B} = \vec{C} + \vec{j}'$

schematically in Figure 2.1. State B, with  $J^\pi$  either  $1/2^-$  or  $3/2^-$ , is formed from a  $0^+$  ground state by the addition of a proton with intrinsic angular momentum  $1/2$  and orbital angular momentum  $\ell = 1$ . The state can emit a proton and leaves the residual nucleus in the first excited  $2^+$  state which subsequently decays by gamma-ray emission. The inelastically scattered proton must have orbital angular momentum consistent with the triangle condition for angular momentum addition. If parity is conserved this condition allows only  $\ell' = 1$  and  $\ell' = 3$  orbital angular momentum.

Yang (1948) has shown that maximum angular complexity of the angular distribution of any reaction product is limited to  $(\cos\theta)^{2J}$  for a compound nuclear state of total momentum  $J$ . In the compound nuclear systems examined in these experiments only even powers of the cosine can be admitted due to the definite parity of the system. These criteria limit the maximum angular complexity for reaction product angular distributions for a  $3/2^-$  state to  $\cos^2\theta$ . These criteria also require a  $1/2^-$  state to have an isotropic decay. These requirements hold for the angular distributions of both the inelastically scattered proton and de-excitation gamma-ray. A detailed discussion of these considerations is given by Blatt and Weisskopf (1952).

## 2.2 General Angular Correlation Formulas

There are two equivalent ways that the angular correlation of nuclear reaction products may be described. One is the wave function--scattering matrix formalism, described by Biedenharn and Rose (1953). The other is the density matrix formalism of Fano (1952) and Coester and Jauch (1953). The wave function formalism was used by Kraus (1956) to give the angular correlation formulas for the reaction studied in the experiments described in this work. The formulas obtained by Kraus were only determined for the channel spin representation. The density matrix formalism was used by Dittrich (1976) to describe the same reaction in both the channel spin representation and the total angular momentum representation. A discussion of this method is found in works by Ferguson (1965) and Thompson and van Rijn (1968). The density matrix formalism will be used in the present discussion.

In the density matrix approach one finds the density matrix,  $\rho$ , for the states of the nucleus and radiation fields and the efficiency matrix,  $\epsilon$ , for the detection of the outgoing radiation and the residual nucleus. These matrices are sufficient to describe an angular correlation measurement specified by  $\epsilon$  with

$$W \equiv \langle \epsilon \rangle = \text{Tr}(\rho \epsilon) \quad (2.2.1)$$

where  $\langle \epsilon \rangle$  is the expectation value of a measurement

described by the efficiency matrix  $\epsilon$  and  $\text{Tr}(\rho\epsilon)$  is the trace of the matrix product of  $\epsilon$  times  $\rho$ . The equation (2.2.1) is the basic equation for determining angular correlations using the density matrix formalism. The operators  $\epsilon$  and  $\rho$  must be spherical tensors in order to make use of the spherical symmetry of the system. As shown in Figure 2.1, there are three angular momentum vectors which must be coupled in order to describe both the formation and decay of state B. The two ways of adding these vectors to give B in both the entrance and exit channels are shown in the table in Figure 2.1. With these two coupling schemes, two sets of angular correlation formulas can be derived for the protons and de-excitation gamma-rays. The two representations for these formulas are the channel spin and total angular momentum representations. General formulas for angular correlations of this kind are given by Ferguson (1965). The notation of Dittrich (1976) will be followed in this work. The general formulas for the total angular momentum representation for the distribution of inelastically scattered protons is

$$\begin{aligned}
 W(\Theta_p) = & \sum (-)^{A-2B_2+C-2j_1+l_p+l_p'+3K+(l_1-l_2+l_1'-l_2')/2} (\hat{B}_1 \hat{B}_2)^2 (\hat{A} \hat{l}_p \hat{l}_p' 4\pi)^2 Z(l_1 j_1, l_2 j_2; l_p k) \\
 & \cdot W(j_2 B_2 j_1 B_1; A R) Z(l_1' j_1' l_2' j_2'; l_p' k) W(j_2' B_2' j_1' B_1'; C k) P_2(\Theta_p) \\
 & \cdot \langle B_1 C_1 j_1 | O_c | B_1 \rangle \langle B_2 C_2 j_2 | O_c | B_2 \rangle^* \quad (2.2.2)
 \end{aligned}$$

and for the de-excitation gamma-rays in the same representation is

$$\begin{aligned}
 W(\Theta_\gamma) = \sum (-)^{A-B_1-B_2-2C_2+D+l_p-2j_1+j'-L_1+L_2+(7/2)k+(l_1-l_2)/2} & \\
 \frac{\hat{C}_1 \hat{C}_2 \hat{L}_1 \hat{L}_2 (\hat{B}_1 \hat{B}_2)^2}{8\pi (\hat{A} \hat{l}_p \hat{l}_p)^2} Z(l_1 j_1 l_2 j_2; L_p k) W(j_2 B_2 j_1 B_1; A k) & \\
 \cdot W(B_2 C_2 B_1 C_1; j' k) W(L_2 C_2 L_1 C_1; D k) (L_1 1 L_2 -1 | k 0) J_k P_2(\Theta_\gamma) & \\
 \cdot \langle B_1 C_1 j' | O_c | B_1 \rangle \langle B_2 C_2 j' | O_c | B_2 \rangle^* \langle C_1 | O_b | C_1 D L_1 \rangle^* \langle C_2 | O_b | C_2 D L_2 \rangle & \\
 (2.2.3) &
 \end{aligned}$$

Distribution formulas may also be obtained in the channel spin representation. The distribution of inelastically scattered protons in this representation is

$$\begin{aligned}
 W(\Theta_p) = \sum (-)^{s+s'-2B_2+(l_2-l_1+l_2'-l_1')/2} & \\
 (4\pi \hat{A} \hat{l}_p)^{-2} Z(l_1 B_1 l_2 B_2; s k) & \\
 \cdot Z(l_1' B_1 l_2' B_2; s' k) P_2(\Theta_p) \langle B_1 s' l_1' | O_c | B_1 \rangle & \\
 \cdot \langle B_2 s' l_2' | O_c | B_2 \rangle^* & \\
 (2.2.4) &
 \end{aligned}$$

and for the de-excitation gamma rays is

$$\begin{aligned}
 W(\Theta_\gamma) = \sum (-)^{s-B_2-B_1-s_1'-s_2'-2C_2+D+l'+l_p'+L_2-L_1-1+(l_2-l_1+7k)/2} & \\
 \frac{\hat{B}_1 \hat{B}_2 \hat{s}_1' \hat{s}_2' \hat{C}_1 \hat{C}_2 \hat{L}_1 \hat{L}_2}{8\pi (\hat{l}_p \hat{l}_p \hat{A})^2} Z(l_1 B_1 l_2 B_2; s k) & \\
 \cdot W(B_2 s_2' B_1 s_1'; j' k) W(s_2' C_2 s_1' C_1; l_p k) W(L_2 C_2 L_1 C_1; D k) & \\
 \cdot (L_1 1 L_2 -1 | k 0) J_k P_2(\Theta_\gamma) \langle B_1 s_1' l_1' | O_c | B_1 \rangle \langle B_2 s_2' l_2' | O_c | B_2 \rangle^* & \\
 \cdot \langle C_1 | O_b | C_1 D L_1 \rangle^* \langle C_2 | O_b | C_2 D L_2 \rangle & \\
 (2.2.5) &
 \end{aligned}$$

In these general equations the sum is over  $B, B_1, B_2, l, l_1, l_2, l', l_1', l_2', j, j_1, j_2, j', j_1', j_2', s, s_1, s_2, s'$ .

$s_1'$ ,  $s_2'$ , and  $k$ . The circumflex over quantities denotes the recurring relation

$$\hat{B} = (2B+1)^{1/2} \quad (2.2.6)$$

Since these equations are rather general, they are not useful unless certain simplifying assumptions are made.

### 2.3 Distribution Equations for Isolated $3/2^-$ Resonances

From general considerations all  $1/2^-$  resonances will have isotropic angular distributions of both de-excitation gamma-rays and inelastically scattered protons; further analysis in this chapter will deal only with  $3/2^-$  resonances. If it is assumed that all the  $3/2^-$  resonances studied are isolated, then the general equations have  $B = B_1 = B_2 = 3/2$ ,  $C = C_1 = C_2 = 2$ ,  $l = l_1 = l_2 = 1$ ,  $A = 0$ ,  $D = 0$ ,  $i_p = i_p' = 1/2$ ,  $j = j_1 = j_2 = 3/2$ , and  $s = s_1 = s_2 = 1/2$ . The sum over  $j'$ ,  $j_1'$ ,  $j_2'$  runs through values  $1/2$ ,  $3/2$ ,  $5/2$ , and  $7/2$ ;  $l'$ ,  $l_1'$ , and  $l_2'$  through values 1 and 3;  $s'$ ,  $s_1'$ , and  $s_2'$  through values  $3/2$  and  $5/2$ ; and  $k$  through values 0 and 2. With these constraints one obtains the angular distribution formulas for inelastically scattered protons in the total angular momentum representation,

$$W(\theta_p) = \sum_{k, l_1', l_2', j_1', j_2'} (-)^{3-2j_1 + (l_1' - l_2')/2 + 3k} Z(1 \ 3/2 \ 1 \ 3/2; 1/2 \ k) W(3/2 \ 3/2 \ 3/2 \ 3/2; 0 \ k) \\ \cdot Z(l_1' \ j_1' \ l_2' \ j_2'; 1/2 \ k) W(j_2' \ 3/2 \ j_1' \ 3/2; 2 \ k) P_2(\theta_p) Y_{j_1'}^{s_1'} Y_{j_2'}^{s_2'} \quad (2.3.1)$$

and for the de-excitation gamma-rays in the same representation,

$$\begin{aligned}
 W(\Theta_\gamma) &= \sum_{j'k} (-)^{-19/2 + j' + (7/2)k} Z(1\ 3/2\ 1\ 3/2; 1/2\ k) W(3/2\ 3/2\ 3/2\ 3/2; 0\ k) \\
 &\cdot W(3/2\ 2\ 3/2\ 2; j'k) W(2222; 0k) (212-1|k0) \\
 &\cdot J_k P_k(\Theta_\gamma) \gamma_{j'} \gamma_{j'}^* \quad (2.3.2)
 \end{aligned}$$

Formula in the channel spin representation for inelastically scattered protons is

$$\begin{aligned}
 W(\Theta_{p'}) &= \sum_{R, S', l'_1, l'_2} (-)^{-5/2 + S' + (l'_2 - l'_1)/2} Z(1\ 3/2\ 1\ 3/2; 1/2\ k) Z(l'_1\ 3/2\ l'_2\ 3/2; S'k) \\
 &\cdot P_k(\Theta_{p'}) \gamma_{S'} \gamma_{S'}^* \quad (2.3.3)
 \end{aligned}$$

and for de-excitation gamma-rays the formula is

$$\begin{aligned}
 W(\Theta_\gamma) &= \sum_{S'_1, S'_2, l'k} (-)^{-7 - S'_1 - S'_2 + l' + (7/2)k} \hat{S}'_1 \hat{S}'_2 Z(1\ 3/2\ 1\ 3/2; 1/2\ k) \\
 &\cdot W(3/2\ S'_2\ 3/2\ S'_1; l'k) W(S'_2\ 2\ S'_1\ 2; 1/2\ k) W(2222; 0k) \\
 &\cdot (212-1|k0) J_k P_k(\Theta_\gamma) \gamma_{S'_1} \gamma_{S'_1}^* \quad (2.3.4)
 \end{aligned}$$

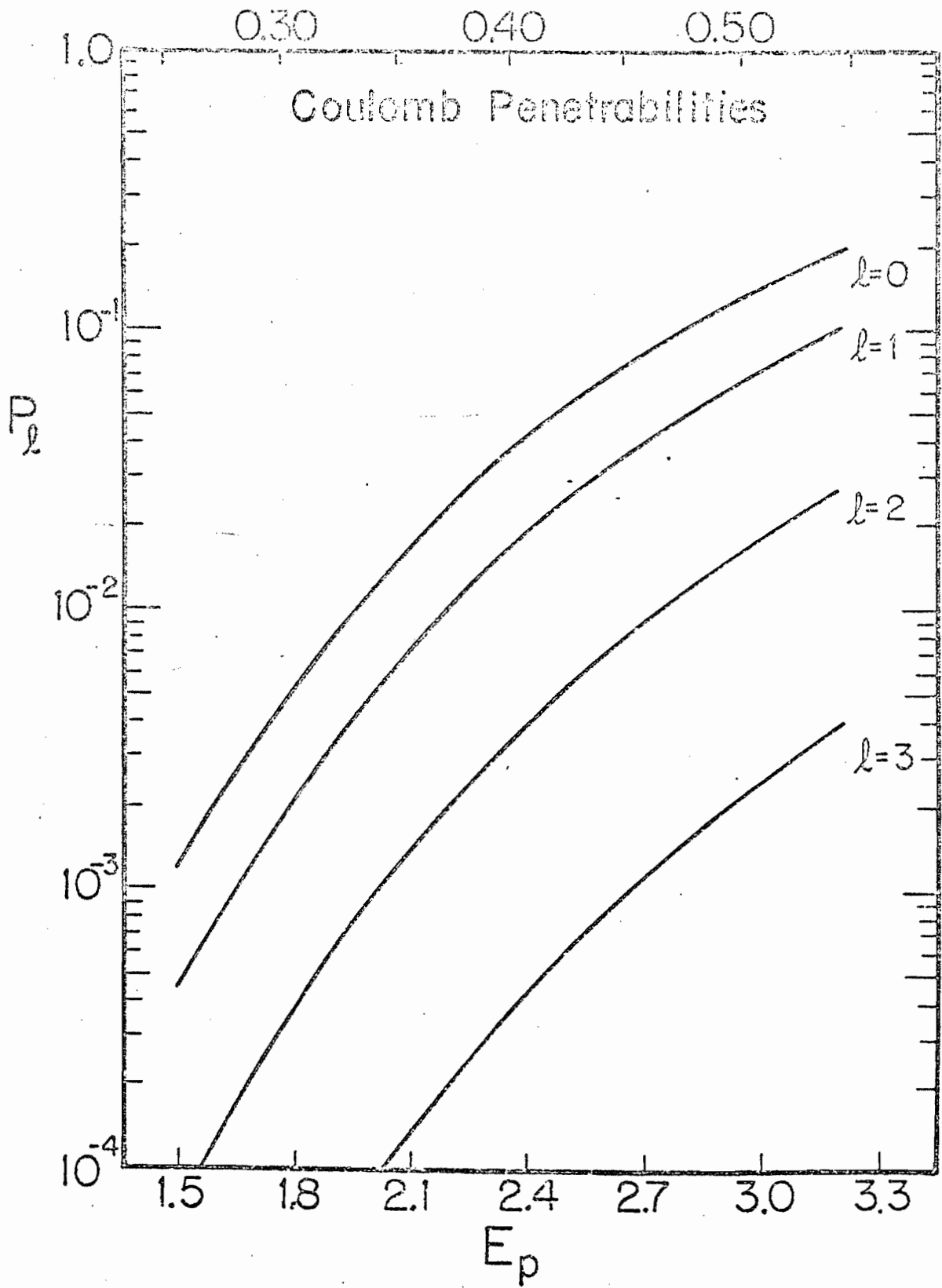


In these expressions all constants have been removed, since only relative measurements are necessary for the determination of the mixing ratios of the inelastic decay amplitudes.

Further simplification of these equations is necessary to allow determination of amplitude mixing ratios from experimental data. The case where all  $l'=3$  amplitudes are zero is particularly useful and the expression for this is easily obtained. If  $l'=3$  amplitudes are included, however, the evaluation of the angular distribution equations becomes extremely tedious. To avoid the mistakes which are possible in a calculation of this type, a computer program was written to evaluate equations with the form of sums of products algebraically using an IBM supplied computer language--FORTRAN. This program and its use are described in Appendix C.

The approximation that all  $l'=3$  amplitudes are zero is used in deriving the set of equations employed in determining the amplitude mixing ratios for the inelastic decay of the  $3/2$  resonances studied in this experiment. This approximation is reasonable and follows from Coulomb penetrability considerations. The Coulomb penetrabilities for protons on  $^{52}\text{Cr}$  are shown for  $l=0, 1, 2, 3$  in Figure 2.2. At  $E = 3.3$  MeV the ratio of  $l=3$  penetrability to  $l=1$  penetrability is approximately 50. Therefore, given equal reduced widths for both  $l=1$  and  $l=3$  components, laboratory

Figure 2.2 Coulomb Penetrabilities for  $l=0,1,2,3$  for  $^{52}\text{Cr}$ .



widths will be 50 times smaller for the  $l=3$  resonances than for  $l=1$  resonances at 3.3 MeV. For inelastic scattering the relevant energy for determining the penetrability is  $E_p$  minus the excitation energy of the first excited state. Thus the Coulomb penetrability strongly inhibits the observation of resonances with high orbital angular momentum. More specifically, in  $^{48}\text{Ti}$  the ratio of the  $l=3$  to  $l=1$  Coulomb penetrability for proton inelastic scattering varies from 123 at 2.0 MeV to 57 at 3.0 MeV.

In the earlier elastic scattering measurements performed by Prochnow (1971) no  $l=3$  elastic scattering resonances were observed. The minimum observable  $l=3$  elastic resonance has a laboratory width of about 1 eV; and the maximum average width from consideration of the Porter Thomas width distribution is approximately a tenth of this, or 0.1 eV. This gives a maximum average reduced width of 0.013 keV for  $l=3$  resonances. The average reduced width for  $l=1$  resonances in  $^{48}\text{V}$  is around 1.00 keV. If the ratio of  $l=1$  to  $l=3$  reduced widths is the same in elastic scattering as in inelastic scattering then,

$$\frac{\overline{\delta_{P,l=1}^2}}{\overline{\delta_{P,l=3}^2}} \geq 75 \quad (2.3.5)$$

Thus an average admixture of 1 to 2 percent may be expected in the widths for inelastic scattering. Similar considerations hold for  $^{56}\text{Fe}$ . Using the approximation that all  $l=3$  amplitudes are zero, the equations for the angular

distributions in the channel spin representation are

$$W(\Theta_p) = 1 + \frac{(\gamma_{5/2}^2 - 4\gamma_{3/2}^2)}{5(\gamma_{5/2}^2 + \gamma_{3/2}^2)} P_2(\Theta_p) \quad (2.3.6)$$

$$W(\Theta_s) = 1 + \frac{(\gamma_{3/2}^2 - 2(\gamma_{3/2}\gamma_{5/2}^* + \gamma_{5/2}\gamma_{3/2}^*) + 4\gamma_{5/2}^2) Q_2 P_2(\Theta_s)}{10(\gamma_{3/2}^2 + \gamma_{5/2}^2)} \quad (2.3.7)$$

The formulas in the total angular momentum representation are

$$W(\Theta_p) = 1 - \frac{2(\gamma_{1/2}\gamma_{3/2}^* + \gamma_{3/2}\gamma_{1/2}^*) + 3\gamma_{3/2}^2}{5(\gamma_{3/2}^2 + \gamma_{1/2}^2)} P_2(\Theta_p) \quad (2.3.8)$$

$$W(\Theta_s) = 1 + \frac{\gamma_{1/2}^2 Q_2 P_2(\Theta_s)}{2(\gamma_{3/2}^2 + \gamma_{1/2}^2)} \quad (2.3.9)$$

These equations are normalized to give a leading term equal to unity since only relative reaction yield as a function of angle is important in determining the amplitude mixing ratios. All the equations are of the form

$$W(\Theta) = 1 + a_2 P_2(\Theta) \quad (2.3.10)$$

where  $a_2$  is an experimentally determined quantity obtained from fitting in a least squares sense a measured angular distribution to equation (2.3.8).

Equations (2.3.3) and (2.3.4) and equations (2.3.5) and (2.3.6) have the same physical content and may be transformed into one another. Satchler (1955) and Devons

(1959) give this transformation between representations as

$$\gamma_{s',l'} = \sum_{j'} \gamma_{j'} (-)^{l'+l_{p'}-j'} \sqrt{\frac{s'}{j'}} W(C l_{p'} B l'; s' j') \quad (2.3.11)$$

For the approximation that only  $l'=1$  amplitudes are important equation (2.3.11) becomes

$$\begin{aligned} \gamma_{s'=3/2} &= \frac{1}{\sqrt{5}} (\gamma_{j'=1/2} + 2\gamma_{j'=3/2}) \\ \gamma_{s'=5/2} &= \frac{1}{\sqrt{5}} (\gamma_{j'=3/2} - 2\gamma_{j'=1/2}) \end{aligned} \quad (2.3.12)$$

This transformation is orthogonal and possesses an inverse, thereby preserving the magnitude of the total inelastic decay amplitude. The approximation that all  $l'=3$  amplitudes are zero is not necessary, but the resulting equations are unwieldy. The equations for the reaction products in the channel spin representation are,

$$W(\Theta_{p'}) = 1 - \frac{1}{5} \left\{ 4(\gamma_{3/2,1}^2 - \gamma_{3/2,3}^2) + (\gamma_{5/2,3}^2 - \gamma_{5/2,1}^2) + 3(\gamma_{3/2,3}^* \gamma_{3/2,1} + \gamma_{3/2,1}^* \gamma_{3/2,3}) + 2\sqrt{6}(\gamma_{5/2,3}^* \gamma_{5/2,1} + \gamma_{5/2,1}^* \gamma_{5/2,3}) \right\} P_2(\Theta_p) / (\gamma_{3/2,1}^2 + \gamma_{3/2,3}^2 + \gamma_{5/2,1}^2 + \gamma_{5/2,3}^2) \quad (2.3.13)$$

$$W(\Theta_s) = 1 + \frac{1}{5} \left\{ 2\gamma_{5/2,1}^2 - \frac{11}{7}\gamma_{5/2,3}^2 + \frac{1}{2}(\gamma_{3/2,1}^2 + \gamma_{3/2,3}^2) + \frac{2\sqrt{6}}{7}(\gamma_{3/2,3}^* \gamma_{5/2,3} + \gamma_{5/2,3}^* \gamma_{3/2,3}) - (\gamma_{3/2,1}^* \gamma_{5/2,1} + \gamma_{5/2,1}^* \gamma_{3/2,1}) \right\} Q_2 P_2(\Theta_s) / (\gamma_{3/2,1}^2 + \gamma_{3/2,3}^2 + \gamma_{5/2,1}^2 + \gamma_{5/2,3}^2) \quad (2.3.14)$$

The distribution equations in the total angular momentum representation are

$$W(\Theta_{p'}) = 1 + \frac{1}{35} \left\{ 25\gamma_{7/2}^2 - 21\gamma_{3/2}^2 - 4\gamma_{5/2}^2 - 14(\gamma_{3/2}^* \gamma_{1/2} + \right.$$

$$\begin{aligned} & \gamma_{1/2}^* \gamma_{3/2} - 7\sqrt{21} (\gamma_{5/2}^* \gamma_{1/2} + \gamma_{1/2}^* \gamma_{5/2}) + 2\sqrt{21} (\gamma_{5/2}^* \gamma_{3/2} + \gamma_{3/2}^* \gamma_{5/2}) - \\ & 6\sqrt{14} (\gamma_{7/2}^* \gamma_{3/2} + \gamma_{3/2}^* \gamma_{7/2}) + 4\sqrt{6} (\gamma_{7/2}^* \gamma_{5/2} + \gamma_{5/2}^* \gamma_{7/2}) \} P_2(\theta_p) / \\ & (\gamma_{1/2}^2 + \gamma_{3/2}^2 + \gamma_{5/2}^2 + \gamma_{7/2}^2) \quad (2.3.15) \end{aligned}$$

$$W(\theta_s) = 1 + 10 \frac{(\frac{1}{20} \gamma_{1/2}^2 - \frac{1}{28} \gamma_{5/2}^2 + \frac{1}{70} \gamma_{7/2}^2) Q_2 P_2(\theta_s)}{(\gamma_{1/2}^2 + \gamma_{3/2}^2 + \gamma_{5/2}^2 + \gamma_{7/2}^2)} \quad (2.3.16)$$

These equations also transform according to equation (2.3.11).

The set of equations for the transformation in the general case for  $3/2^-$  inelastic resonances is

$$\begin{aligned} \gamma_{j'=1/2} &= \frac{1}{\sqrt{5}} (\gamma_{3/2,1} - 2\gamma_{5/2,1}) \\ \gamma_{j'=3/2} &= \frac{1}{\sqrt{5}} (\gamma_{5/2,1} + 2\gamma_{3/2,1}) \\ \gamma_{j'=5/2} &= \frac{1}{\sqrt{35}} (\sqrt{3}\gamma_{3/2,3} - 4\sqrt{2}\gamma_{5/2,3}) \\ \gamma_{j'=7/2} &= \frac{1}{\sqrt{35}} (\sqrt{3}\gamma_{3/2,3} + 4\sqrt{2}\gamma_{5/2,3}) \end{aligned} \quad (2.3.17)$$

The equations in this section have been written with amplitudes as complex quantities. Since the nuclear Hamiltonian is rotationally and time reversal invariant, reduced width amplitudes are real,

$$\gamma = |\gamma| e^{i\varphi} \quad \varphi = 0, \pi$$

#### 2.4 Amplitude Mixing Ratios.

Equations (2.3.13) and (2.3.14) or (2.3.15) and

(2.3.16) for the angular distributions have four nuclear decay amplitudes for the  $l'=1$  and  $l'=3$  case. Two amplitudes exist in the  $l'=1$  case. Mixing parameters can be defined for both cases. The definitions used are similar in both representations. In the total angular representation these mixing parameters are

$$\delta_{f'} \equiv \frac{\delta_{7/2}}{\delta_{5/2}} \quad \delta_{g'} \equiv \frac{\delta_{3/2}}{\delta_{1/2}} \quad (2.4.1)$$

$$\epsilon_{f'}^2 \equiv \frac{\delta_{7/2}^2 + \delta_{5/2}^2}{\delta_{7/2}^2 + \delta_{5/2}^2 + \delta_{3/2}^2 + \delta_{1/2}^2}$$

In the channel spin representation the parameters are

$$\delta_{s'} \equiv \frac{\delta_{5/2,3}}{\delta_{3/2,3}} \quad \delta_{s'c} = \frac{\delta_{5/2,1}}{\delta_{3/2,1}} \quad (2.4.2)$$

$$\epsilon_{s'}^2 \equiv \frac{\delta_{5/2,3}^2 + \delta_{3/2,3}^2}{\delta_{5/2,3}^2 + \delta_{3/2,3}^2 + \delta_{5/2,1}^2 + \delta_{3/2,1}^2}$$

The mixing ratios  $\delta_s$  and  $\delta_c$  can take on all real values.

$\epsilon^2$  is the ratio of  $l'=3$  reduced width to the total reduced width. The sign of  $\epsilon$  is defined to have the same sign as  $\delta_s$ . This definition of the sign of  $\epsilon$  is arbitrary and could be defined as the sign of  $\delta_c$ . Using the approximation that only  $l'=1$  inelastic scattering amplitudes exist,  $\delta_c$  can be written as a simple function of  $a_2$ . The equations for  $\delta_c$  as a function of  $a_2$  in the total angular momentum representation are

$$\delta_{p'g'} = \frac{-2 \pm \sqrt{4 - 26a_2^2 - 15a_2}}{5a_2 + 3} \quad )$$



$$\delta_{\gamma\gamma'} = \pm \sqrt{(1-2a_2)/2a_2} \quad (2.4.3)$$

where  $\delta_{p\gamma}$  are the values obtained from the charged particle experiment and  $\delta_{\gamma\gamma'}$  are the values obtained from the gamma-ray experiment. Similar equations for the channel spin representation are

$$\delta_{p's'} = \pm \sqrt{(4+5a_2)/(1-5a_2)} \quad (2.4.4)$$

$$\delta_{\gamma s'} = \frac{2 \pm 3\sqrt{2a_2 - 4a_2^2}}{4 - 10a_2}$$

where  $\delta_{p's'}$  are the values obtained from the charged particle experiment and  $\delta_{\gamma s'}$  are the values obtained from the gamma-ray experiment. It can be seen from either equations (2.4.3) or (2.4.4), that each angular distribution in general will give an  $a_2$  consistent with two mixing ratios. The two angular distributions measured for each resonance give sufficient information to remove this ambiguity. Using the transformation equations (2.3.9) the mixing ratios are found to transform as

$$\delta_{\gamma'} = \frac{2 + \delta_{s'}}{1 - 2\delta_{s'}} \quad (2.4.5)$$

or inversely as

$$\delta_{s'} = \frac{-2 + \delta_{\gamma'}}{1 + 2\delta_{\gamma'}} \quad (2.4.6)$$

Since the mixing ratios have inconvenient infinities, it is useful to define a quantity  $\varphi$  as

$$\varphi = \text{TAN}^{-1} \delta \quad (2.4.7)$$

This definition compresses the information on the mixing ratios so that a finite parameter can be used to describe the mixing. With this definition the  $\varphi$  in different representations transform as

$$\varphi_{3'} = \varphi_{2'} + \text{TAN}^{-1}(-2) \quad (2.4.8)$$

These relationships can be seen in Figure 2.3 and Figure 2.4 which show the functional relationship between  $\varphi$  and  $a_2$  in both the channel spin and total angular momentum representations. The transformation from one representation to another is a rotation of approximately sixty three degrees.

If  $l'=3$  amplitudes are included in the analysis, simple formulas for  $\delta_3$ ,  $\delta_4$ , and  $\epsilon$  as a function  $a_2$  are not obtained. However, since penetrability considerations indicate a small value of  $\epsilon^2$  (approximately one percent), an equation for  $a_2$  as a function of  $\delta_3$ ,  $\delta_4$ , and  $\epsilon$  is useful in determining the effect of small admixtures of  $l'=3$  amplitudes. In the angular momentum representation for inelastically scattered protons, one obtains an equation for  $a_2$  as a function of  $\delta_3$ ,  $\delta_4$ , and  $\epsilon$

$$a_2 = \frac{-1}{35} \frac{(21\delta_z^2 + 28\delta_z)}{(1 + \delta_z^2)} (1 - \epsilon^2) + \frac{\epsilon^2}{35} \frac{(25\delta_z^2 + 8\sqrt{6}\delta_z + 4)}{(1 + \delta_z^2)} - \frac{\epsilon(1 - \epsilon^2)^{1/2}}{35} \frac{(14\sqrt{21} + 12\sqrt{14}\delta_z\delta_z - 4\sqrt{21}\delta_z)}{(1 + \delta_z^2)^{1/2}(1 + \delta_z^2)^{1/2}} \cos(\ ) \quad (2.4.9)$$

and for the de-excitation gamma-rays

$$a_2 = \frac{1}{2} \frac{(1 - \epsilon^2)}{(1 + \delta_z^2)} - \frac{\epsilon^2}{14} \frac{(5 - 2\delta_z^2)}{(\delta_z^2 + 1)} \quad (2.4.10)$$

The first term in both equations is the same as that obtained with only  $l'=1$  amplitudes except for an attenuation factor proportional to  $(1 - \epsilon^2)$ . For small  $\epsilon$ , no appreciable variation as a function of  $\epsilon$  occurs in this term of the formula. The second term in both equations gives a displacement of the  $a_2$  curve. The displacement for all values of  $\epsilon$  has a maximum of  $(25/35)\epsilon^2$  for protons and  $-(5/14)\epsilon^2$  for gamma-rays. This displacement is small for small  $\epsilon^2$ . The only remaining term is in the equation for the protons. This term is proportional to  $(1 - \epsilon^2)^{1/2}\epsilon$  or for small  $\epsilon^2$  is proportional to  $\epsilon$ . A plot of  $\varphi$  for  $l'=1$  amplitudes with an admixture of  $l'=3$  strength equal to one percent is shown in Figure 4.5. The gamma-ray plot is essentially unchanged. The proton curve, however, has a band in which  $a_2$  can vary for a constant  $\delta_z$  and a varying  $\delta_z$  and  $\epsilon$ . The curves marked with  $|\epsilon|=0.1$  show the maximum extent of this band when  $|\epsilon|=0.1$  with  $\delta_z$  assuming any arbitrary value. This effect can cause confusion as to

Figure 2.3  $a_2$  Versus  $\varphi$  in the Channel Spin Representation.

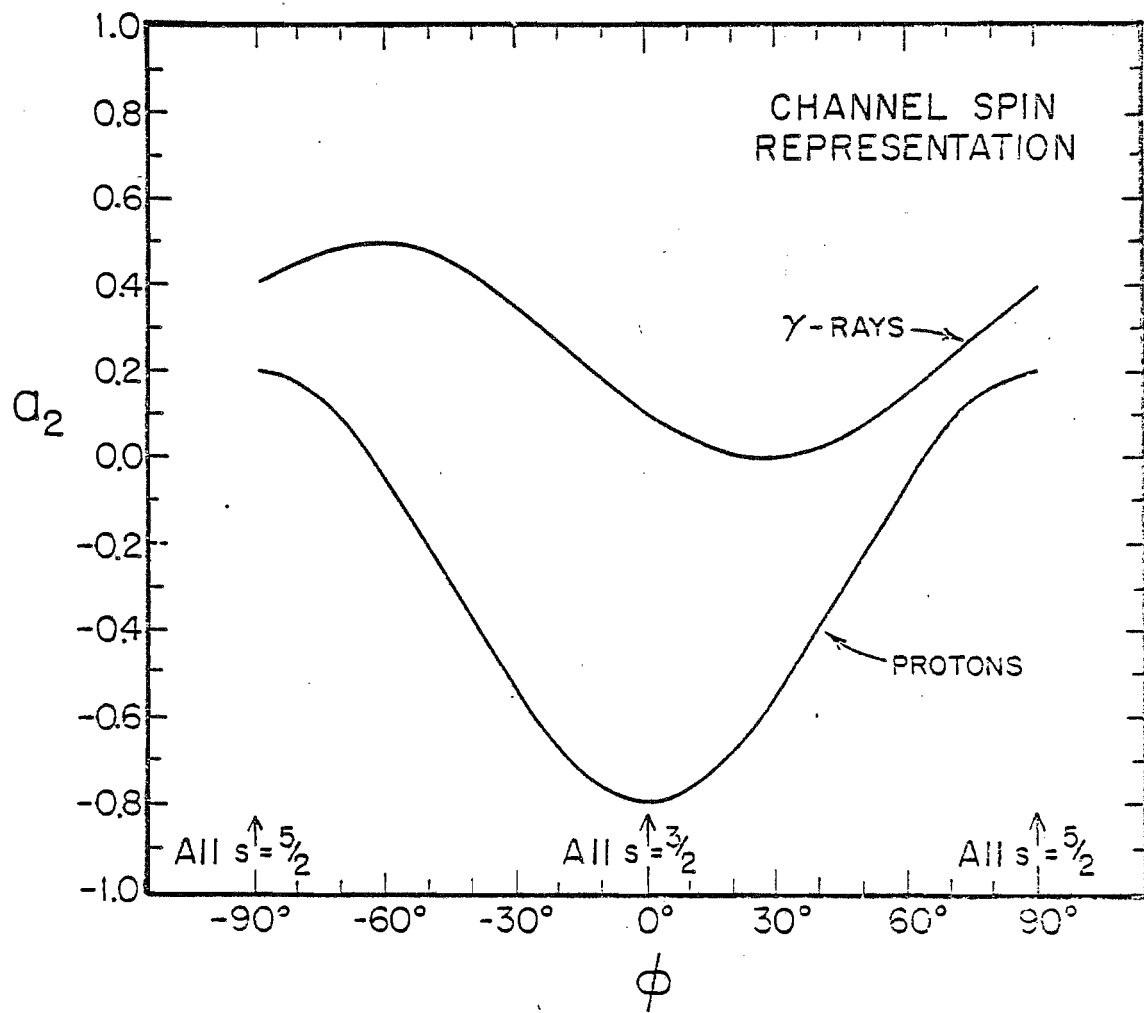


Figure 2.4  $a_2$  Versus  $\varphi$  in the Total Angular Momentum Representation.

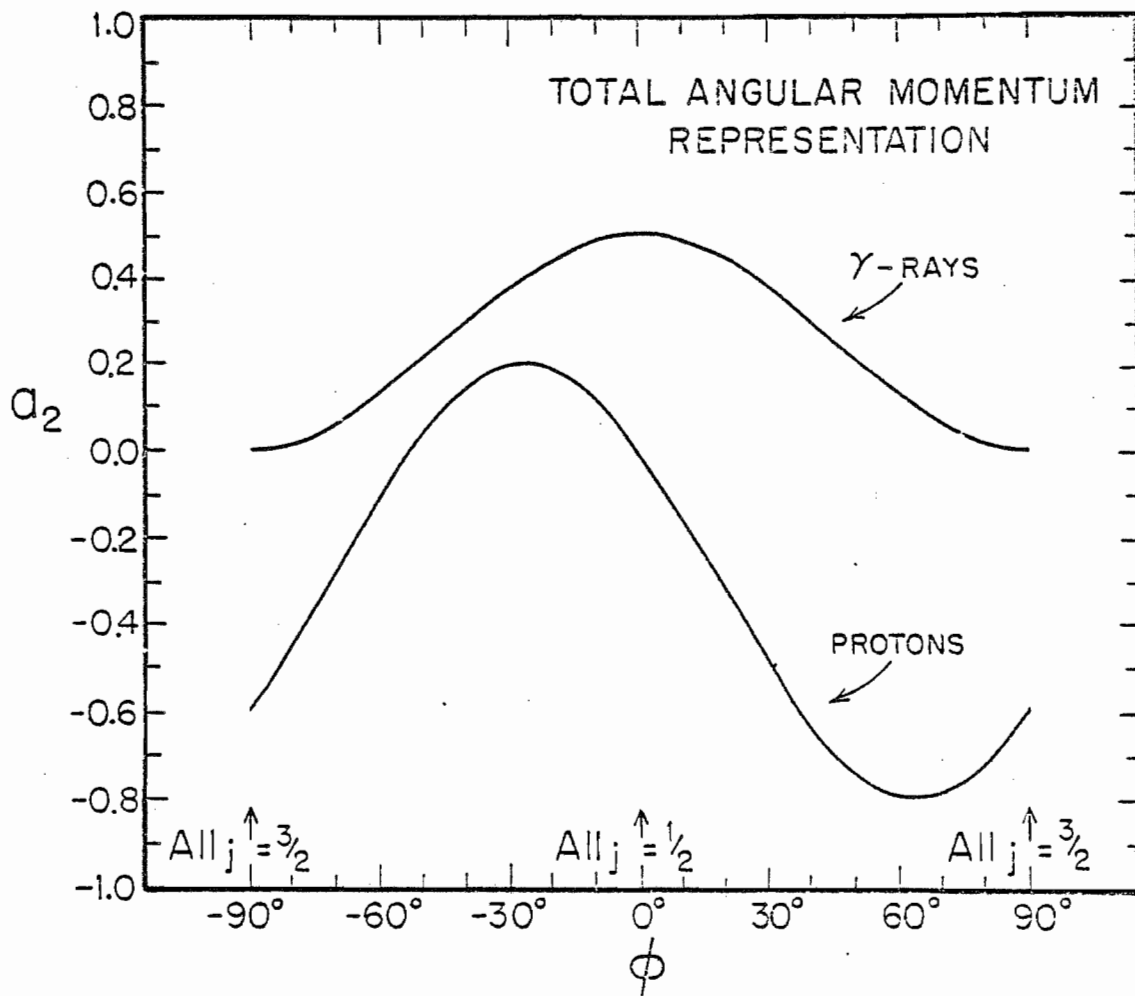
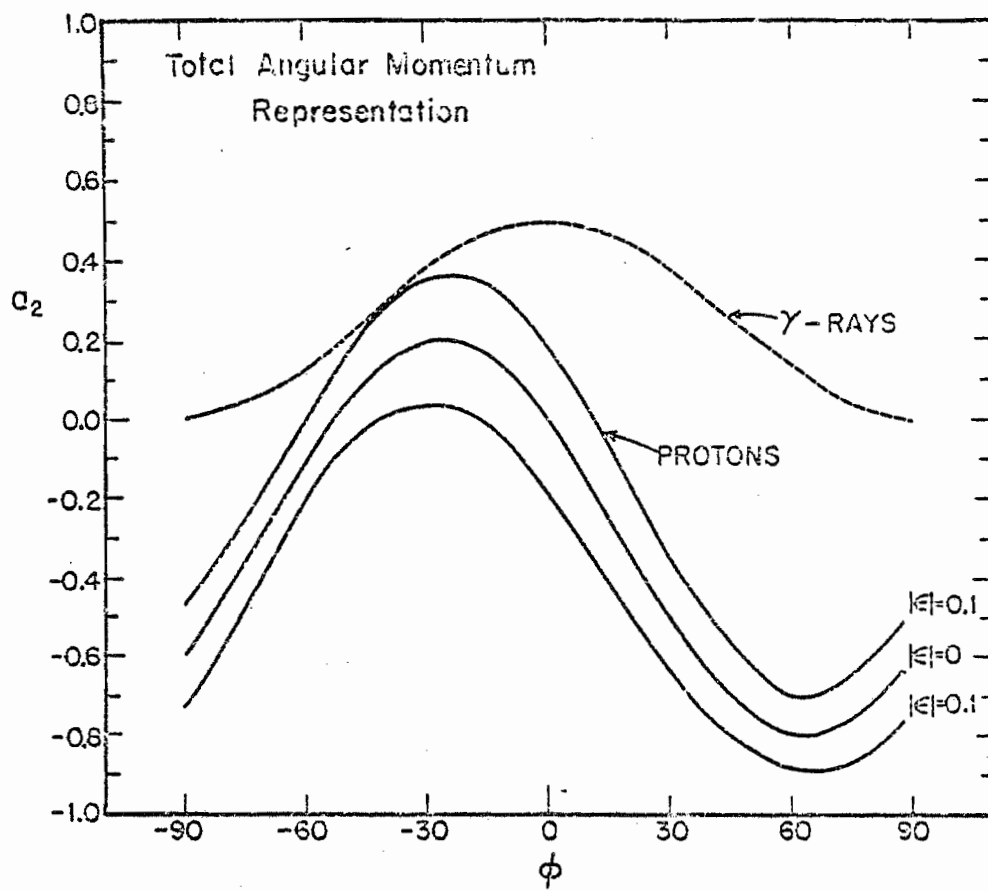


Figure 2.5  $a_2$  Versus  $\varphi$  in the Total Angular Momentum Representation with  $l'=3$  Amplitude Admixtures. The bands in the lower curve marked with  $|\epsilon|=0.1$  show the maximum excursion that  $a_2$  can make for a given  $\varphi$  with  $|\epsilon|$  less than 0.1 and with  $\delta_2$  assuming an arbitrary value .





which value of  $\varphi$  or  $\delta$  is the correct solution given the four values computed from equations (2.4.3) or (2.4.4). If the  $a_2$  values have sufficiently small statistical errors, then an admixture of one percent or greater  $l'=3$  strength will give inconsistent results if one uses the equations derived assuming that  $l'=3$  amplitudes are zero. No systematic inclusion of  $\delta_2$  where an appreciable value of  $\delta_2$  exists is possible if reasonable rejection criterion for inconsistent results are used. Experimentally only one inconsistent result was obtained in these experiments for which there was no obvious level interference.

## Chapter 3

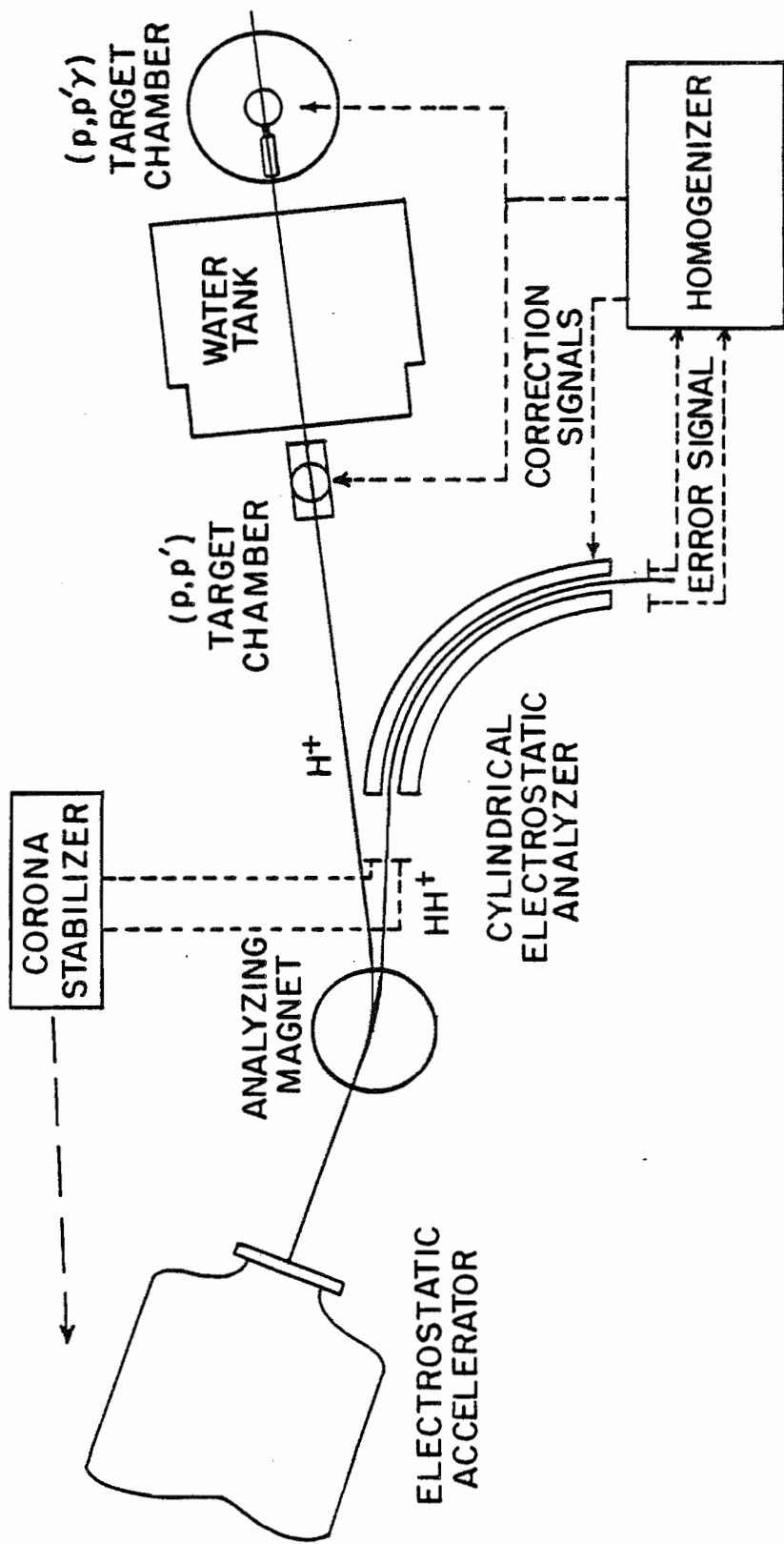
### EQUIPMENT AND EXPERIMENTAL PROCEDURES

#### 3.1 3 MV Van de Graaff Accelerator

The data in the experiments described in this dissertation were taken using the Triangle Universities Nuclear Laboratory's 3 MV Van de Graaff accelerator and beam homogenizer system. The original homogenizer system was described by Paris (1958). Details of this homogenizer system, which has since undergone substantial changes, are given in Appendix A.

The accelerator and its control system are shown in Figure 3.1. The accelerator ion source produces two species of charged ions,  $H^+$  and  $HH^+$ , which are accelerated and analyzed by the 25 degree bending magnet. The  $H^+$  beam is directed to the experimental scattering chambers and plays no direct role in subsequent stabilization of the beam energy. The  $HH^+$  beam is intercepted by a pair of slits and the difference in current on these slits is used to derive

Figure 3.1 The Floor Plan of the 3 MV Van de Graaff Accelerator Laboratory.



an energy control signal for a conventional corona stabilization system. These slits also serve as object slits for the electrostatic analyzer. Feedback control systems of the coronal discharge type, control low frequencies (less than 10 hertz) very well, but have little or no effect on the higher frequencies due to finite transit times of the ions in the discharge. A discussion of this problem and some of the methods for overcoming the difficulty are given by Bleck (1978).

The  $\text{HH}^+$  beam enters the one meter radius electrostatic analyzer. A negative high voltage is applied to the inner plate of the analyzer and the outer plate is maintained at zero potential. An image is formed on the slits at the output of the analyzer and the difference of the current on these slits is amplified and applied to the outer plate. This outer plate correction voltage keeps the beam centered on the image slits and thus is proportional to the energy fluctuations in the beam. The fluctuations in the incident proton energy can be cancelled by applying a voltage to a target rod in one of the scattering chambers. The ratio of the target rod voltage to outer plate correction voltage depends only upon the geometry of the analyzer. This ratio for the analyzer used in this experiment is approximately 111.

### 3.2 Targets

Two nuclei were studied in this dissertation,  $^{56}\text{Fe}$  and  $^{48}\text{Ti}$ . These isotopes were both isotopically enriched to greater than 99%. Iron targets were prepared from the chemical compound  $\text{Fe}_2\text{O}_3$  and titanium targets from a crystal bar. The target material was obtained from Oak Ridge National Laboratory.

Targets were 1-5  $\mu\text{g}/\text{cm}^2$  thick and were evaporated onto 2-5  $\mu\text{g}/\text{cm}^2$  carbon foils obtained from the Arizona Carbon Foil Company. The targets were prepared to give the maximum possible yield of reaction products without sacrificing the necessary resolution in the proton bombarding energy used for that target. This thickness corresponds to an average energy loss of approximately 200-300 eV. The vacuum in the evaporator used for the preparation of the targets was maintained at less than  $10^{-5}$  torr during the deposition of the target material on the self supporting foils. Glass slides were placed over the foils to prevent deposition of target material on the reverse side of the foil.

Iron targets were prepared by reducing the  $\text{Fe}_2\text{O}_3$  in a carbon crucible placed in a high current heater. The  $\text{Fe}_2\text{O}_3$  was reduced at increasingly elevated temperatures, while keeping the vacuum less than  $10^{-4}$  torr. Without this constraint the reaction proceeded at a high rate and ejected the isotope from the crucible. At the point where increasing temperatures did not produce any more

reduction--as indicated by the vacuum in the evaporator--the  $^{56}\text{Fe}$  metal was then deposited on the carbon backings. During the reduction process a metal shutter was kept between the backings and the crucible to prevent contaminating the foils and causing them to fracture from excess heat. These targets were stored in vacuum to prevent the iron from oxidizing.

Titanium targets were much easier to prepare. They were produced by evaporating a small piece of the  $^{48}\text{Ti}$  crystal bar placed in an open tantalum evaporation boat. These targets can be stored in air without appreciable oxidation for several months.

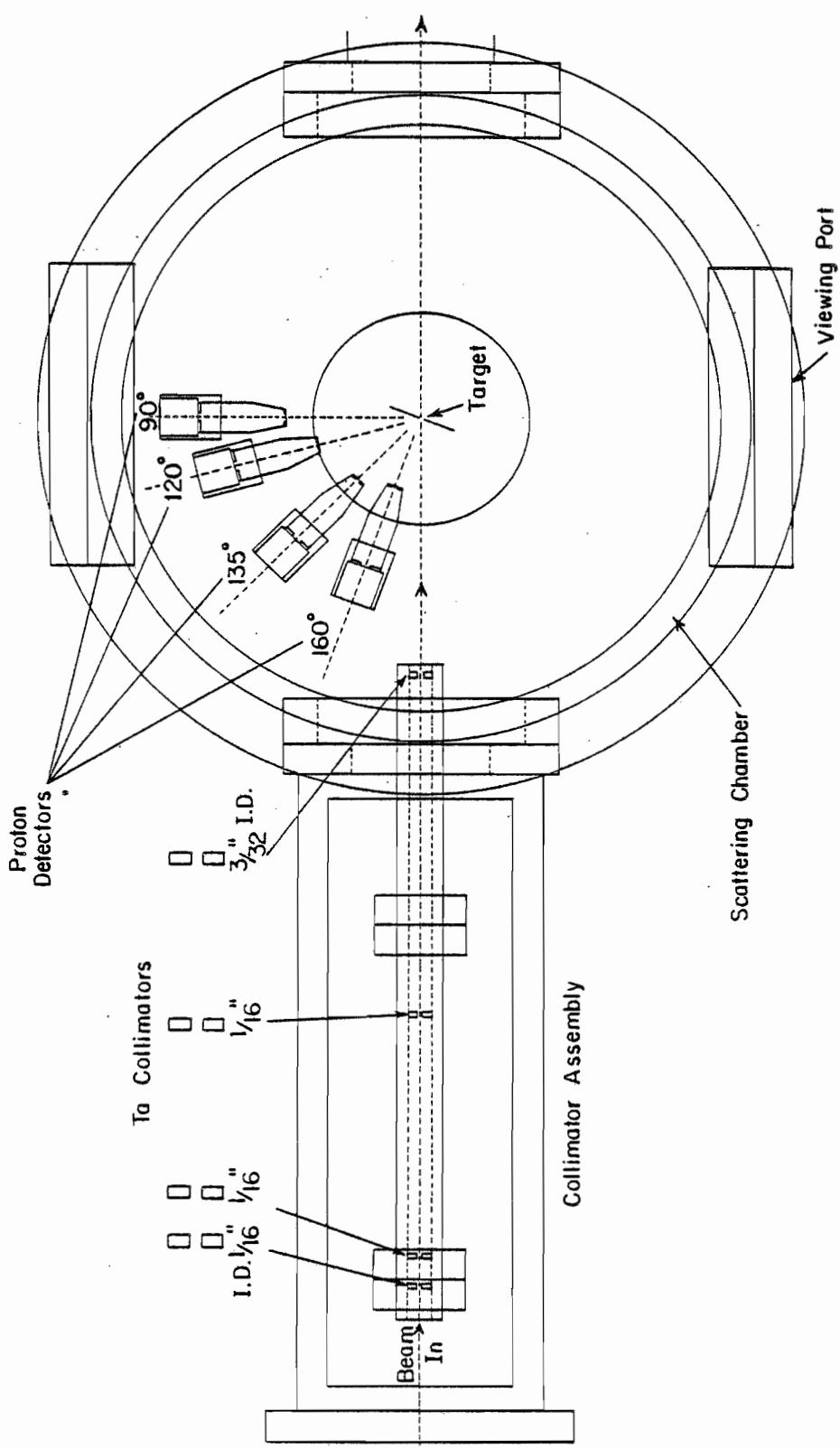
### 3.3 Scattering Chambers and Detectors

The experiments described in this dissertation were performed in two scattering chambers. Charged particle angular distributions were measured in a chamber designed by Browne (1969). Gamma-ray angular distributions were measured in a chamber designed by Wimpey (1974). The location of these chambers in the laboratory is shown in Figure 3.1.

The chamber and beam collimation system for the charged particle work are shown in Figure 3.2. The vacuum in this chamber was maintained at less than  $10^{-6}$  torr to prevent the accumulation of contaminants, which degrade the resolution.



Figure 3.2 Schematic Diagram of the Charged Particle Scattering Chamber and its Associated Collimator Assembly.



Proton Detectors

Ta Collimators

3/32" I.D.

I.D. 1/16"

Beam In

Collimator Assembly

Target

Scattering Chamber

Viewing Port

90°

120°

135°

160°

The beam is limited by the first of two collimators as it enters the collimator assembly. The third collimator disk is used to insure that the beam is centered in the scattering chamber. The final collimator is used as a monitor to minimize the slit scattering from the previous collimators. The final collimator is electrically insulated; by minimizing the current intercepted by this collimator, low energy proton scattering background can be minimized in the charged particle spectra. This is a very important requirement since inelastic scattering from weak resonances requires small background in order to reduce background subtraction errors.

Charged particles were detected in four Ortec surface barrier detectors whose collimators subtended the same solid angle. The original design of the scattering chamber allowed only certain discrete angular positions for the detectors. These angular positions were selected for their utility in elastic scattering resonance shape analysis. In the  $^{56}\text{Fe}$  experiment, particles were detected at  $90^\circ$ ,  $105^\circ$ ,  $135^\circ$ , and  $150^\circ$ . The angles  $90^\circ$  and  $105^\circ$ , however, are redundant for a measurement of the  $a_2$  coefficient of an angular distribution. In the  $^{48}\text{Ti}$  experiment a jig for positioning and holding a detector at  $120^\circ$  was built and the  $150^\circ$  detector was replaced by a detector at  $160^\circ$ . This geometrical arrangement provided a better determination of  $a_2$  than the previous detector configuration. However, the

120° detector was not as positionally stable as was initially intended; small motions and vibrations in the experimental area caused the error associated with the yield in this detector to be about twice that of the other detectors.

The collimation system and scattering chamber used to measure the gamma-ray angular distributions in this experiment are shown in Figure 3.3. The collimation system is similar in design to the one used with the charged particle chamber. The angular distributions were measured using four 3 inch by 3 inch NaI(Tl) crystal scintillation detectors coupled to RCA 8575 photomultiplier tubes obtained from Harshaw Chemical Company. These detectors were mounted at 90°, 60°, 45°, and 30° and were shielded with a two inch thick lead collar. Charged particles were detected in this chamber at 135° with a surface barrier detector. Not shown in Figure 3.3 is the 80 cc. Ge(Li) detector used as a high resolution gamma-ray monitor and the lead shielding around both the collimator and the beam dump.

#### 3.4 Counting Electronics

The counting electronics used in these experiments are shown as used for one detector in Figure 3.4. The electronics are shown for both gamma-rays and charged particle detectors. Two computers were used for collecting the data in this experiments. The majority of the data was

Figure 3.3 Schematic Diagram of the Gamma-Ray Scattering Chamber and Associated Collimator Assembly. The upper drawing is a top view and the lower drawing is a side view of the chamber and collimator.

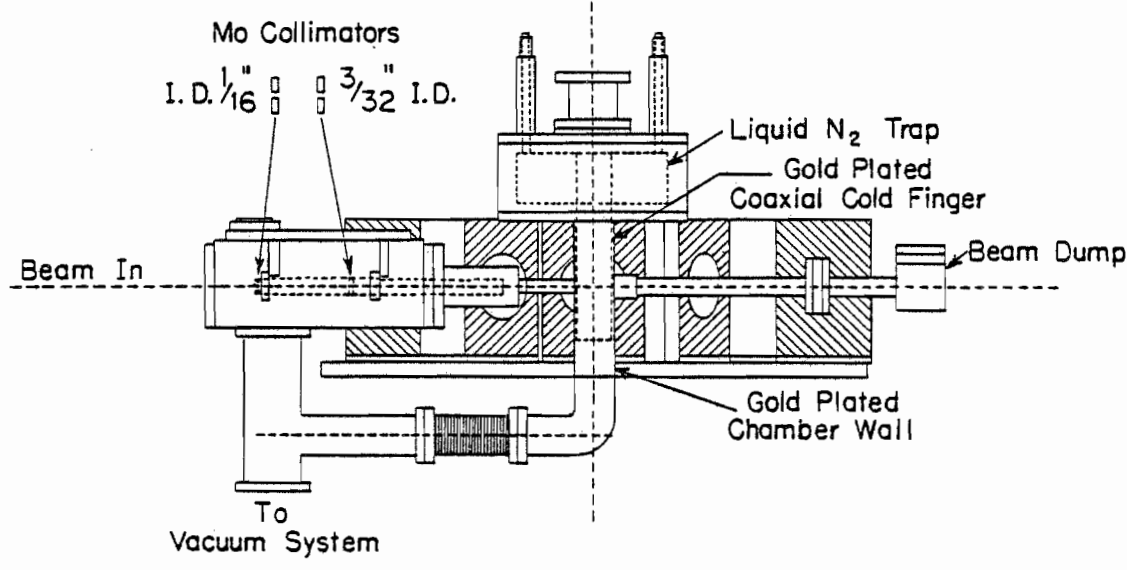
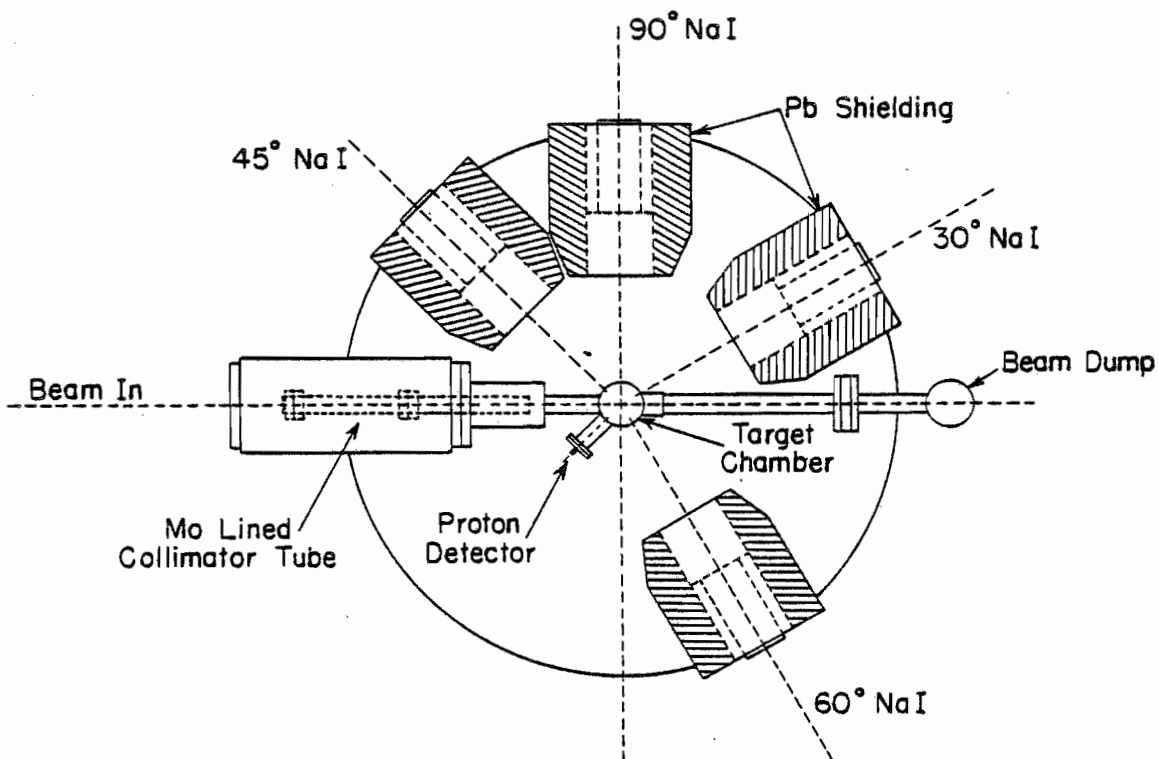
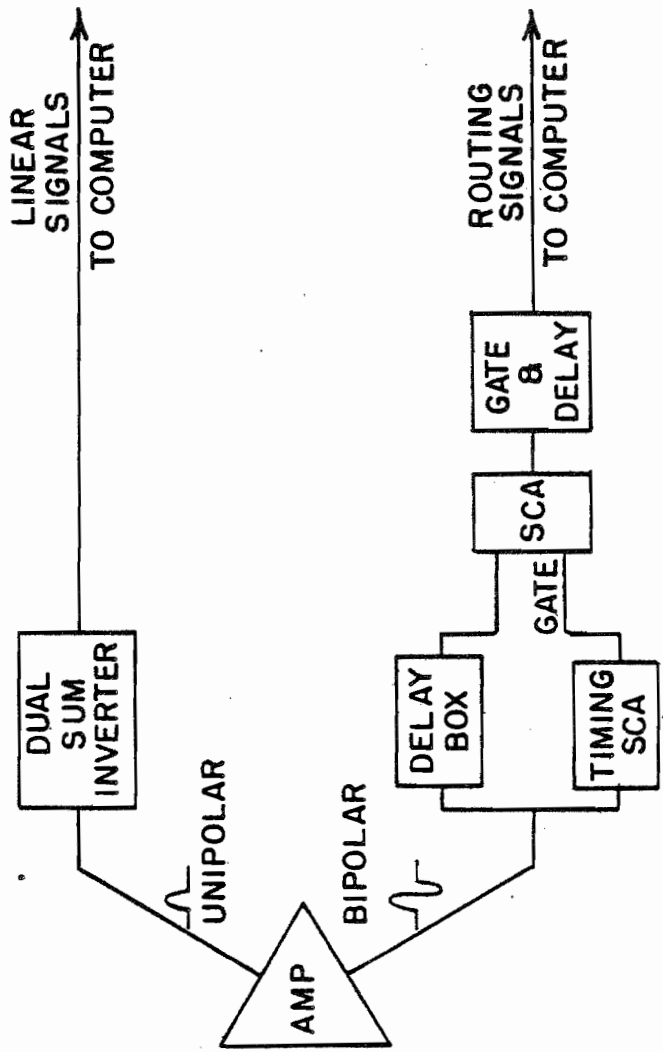
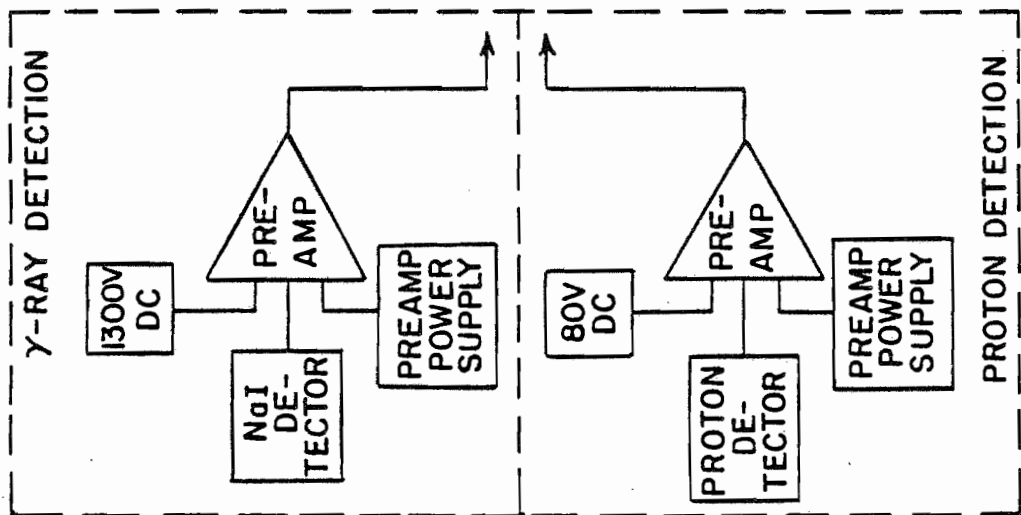


Figure 3.4 Schematic Diagram of the Charged Particle and Gamma-Ray Detection Electronics.





taken using a DDP-224 computer; the rest was taken with a Prime 300 computer. The operation of the electronics is similar for both gamma-ray and charged particles.

First consider the operation of the counting system when used for the detection of charged particles. Pulses from the surface barrier detector are amplified by an Ortec 109A preamplifier. The preamplifier pulses are then amplified and shaped by a Tennelec 203 spectroscopy amplifier which produces unipolar and bipolar pulses. The unipolar pulses from all four detector systems are summed in an Ortec 433 dual sum and invert amplifier. These summed signals are then sent to a Northern Scientific (model 621) analogue to digital converter (ADC).

The bipolar signals from each separate spectroscopy amplifier are sent to an Ortec 420A timing single channel analyzer (SCA). The Ortec SCA is used to generate a signal to gate out selected pulses from a Hewlett Packard SCA, whose input is a delayed bipolar signal from the Tennelec spectroscopy amplifier. The pulses gated out are those due to proton elastic scattering from  $^{12}\text{C}$ . The timing signals from the Hewlett Packard SCA are then shaped and delayed by the Ortec 416A gate and delay generator and are then sent to an eight input router in the computer interface. The output of the eight input router consists of a three bit digital signal which records which of the eight inputs received a pulse. The router also generates a gate signal which turns

on the ADC and allows it to digitize the unipolar pulse present at its input. The timing of the unipolar pulses and the router pulses is adjusted with the gate and delay generator so that the unipolar pulse analyzed is associated with the bipolar pulse which activated the router. The output of the router is then combined with the output of the ADC (maximum number of bits is 13) to form a computer input word (16 bits with the Prime 300, 24 bits with the DDP-224). This input word contains all information concerning the digitized pulse height and the detector from which the analyzed pulse came. During the time after the router pulse arrives and the reading and clearing of the computer input word, the router generates a "busy signal". This signal is used for differential "dead time" correction for the rest of the control electronics.

The control electronics consist of a current integration system which allows the data to be normalized to the total charge accumulated on a beam stop after the target. An Ortec 439 current digitizer sends out a pulse for a certain amount of integrated beam current. These pulses are counted by a preset scaler. The scaler and current digitizer are gated off by the "router busy" signal to ensure that the current is integrated only while the computer is capable of accepting and analyzing pulses from the detectors. When the scaler reaches a preset count it sends an output to the computer's external control lines

inactivating the router and ADC. This system thus allows the operator to select a certain amount of integrated beam current to control the accumulation of data. Conversion of yield into cross section is made possible by this system.

The operation of the NaI(Tl) detectors with this electronics system is the same as with the surface barrier detectors except that the Hewlett Packard SCA is not gated. The only purpose of the gating in the charged particle work is to reduce the counting rates input into the computer from  $^{12}\text{C}$  elastic scattering in order to minimize computer dead time.

Examples of spectra obtained with these electronics and the detectors and chambers discussed in section 3.3 are shown in Figures 3.5 and 3.6. A charged particle spectrum with a  $^{56}\text{Fe}$  target with a  $^{12}\text{C}$  elastic scattering peak gated out is shown in Figure 3.5. Contaminant peaks are labelled. A corresponding spectrum of the inelastic de-excitation gamma-rays from  $^{56}\text{Fe}$  is shown in Figure 3.6.

### 3.5 Experimental Procedures

The procedures used for both charged particles and gamma-ray measurements are similar. Only the procedures for the charged particles will be discussed in detail; the differences in the gamma-ray procedures will be explained as needed in the discussion. The experiments consisted of

Figure 3.5 Charged Particle Spectrum from a Resonance Excited via the  $^{56}\text{Fe}(p,p')^{56}\text{Fe}$  Reaction at  $E_p = 3.01$  MeV. The contaminant peaks are marked. Note the absence of the  $^{12}\text{C}$  elastic scattering peak, which has been gated out of the spectrum to reduce the counting rate.

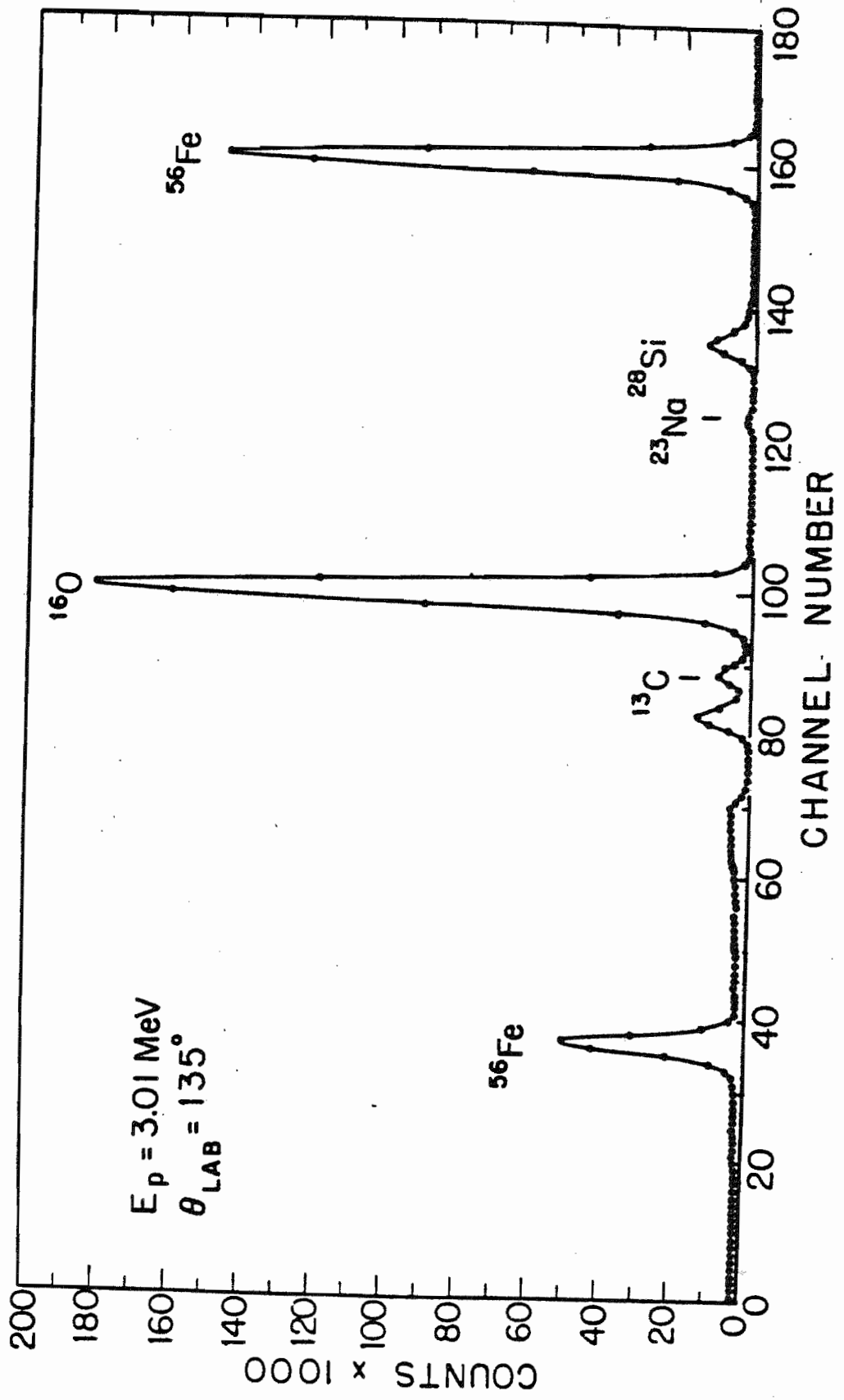
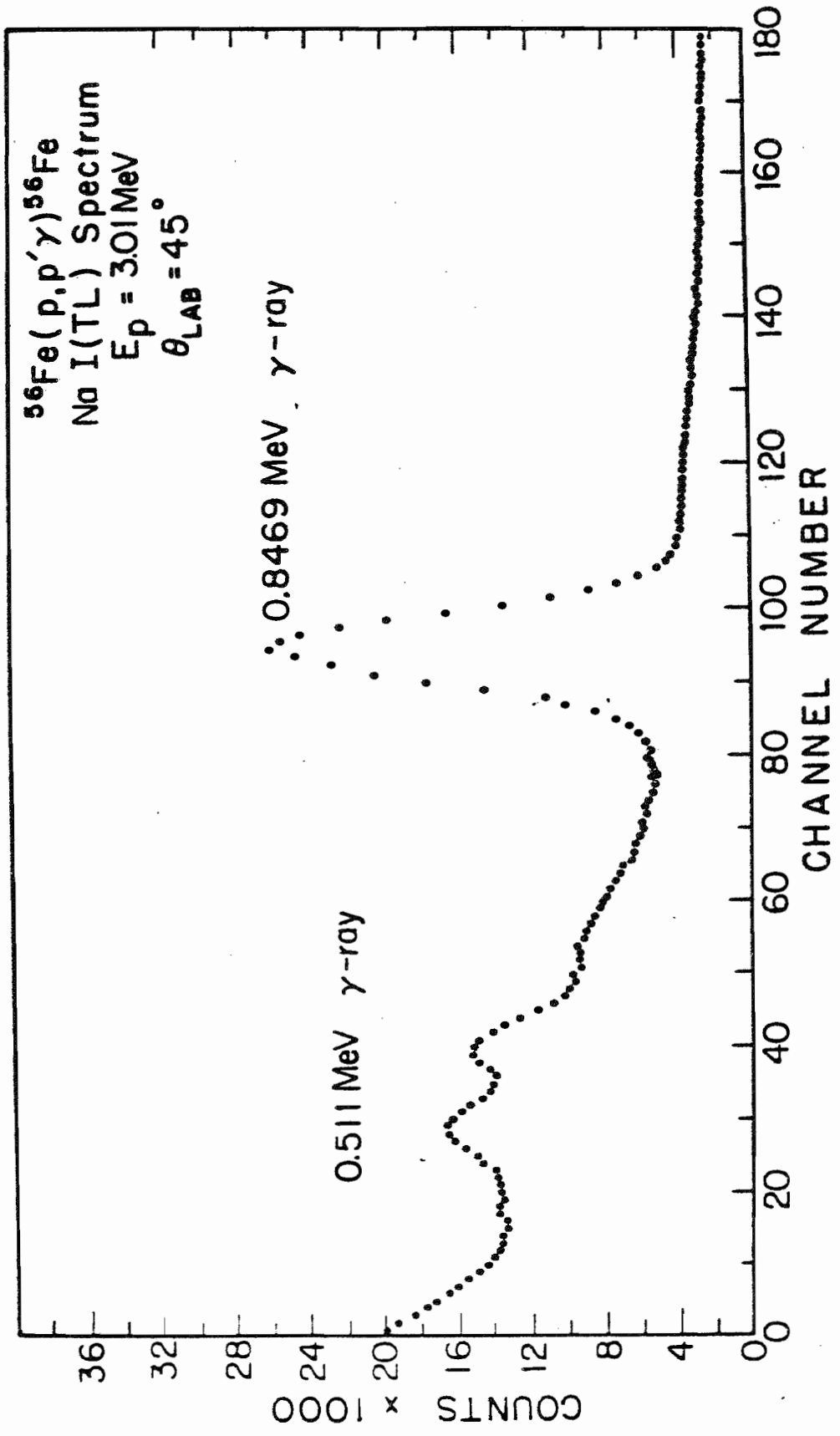


Figure 3.6 De-Excitation Gamma-Ray Spectrum from a Resonance Excited via the  $^{56}\text{Fe}(p,p')^{56}\text{Fe}$  Reaction at  $E_p=3.01$  MeV.



angular distribution measurements of inelastically scattered protons and de-excitation gamma-rays from resonances in the compound systems of  $^{57}\text{Co}$  and  $^{49}\text{V}$ . The compound nuclear states examined were p-wave resonances first studied in the elastic scattering on  $^{56}\text{Fe}$  and  $^{48}\text{Ti}$  by Lindstrom (1970) and Prochnow (1971), respectively.

The states to be studied were located by taking an elastic and inelastic yield curve from approximately 2 keV below the resonance energy (as given in the previously published experiments on elastic scattering) to 2 keV above the state. A plot was made of the yield of elastically and inelastically scattered protons from the  $150^\circ$  or  $160^\circ$  detector. In the gamma-rays a plot was made of the elastically scattered protons in the  $135^\circ$  surface barrier detector and the de-excitation gamma-rays from the  $90^\circ$  NaI(Tl) detector. The yields were written in a notebook and all the spectra taken during the yield curve measurement were recorded on magnetic tape.

Before the yield curve was taken, the target was replaced by a metal disk with a 0.100 inch diameter hole and the disk was connected to a microammeter through the target rod to measure the beam current intercepted by the disk. The beam was then steered and focused to minimize current on the last collimator (minimizing slit scattering). Simultaneously, the beam current intercepted by the disk on the target rod was minimized (insuring that the beam was



centered in the scattering chamber) and maximized on the beam stop (maximizing yield). A spectrum was taken with the disk in place of the target and with the target rod totally removed from the path of the beam to record the success of the beam steering and focusing. A similar procedure was performed in the gamma-ray scattering chamber. The disk used in the gamma-ray chamber was made of aluminium which has a large proton capture cross section. The yield of capture gamma-rays resulting from the beam hitting the ring was also used as a measure of beam centering in the steering and focusing procedures. A count rate of less than 2000 counts per second from all four gamma-ray detectors gave an acceptable background.

After the focusing and steering of the beam was accomplished and the yield curve for the resonance under study was taken, the proton beam energy was adjusted to the resonant energy. A set of spectra for the reaction product being studied was then accumulated for an integrated beam current sufficient to give an accurate determination of the coefficients of the angular distribution. The relative efficiencies of the detectors were normalized with Rutherford scattering for the proton detectors. Calibrated radioactive gamma-ray sources were used to obtain the relative efficiencies of the NaI(Tl) detectors. The Rutherford scattering normalization was performed for each resonance in the experiment with  $^{48}\text{Ti}$  using a thin gold

target backed with a carbon foil. In the  $^{56}\text{Fe}$  experiment the normalization was performed only periodically. Better results were obtained when the charged particle detectors were normalized for each resonance to compensate for beam and detector movements. The gamma-ray detectors did not need such frequent normalization. More severe constraints were placed on the beam position in the gamma-ray experiments since the beam passed through both the proton and the gamma-ray chamber collimators.

The criterion for necessary yield for an angular distribution measurement was set at 10,000 counts in the  $90^\circ$  detector or until 30,000  $\mu\text{C}$  of integrated beam current was accumulated (in practice about one and one half hours). This rather arbitrary criterion was established as a compromise between measuring as many angular distributions from separate resonances as possible and making the measurements with as small a statistical error as possible.

Once the distribution was measured, the beam energy was changed and the process was repeated. It was more economical to measure the gamma-ray distributions first, since with targets of equal thickness, the yield of gamma-rays to inelastically scattered protons was approximately ten to one. Thus, once a resonance yield was determined to be too weak in the gamma-ray measurement, no more measurements were made on the resonance.

Rutherford scattering normalization, which was

required in the measurement of the charged particles, was necessary because of small movements in the  $120^\circ$  detector due to vibrations in the experimental area. The close positioning of the surface barrier detectors because of the design of the chamber made the detectors more sensitive to beam movement. The movement of the  $120^\circ$  detector, because of its mounting, has now been largely eliminated. The beam motion problem is eliminated to some extent by using a gold Rutherford scattering normalization before every measurement of a charged particle angular distribution. The motion problem is not as severe in the gamma-ray experiment due to the larger distance between the detectors and the target. In addition, the use of two sets of collimators helps alleviate this problem at the expense of increasing the difficulty of steering and focusing the beam into the gamma-ray chamber.

## Chapter 4

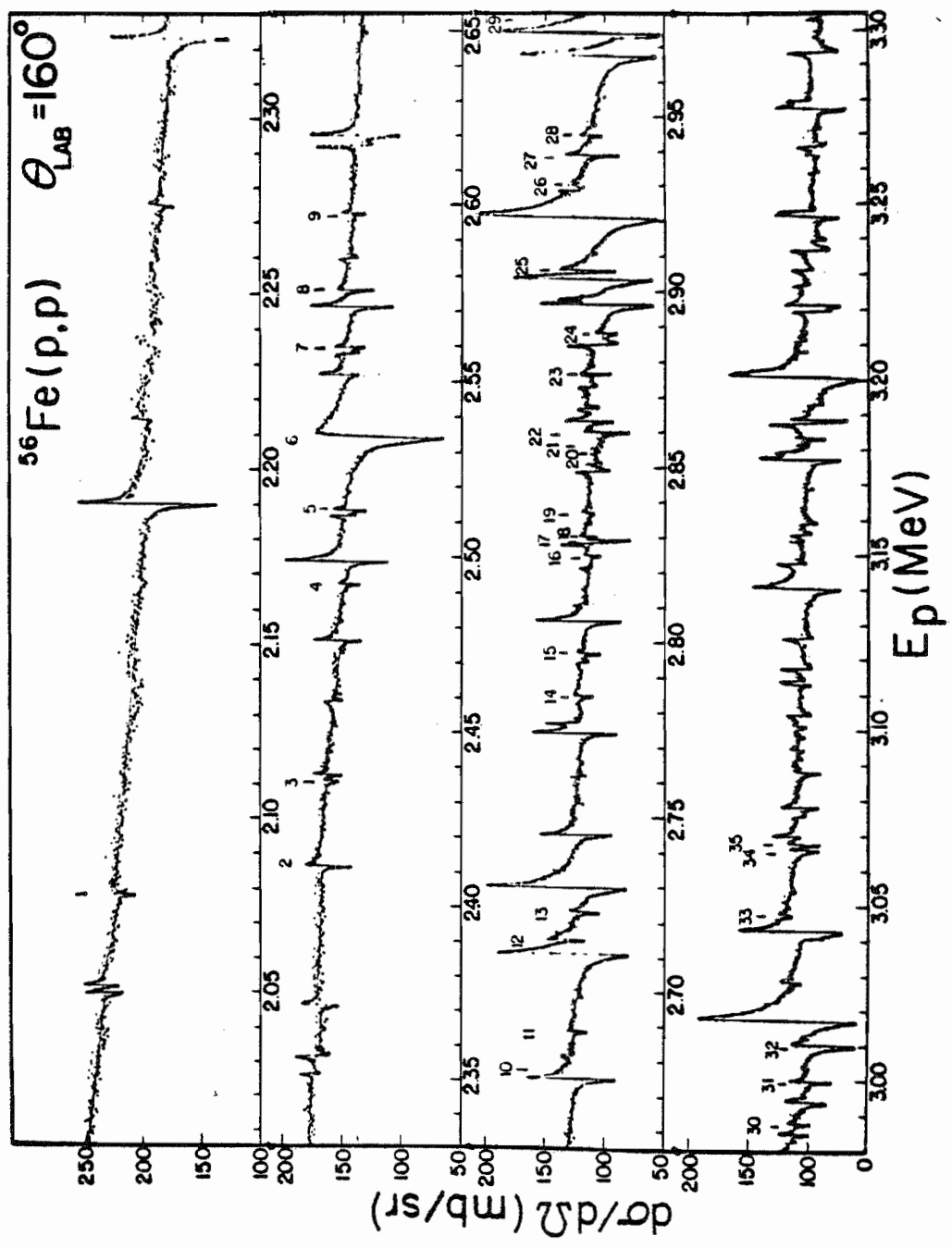
### DATA AND PRELIMINARY ANALYSIS

#### 4.1 Elastic Scattering Experiments

The first high resolution proton scattering studies of  $^{56}\text{Fe}$  and  $^{48}\text{Ti}$  were designed primarily as elastic scattering experiments with only secondary emphasis on inelastic scattering. The elastic scattering experiment on  $^{56}\text{Fe}$  by Lindstrom(1970) ignored inelastic contributions on all but a few resonances. The small average inelastic yield in  $^{56}\text{Fe}$  made the detection of inelastically scattered protons very difficult with the methods employed at that time. In Figure 4.1 is shown the differential cross section at the laboratory scattering angle of 160 degrees for the energy range studied. The solid line is a guide to the eye. Numbers indicate the p-wave resonances studied in the present experiment.

The first high resolution work on  $^{48}\text{Ti}$  by Prochnow(1971) showed a higher and denser inelastic

Figure 4.1 Differential Cross Section of Proton Elastic Scattering at 160 Degrees on  $^{56}\text{Fe}$ . Numbers refer to the resonances studied in the present experiment. The solid line is a guide to the eye.

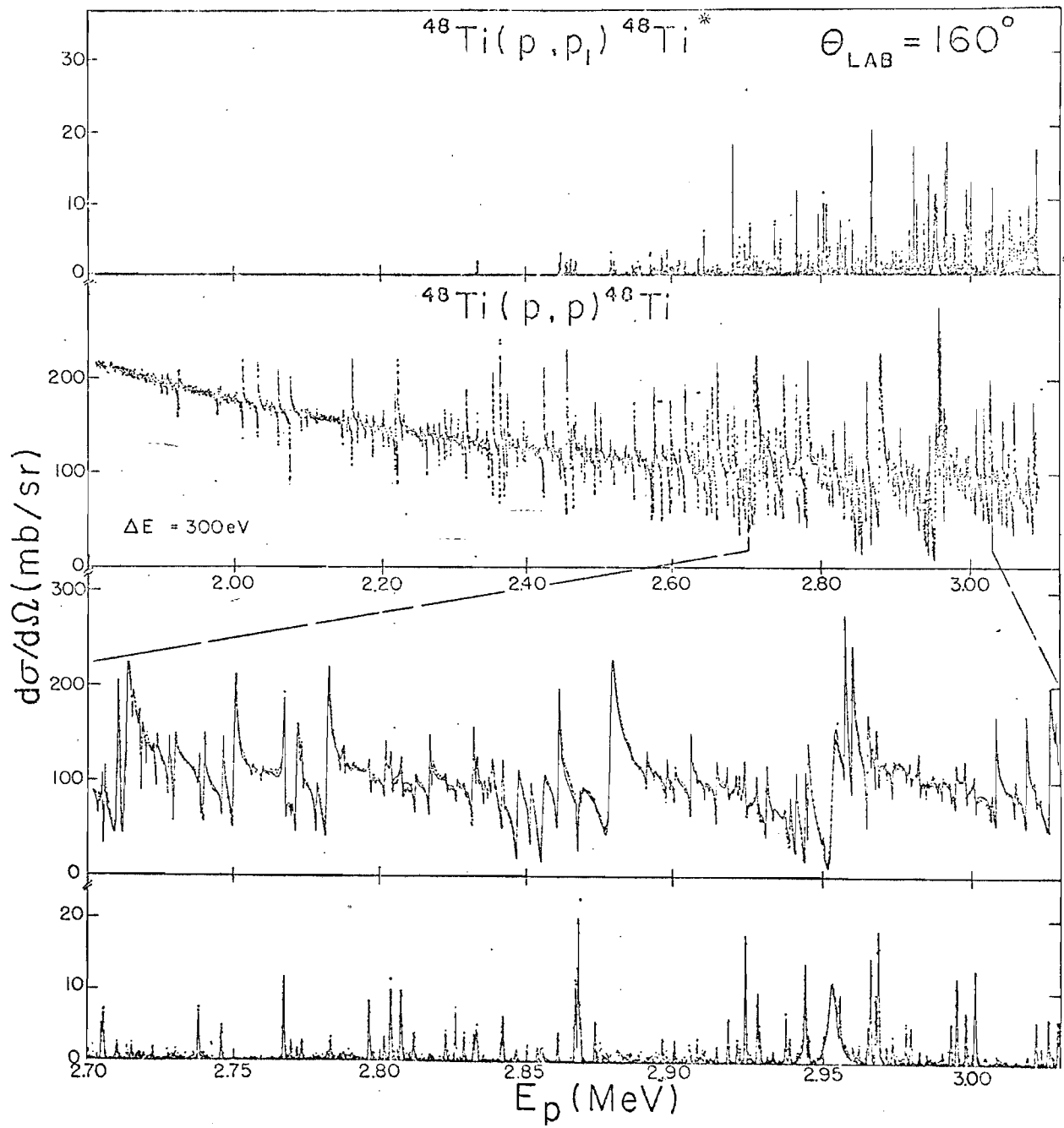


scattering yield which necessitated a multichannel analysis of the data. Elastic and inelastic differential cross section of  $^{48}\text{Ti}$  at the laboratory scattering angle of 160 degrees are shown in Figure 4.2. The solid line is a multilevel, multichannel fit. The data are also shown on an expanded energy scale in a portion of the higher level density region. The density of states in this nucleus is much higher than in  $^{56}\text{Fe}$ . The method of obtaining this data was much the same as that used by Lindstrom (1970) which precluded the observation of many of the weak levels in the inelastic channel which are seen in the present work. One hundred and twenty p-wave resonances were studied in  $^{48}\text{Ti}$  and thirty-six p-wave resonances were studied in  $^{56}\text{Fe}$ . Some of the resonances studied had insufficient yield for study and some had interference from neighboring states which led to inconsistencies in the analysis. In all, seventy two  $3/2^-$  resonances and fourteen  $1/2^-$  resonances were analyzed in  $^{48}\text{Ti}$ . There were eighteen resonances which had no inelastic yield and sixteen resonances for which the analysis led to inconsistent results. In  $^{56}\text{Fe}$ , twenty  $3/2^-$  resonances and two  $1/2^-$  resonances were analyzed; nine resonances had no yield, and five resonances had inconsistent results.

#### 4.2 Resonance Parameters

Figure 4.2 Differential Cross Section of Proton Elastic and Inelastic Scattering on  $^{48}\text{T}$  at 160 Degrees. The expanded region shows the data in the region of high level density. The solid line is a multilevel, multichannel fit to the data.





The present experiment consisted of measuring the inelastic scattering from all the p-wave resonances from  $E = 2.0$  to  $3.1$  MeV seen in previous high resolution elastic scattering experiments on  $^{56}\text{Fe}$  and  $^{48}\text{Ti}$ . The procedures of section 3.5 were followed. The resonances studied are specified by the following set of parameters:

- $E_p$  the proton excitation energy of the resonance,
- $J^\pi$  the spin and parity of the resonance,
- $\gamma_p^2$  the elastic proton reduced width,
- $\gamma_p^2$  the total inelastic proton reduced width, and
- $\delta$  the ratio of the inelastic reduced width amplitudes.

Other useful parameters can be derived from this set. Tables listing the different parameters used in this work are presented in Appendix B. Tables B.1 and B.5 list the first four of the above basic parameters for  $^{56}\text{Fe}$  and  $^{48}\text{Ti}$ , respectively. An asterisk following the spin and parity of a resonance denotes a change in the assignment. Parentheses around the spin and parity denote an ambiguous spin. When there are no entries for  $\Gamma_p$  and  $\gamma_p^2$ , either the inelastic strength was too small for analysis or the resonance had interference from neighboring states which prevented analysis.

It must be emphasized that only those p-wave resonances

which are observable in elastic scattering were studied. Analysis of elastic scattering data uniquely determines the parity of the compound nuclear states thereby marking the p-wave resonances for more detailed study, at the expense of missing that fraction of states which have low elastic yield. Without this information, extensive yield curve measurements with long counting times per point would be required to locate inelastic scattering resonances, and only a fraction of these would be p-wave resonances.

The measured four point angular distributions for both inelastically scattered protons and de-excitation gamma-rays were fitted to a function  $-a_0(1+a_2P_2(\cos \theta))$ . The yields were obtained from spectra accumulated after the resonance was located. The peaks in the spectra were summed with appropriate background subtraction and normalized before fitting to obtain the  $a_0$  and  $a_2$  coefficients and their errors. Mixing ratios were determined from the  $a_2$  coefficients determined from both gamma-ray and proton experiments using equations (2.4.4) in the channel spin representation. Using the definition  $\varphi = \tan^{-1} \delta$ , the values of  $\varphi$  for the channel spin representation were calculated. The consistent values for  $\delta$  and its associated  $\varphi$  were then selected. Values from the proton and gamma-ray experiments which disagreed by more than two standard deviations were considered inconsistent. This analysis was repeated for the total angular momentum representation. The results of this

analysis are summarized in Table B.2 for  $^{56}\text{Fe}$  and Table B.6 for  $^{48}\text{Ti}$ . Note that the values of the mixing ratio,  $\delta$ , selected for each resonance as consistent do not have exactly the same values in each experiment due to experimental errors. These values must be combined into one value for use in further calculations. The final value for the mixing ratio is calculated using equations

$$\delta_{\gamma'} = \frac{\Delta P \delta_{\gamma\gamma'} + \Delta G \delta_{\gamma' \gamma}}{\Delta P + \Delta G}$$

$$\delta_{\gamma'} = \frac{\Delta P \delta_{\gamma\gamma'} + \Delta P \delta_{\gamma' \gamma}}{\Delta P + \Delta G}$$

where  $\Delta P$  and  $\Delta G$  are the errors in the mixing ratios in the proton and gamma-ray data, respectively. The composite error for each mixing ratio was determined in the same fashion. These results are given in table B.3 for  $^{56}\text{Fe}$  and table B.7 for  $^{48}\text{Ti}$ . The finite range of  $\varphi$  makes it a more convenient variable to plot than  $\delta$ . Plots of  $\varphi$  versus proton bombarding energy in the total angular momentum representation are shown for  $^{56}\text{Fe}$  in Figure 4.3 and for  $^{48}\text{Ti}$  in Figure 4.4. This plot is useful in showing any gross regularity in the inelastic decay patterns of the observed compound nuclear states. The groupings of  $\varphi$  around zero degrees and minus sixty degrees for  $^{48}\text{Ti}$  are not expected. This anomaly is considered in the next chapter.

Figure 4.3  $\phi$  versus  $E_p$  in the Channel Spin Representation  
for  $^{56}\text{Fe}$ .

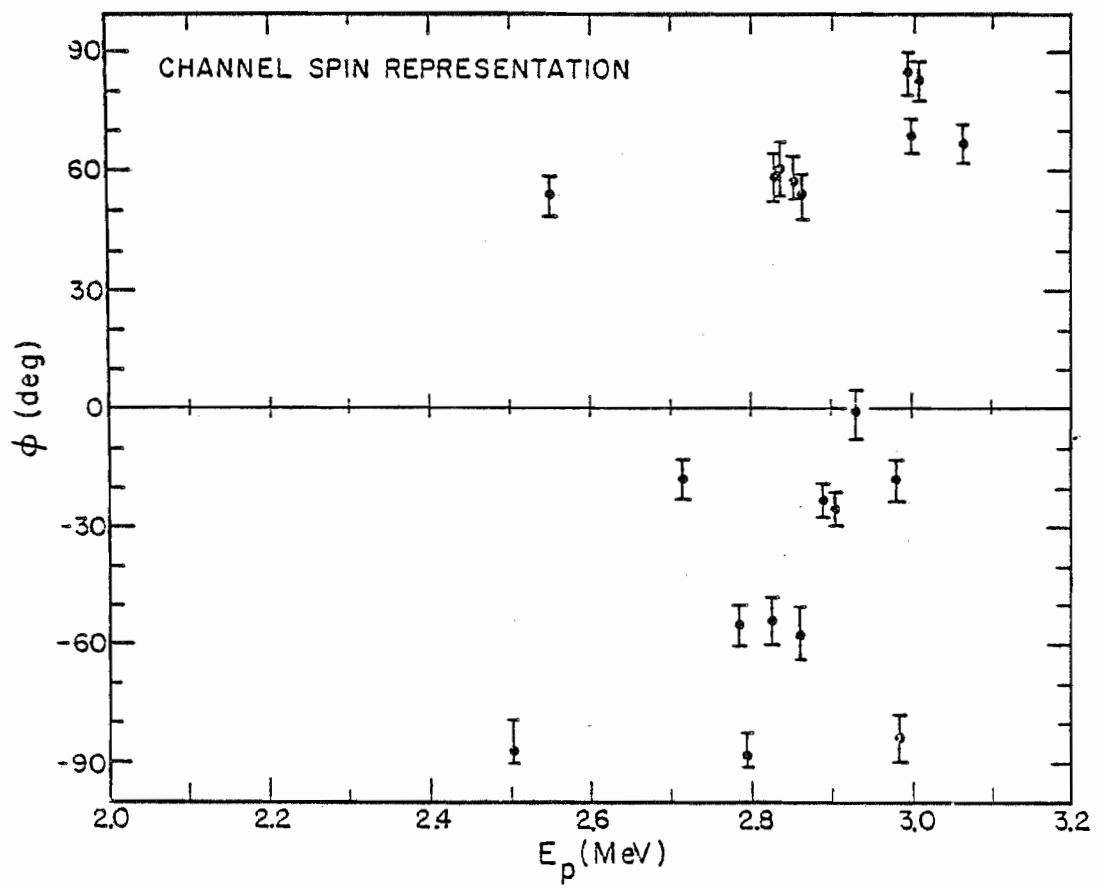
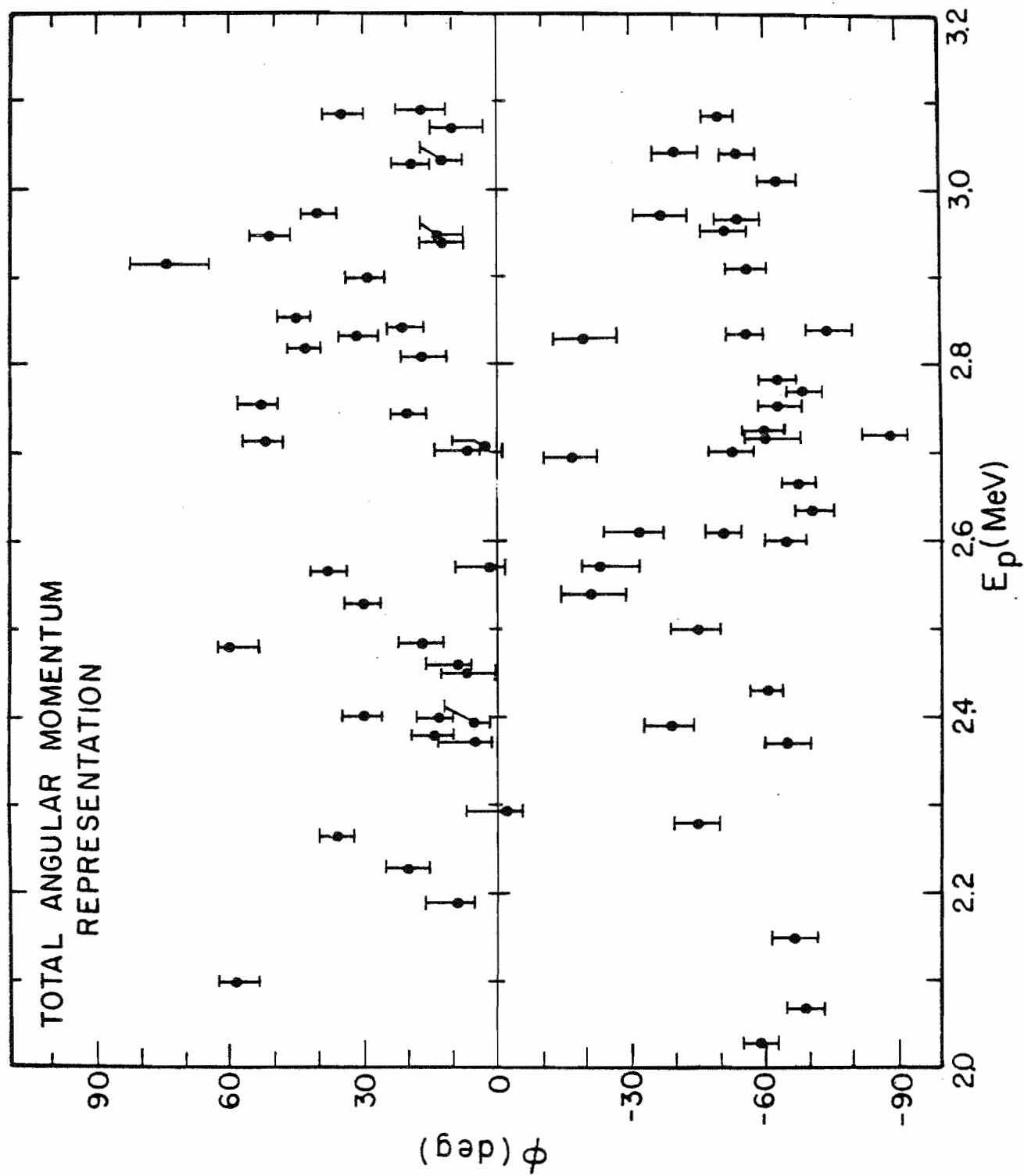


Figure 4.4  $\varphi$  versus  $E_p$  in the Total Angular Momentum Representation for  $^{48}\text{Ti}$ .





When the spin assignments were correct, the elastic widths,  $\Gamma_p$ , for the resonances in the present experiments were taken from previous elastic scattering experiments. When spin assignments were uncertain or incorrect, the widths for small resonances were modified by the ratio of the states' spin statistical factors. Large resonances were refitted using a multilevel, multichannel R-matrix computer program, MULTI, written by D. L. Sellin (1969). The inelastic widths,  $\Gamma_p'$ , were also determined with MULTI for large resonances, but for small widths a procedure outlined by Gove (1953) was followed. The widths were determined from the equation

$$(2J+1) \frac{\Gamma_p' \Gamma_p}{\Gamma} = 2Y/\lambda^2 t$$

where  $J$  is the spin of the compound nuclear state of total width  $\Gamma$  (energy),  $Y$  is the thin target reaction yield (reactions times energy per incident particle),  $\lambda$  is the center of mass wavelength of the incident particle (centimeters),  $t$  is the areal target thickness (atoms per square centimeter),  $\Gamma_p$  is the elastic width (energy) and  $\Gamma_p'$  is the inelastic width (energy). The approximation that total and elastic widths are equal was used for the weak resonances. Widths calculated with these methods are compiled in tables B.1 for  $^{56}\text{Fe}$  and B.5 for  $^{48}\text{Ti}$ . The reduced widths in these tables are calculated from

$$\gamma_{\lambda c}^2 = \Gamma_{\lambda c} / 2R$$

where  $\Gamma_{\lambda c}$  is the partial width of resonance  $\lambda$  in channel  $c$  and  $P_c$  is the Coulomb penetrability in channel  $c$ . The penetrability was evaluated at a channel radius  $1.25(A^{1/3} + 1)R$ , where  $A$  is the mass number of the target. Reduced widths in each channel for each representation can be calculated for inelastic scattering from the total reduced width and the mixing ratios. These data are presented in table B.4 for  $^{56}\text{Fe}$  and table B.8 for  $^{48}\text{Ti}$ .

Graphical representations are useful in discussions of these data. Figure 4.5 shows a plot of the total inelastic reduced widths versus proton bombarding energy for  $^{48}\text{Ti}$ . In this plot the wide variations in the reduced widths typical of such experiments are evident. The inelastic reduced widths in the  $J=3/2^-$  and  $J=1/2^-$  channels are shown in Figure 4.6 as well as the elastic reduced widths. The large reduced width at 2.953 MeV in all three channels is an isobaric analogue state previously identified by Prochnow (1970).

Figure 4.5 Plot of Total Inelastic Reduced Widths versus  $E_p$ .

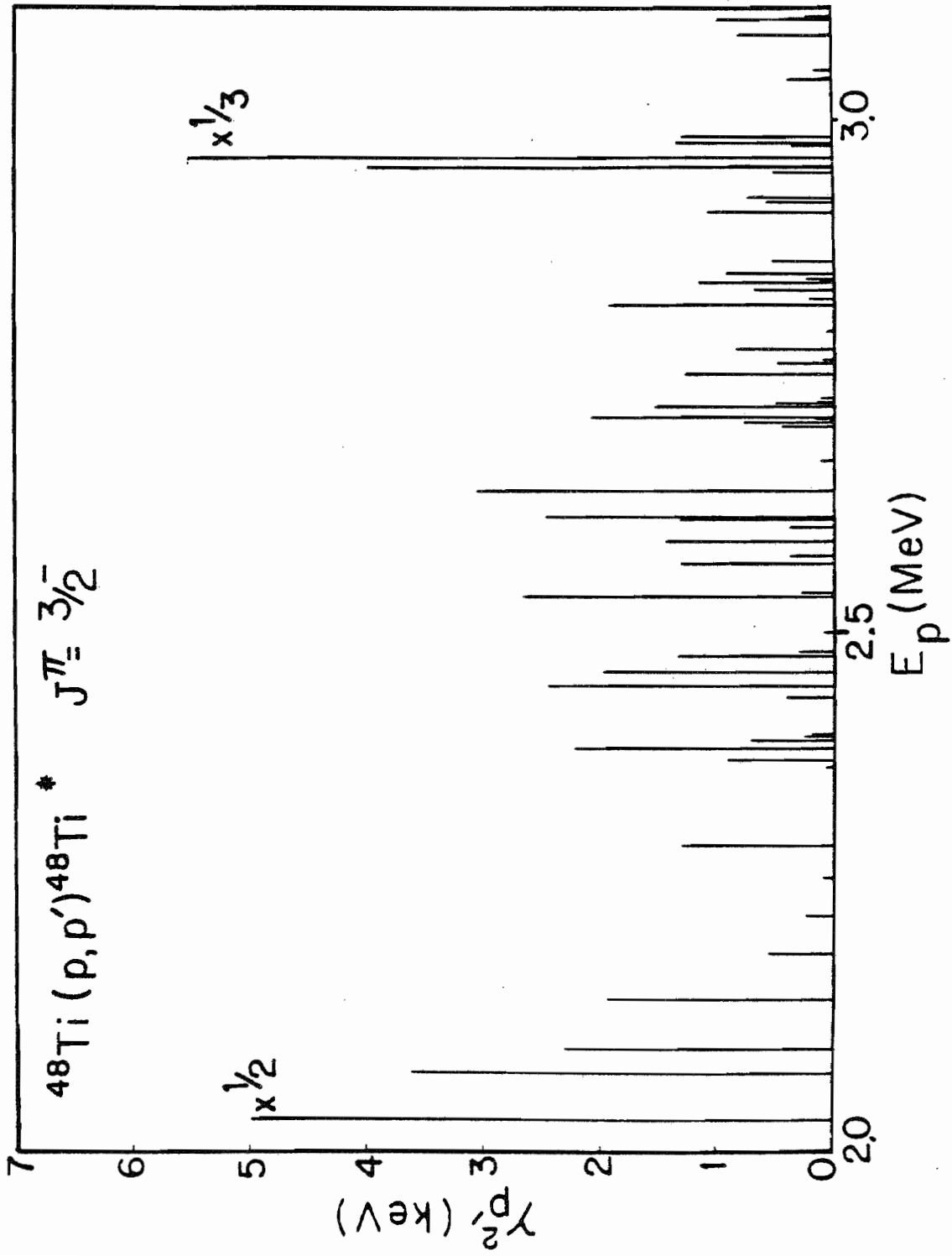
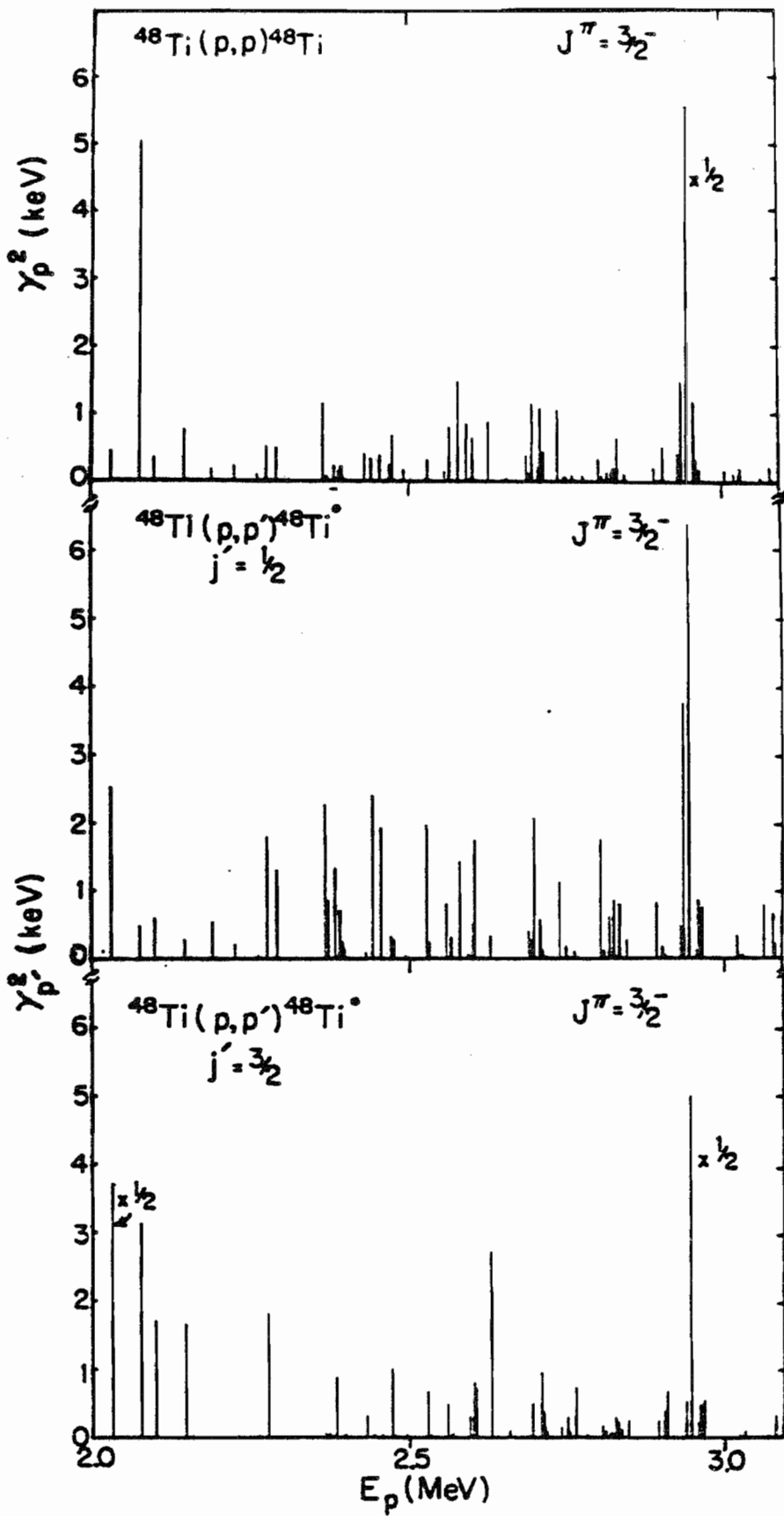


Figure 4.6 Elastic and Inelastic Reduced Widths versus  $E_p$ .

This plot depicts the elastic reduced widths and the inelastic reduced widths in  $j=1/2$  and  $j=3/2$  channels in the total angular momentum representation.



## Chapter 5

### WIDTH DISTRIBUTIONS

#### 5.1 General Theoretical Background

In highly excited quantum mechanical systems with the number of interacting particles of order 100, dynamical properties are in practice impossible to predict from first principles. For the atomic nucleus even the validity of the standard methods (non-relativistic quantum mechanics) are suspect. Similarities in the spectra of Hamiltonians of different highly excited systems have led to the description of these spectra in terms of fluctuations about average values. Such descriptions in terms of fluctuations have permitted the distribution functions to assume a "universal" quality. Familiar examples of such distribution functions for describing complex systems are the well known Wigner (1956) spacing distribution and the Porter-Thomas (1956) width distribution.

One's ignorance of a complex system can be precisely

defined by a probability distribution for the matrix elements of the Hamiltonian. By specifying the Hamiltonian's symmetries, it is possible to obtain both the Porter-Thomas and the Wigner distributions. These distributions are not unique for all possible symmetries. The program of determining the distributions of spectral quantities has become known as the study of the "statistical theories of spectral fluctuations". There is, of course, nothing "statistical" about the measurement of a resonance spacing or width, just as there is nothing statistical about the measurement of pressure in a macroscopic quantity of gas. The "statistical" nature of both problems is embodied in the manner in which one's ignorance is specified. In the nuclear problem the model uses ensembles of Hamiltonians to simulate fluctuations of spectral quantities.

If a quantum mechanical Hamiltonian is represented as a matrix, examination of the behavior of the Hamiltonian under time reversal and rotation becomes the study of the different groups of matrix similarity transformations which leave the Hamiltonian invariant. In discussions of the properties of spacing and width distributions, the dimension of the matrices normally employed is finite. Nuclear Hamiltonian matrices are in general infinite and the finite dimensional matrices conventionally adopted for the study of fluctuations must, therefore, produce dimensionally



independent results.

The classification of the groups of matrix similarity transformations which leave Hamiltonian matrices invariant was given by Dyson(1962). If a Hamiltonian matrix is invariant with respect to time reversal and rotation, it is a real symmetric matrix and is unchanged by a similarity transformation by a member of the orthogonal group. Similarity transformations by a member of the unitary group leave invariant complex Hamiltonians which may or may not possess rotational symmetry and which have no time reversal symmetry. The orthogonal group also leaves invariant Hamiltonians of systems with integral spin which have time reversal symmetry but no rotational symmetry. Similarity transformations by elements of the symplectic group leave invariant real quaternion matrix Hamiltonians of systems with half-integral spin which have time reversal symmetry but no rotational symmetry.

For the study of compound nuclear resonances, the orthogonal group and its associated real symmetric Hamiltonian matrices is the appropriate choice. The requirement that all the resonances be of the same spin and parity simplifies the problem by eliminating troublesome degeneracies. The fluctuations in spacing can be determined once the joint probability distribution for the elements of the Hamiltonian matrix

$$P(H) = P(H_{11}, H_{22}, \dots, H_{N,N}, H_{12}, H_{13}, \dots, H_{N-1,N}) \quad (5.1.1)$$

is found. The probability that Hamiltonian  $H$  has elements  $H_{11}$  at  $H_{11}$  in interval  $dH_{11}$ ,  $H_{22}$  at  $H_{22}$  in interval  $dH_{22}$ , etc. is

$$dP = P(H) dH \quad (5.1.2)$$

where

$$dH = 2^{N(N-1)/4} dH_{11} dH_{22} dH_{33} \dots dH_{NN} dH_{12} dH_{13} \dots dH_{N-1,N}$$

The actual form which the function (5.1.1) may take is limited by the symmetries of the Hamiltonian.

The joint probability,  $dP$ , may be brought to a more useful form if the volume element  $dH$  can be made diagonal. This program has been carried out by Porter and Rosenzweig (1960). Using the Schrodinger equation in matrix form  $H$  may be obtained from a diagonal matrix  $H_D$ ,

$$H = O H_D \tilde{O}.$$

$O$  contains the eigenvectors of  $H$  and  $H_D$  the eigenvalues. Porter (1965) has examined the simple case of an orthogonal transformation of the form

$$O = \begin{pmatrix} \cos \alpha & \sin \alpha & 0 & 0 & \dots \\ -\sin \alpha & \cos \alpha & 0 & 0 & \dots \\ 0 & 0 & 1 & & \\ 0 & \dots & & 1 & \\ & & & & \dots \end{pmatrix} \quad (5.1.3)$$

With the transformation given in equation (5.1.3), the

hypotheses used to determine the joint probability distribution are

$$\frac{dP}{d\alpha} = 0 \quad (5.1.4)$$

and

$$P(H) = P_{11}(H_{11}) P_{22}(H_{22}) \cdots P_{NN}(H_{NN}) P_{12}(H_{12}) P_{13}(H_{13}) \cdots P_{N-1,N}(H_{N-1,N}) \quad (5.1.5)$$

Equation (5.1.4) requires that the distribution  $P$  be an invariant function of  $H$  and equation (5.1.5) is assumed for simplicity. Much theoretical work has been performed assuming these hypotheses, but the lack of good experimental data has limited progress in this area. The first experimental work to accurately test the spacing distributions was performed by Liou et al. (1972), using neutron resonances. Wilson (1975) made similar tests using spacing data obtained from proton elastic scattering.

In this dissertation only the distribution of resonance widths is studied. As each Hamiltonian matrix  $H$  in an ensemble has matrix elements determined by some distribution function, so must the matrix elements of  $O$  that diagonalize  $H$  have a distribution function specifying its elements. The postulates of invariance and independence when applied to  $O$  give equations which are vector analogs to the matrix equations for  $H$ . The eigenvectors are conveniently discussed in the rotation of P-matrix theory as reviewed by Lane and Thomas (1958). The eigenvectors  $\chi_\lambda$  are

represented by the channel surface overlap of  $\chi_\lambda$  with the various channel functions  $\varphi_c$ . This overlap defines the reduced width amplitude,

$$\gamma_{\lambda c} = \left( \frac{\hbar^2}{2m_c a_c} \right) \int \chi_\lambda \varphi_c dS \quad (5.1.6)$$

where  $m_c$  is the channel mass,  $a_c$  is the channel radius, and  $dS$  is the surface element specified by the choice of channel  $c$ .

The hypothesis of independence is

$$P(\{\gamma_{\lambda c}\}_{\lambda c}) = \prod_\lambda f_\lambda(\{\gamma_{\lambda c}\}_c) \quad (5.1.7)$$

where  $\{\gamma_{\lambda c}\}_{\lambda c}$  is the collection of  $\gamma_{\lambda c}$  over levels and channels and  $\{\gamma_{\lambda c}\}_c$  is the collection of  $\gamma_{\lambda c}$  over channels.  $f_\lambda$  is a function only of the partial reduced width amplitudes associated with level  $\lambda$ . The invariance condition is

$$P(\{\gamma_{\lambda c}\}_{\lambda c}) = P(\{\gamma'_{\lambda c}\}_{\lambda c}), \quad (5.1.8)$$

where  $\{\gamma_{\lambda c}\}_{\lambda c}$  is related to  $\{\gamma'_{\lambda c}\}_{\lambda c}$  by the relation

$$\gamma = O\gamma' \quad (5.1.9)$$

The vectors  $\gamma$  and  $\gamma'$  are formed from the elements of  $\{\gamma_{\lambda c}\}_{\lambda c}$  and  $\{\gamma'_{\lambda c}\}_{\lambda c}$ , respectively. Following the development of Krieger and Porter (1963) and integrating out all but two levels in the distribution function  $P$ , the independence condition becomes

$$P(\{\delta_{1c}\}\{\delta_{2c}\}) = f_1(\{\delta_{1c}\}) f_2(\{\delta_{2c}\}) \quad (5.1.10)$$

and the invariance condition is

$$P(\{\delta_{1c}\}\{\delta_{2c}\}) = P(\{\delta'_{1c}\}\{\delta'_{2c}\}) \quad (5.1.11)$$

with

$$\begin{pmatrix} \{\delta_{1c}\} \\ \{\delta_{2c}\} \end{pmatrix} = O \begin{pmatrix} \{\delta'_{1c}\} \\ \{\delta'_{2c}\} \end{pmatrix}. \quad (5.1.12)$$

where  $O$  has the form of the orthogonal transformation matrix in equation (5.1.3). The equation (5.1.12) is symbolically expressed as

$$\gamma = O\gamma' \quad (5.1.13)$$

In the two dimensional case under consideration  $O$  can be written

$$O = e^{i\alpha V_y} \quad (5.1.14)$$

where  $V_y$  is the Pauli spin matrix

$$\begin{pmatrix} 0 & -i \\ i & 0 \end{pmatrix}$$

Letting  $g_\lambda = \ln f_\lambda$ , the invariance condition (5.1.11) becomes

$$\sum_{\lambda=1}^2 \sum_c \left( \frac{\partial g_\lambda}{\partial \delta_{\lambda c}} \frac{d\delta_{\lambda c}}{d\alpha} \right) = 0 \quad (5.1.15)$$

The derivative  $d\delta_{\lambda c}/d\alpha$  can be determined from equations (5.1.13) and (5.1.14)

$$\frac{d\delta_{\lambda c}}{d\alpha} = \frac{dO}{d\alpha} \delta'_{\lambda c}$$

$$= \frac{dO}{d\alpha} \tilde{O} O' \delta_{\lambda c}$$

$$\frac{d\delta_{\lambda c}}{d\alpha} = \frac{dO}{d\alpha} \tilde{O} \delta_{\lambda c} \quad (5.1.16)$$

Since

$$\frac{dO}{d\alpha} = i\sigma_y O$$

and

$$\frac{dO}{d\alpha} \tilde{O} = i\sigma_y = \begin{pmatrix} 0 & 1 \\ -1 & 0 \end{pmatrix} \quad (5.1.17)$$

then

$$\frac{d\delta_{\lambda c}}{d\alpha} = \delta_{\lambda c} \quad (5.1.18)$$

and

$$\frac{d\delta_{\lambda c}}{d\alpha} = -\delta_{\lambda c} \quad (5.1.19)$$

Substituting (5.1.18) and (5.1.19) into (5.1.15)

$$\sum_c \left( \frac{\partial g_\lambda}{\partial \delta_{\lambda c}} \delta_{\lambda c} - \frac{\partial g_\lambda}{\partial \delta_{\lambda c}} \delta_{\lambda c} \right) = 0 \quad (5.1.20)$$

For equation (5.1.20) to be true the quantity  $\frac{\partial g_\lambda}{\partial \delta_{\lambda c}}$  must be a linear function of all  $\delta_{\lambda c}$  for a fixed  $\lambda$ , i.e.

$$\frac{\partial g_\lambda}{\partial \delta_{\lambda c}} = \sum_{c'} M_{cc'}^{(\lambda)} \delta_{\lambda c'} \quad (5.1.21)$$

As a substitution of (5.1.21) into (5.1.20) shows, the  $M_{cc'}^{(\lambda)}$  must not depend upon  $\lambda$ . Therefore, solving for  $g_\lambda$

$$g_{\lambda} = -\frac{1}{2} \sum_c M_{cc} \gamma_{\lambda c}^2 - \sum_{c' < c} M_{cc'} \gamma_{\lambda c} \gamma_{\lambda c'} - a_{\lambda} \quad (5.1.22)$$

which can be written as a convenient scalar product

$$g_{\lambda} = -\frac{1}{2} (\gamma_{\lambda}, M \gamma_{\lambda}) - a_{\lambda} \quad (5.1.23)$$

The constant  $a_{\lambda}$  is only for normalization and may be dropped.  $M$  is defined in the equations above as a real symmetric positive definite channel matrix. Therefore, the probability distribution for two levels is

$$P(\{\gamma_{\lambda c}\} \{\gamma_{\lambda c'}\}) \propto \prod_{\lambda=1}^2 \text{EXP}[-\frac{1}{2} (\gamma_{\lambda}, M \gamma_{\lambda})] \quad (5.1.24)$$

For the general case of  $N$  levels and  $m$  channels the normalized distribution function is

$$P(\{\gamma_{\lambda c}\}_{\lambda c}) = \prod_{\lambda=1}^N \frac{|M|^{N/2}}{(2\pi)^{Nm/2}} \text{EXP}[-\frac{1}{2} (\gamma_{\lambda}, M \gamma_{\lambda})] \quad (5.1.25)$$

If all but one channel is integrated out of equation (5.1.26), then

$$P(\gamma_{\lambda}) = \prod_{\lambda=1}^N \frac{\text{EXP}[-\frac{1}{2} \gamma_{\lambda c}^2 / \overline{\gamma_{\lambda c}^2}]}{(2\pi \overline{\gamma_{\lambda c}^2})^{1/2}} \quad (5.1.26)$$

With the levels viewed as the sample space, the one channel reduced width distribution is

$$P(\gamma^2) = \frac{\text{EXP}(-\gamma^2 / 2 \overline{\gamma^2})}{(2\pi \overline{\gamma^2} \gamma^2)^{1/2}} \quad (5.1.27)$$

This is the equation first proposed by Porter and Thomas (1956) for the most probable distribution for width fluctuations. For more than one channel the distribution

for reduced width amplitudes becomes

$$P(\gamma) = \frac{|M|^{1/2}}{(2\pi)^{m/2}} \text{EXP} \left[ -\frac{1}{2} (\gamma, M\gamma) \right] \quad (5.1.28)$$

Equation (5.1.26) identifies the elements of the channel matrix  $M$ . The channel covariance matrix is defined as

$$\Sigma \equiv \overline{\gamma_\lambda \times \gamma_\lambda} \quad (5.1.29)$$

where the bar is the level average of the dyadic  $\gamma_\lambda \times \gamma_\lambda$ . If  $M$  is defined as the inverse of  $\Sigma$ , the correct form for equation (5.1.25) is obtained in the one channel case. For two channels the reduced width amplitude distribution function is

$$P(\gamma_1, \gamma_2) = \frac{1}{2\pi (\overline{\gamma_1^2 \gamma_2^2} - \overline{\gamma_1 \gamma_2}^2)^{1/2}} \text{EXP} \left[ -\frac{1}{2} M_{11} \gamma_1^2 - \frac{1}{2} M_{22} \gamma_2^2 - M_{12} \gamma_1 \gamma_2 \right] \quad (5.1.30)$$

where

$$\begin{aligned} M_{11} &= \overline{\gamma_2^2} / (\overline{\gamma_1^2 \gamma_2^2} - \overline{\gamma_1 \gamma_2}^2) \\ M_{22} &= \overline{\gamma_1^2} / (\overline{\gamma_1^2 \gamma_2^2} - \overline{\gamma_1 \gamma_2}^2) \\ M_{12} &= -\overline{\gamma_1 \gamma_2} / (\overline{\gamma_1^2 \gamma_2^2} - \overline{\gamma_1 \gamma_2}^2) \end{aligned}$$

The off-diagonal elements of  $M$  are intimately related to the linear correlation between reduced width amplitudes between channels.

The linear correlation coefficient between two sets of data  $\{x_i\}$  and  $\{y_i\}$  with set averages  $\bar{x}$  and  $\bar{y}$  is



$$r(x, y) = \frac{\sum_{i=1}^N (x_i - \bar{x})(y_i - \bar{y})}{\left[ \sum_{i=1}^N (x_i - \bar{x})^2 (y_i - \bar{y})^2 \right]^{1/2}} \quad (5.1.31)$$

If the distributions of  $\{x_i\}$  and  $\{y_i\}$  are symmetric about zero, then

$$r(x, y) = \overline{xy} / (\overline{x^2} \overline{y^2})^{1/2} \quad (5.1.32)$$

Letting  $x_i = \gamma_{1c}$  and  $y_i = \gamma_{2c}$ , and  $M_{12}$  be small,

$$r = \frac{\overline{\gamma_1 \gamma_2}}{(\overline{\gamma_1^2} \overline{\gamma_2^2})^{1/2}} = \frac{\sum_{12}}{[\sum_{11} \sum_{22}]^{1/2}} = \frac{M_{12}}{[M_{11} M_{22}]^{1/2}} \quad (5.1.33)$$

Under these restrictions  $M_{12}$  as a function of  $r$  is

$$M_{12} \cong \frac{r}{(r^2 - 1)} \frac{1}{(\overline{\gamma_1^2} \overline{\gamma_2^2})^{1/2}} \quad (5.1.34)$$

The assumption that the distribution for  $\gamma_1$  and  $\gamma_2$  is symmetric about zero is valid only for  $M_{12} = 0$ . However the expression (5.1.34) is a good approximation for small correlations, i.e.,

$$M_{12} \cong r / (\overline{\gamma_1^2} \overline{\gamma_2^2})^{1/2} \quad (5.1.35)$$

From the definition of the channel covariance matrix (equation (5.1.29)) and the result for the linear correlation coefficient (equation (5.1.33)), it is evident that the linear correlation coefficient is proportional to the off-diagonal covariance matrix element

$$r \propto \sum_{i_2}$$

The extreme statistical hypothesis assumes no correlation between channels. Lane (1971) has shown that a doorway state common to two channels may be the cause of a linear correlation between the partial reduced widths of the two channels. The reduced width correlation can be written as

$$r(\gamma_1^2, \gamma_2^2) = \frac{\sum_i \gamma_{i1}^2 \gamma_{i2}^2}{N} - \frac{\sum_i \gamma_{i1}^2}{N} \frac{\sum_i \gamma_{i2}^2}{N} \left[ \left( \frac{\sum_i \gamma_{i1}^4}{N} - \left( \frac{\sum_i \gamma_{i1}^2}{N} \right)^2 \right) \left( \frac{\sum_i \gamma_{i2}^4}{N} - \left( \frac{\sum_i \gamma_{i2}^2}{N} \right)^2 \right) \right]^{1/2} \quad (5.1.36)$$

or

$$r_{\gamma_1^2, \gamma_2^2} = \frac{\overline{\gamma_2^2 \gamma_1^2} - \overline{\gamma_1^2} \overline{\gamma_2^2}}{[(\overline{\gamma_1^4} - \overline{\gamma_1^2}^2)(\overline{\gamma_2^4} - \overline{\gamma_2^2}^2)]^{1/2}} \quad (5.1.37)$$

It can be shown from equations (5.1.37) and (5.1.32) that

$$r_{\gamma_1^2, \gamma_2^2} = (\gamma_{\gamma_1, \gamma_2})^2 \quad (5.1.38)$$

which implies that only positive width correlations are possible.

The definition of  $\sum$  is ambiguous since the size of the averaging interval is not exactly specified. If  $\sum_{i_2}$  deviates from zero, the question arises as to the significance of this deviation, since a change in the averaging interval will modify its value. This problem is alleviated if instead of  $\sum_{i_2}$ , one considers the cumulative sum of  $\gamma_{\lambda_1} \gamma_{\lambda_2}$  versus resonance energy. The requirement that  $\sum_{i_2}$  is zero is equivalent to the sum of  $\delta_{\lambda_1} \delta_{\lambda_2}$  versus energy having zero

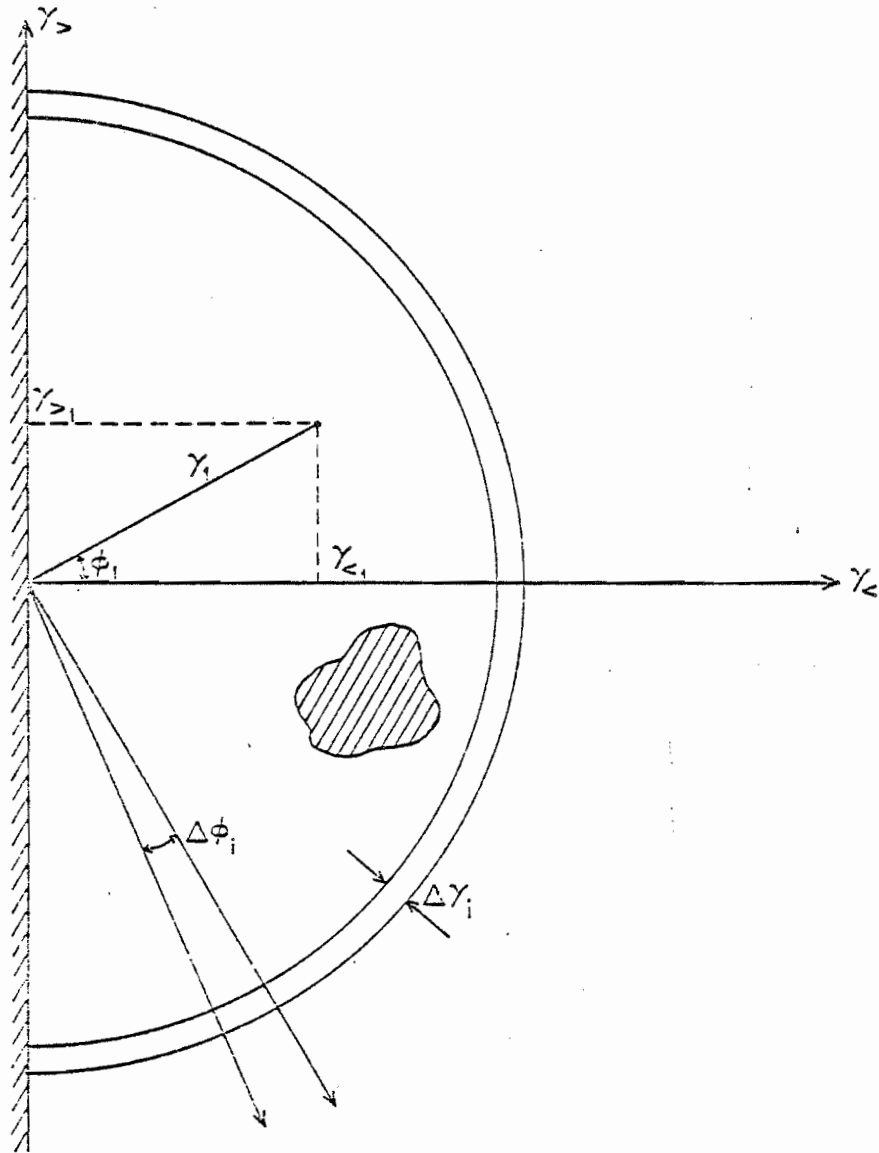
slope. In regions of non-zero slope the linear correlation coefficient between the set  $\{\delta_{\lambda_1}\}$  and the set  $\{\delta_{\lambda_2}\}$  can be calculated. The significance of such linear correlation coefficients may be determined using Monte-Carlo techniques or by a distribution free technique described by Baudinet-Rcbinet (1974).

## 5.2 Probability Distributions for Mixing Ratios

The probability distribution function for reduced width amplitudes in two channels, equation (5.1.28), derived in section 5.1 is not very useful in its present form. The most directly measured quantity in this experiment is  $\delta$ , the mixing ratio of the reduced width amplitudes of the two inelastic decay channels. The mixing ratio is more conveniently parameterized in terms of  $\varphi = \tan^{-1} \delta$ . Equation (5.1.28) can be converted into a distribution function for both  $\delta$  and  $\varphi$ .

The mixing may be described in a geometrical manner which more readily shows the relationship between the two parameterizations of the data. Consider the diagram in Figure 5.1 which shows the relationship of the mixing parameters and the reduced width amplitudes.  $\gamma_{<}$  is the reduced width amplitude in the channel labeled with the smaller quantum number and  $\gamma_{>}$  is the amplitude from the channel labeled with the larger quantum number. There is a

Figure 5.1 Geometrical Relationships Between Reduced Width  
Amplitudes and Mixing Parameters.



restriction to the half plane ( $\gamma_2 > 0$ ) since only the relative phase of the amplitudes is measured. The allocation of positive and negative values to  $\gamma_2$  is arbitrary. In this diagram the probability distribution is a scalar plotted out of the plane of the page.

A probability distribution for  $\varphi$  (or  $\delta$ ) is a projection of  $\varphi$  (or  $\delta$ ) from the distribution function (5.1.29) with the remaining variable integrated over its entire range. In the distribution for  $\varphi$  (or  $\delta$ ) the information regarding the total width of the resonance is integrated out. This corresponds to summing the density of resonances for each element,  $\Delta\varphi_i$ , removing all strength information. In the distribution for the total reduced width amplitude, the mixing information is integrated out. This corresponds to summing the density of resonances for each element  $\Delta\delta_i$ . The distribution for  $\delta$  may be written

$$P(z) = C \int_0^x \int_0^y \delta(z - y/x) \exp\left[-\frac{x^2}{2} - \frac{y^2}{2} - M'xy\right] dx dy \quad (5.2.1)$$

where  $Z$  is the reduced mixing ratio defined as

$$Z = y/x \quad (5.2.2)$$

where

$$y = \delta_1 \left\{ \frac{\delta_2^2}{(\delta_1^2 \delta_2^2 - \delta_1 \delta_2^2)^{1/2}} \right\} \quad \delta_1 \equiv \delta_2 \quad (5.2.3)$$

$$x = \delta_2 \left\{ \frac{\delta_1^2}{(\delta_1^2 \delta_2^2 - \delta_1 \delta_2^2)^{1/2}} \right\} \quad \delta_2 \equiv \delta_2 \quad (5.2.4)$$

and

$$M' = \frac{\overline{\delta_1 \delta_2}}{(\overline{\delta_1^2} \overline{\delta_2^2})^{1/2}} \quad (5.2.5)$$

$$C = \frac{1}{\pi} \frac{(\overline{\delta_1^2} \overline{\delta_2^2} - \overline{\delta_1 \delta_2}^2)^{1/2}}{(\overline{\delta_1^2} \overline{\delta_2^2})^{1/2}} \quad (5.2.6)$$

These reduced variables remove the average properties from the distribution function, and emphasize the fluctuations. If  $R$  is defined as

$$R^2 = x^2 + y^2 \quad (5.2.7)$$

the distribution function becomes

$$P(z) = C \int_{-\pi/2}^{\pi/2} d\varphi' \int_0^R dR d\varphi' R \delta(z - \tan \varphi') \exp\left[-\frac{R^2}{2}(1 - M' \sin 2\varphi')\right] \quad (5.2.8)$$

where

$$\varphi' = \tan^{-1} y/x$$

After integration over the variable  $R$

$$P(z) = C \int_{-\pi/2}^{\pi/2} \delta(z - \tan \varphi') \frac{1}{1 - M' \sin 2\varphi'} d\varphi' \quad (5.2.9)$$

From this equation either the probability density function for  $\varphi$  or  $Z$  may be determined to be

$$\frac{dP(\varphi)}{d\varphi} = \frac{C}{1 - M \sin 2\varphi'} \quad (5.2.10)$$

or

$$\frac{dP(z)}{dz} = \frac{c}{1+z^2-2M'z} \quad (5.7.11)$$

Both equations (5.2.10) and (5.2.11) take a particularly simple form when the correlation between the channels is zero. This extreme statistical model ( $M'=0$ ) produces a Cauchy distribution for  $Z$ , and a uniform distribution for  $\varphi'$ . The reason for defining the dependent variable in the distribution functions is evident in Figure 5.2 and Figure 5.3. The values for the abscissa on these plots are not the reduced variables but the originally defined  $\varphi$  and  $\delta$ . The two distributions are plotted for various values of  $(\overline{\delta^2}/\overline{\varphi^2})^{1/2}$ . The plotted distributions labeled with the value of  $(\overline{\delta^2}/\overline{\varphi^2})^{1/2}=1.0$  are the same as those obtained using the reduced parameters  $\varphi'$  or  $Z$ .

The distribution function to use for the easiest visual inspection of the data is equation (5.2.10). If the channel matrix  $M$  is diagonal, the distribution of  $\varphi'$  should be uniform. However, correlations between channels ( $M_{12} \neq 0$ ) cause some  $\sin 2\varphi'$  modulation of the uniform distribution. Other possibilities are shown in Figure 5.4. If there is a special state in a statistical background it should cause an anomalous peak in the distribution of  $\varphi'$ , since a special state will have one definite decay pattern. If an anomalously high density of states with a certain decay pattern (for example the hatched area in Figure 5.1) existed, the distribution of  $\varphi'$  would show some peak like



Figure 5.2 Distribution Function for Mixing Ratios. The number near each curve is the value of  $\left(\frac{\gamma^2}{\delta^2}\right)^{1/2}$  used in the plot of the function.

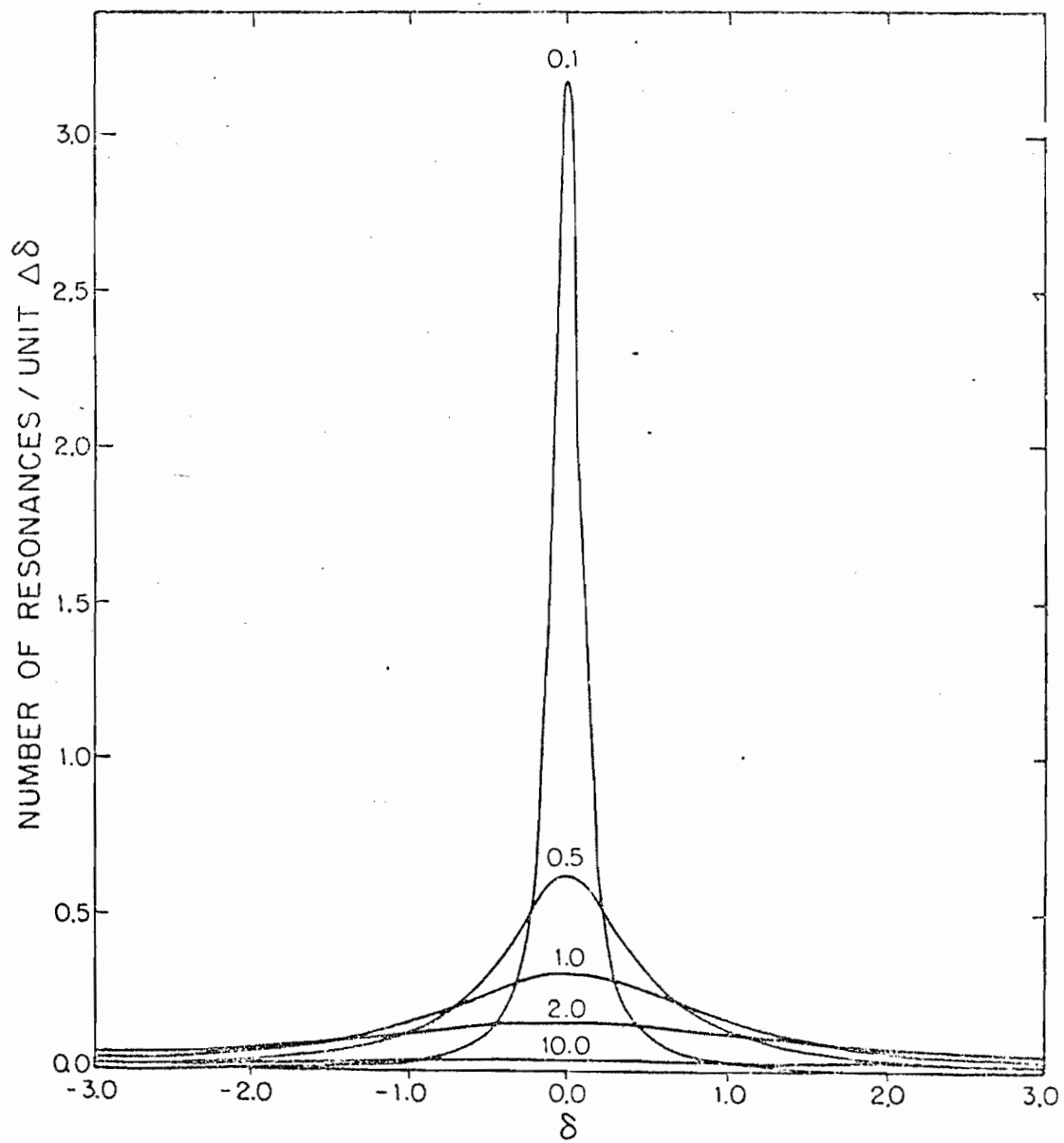


Figure 5.3 Distribution Function for  $\varphi$ . The number near each curve is the value of  $\left\{ \frac{\delta^2}{\delta_2^2} \right\}$  used in the plot of the function.

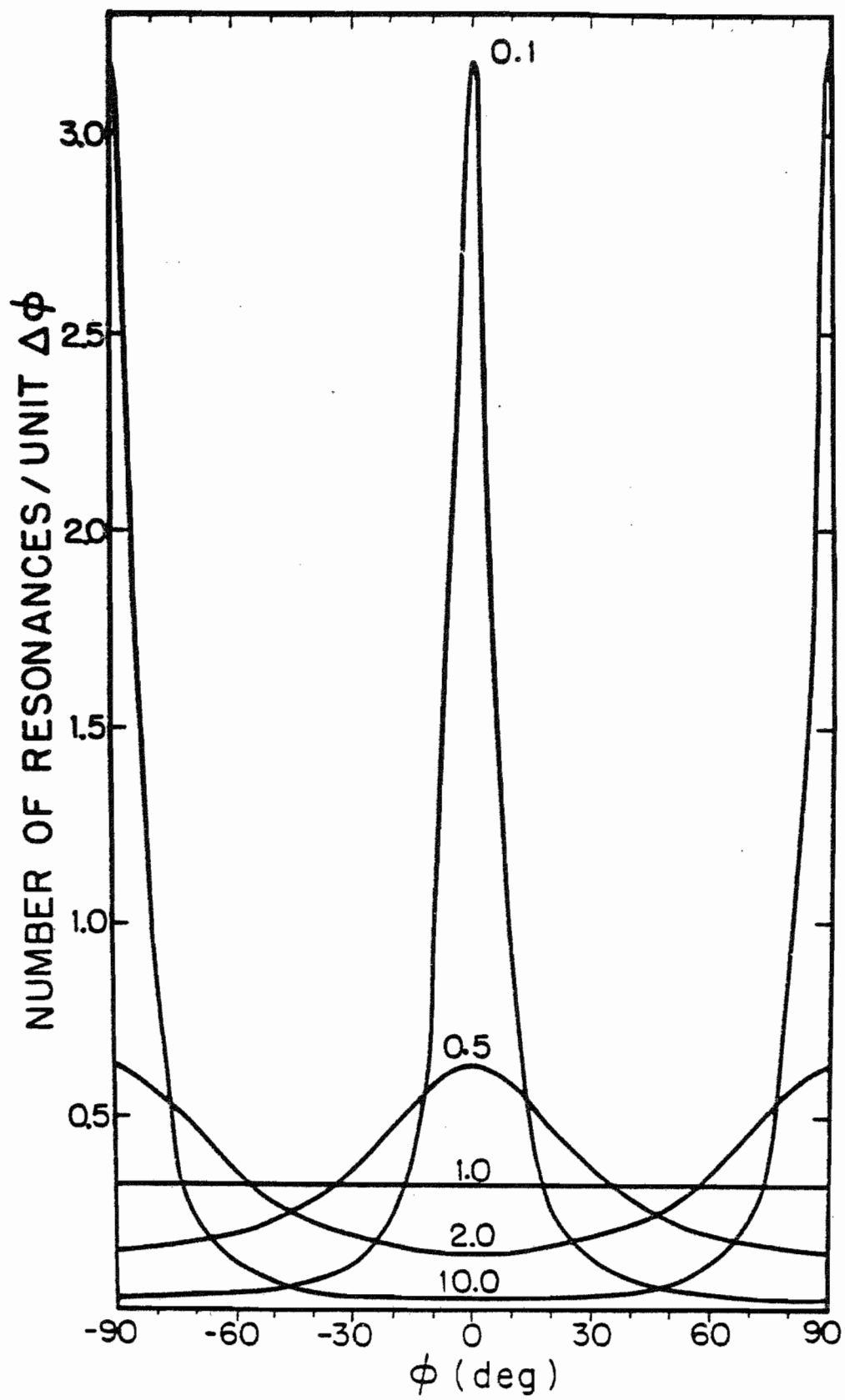
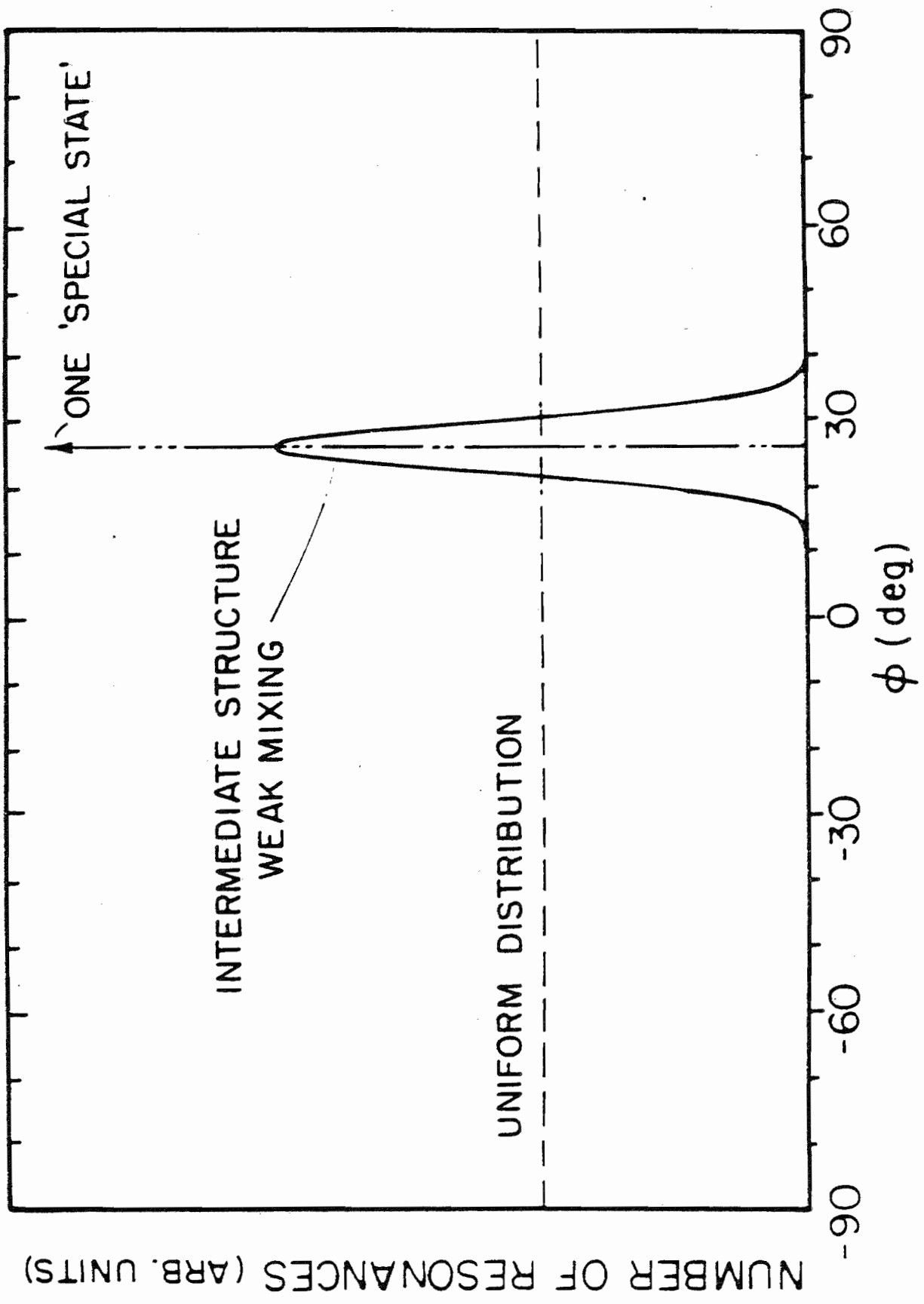


Figure 5.4 Effects of Intermediate Structure on the  
Distribution of  $\varphi$ .



structure. The distribution of  $R = (x^2 + y^2)^{1/2}$  might also exhibit anomalous behavior. However, if the probability density was small in a region near the same value of  $R$  but at a different  $\phi$  as an excess density, then the distribution of  $R$  would be little affected. The power of the method of measuring mixing ratios is the ability to look at both strength fluctuations and decay pattern fluctuations.

### 5.3 Inelastic Decay of Isobaric Analogue States

The inelastic decay from five analogue states was measured in this experiment. In the compound system  $^{57}\text{Co}$  there was one  $1/2^-$  and two  $3/2^-$  analogue states, each with only one fragment. In the  $^{99}\text{V}$  compound system two fragmented analogue states were studied. The  $1/2^-$  analogue state had only weak inelastic decay. The inelastic decay mixing ratios of resonances in the region around the  $3/2^-$  state indicate the previously identified fragmented analogue state has only one fragment.

The mixing ratios of inelastic decay amplitudes for fragments of an analogue should exhibit similar decay patterns. The simple arguments presented in Section 5.2 for the parameter  $\phi'$  being the same for fragments of a "special state" have been made precise by Lane (1978) for the case of analogue states. Lane discusses the phenomenon in terms of a generalized strength function defined as

$$S_{cc'} = A_{cc'} + \frac{1}{\pi} \frac{B_{cc'} (\bar{E}_\lambda - E) + C_{cc'}}{(\bar{E}_\lambda - E)^2 + W_\lambda^2/4} \quad (5.3.1)$$

where  $A_{cc'}$  is the "background" strength function and  $\bar{E}_\lambda$  and  $W_\lambda$  are the energy and width of the analogue state. It can be shown that

$$(C_{cc'} + \frac{i}{2} W_\lambda B_{cc'})^2 = (C_{cc'} + \frac{i}{2} W_\lambda B_{cc'}) (C_{cc} + \frac{i}{2} W_\lambda B_{cc}) \quad (5.3.2)$$

Thus if fits to the diagonal strength function data can be obtained, then the off-diagonal strength function can be predicted. The constants in equation (5.3.1) for the diagonal case are related to the usual background strength function  $S_0$ , asymmetry  $\Delta_{\lambda c}$ , analogue spreading width  $W_0$ , and analogue reduced width  $\gamma_\lambda^2$  by

$$\begin{aligned} B_{cc} &= 2\pi S_0 \Delta_{\lambda c} \\ C_{cc} &= \gamma_\lambda^2 W_0 / 2 \\ A_{cc} &= S_0 \\ W_\lambda &= W_0 \\ \bar{E}_\lambda &= E_\lambda \end{aligned}$$

The diagonal fine structure parameters were determined for the  $3/2^-$  analcque in  $^{99}\text{V}$  using the procedure described by Bilpuch et al. (1976) with the following constraints. The elastic and total inelastic fine structure were fit and  $E_\lambda$  and  $W_0$  were fixed. The asymmetry  $\Delta$  was set to zero, since there was no obvious asymmetry in the data. The fits and the data are shown in Figure 5.5 and Figure 5.6. The fine structure of the two inelastic decay channels was fit



Figure 5.5 The Fine Structure Distribution for  $^{48}\text{Ti}(p,p)^{48}\text{Ti}$ . The fine structure distribution in the differential (lower) and integral (upper) representations is shown with the integral of the Lane strength function (smooth solid line).

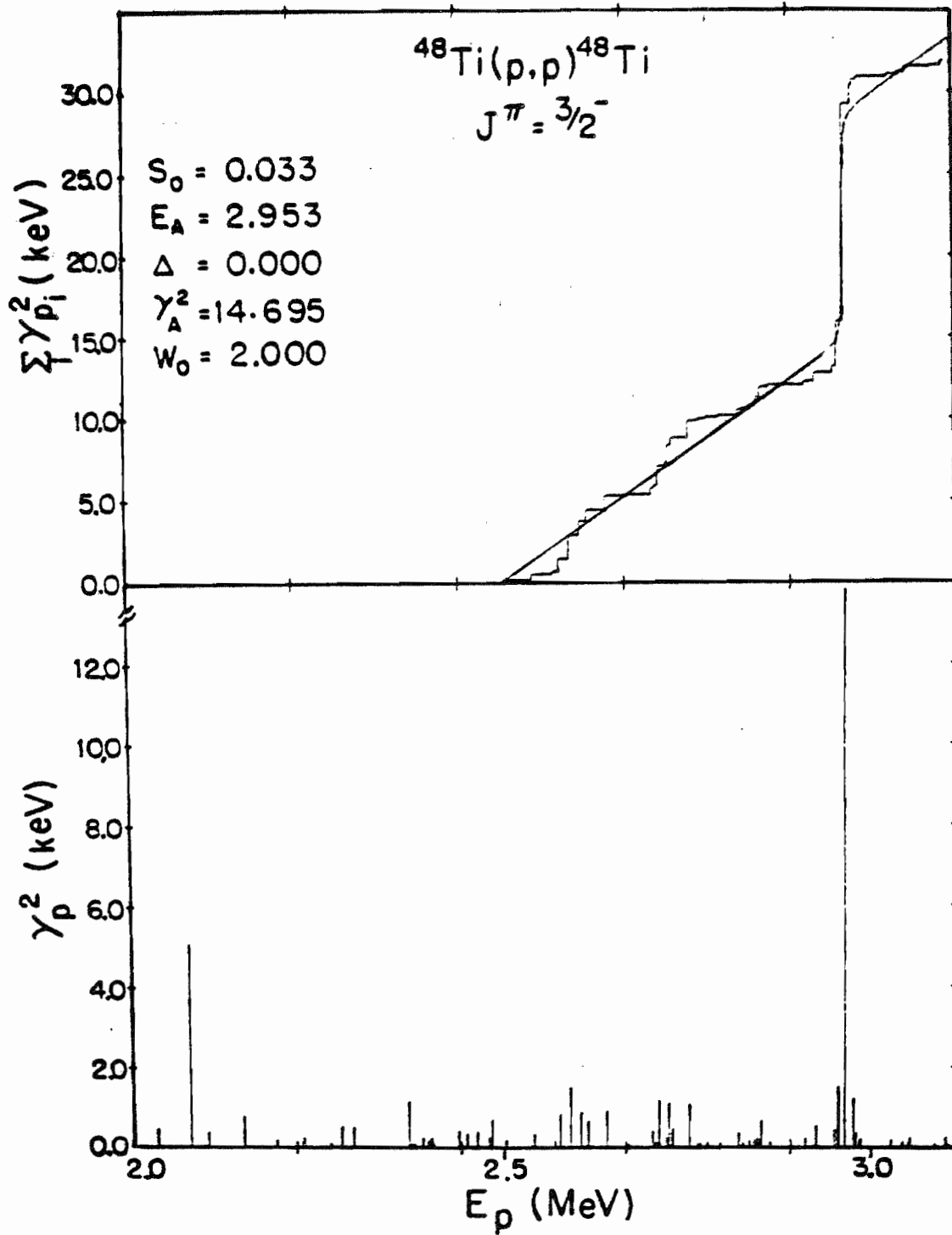
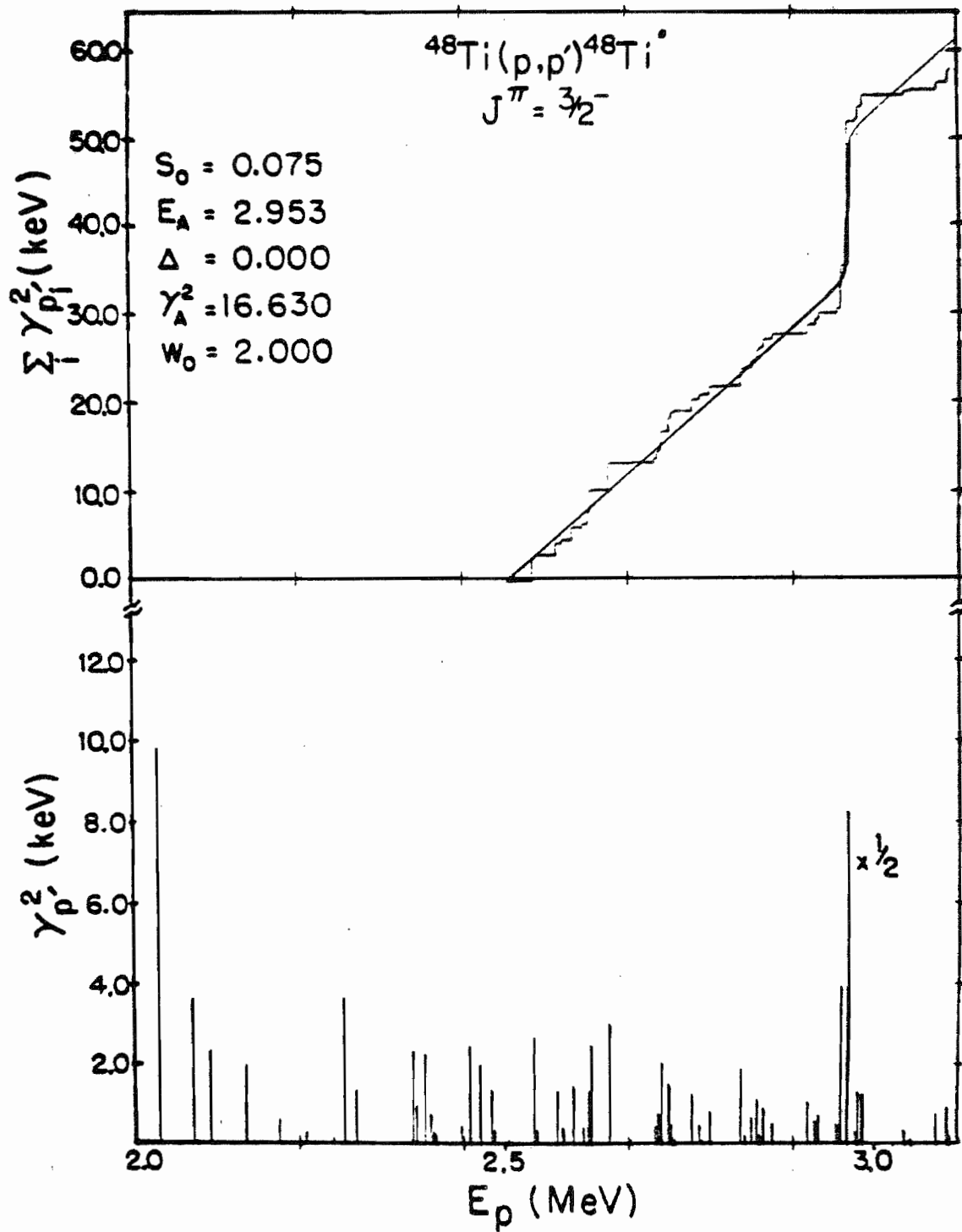


Figure 5.6 The Fine Structure Distribution for  
 $^{48}\text{Ti}(p,p')^{48}\text{Ti}$ .



separately with the constraint that  $W_0$  and  $E_A$  were the same as in the total inelastic and elastic channel fits. Also, the analogue reduced widths in each inelastic decay channel must sum to the total inelastic analogue reduced width. The fits and data for the inelastic fine structure are shown in Figure 5.7 and Figure 5.8 for the channel spin representation. The parameters determined for the inelastic channel fine structure were then combined to determine the parameters for the off-diagonal strength function.

To compare the data for the strength function with experiment the data shown in Figure 5.9 were averaged with a Lorentzian weighting function with a 20 keV width. The predicted strength function was similarly averaged. The parameters used for the off-diagonal strength function prediction are

Representation	A (MeV)	B (MeV)	C (MeV <sup>2</sup> )
Channel Spin	0	0	$2.4 \times 10^{-6}$
Total Angular Momentum	0	0	$2.1 \times 10^{-6}$

The averaged data and predictions are shown in Figure 5.10 for the channel spin representation. There is a sign ambiguity for  $S_{cc}$  due to the quadratic nature of equation (5.3.2). Both solutions given by the theory are shown in the figure. Although the agreement between experiment and theory is good, the small analogue spreading width and the

Figure 5.7 The Fine Structure Distribution for  
 $^{48}\text{Ti}(p,p')^{48}\text{Ti}$  in the  $s'=3/2$  Channel.

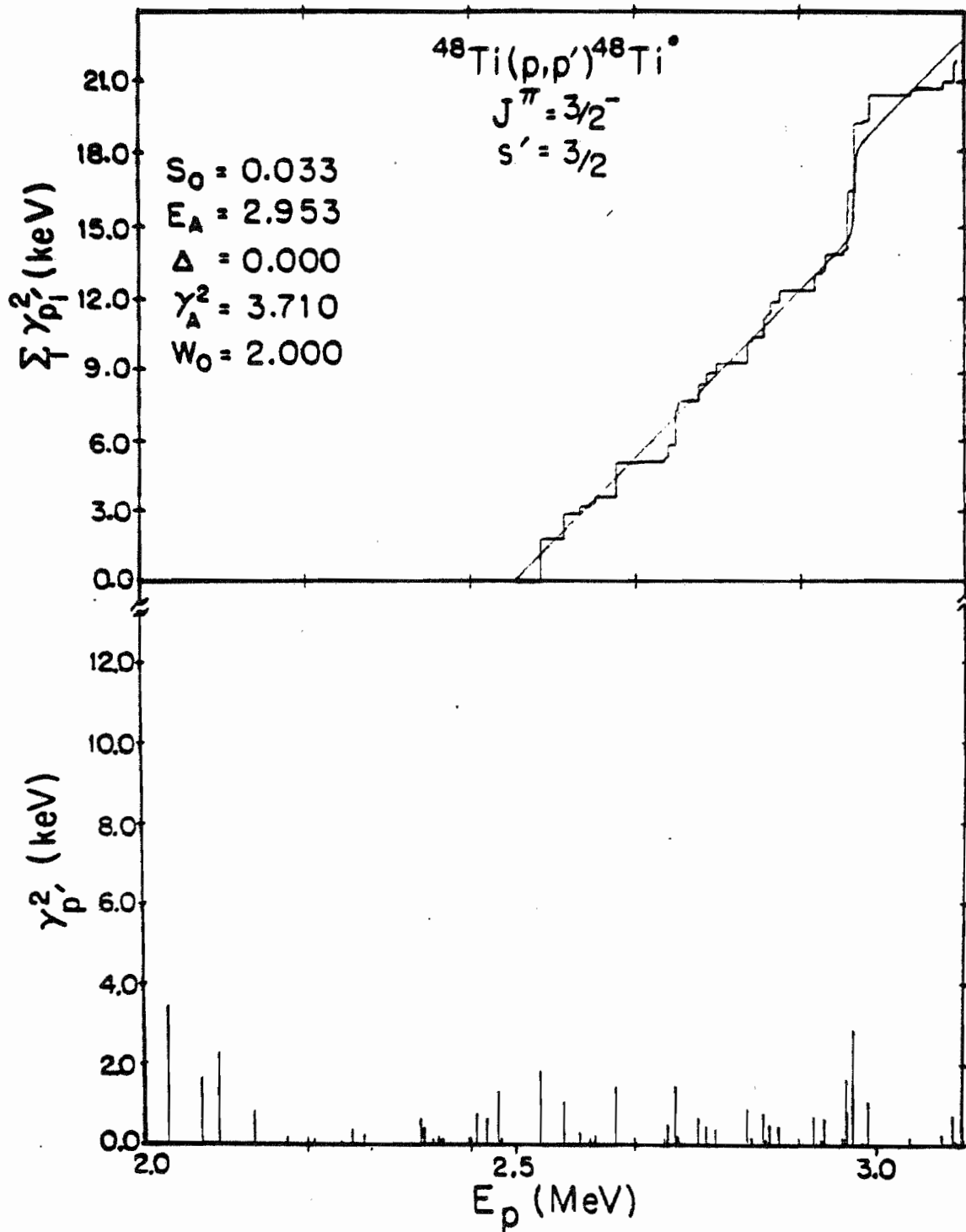


Figure 5.8 The Fine Structure Distribution for  
 $^{48}\text{Ti}(p,p')^{48}\text{Ti}$  in the  $s'=5/2$  Channel.



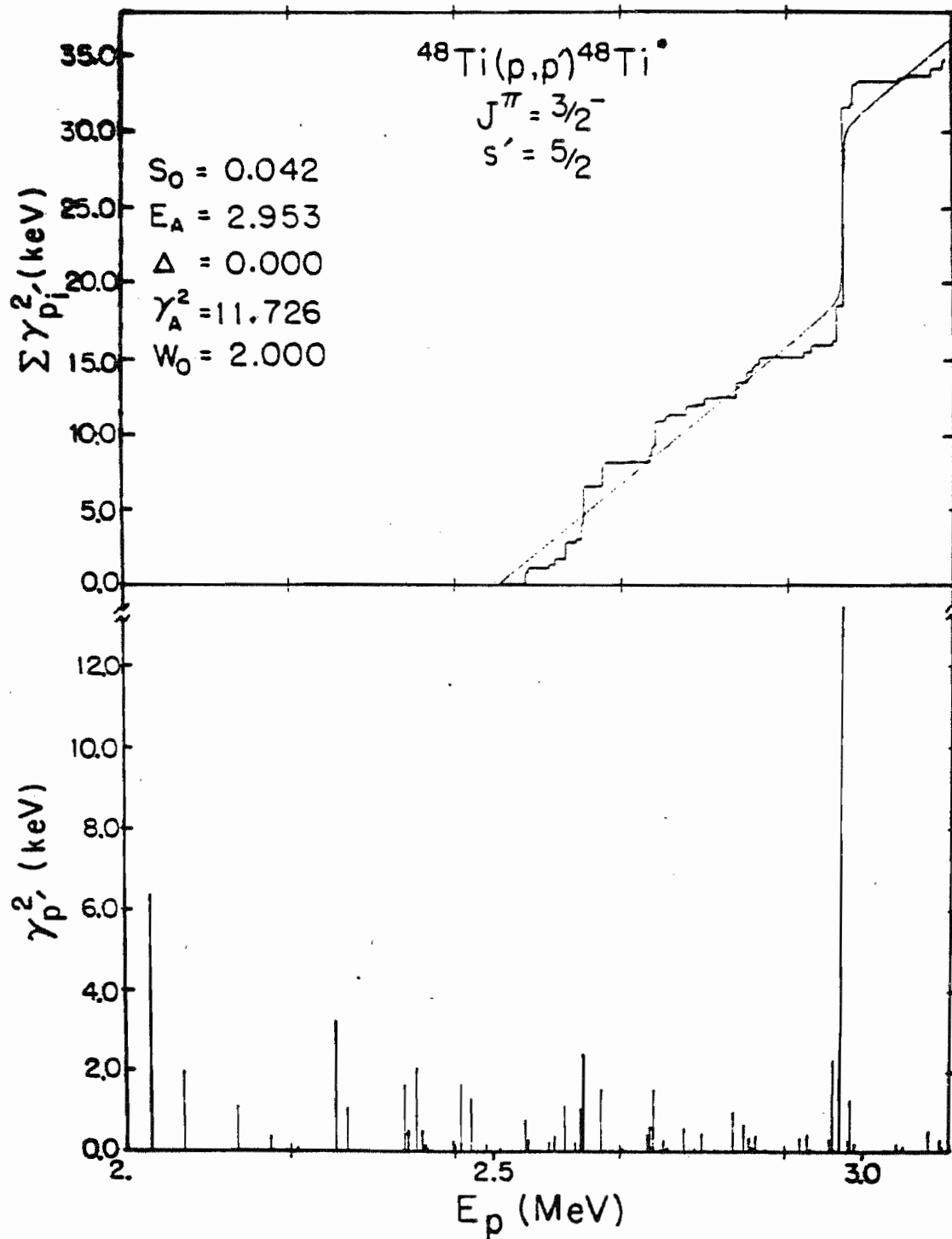


Figure 5.9  $\delta_{S=3/2}$   $\delta_{S=5/2}$  versus Proton Bombarding Energy.

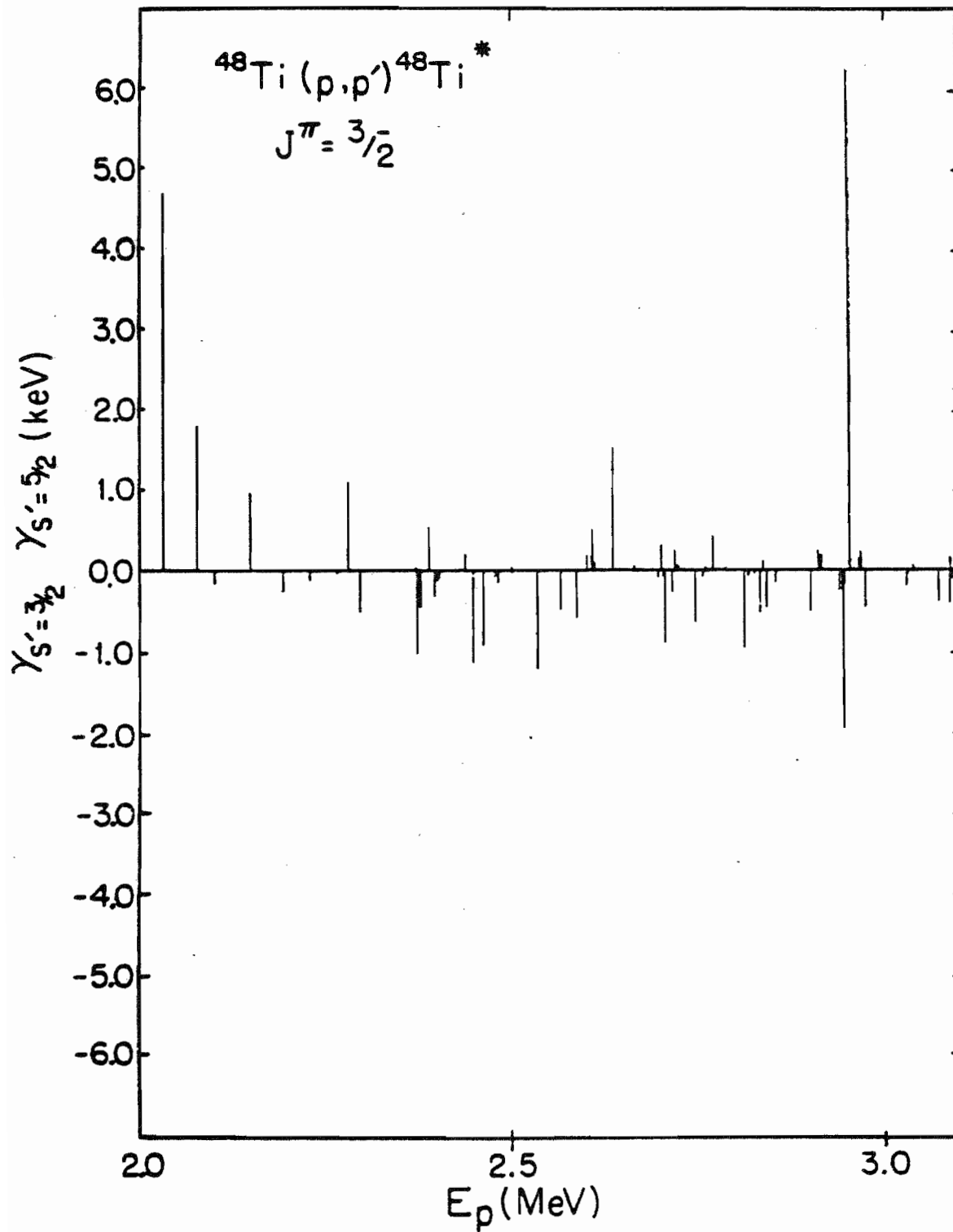
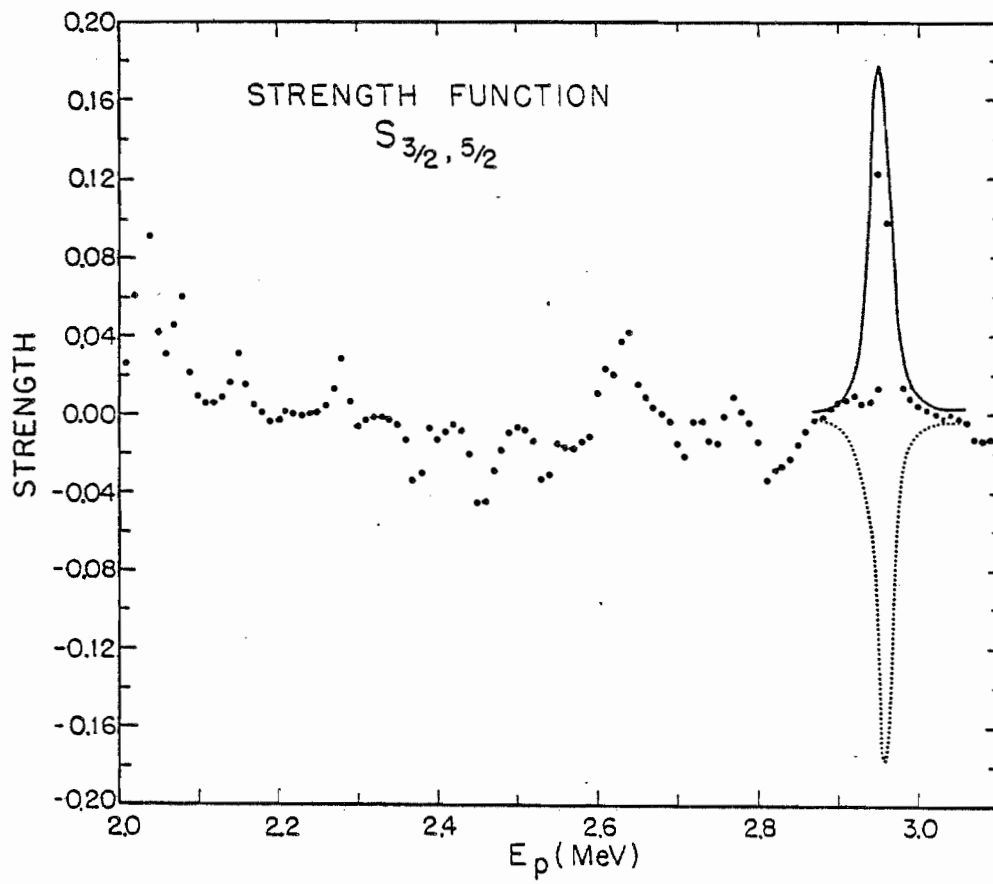


Figure 5.10 Off-Diagonal Strength Function in the Channel Spin Representation. Data (dots) and prediction (solid and dashed curves) are averaged with a Lorentzian weighting function with a 20 keV width.



lack of similarity in the decay patterns near the large state at  $E = 2.953$  lead one to assign only one resonance to the analogue state. Therefore, the effects of the analogue state can be eliminated by removing the one state at 2.953 Mev when the sequence of  $3/2^-$  resonances are used for statistical analysis.

The analogue inelastic spectroscopic factor is defined as

$$S_{p'} = 2T_0 + 1 \frac{\Gamma_{p'}}{\Gamma_{p'sp}}$$

where  $T_0$  is the  $z$  projection of the isospin of the target,  $\Gamma_{p'}$  is the measured analogue inelastic width, and  $\Gamma_{p'sp}$  is the inelastic analogue single particle width. Since  $\Gamma_{p'}$  is the sum of all analogue fragment inelastic widths, the inelastic spectroscopic factors for the analogue states in  $^{59}\text{Co}$  and  $^{49}\text{V}$  can be computed once the single particle inelastic width is known. The single particle widths were calculated with a computer code "HANS" written by Harney (1969) which calculates the analogue width using three different methods. The methods are designated as ZDH (method of Zaidi, Darmodjo (1967) and Harney (1968)), MM (method of Mekjjar and McDonald (1968)), and TAR (method of Thompson, Adams, and Robson (1968)). Table 5.1 lists the inelastic single particle widths and inelastic spectroscopic factors for all three methods for all the five analogue

Table 5.1 Inelastic Spectroscopic Factors

Target	$J^\pi$	$E_p^{LAB}$	$\Gamma_{3/2}^p$ (keV)		
			TAR	ZDH	MM
$^{56}\text{Fe}$	1/2-	2.534	$J'=1/2$	$J'=3/2$	$J'=3/2$
	3/2-	2.905	$J'=1/2$	$J'=3/2$	$J'=1/2$
	3/2-	3.010	$J'=3/2$	$J'=3/2$	$J'=3/2$
$^{48}\text{Tl}$	1/2-	2.856	0.120	0.150	0.150
	3/2-	2.951	0.774	0.946	0.907
$^{48}\text{Tl}$	1/2-	2.856	1.164	1.417	1.359
	3/2-	2.951	1.540	1.870	1.890
$^{48}\text{Tl}$	1/2-	2.856	2.381	2.803	2.700
	3/2-	2.951	2.216	2.673	2.831

Target	$J^\pi$	$E_p^{LAB}$	$S_{p'}$		
			TAR	ZDH	MM
$^{56}\text{Fe}$	1/2-	2.534	$J'=1/2$	$J'=3/2$	$J'=3/2$
	3/2-	2.905	$J'=1/2$	$J'=3/2$	$J'=1/2$
	3/2-	3.010	$J'=3/2$	$J'=3/2$	$J'=3/2$
$^{48}\text{Tl}$	1/2-	2.856	0.005	0.004	0.004
	3/2-	2.951	0.034	0.027	0.027
$^{48}\text{Tl}$	1/2-	2.856	0.070	0.058	0.043
	3/2-	2.951	0.054	0.043	0.043
$^{48}\text{Tl}$	1/2-	2.856	0.026	0.021	0.021
	3/2-	2.951	0.047	0.039	0.039

states studied.

One of the other average properties which can be extracted from the resonance data is the diagonal strength functions. These strength functions are defined as

$$S_c = \overline{\gamma_c^2} / D$$

where  $\overline{\gamma_c^2}$  is the average reduced width in channel  $c$  and  $D$  is the average resonance spacing. The strength functions measured in this experiment are listed in Table 5.2 along with the average reduced widths and average resonance spacing.

#### 5.4 Reduced Width Fluctuations

The sequences of  $3/2^-$  resonances obtained in this experiment have missing levels. Since accurate experimental determination of the spins of p-wave resonances requires that the resonance have inelastic decay, the fraction of resonances studied without inelastic decay are considered to have uncertain spin assignments. Resonances with uncertain spin assignments were not included in the analysis of statistical properties. Resonances with uncertain spin assignments were not the only missing resonances, since resonances with small elastic scattering cross section were also not observed. This omission is the cause of the definite hole ( $\gamma < 0.01$ ) which is seen in Figure 5.11 where



Table 5.2 P-wave Strength Functions

Target	$J^\pi$	Average Spacings and Average Widths					Strength Functions					
		Number of Resonances	D (keV)	$\gamma_p^2$ (keV)	$\gamma_{p'}^2$ (keV)	$\gamma_{j'=1/2}^2$ (keV)	$\gamma_{j'=3/2}^2$ (keV)	$\gamma_{s'=3/2}^2$ (keV)	$\gamma_{s'=5/2}^2$ (keV)	$S_{j'=1/2}$	$S_{j'=3/2}$	$S_{s'=3/2}$
$^{56}\text{Fe}$	1/2-	14	73.8	0.762	0.269	.....	.....	.....	.....	.....	.....	.....
$^{56}\text{Fe}$	3/2-	22	24.8	0.328	0.891	0.533	0.358	0.294	0.597	.....	.....	.....
$^{48}\text{Tl}$	1/2-	45	24.4	0.642	0.297	.....	.....	.....	.....	.....	.....	.....
$^{48}\text{Tl}$	3/2-	75	14.6	0.634	1.314	0.715	0.598	0.504	0.809	.....	.....	.....

the seventy two elastic reduced widths measured in  $^{49}\text{V}$  are compared to the Porter-Thomas distribution. The logarithmic scales enhance the effect of the small reduced widths.

It has been shown by Wilson (1975) that comparison of spacing distributions and experimental spacings requires data with few missing levels if an accurate test of the theory is to be made. Since the number of missing levels in the sequence of  $3/2^-$  levels obtained in this experiment is not small, tests of spacing distributions would not be productive. However, all that is needed to test width distributions is an unbiased sampling of the distribution, since missing levels in this case only effect the normalization.

Reference to Figure 5.11 shows that the sampling of the elastic and total inelastic reduced widths for the  $^{49}\text{V}$  data is biased against small widths. The total inelastic reduced width sequence is a combination of two decay channels. If the elastic channel and the two inelastic channels are independent to first order, the inelastic channels should show little bias in their sampling. This lack of bias is shown in Figure 5.12 where the Porter-Thomas distribution is compared with the experimental sampling in the total angular momentum representation. The sampling for the channel spin representation is shown in Figure 5.13. Similar plots for reduced widths from  $^{57}\text{Co}$  are not shown since the small number of levels measured have very large fluctuations.

Figure 5.11 The Distribution of Elastic and Inelastic Partial Reduced Widths. The smooth solid line is the Porter-Thomas distribution.

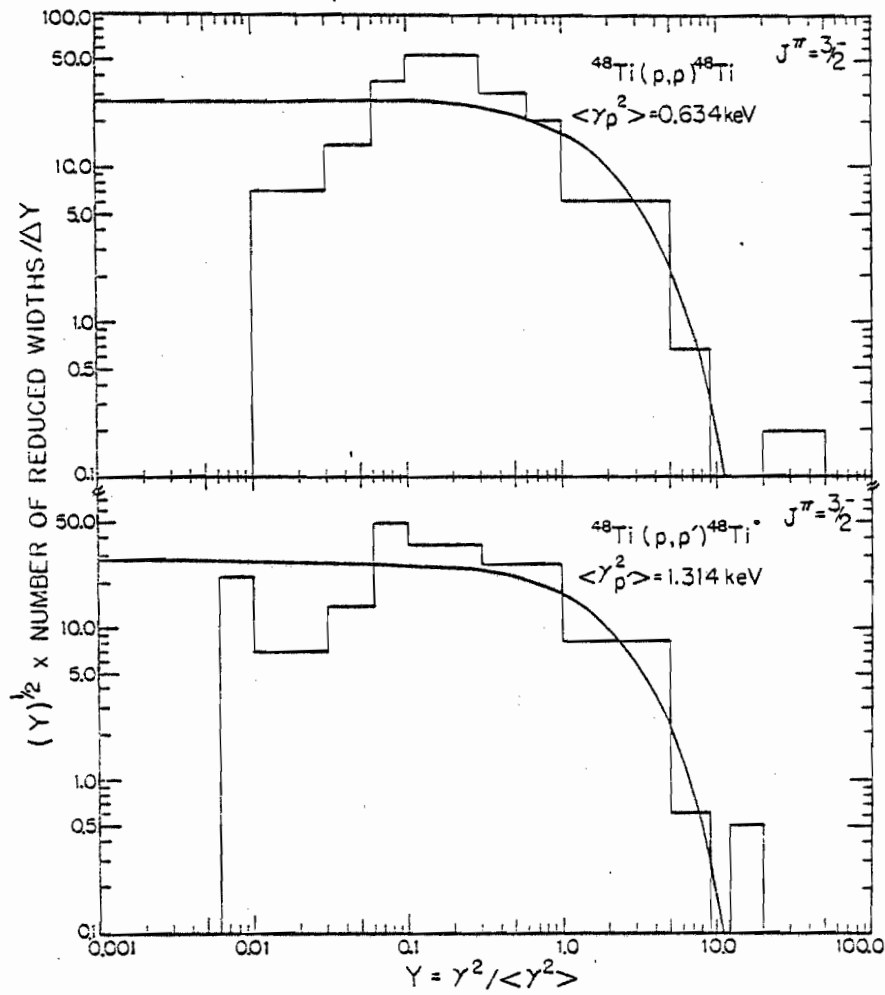


Figure 5.12 The Distribution of Inelastic Reduced Widths in the  $j'=1/2$  and  $j'=3/2$  Channels. The smooth solid line is the Porter-Thomas distribution.

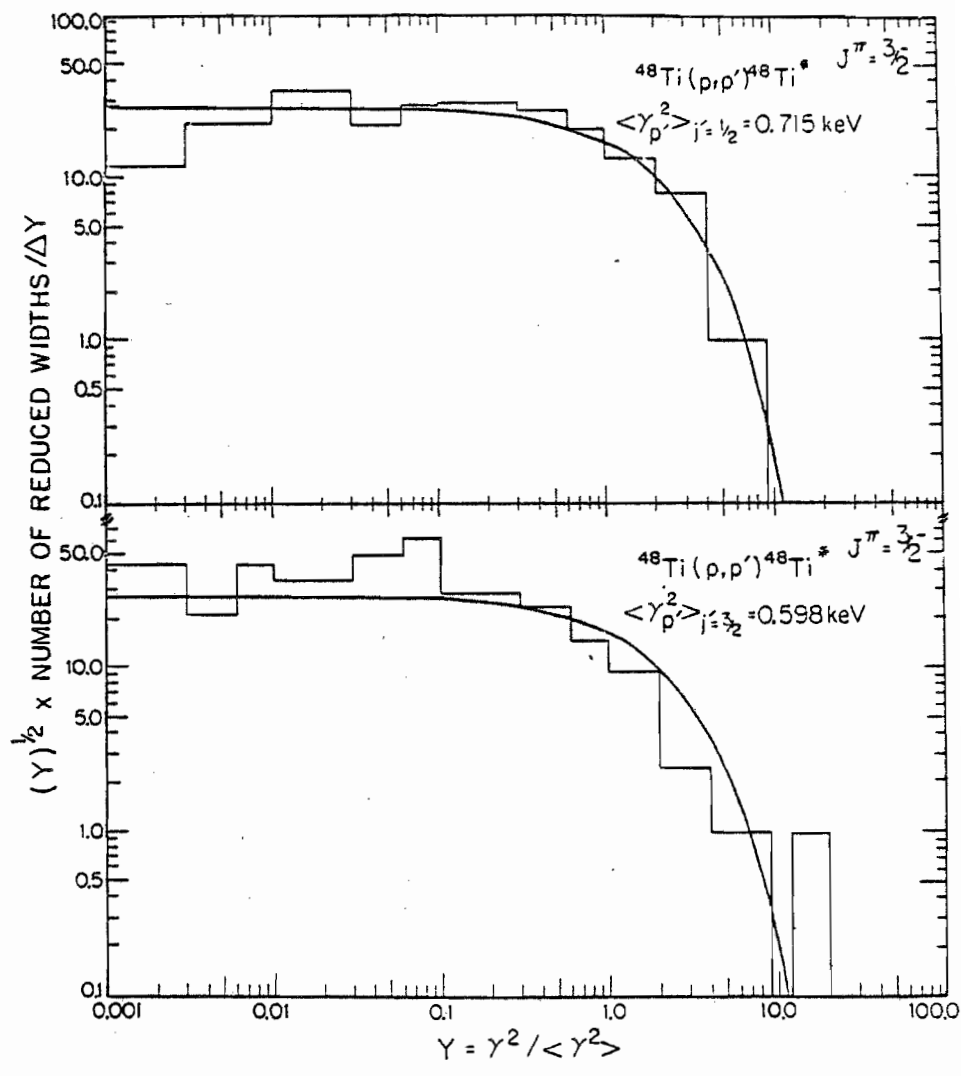
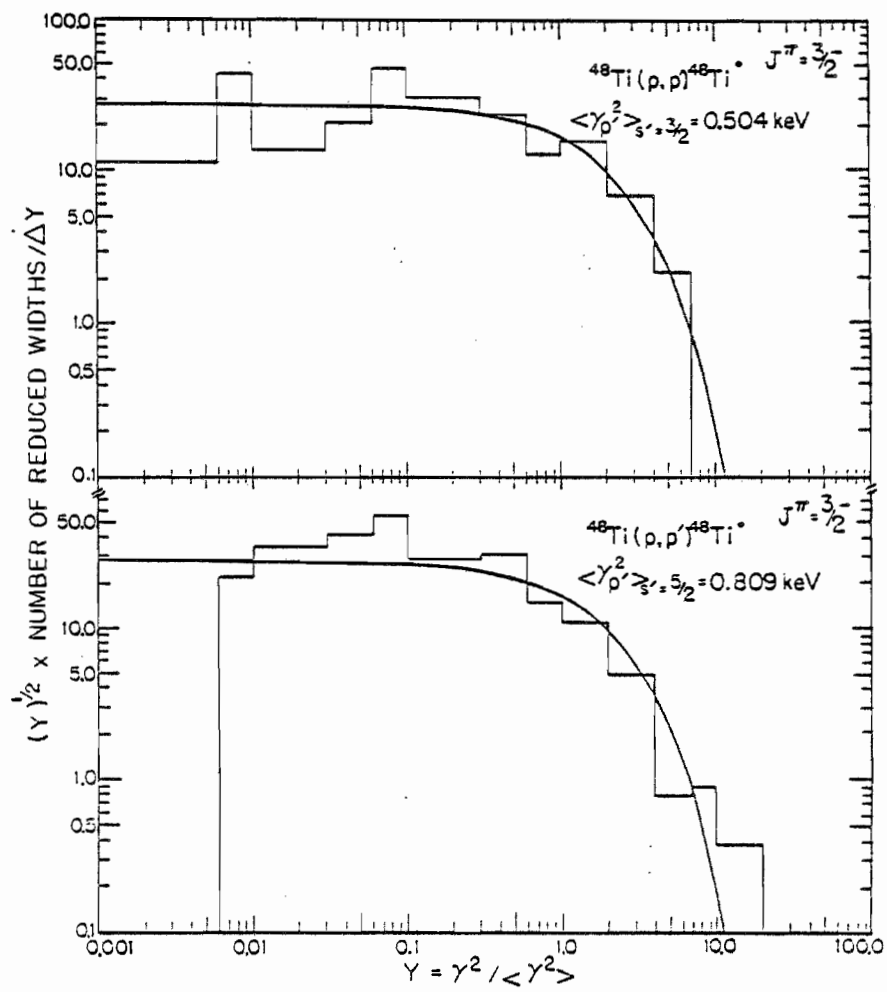


Figure 5.13 The Distribution of Inelastic Reduced Widths in the  $s'=3/2$  and  $s'=5/2$  Channels. The smooth solid line is the Porter-Thomas distribution.





One of the more traditional methods of evaluating agreement between reduced width data and the Porter-Thomas distribution is to assume that the distribution of reduced widths is a  $\chi^2$  distribution of  $\nu$  degrees of freedom,

$$P(\nu, x) = \frac{1}{\Gamma(2\nu)} (2\nu x)^{2\nu-1} e^{-2\nu x} \nu dx \quad (5.4.1)$$

This distribution is shown in Figure 5.14 for various degrees of freedom. Once this assumption is made,  $\nu$  is treated as a free parameter and is determined using the maximum-likelihood method. This procedure was the one originally employed by Porter and Thomas (1958) to obtain the reduced width distribution. The degree of freedom parameter obtained for the various channels from the  $^{39}\text{V}$  data is listed in Table 5.3. The maximum-likelihood method has until now been one of the few methods of comparing experimental width distributions with the various statistical hypotheses.

The most directly measured quantity in these experiment is  $\varphi = \text{TAN}^{-1} \delta$ . A comparison of this data with theory brings new information (relative phase between the amplitudes) into the analysis. A number plot of  $\varphi$  for  $3/2^-$  resonances in the channel spin representation for  $^{57}\text{Co}$  is shown in Figure 5.15. Again, the small number of resonances preclude drawing any strong conclusions. However, this is not the case for the set of  $\varphi$  obtained for  $^{39}\text{V}$ .

The dashed line in Figure 5.16 is the predicted

Figure 5.14 The  $\chi^2$  Distribution for 2 Degrees of Freedom.

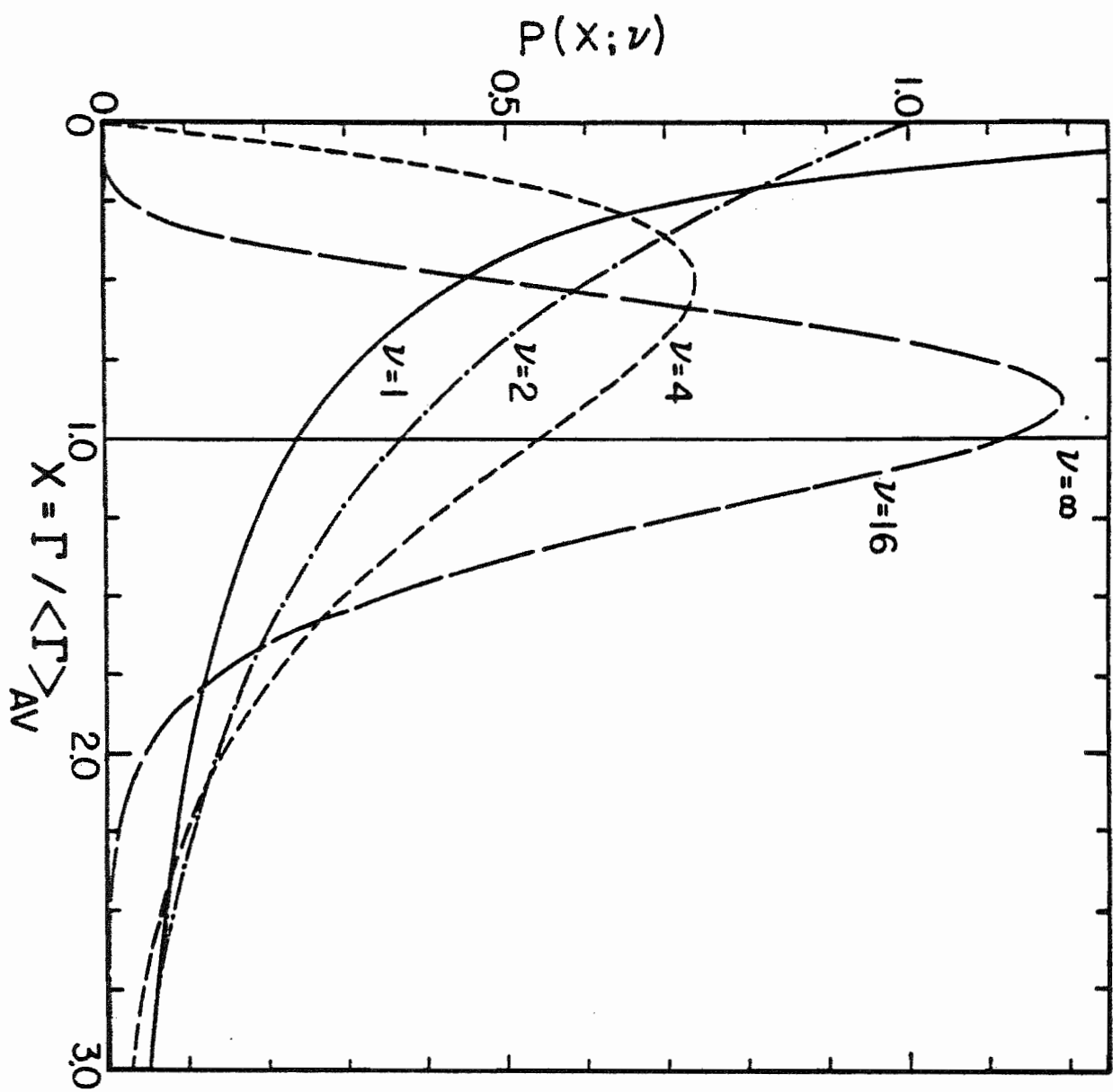
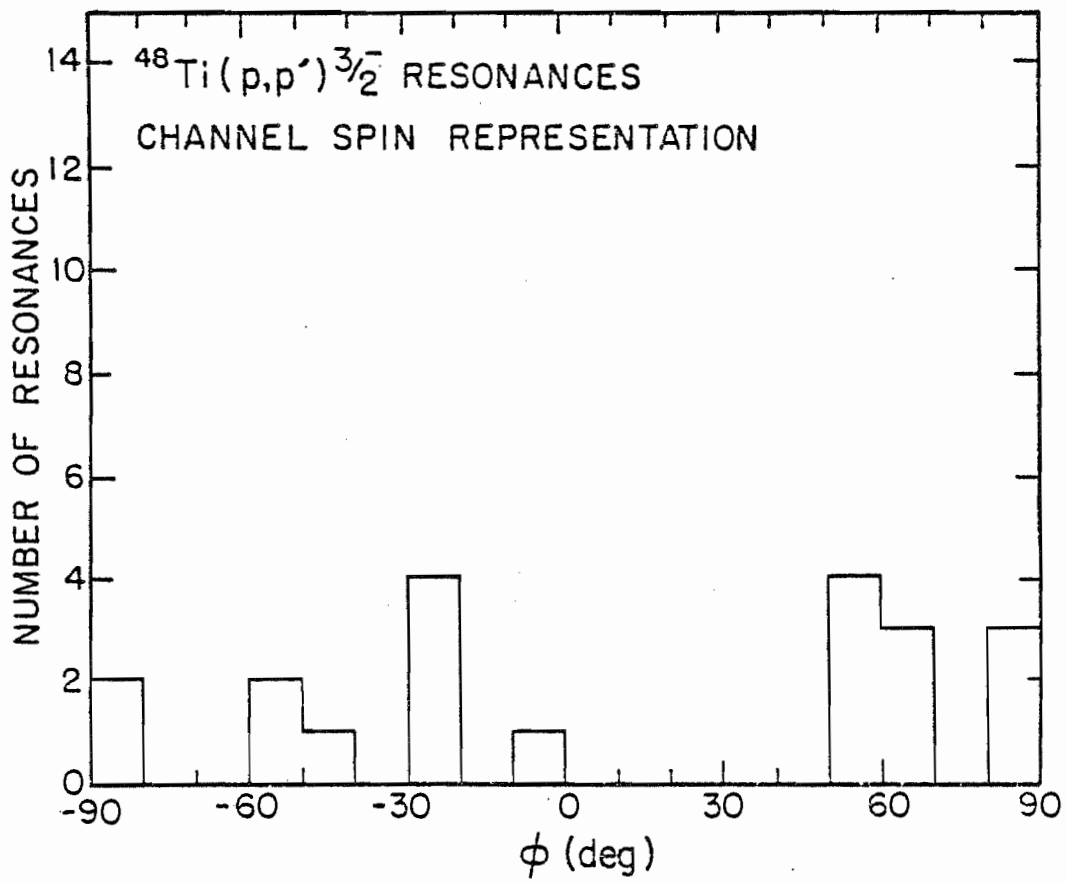


Table 5.3 Degrees of Freedom  
(Maximum-Likelihood Method)

Channel	$^{48}\text{Tl}(P,P)$	$^{48}\text{Tl}$	Total	$^{48}\text{Tl}(P,P')$ $j'=1/2$	$^{48}\text{Tl}$ $j'=3/2$	$s'=3/2$	$s'=5/2$
Degree of Freedom ( $\nu$ )	1.87		1.75	1.40	0.92	1.31	1.23

Figure 5.15 Distribution of  $\varphi$  for Inelastic Decay from  $3/2^-$   
Resonances in  $^{57}\text{Co}$  in the Channel Spin  
Representation.



distribution for the extreme statistical case where the channel matrix  $M$  is diagonal. If  $M$  is not diagonal, some  $\sin 2\phi'$  modulation of the uniform distribution is expected. The measured sample for the channel spin representation agrees with neither of these predictions. The significance of the large bumps in the distribution was estimated using a Monte-Carlo technique. A statistic was defined as

$$Z = \sum_{i=1}^{N_b} \left( N_i - \frac{N_k}{N_b} \right)^2$$

where  $Z$  is the sum of squares statistic,  $N_i$  is the number of resonances with value of  $\phi$  in the  $i^{\text{th}}$  bin (bins were of equal width),  $N_k$  is the number of resonances measured, and  $N_b$  is the number of bins. This statistic is distributed as shown in Figure 5.17. This histogram was determined by generating seventy two random numbers on the interval between zero and one hundred and eighty. These random numbers were treated as  $\phi$  and sorted into bins. The sum of squares statistic was then calculated. This procedure was repeated for 100,000 cases. The various  $Z$  were then sorted and plotted as shown in Figure 5.17. The three plots for various values of  $N_b$  demonstrate that the distribution is not a sensitive function of bin size. The values of  $Z$  calculated from the data, for both  $\phi$  and  $\phi'$ , in the total angular momentum and channel spin representations are

Figure 5.16 Distribution of  $\phi$  for Inelastic Decay from  $3/2^-$  Resonances in  $^{49}\text{V}$  in the Channel Spin Representation. The dashed line is the uniform distribution predicted with no correlations between channels.



$^{48}\text{Ti}(p,p')\ ^{3/2}_-$  RESONANCES  
CHANNEL SPIN REPRESENTATION

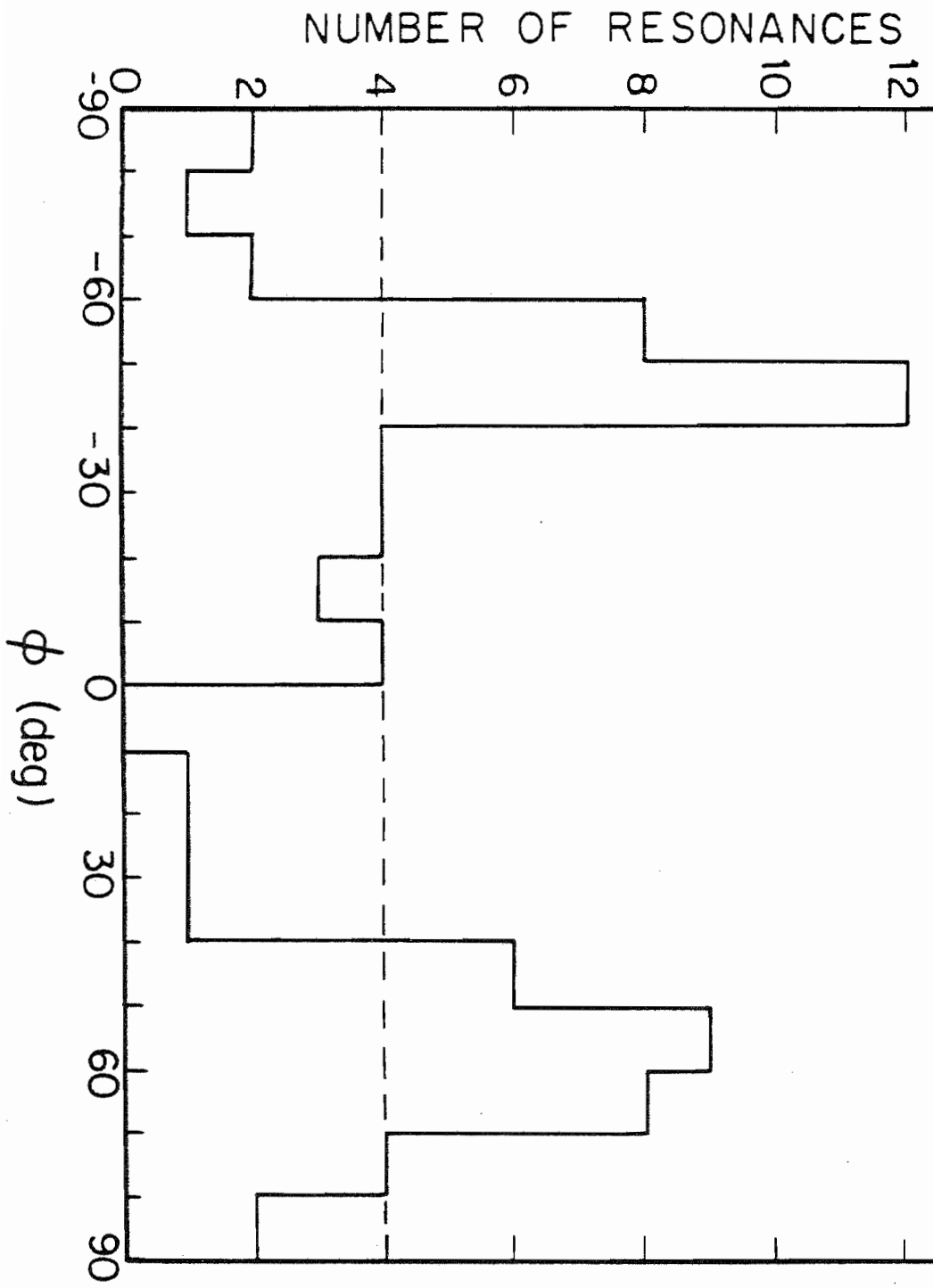
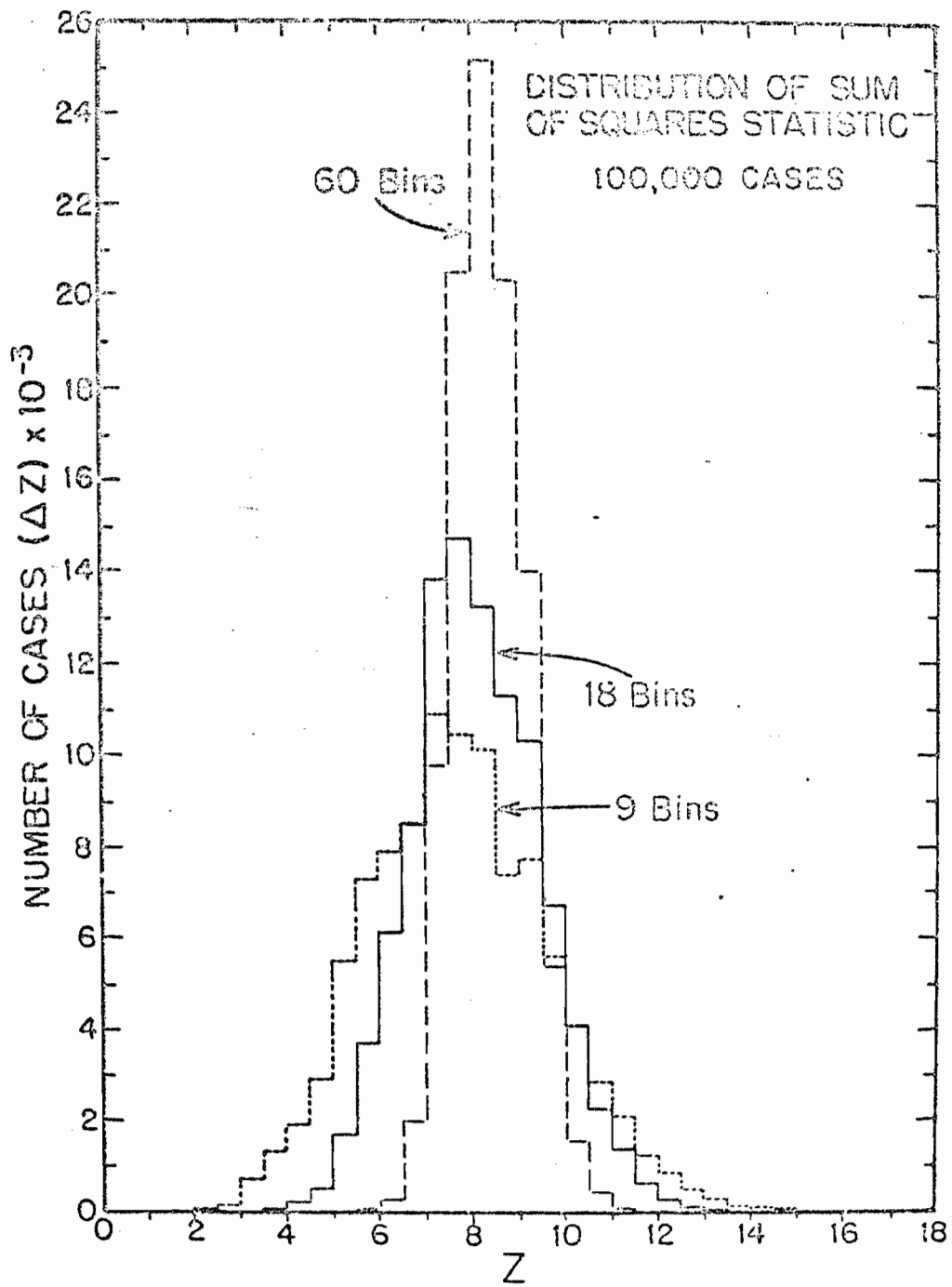


Figure 5.17 Distribution of Sum of Squares Statistic for  
Different Number of Bins.



	$\varphi_3$	$\varphi_4$	$\varphi'_3$	$\varphi'_4$	142
$Z_{18}$	14.8	13.9	15.9	14.4	
$Z_9$	15.2	16.8	15.2	17.3	

The number of cases of  $Z_{18} > 13.9$  calculated from the number of bins equal to 18 was 11. There were no cases of  $Z_{18} > 14.8$  for the 18 bin calculation. There were only 17 cases of  $Z_9 > 16.0$  with 9 bins. Therefore, the probability that the data shown in Figure 5.18 could have been sampled from a uniform distribution is less than 1 in  $10^4$ .

Another method of determining whether the data on mixing ratios from the  $^{48}\text{Ti}(p,p')$  experiment satisfies the statistical hypothesis made in section 5.1 is to compute the linear correlation coefficient between inelastic decay channels. To find regions of linear correlation between channels a plot of  $\sum \gamma_i \gamma_{2i}$  versus energy was constructed. Two obvious regions of large slope are seen in Figure 5.18. Region 1 is between 2.4 and 2.6 MeV and region 2 is between 2.7 and 3.0 MeV. The large jump at 2.95 MeV is caused by the  $3/2^-$  analogue state. The linear correlation coefficients between the different channels in region 1 are listed in Table 5.4 and the correlation coefficients for region 2 are listed in Table 5.5. The significance level in these tables was determined with the method of Baudinet-Robinet discussed in section 5.2. These regions of large

Figure 5.18  $\sum_i \delta_{\alpha_i} \delta_{\beta_i}$  versus  $E_p$  for Inelastic Decay from  $3/2^-$  Resonances in  $^{99}\text{V}$  in both Channel Spin and Total Angular Momentum Representations.

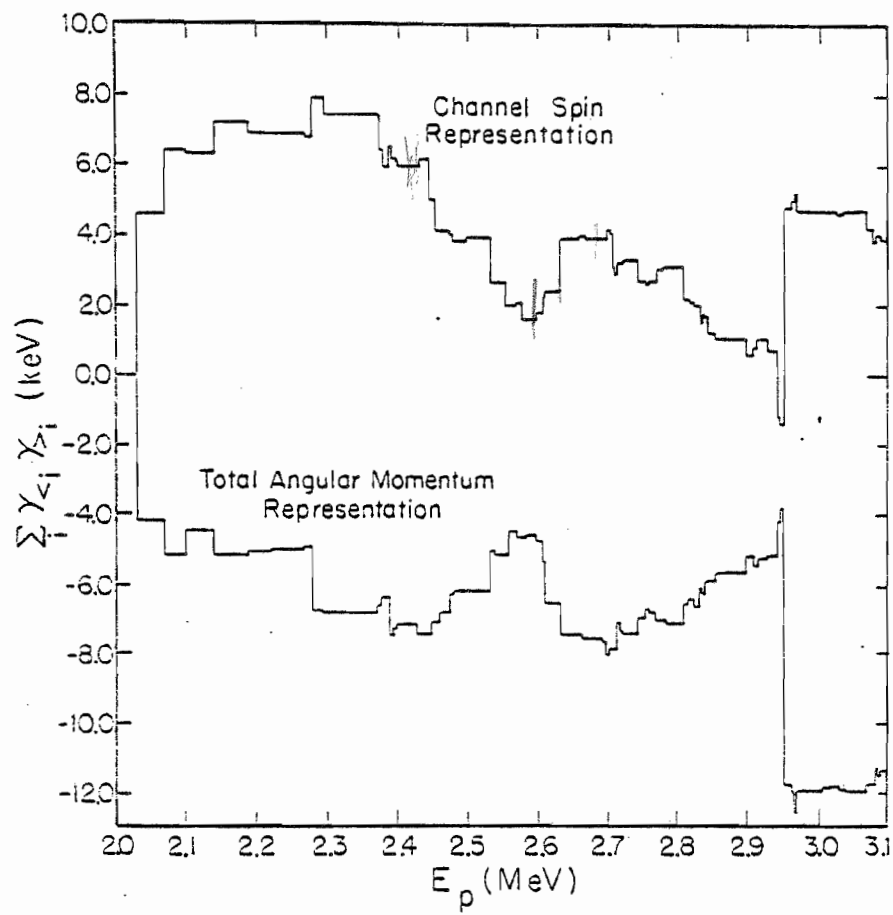


Table 5.4 Linear Correlation Coefficients Between Channels

Region 1  
14 Resonances

	$\gamma_p^2$	$\gamma_{p'}^2$	$\gamma_{s'=3/2}^2$	$\gamma_{s'=5/2}^2$	$\gamma_{j'=1/2}^2$	$\gamma_{j'=3/2}^2$	$\gamma_{s'=3/2}^2$	$\gamma_{j'=1/2}^2$
$\gamma_p^2$	1.0	-0.087	-0.367	0.255	0.024	-0.317	...	...
$\gamma_{p'}^2$		1.0	0.818	0.778	0.938	0.357	...	...
$\gamma_{s'=3/2}^2$			1.0	0.274	...	...	...	...
$\gamma_{s'=5/2}^2$				1.0	...	...	...	...
$\gamma_{j'=1/2}^2$					1.0	0.011	...	...
$\gamma_{j'=3/2}^2$						1.0	...	...
$\gamma_{s'=5/2}^2$							-0.651	...
$\gamma_{j'=3/2}^2$								0.462

Significance Level

Significance	50%	70%	90%	95%	99%	99.9%
Linear Correlation Coefficient	0.192	0.288	0.428	0.492	0.597	0.688

Table 5.5 Linear Correlation Coefficients Between Channels

Region 2							
39 Resonances							
$\gamma_p^2$	$\gamma_{p'}^2$	$\gamma_{s'=3/2}^2$	$\gamma_{s'=5/2}^2$	$\gamma_{j'=1/2}^2$	$\gamma_{j'=3/2}^2$	$\gamma_{s'=5/2}^2$	$\gamma_{j'=1/2}^2$
$\gamma_p^2$	1.0	0.557	0.414	0.511	0.554	0.096	...
$\gamma_{p'}^2$		1.0	0.812	0.857	0.951	0.304	...
$\gamma_{s'=3/2}^2$			1.0	0.394	...	...	...
$\gamma_{s'=5/2}^2$				1.0	...	...	...
$\gamma_{j'=1/2}^2$					1.0	-0.005	...
$\gamma_{j'=3/2}^2$						1.0	...
$\gamma_{s'=5/2}^2$							-0.451
$\gamma_{j'=3/2}^2$							
							0.310

## Significance Level

Significance	50%	70%	90%	95%	99%	99.9%
Linear Correlation Coefficient	0.111	0.168	0.260	0.307	0.389	0.474



correlations are also the source of the clumps of resonances with the similar values of the parameter  $\varphi$ . The grouping can be seen in the plot of  $\varphi$  versus  $E_p$  shown in Figure 5.19 for the total angular momentum representation.

The conditions of  $\varphi$  being approximately constant or  $\sum_i \gamma_{\alpha i} \delta_{\alpha i}$  having non-zero slope have been shown by Lane (1971) to be consistent with the existence of a doorway state common to two channels.

One of the remaining puzzles presented by this data is the existence of negative correlations between the reduced widths. Correlations between widths have been shown by Ullah (1963) to be positive even in the Unitary ensemble.

A plot of  $\sum_i \gamma_{\alpha i} \delta_{\alpha i}$  for resonances in  $^{57}\text{Co}$  is shown in Figure 5.20. The two  $3/2^-$  analogue states stand out dramatically as the large changes in  $\sum_i \gamma_{\alpha i} \delta_{\alpha i}$  at 2.9 and 3.0 Mev. No correlations are apparent in these data if the analogue states are removed. Experience with both  $^{57}\text{Co}$  and  $^{99}\text{Tc}$  indicate that large ( $N > 50$ ) and fairly complete sequences of resonances are needed to perform statistical analyses of width fluctuations.

Figure 5.19  $\phi'$  in the Total Angular Momentum Representation  
versus  $E_p$  for Inelastic Decay from  $3/2^-$   
Resonances in  $^{99}\text{V}$ .

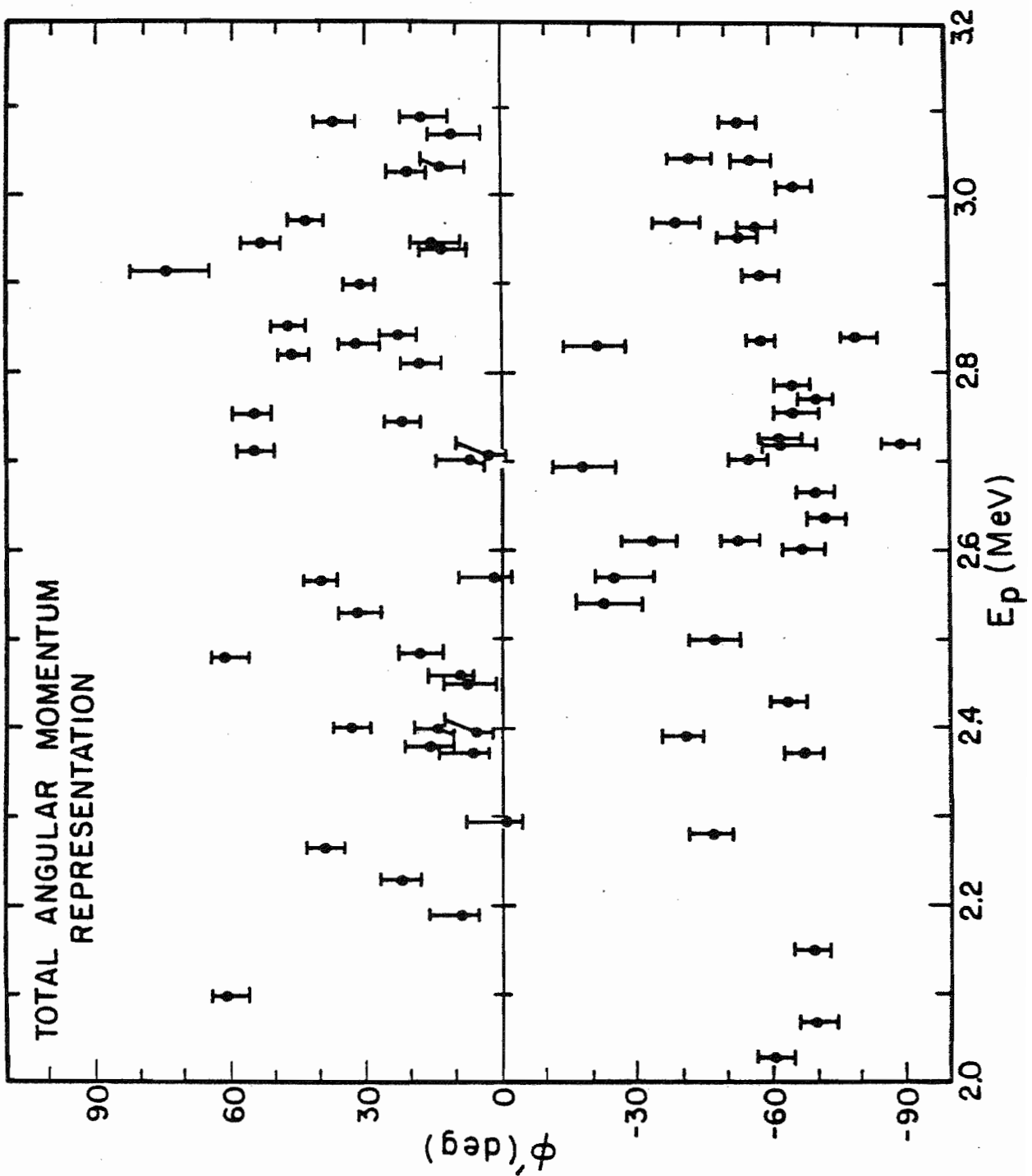
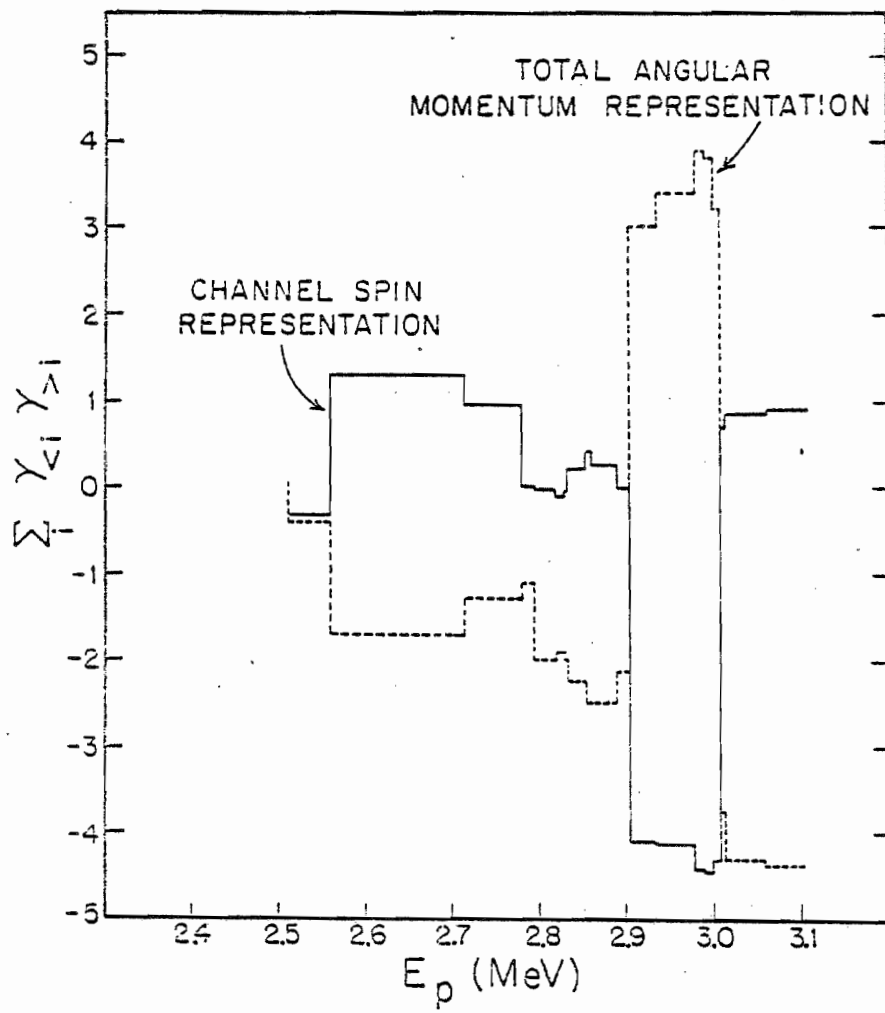


Figure 5.20  $\sum_i |\alpha_i \delta_i|$  versus  $E_e$  for Inelastic Decay from  $3/2^-$   
Resonances in  $^{57}\text{Co}$ .



## Chapter 6

### SUMMARY

Inelastically scattered proton and de-excitation gamma-ray angular distributions were measured for the reactions  $^{56}\text{Fe}(p,p')^{56}\text{Fe}$  and  $^{48}\text{Ti}(p,p')^{48}\text{Ti}$ . One hundred and twenty p-wave resonances in  $^{49}\text{V}$  and thirty-six p-wave resonances in  $^{57}\text{Co}$  were examined between proton bombarding energies 2.0 and 3.1 MeV. It was shown that the method of measuring two singles angular distributions could be used to assign spins to p-wave resonances. Also, the mixing ratio of the inelastic decay amplitudes could be extracted for  $3/2^-$  resonances.

Spectroscopic information was obtained from the sequences of  $1/2^-$  and  $3/2^-$  resonances. The strength functions in both elastic and inelastic channels in  $^{49}\text{V}$  and  $^{57}\text{Co}$  were obtained. The analogue inelastic spectroscopic factors were determined for the five p-wave analogues observed. The proposed fine structure for the  $3/2^-$  analogue

state in  $^{99}\text{V}$  was shown to be inconsistent with the results of the inelastic decay mixing ratio measurements. The  $3/2^-$  analogue in  $^{99}\text{V}$  is an extreme weak mixing case.

The probability distribution for reduced width amplitudes in the orthogonal ensemble for the two channel case was given. This distribution function was modified to obtain the distribution functions for the mixing parameters  $\varphi$  and  $\delta$ . The inelastic decay of a sequence of 72  $3/2^-$  resonances in  $^{99}\text{V}$  was compared to these distribution functions and found to be inconsistent. The off diagonal strength function  $S_{cc'}$  was non-zero in two energy regions, in violation of the random phase approximation. The linear correlations between channels in these regions were significant and were consistent with existence of two doorway states common to the inelastic channels. The prediction that the linear correlation coefficient for reduced widths is equal to the square of the linear correlation coefficient for the reduced width amplitudes was not borne out by experiment. Also, negative reduced width linear correlation coefficients were calculated between some channels which violates the strongest prediction of the theories of width distributions.

Since the methods used in this experiment are more sensitive than previously used techniques, it has led to more questions than answers. The main question, which can only be answered by additional experiments of this type, is

related to the probable doorway states in  $^{49}\text{V}$ . The simplest explanation of the nonstatistical behavior of the off-diagonal strength function is the existence of doorway states. However, another possibility is that the random phase approximation is not valid and that energy dependent correlations between reaction channels must be incorporated into the theories of width fluctuations.



## Appendix A

### A.1 Introduction

This appendix provides the pertinent details of the present beam energy control system utilized at the Triangle Universities Nuclear Laboratory (TUNL) 3 MV Van de Graaff accelerator laboratory. The primary beam energy stabilization is accomplished by a standard corona control system which monitors the HH beam which is accelerated along with the H beam used to perform experiments. The fluctuations of the HH beam are further examined in an electrostatic analyzer and associated control system (homogenizer) in order to first measure and then cancel the remaining energy fluctuations in the experimental H beam. In section A.2 a simplified model of the system is defined and considered as a position regulator. The components of the present system and circuits are reviewed in Section A.3. The linear control analysis used in Section A.4 to model the complete regulation system is not carried out to the actual modeling of the individual components. The complexity added by complete detail modeling does not enhance understanding of the general operation of the system. Some modifications and improvements are suggested

in Section A.5.

#### A.2 Model of the TUNL Homogenizer as a Position Regulator.

Electrostatic analyzers or prisms have long been used in experimental nuclear physics. Herzog (1935) first described the properties of electrostatic prisms. These devices were first used in the way that glass prisms are used in optical spectroscopy. Charged particles with different energies have different orbits in the analyzer and slits select a range of particle energies to be used in experiments. Such an instrument was described by Warren (1947). In these devices as in their optical analogs, high resolution implies smaller slit aperture and low beam intensities.

The Van de Graaff accelerator produces ion beams which on small time scales have essentially monochromatic beam energies. With high energy ions from a Van de Graaff accelerator, the electrostatic analyzer with appropriate control electronics can be made into a beam position regulator. If the beam's position through the analyzer is made time independent by changing the "index of refraction", the varying "index of refraction" can be related to the time dependent variations in the beam energy. Once this energy variation is detected, corrections can be placed on the target via a high voltage, cancelling time dependent

energy fluctuations. Such a system was initially described by Parks (1958). These regulators are best understood with linear feedback analysis.

Consideration of Newton's equations of motion in an ideal analyzer will explain the previous analogy to optical prisms. Detailed descriptions of ion optics for analyzers are given by Bendelid (1958) and by Wollnik (1967). Consider the diagram of an analyzer in Figure A.1. The beam from the accelerator is defined by the object slits  $\odot$  which have a separation  $2b$ . The beam enters the analyzer and experiences a radial acceleration arising from the potential difference on the analyzer plates. In the following discussion the voltage is assumed to be symmetrically placed on the plates of the analyzer to eliminate any acceleration in the direction of the beam's motion. The electric field in a cylindrical analyzer is

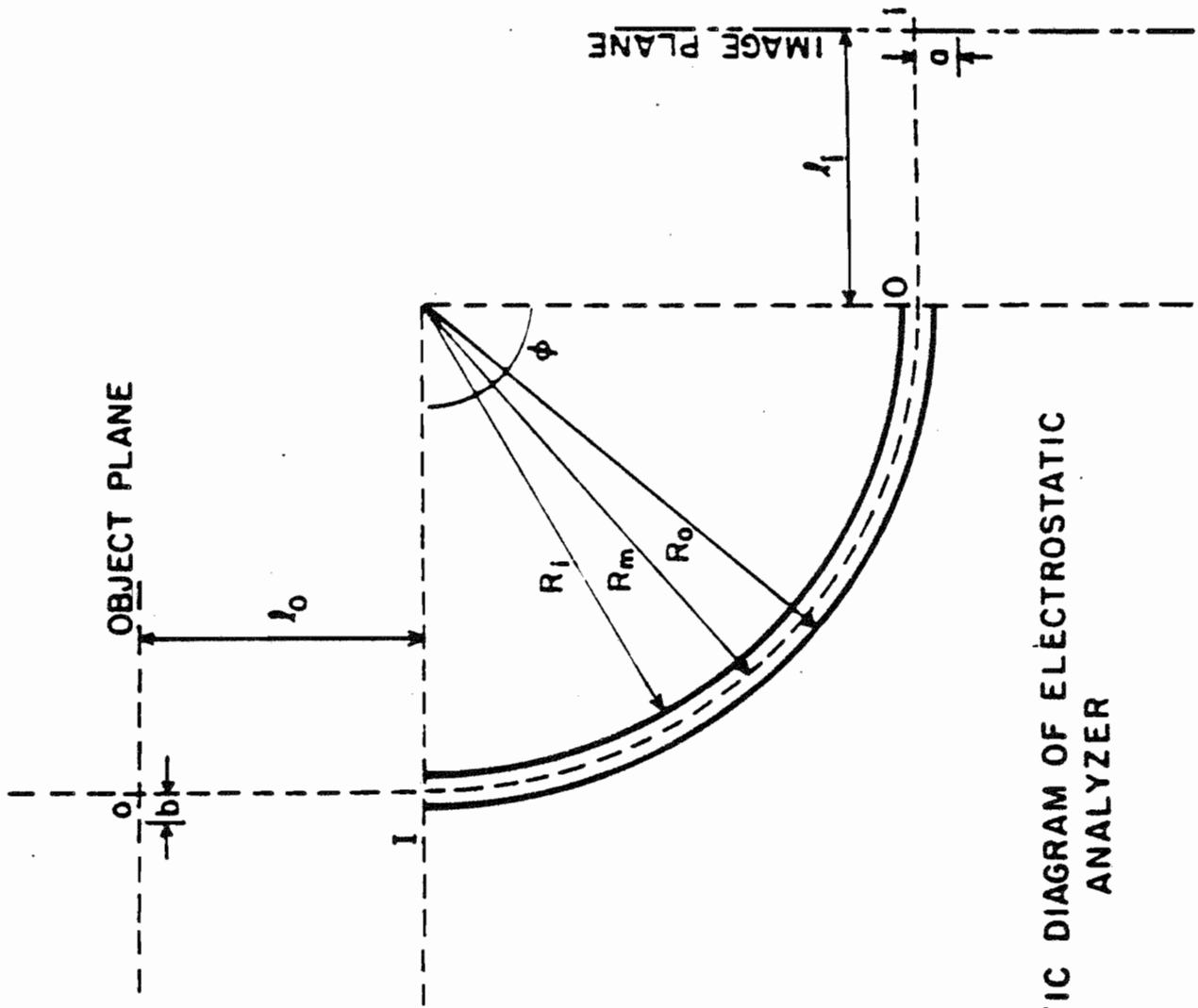
$$\vec{E} = \frac{V}{\ln(R_o/R_i)} \frac{\vec{R}}{R^2} \quad (\text{A.2.1})$$

where  $V$  is the potential across the plates,  $R_o$  is the radius of the outer plate,  $R_i$  is the radius of the inner plate, and  $R$  is the radial position between the plates of the analyzer. The radial force on a particle in the beam moving along the median radius  $R_m$  is

$$F = \frac{eV}{\ln(R_o/R_i)} \frac{1}{R_m} \quad (\text{A.2.2})$$

The force required to maintain a non-relativistic particle

Figure A.1 Schematic Diagram of Cylindrical Electrostatic Analyzer.



**SCHEMATIC DIAGRAM OF ELECTROSTATIC ANALYZER**

of mass  $m$  with velocity  $v$  and kinetic energy  $T$  in a circular orbit of radius  $R_m$  is

$$F = \frac{mv^2}{R_m} = \frac{T}{2R_m} \quad (\text{A.2.3})$$

If the kinetic energy is equal to the potential energy through which the particle was accelerated, then  $T = eV_r$ , where  $V_r$  is the acceleration voltage. From equations (A.2.3) and the relation for  $T$  one obtains

$$\frac{V_r}{V} = \frac{2}{\ln(R_o/R_i)} \quad (\text{A.2.4})$$

the ratio of the voltage applied to the plates of the analyzer and the voltage through which the particle was accelerated for a central orbit in the analyzer. This ratio is a geometric constant for an analyzer.

To describe the orbit of a particle in an analyzer, the radius of the particle's orbit must be determined as a function of the total energy of the particle and the voltage  $V$  across the analyzer. The function  $\ln(R_o/R_i)$  can be expanded in a Taylor series to first order as

$$\ln(R_o/R_i) = \frac{2(R_o - R_i)}{(R_o + R_i)} \quad (\text{A.2.5})$$

For radii on the order of a meter and plate separations of 9.525 mm, the error is less than one part in  $10^8$ . Defining the plate separation  $R_o - R_i$  as  $d$ , a very good approximation for the force on a charged particle in the

analyzer is

$$F = \frac{eV}{d} \quad (\text{A.2.6})$$

From equation (A.2.3) the function

$$R(T,v) = 2Td/eV$$

is obtained. The radius of a particle in a median orbit is a function of particle energy and the potential across the analyzer plates. Of more interest in reducing energy fluctuations is the behavior of

$$\Delta R = \left. \frac{\partial R}{\partial T} \right|_V \Delta T + \left. \frac{\partial R}{\partial V} \right|_T \Delta V \quad (\text{A.2.7})$$

which relates changes in the ion's trajectory to changes in T and V. If  $\Delta R$  is constrained to be zero,

$$\Delta V = -\frac{A_1}{A_2} \Delta T \quad (\text{A.2.8})$$

$$A_1 = \left. \frac{\partial R}{\partial T} \right|_V \quad A_2 = \left. \frac{\partial R}{\partial V} \right|_T$$

or,

$$\frac{\Delta V}{\Delta T} = \frac{1}{2} \ln(R_o/R_i) \quad (\text{A.2.9})$$

Therefore, for any energy fluctuation  $\Delta T$  an extra voltage must be imposed upon the analyzer to keep  $\Delta R=0$ . This requires an instantaneous control which cannot be achieved in practice. Correct descriptions must acknowledge the finite transit times for signals in electronic circuits.

The measurement of  $\Delta R$  associated with a variation in beam energy is not possible absolutely, since only finite

gains are obtainable in the electronic circuits used to measure . Analysis of a simple model of the electronic control systems demonstrates this. Consider Figure A.2, where a schematic diagram of the image slit region of the analyzer is displayed. The discussion is simplified by assuming that the beam intensity has a square profile. This square shape arises from the close spacing of the object slits. If the object slits have a spacing of  $2b$ , the beam will have a width of  $2bm$  at the image slits, where  $m$  is the horizontal magnification of the analyzer. With this rectangular beam of uniform current density

$$\rho = I/2mbh \quad (A.2.10)$$

and displacement  $\Delta R$  from the center of the slit opening, the current from the high energy and low energy slits are given by

$$\begin{aligned} I_{he} &= \frac{1}{2}(2bm - 2a)h\rho + \Delta R h\rho \\ I_{le} &= \frac{1}{2}(2bm - 2a)h\rho - \Delta R h\rho \end{aligned} \quad (A.2.11)$$

where  $2a$  is the image slit separation,  $I$  is the total current through the analyzer,  $I_{he}$  is the current intercepted by the high energy slit, and  $I_{le}$  is the current intercepted by the low energy slit. Letting  $Z$  be the impedance of the parallel combination of  $R_s$  and  $C_s$  (capacity from slit to ground) and  $D$  be the ratio of the impedances of  $C_s$  (the capacity between the slits) and  $Z$ , the output voltages from the slits are



$$V_{ne} = I_{ne} Z + I_{le} Z D \quad (A.2.12)$$

$$V_{le} = I_{le} Z + I_{ne} Z D$$

where

$$Z = \frac{R_s \cdot (1 + j\delta (\frac{1}{f_1} + \frac{1}{f_2}))}{1 - 2(\delta^2 / f_1 f_2) - (\delta / f_1)^2 + 2j\delta (\frac{1}{f_1} + \frac{1}{f_2})}$$

$$D = \frac{j\delta / f_2}{1 + j\delta (\frac{1}{f_1} + \frac{1}{f_2})}$$

$$f_1 = \frac{1}{2\pi R_s C_s}$$

$$f_2 = \frac{1}{2\pi R_s C_s'}$$

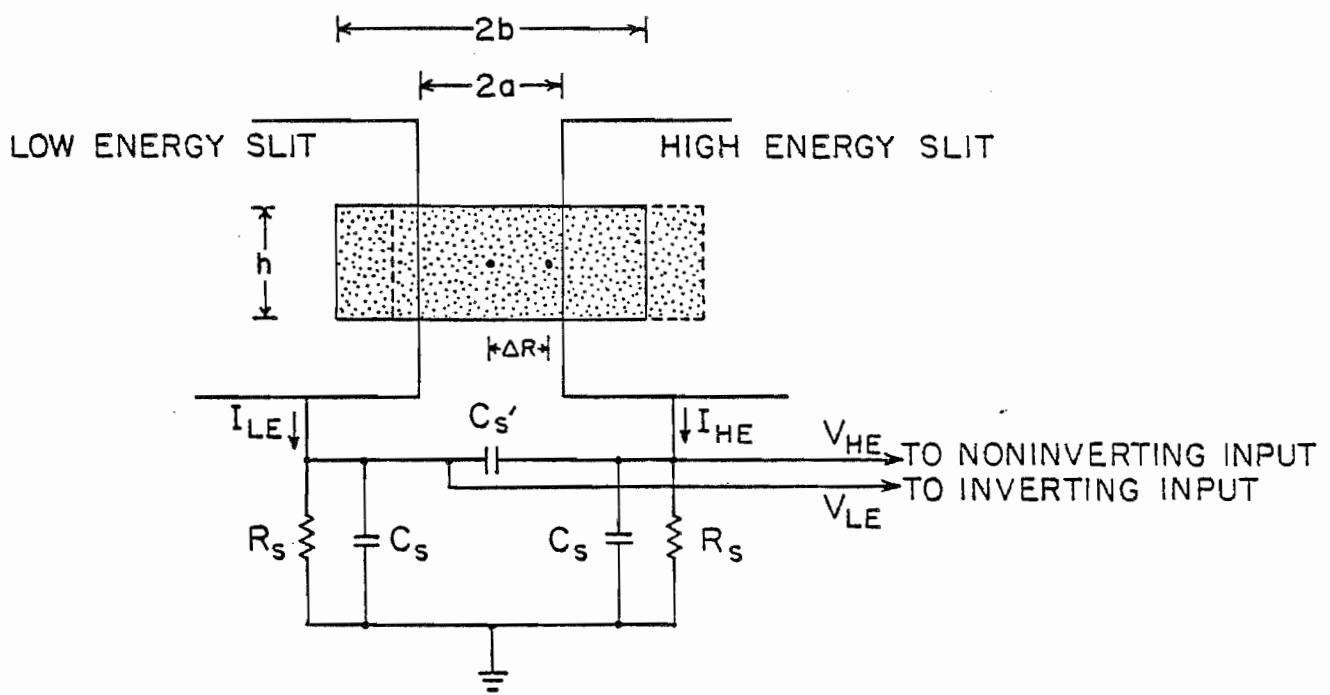
$$j^2 = -1$$

and  $f$  is the frequency of the slit current signals. a complex representation for impedances is standard and can be extended to describe the gain characteristics of active amplifying elements. The gain of an amplifier can also be represented as a complex quantity. The modulus of the complex gain is the ratio of the output to input signals and the phase is the time delay between the input and output signals. In general modulus and phase are a function of frequency. This type of analysis is valid only for sinusoidal signals (or sums of such signals) and linear amplifiers.

If the above slit voltages are input into a difference amplifier, The output voltage of the amplifier is given by

$$V_o = 2ARh_p Z (1-D) B_d + \frac{1}{2} (2b_m - 2a) h_p Z (1+D) B_{cm} \quad (A.2.13)$$

Figure A.2 Diagram of the Analyzer Image Slits. This schematic shows the model of the electrical characteristics used in the analysis of the homogenizer.



where  $B_d$  is the differential gain and  $B_{cm}$  is the common mode gain. Both  $B_d$  and  $B_{cm}$  are in general complex quantities. In a good difference amplifier  $B_{cm}$  is very small and  $V_o$  is given by the first term. If  $V_o$  is applied to the outer plate of the analyzer and the relation for  $\Delta R$  is used, an expression for  $\Delta R$  is

$$\Delta R = A_1 \Delta T + A_2 V_o \quad (\text{A.2.14})$$

$\frac{\Delta R}{\Delta T}$  may be obtained by using the first term in equation (A.2.13).

$$\frac{\Delta R}{\Delta T} = \frac{A_1}{1 - A_2 h \rho Z (1-D) B_d} \quad (\text{A.2.15})$$

At low frequencies  $Z$  is approximately  $R_s$  and  $D$  which is a measure of the cross talk between slits is zero. With these approximations and the definition of  $\rho$  one obtains

$$\frac{\Delta R}{\Delta T} = \frac{A_1}{1 - \frac{A_2 I R_s B_d}{2mb}} \quad (\text{A.2.16})$$

for the variation of  $R$  with a variation in  $T$  in terms of known quantities. Using equation (A.2.10) the outer plate voltage as a function of  $\Delta R$  is

$$\frac{\Delta R}{\Delta V} = \frac{2e A_1 / \ln(R_o/R_i)}{1 - \frac{A_2 I R_s B_d}{2mb}} \quad (\text{A.2.17})$$

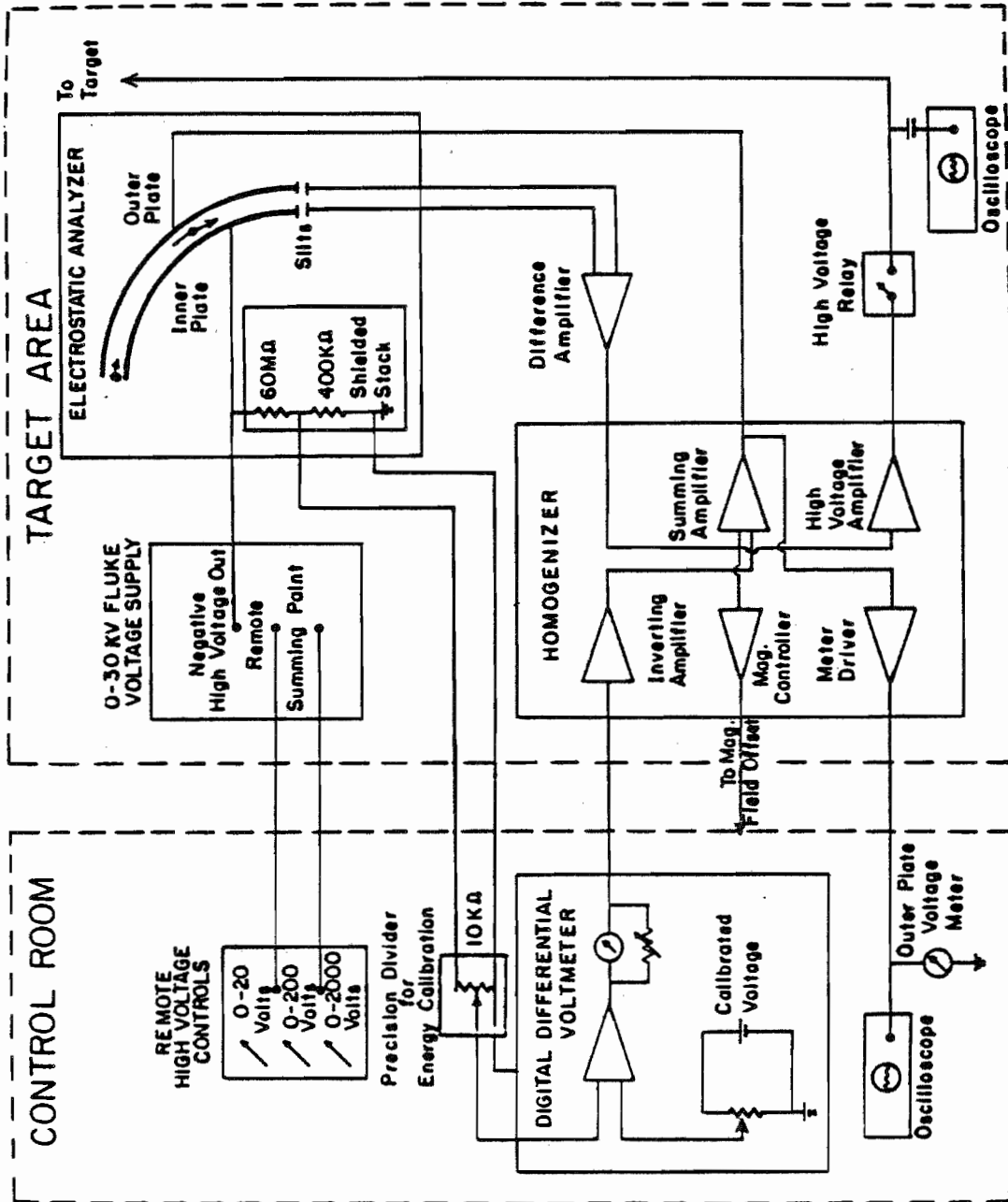
Fluctuations in energy are converted to changes in  $R$  which can be related to changes in the voltage sent to the outer

plate of the analyzer to keep the beam centered on the image slits. These voltages are known to be related by a geometric parameter. Thus, a voltage may be applied to the target used in an experiment to cancel some percentage of the measured fluctuations. Ideally one wants  $\Delta R$  to be zero for any  $\Delta T$ . Reference to equation (A.2.15) shows that this is possible only if the right hand side of the equation is zero. Therefore, only an approximate regulation of  $R$  can be obtained and only then if the system electronics has large gain.

### A.3 Homogenizer Component Description

The homogenizer system used in the TUNL 3 MV accelerator laboratory is shown in Figure A.3. Absolute energy measurements and the absolute stability of the control system are provided by the negative high voltage power supply connected to the analyzer inner plate, shielded resistive divider, and digital differential voltmeter (DVM). A negative high voltage is applied to the inner plate of the analyzer and the resistive divider is calibrated so that the voltage measured from the low voltage side of the resistive divider corresponds to the energy in MeV of the beam going through the analyzer. The ratio of the analyzer voltage to energy is given by Toller (1954) to be 1 to 111. If the differential voltmeter is nulled and the dial reading

Figure A.3 Block Diagram of Homogenizer Circuitry.



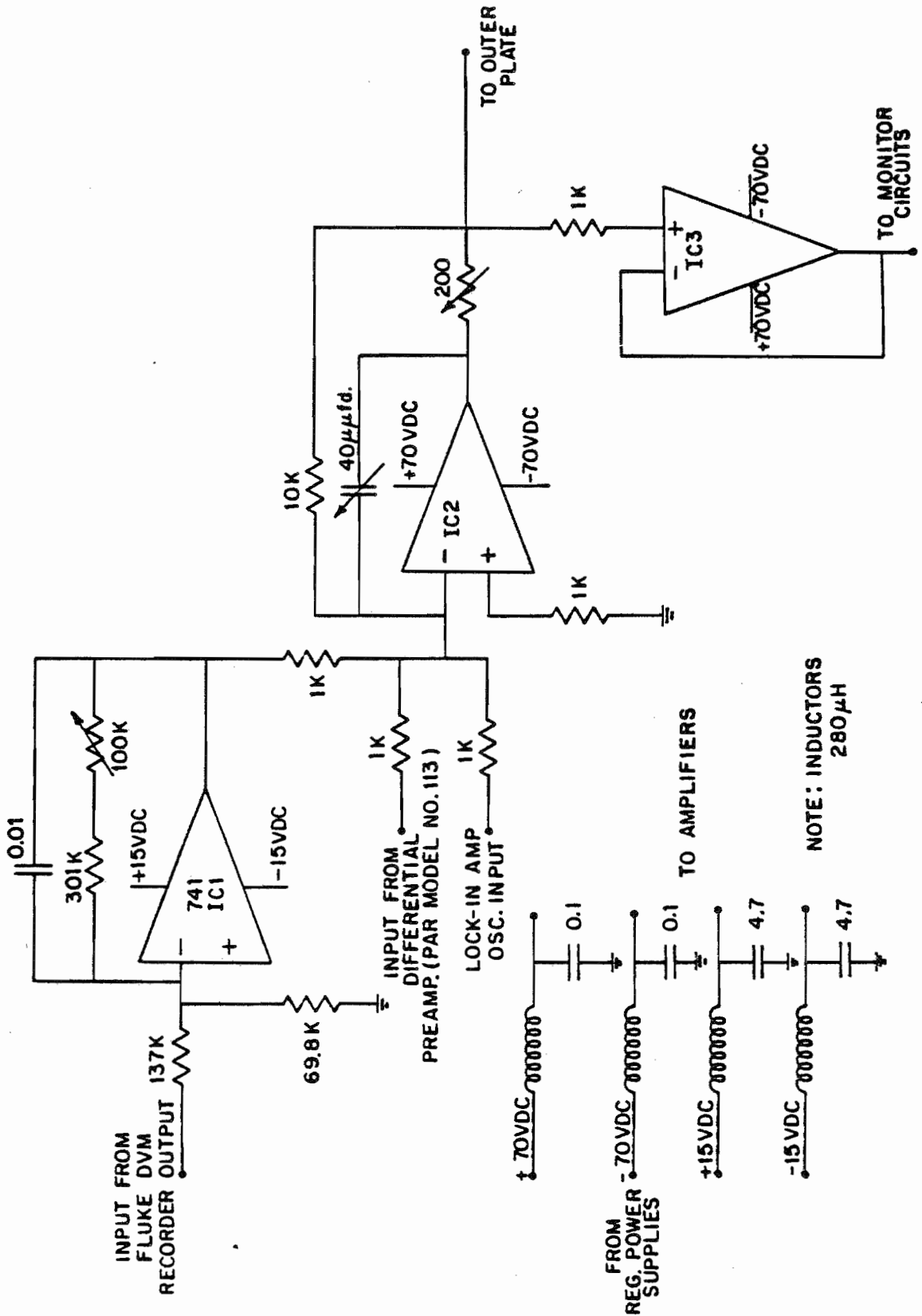
gives the energy, for example,  $-2.5643$  volts corresponds to an energy of  $2.5643$  MeV. This is only approximately correct. Minor corrections must be added for relativistic effects and for the acceleration of the beam into the analyzer. Calculations for these corrections are given by Westerfeldt (1977). If the voltage from the high voltage power supply drifts and the DVM goes off null, a signal from the recorder output goes to the inverting amplifier in the homogenizer to correct for this drift.

The difference amplifier is a Princeton Applied Research model 113 low noise preamplifier. The currents intercepted by the slits are converted to voltages by resistors. The voltages from the resistors are the input for the difference amplifier which has a variable gain. The amplifier has both an adjustable high and low pass filter on its output. The high pass filter is always set at d.c. and the the low pass filter and gain are adjusted as high as possible without inductions system oscillating.

The output of the difference amplifier goes to one of the inputs of the summing amplifier. Schematic diagrams for the summing amplifier are shown in Figure A.4. The summing amplifier IC2 also has an input from the inverting amplifier IC1. The recorder output voltage is amplified in IC1 and IC2 so that a change in high voltage to the analyzer inner plate which would change the beam energy by, say  $555$  eV, places  $5$  volts on the outer plate. The gain of the IC1 and



Figure A.4 Schematic Diagram of Inverter, Summing, and Buffer Amplifiers.



IC2 combination is set by adjusting the potentiometer in the feedback path of IC1 to obtain 5 volts on the outer plate of the analyzer with the DVM inputs shorted and its dial set to 555  $\mu$ V. This calibration requires periodic adjustment. The gain of the summing amplifier is -10 and the difference amplifier has a maximum output of 5 volts peak-to-peak. Therefore, the maximum possible 50 volt peak-to-peak variation on the outer plate corresponds to 5.55 keV energy fluctuations in the beam. This variation is abnormally large. More typically, 20 volts peak-to-peak on the outer plate is a value for a poorly running accelerator. The output of IC2 is trimmed by a small variable capacitor and resistor to aid in driving its capacitive load. The amplifier IC3 is used as a unity gain buffer. The buffer's output drives meters and monitor oscilloscopes. Nothing should be connected to the output of the summing amplifier IC2 except the analyzer outer plate. Any additional load impedance will adversely effect the operation of the homogenizer.

Once the feedback loop has been closed by connecting the slit difference signal to the outer plate through the summing amplifier, the difference signal represents a measure of the true energy fluctuations of the beam through the analyzer. This signal is also sent to the high voltage amplifier. This amplifier was first described by Posakony (1972) and has been modified for use in this application.

The schematic diagram is shown in Figure A.5. The gain of the amplifier from IC1 through the tube section is 2500. The divider on the input of IC1 is used to vary the gain for the correct ratio of outer plate voltage to target rod voltage. This calibration is accomplished by shorting the difference amplifier inputs to ground, grounding the input of the inverting amplifier and using the difference amplifier zero offset to drive the summing and high voltage amplifiers. Plots of high voltage to the target rod versus outer plate voltage should be made while adjusting the potentiometer  $V_2$  until a plot yields a slope of 1:1 which corresponds to the correct analyzer voltage to energy ratio.

The last element in the homogenizer is the magnet controller shown schematically in Figure A.6. This amplifier system drives the field offset input of the analyzing magnet power supply of the corona control system. This input only responds to signals which have a frequency below 0.02 Hz on the 200 gauss range of the field offset normally used. Plate voltage is changed on the analyzer and the beam moves off center generating a small difference signal. This signal will drive the magnet to a higher current, which forces the corona control circuit to increase the accelerator energy. This system allows only one control to change the energy of the entire system automatically. This controller has a limited energy range of approximately 20 keV. The corona control system and homogenizer systems

Figure A.5 High Voltage Amplifier Schematic Diagram.

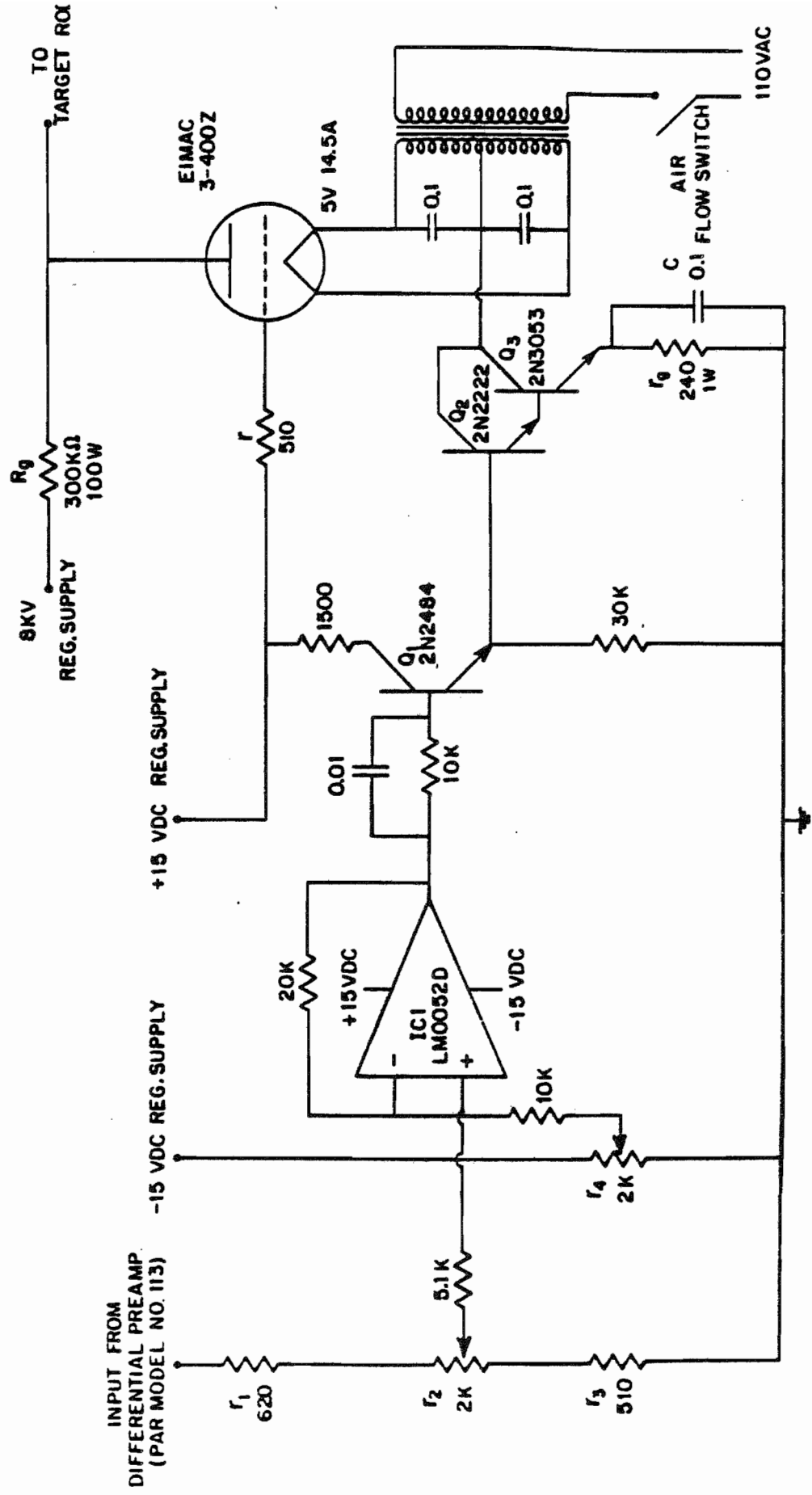
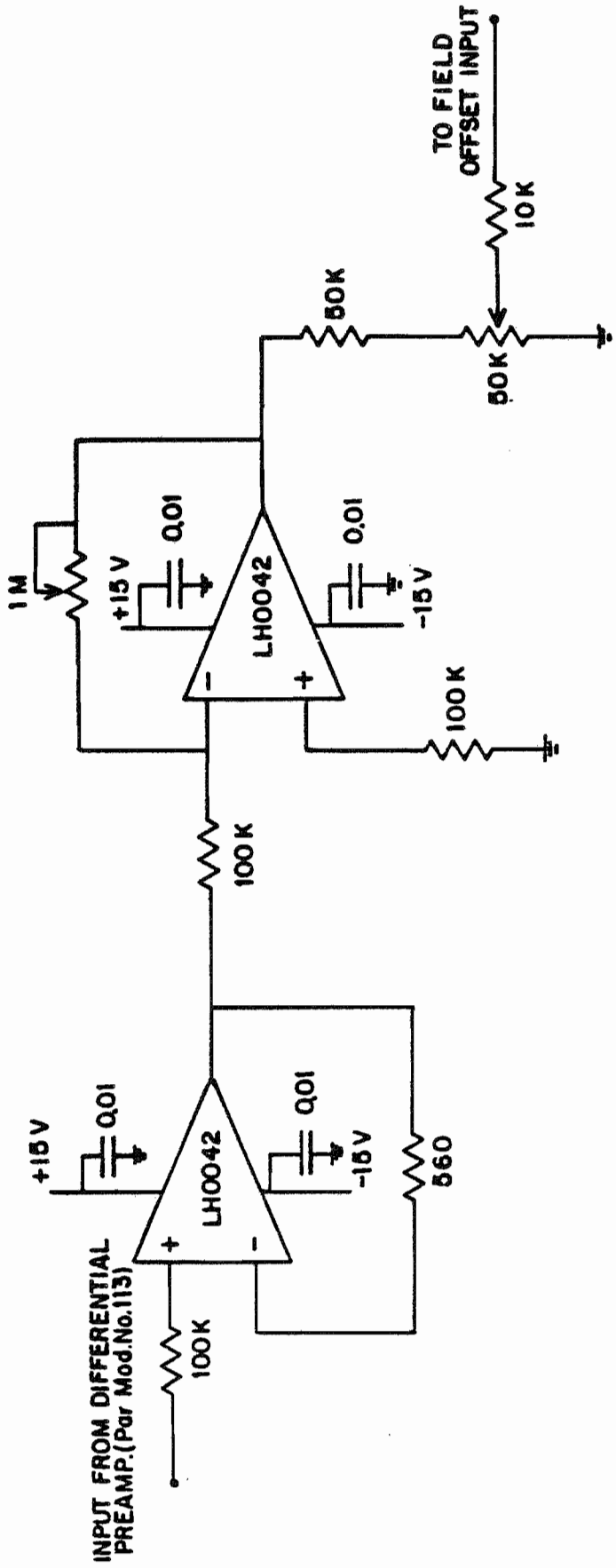


Figure A.6 Magnetic Controller Schematic Diagram.





are weakly coupled via the magnet controller and oscillations will occur if the gain of the magnet controller is too high.

#### A.4 Feedback Analysis

Instability of the magnet control system is only a small fraction of the problem that must be solved in order to keep the control systems stable. In any control system, the closed loop gain has to be less than unity when the total phase shift of the system is  $2\pi$ , or the system will go into uncontrolled oscillations. The gain or transfer function of any passive or active electronic or mechanical system can be defined in terms of a linear transformation which acts on the input to produce an output. This transfer function relates the magnitudes of the input and output and the time delay between them. If signals can be represented as a Fourier series, only sinusoidal inputs and outputs need be considered. The transfer function is then given by

$$\frac{V_o(\omega)}{V_i(\omega)} = |A(\omega)| e^{i\varphi(\omega)}$$

where  $V_o(\omega)$  is the output signal,  $V_i(\omega)$  is the input signal,  $|A(\omega)|$  is the gain of the system, and  $\varphi(\omega)$  is the phase shift between the input and outputs.  $\omega$  is the angular frequency of these signals in radians per second.

In the study of the characteristics of any system where

the transfer function model is applicable, the system may be modeled with the transfer functions of the components of the system. The stability of the system is guaranteed as long as any string of transfer functions which closes upon itself obeys the criterion

$$\prod_i |A_i(\omega)| > 1$$

WHEN  $\sum_i \varphi_i(\omega) \geq 2\pi$

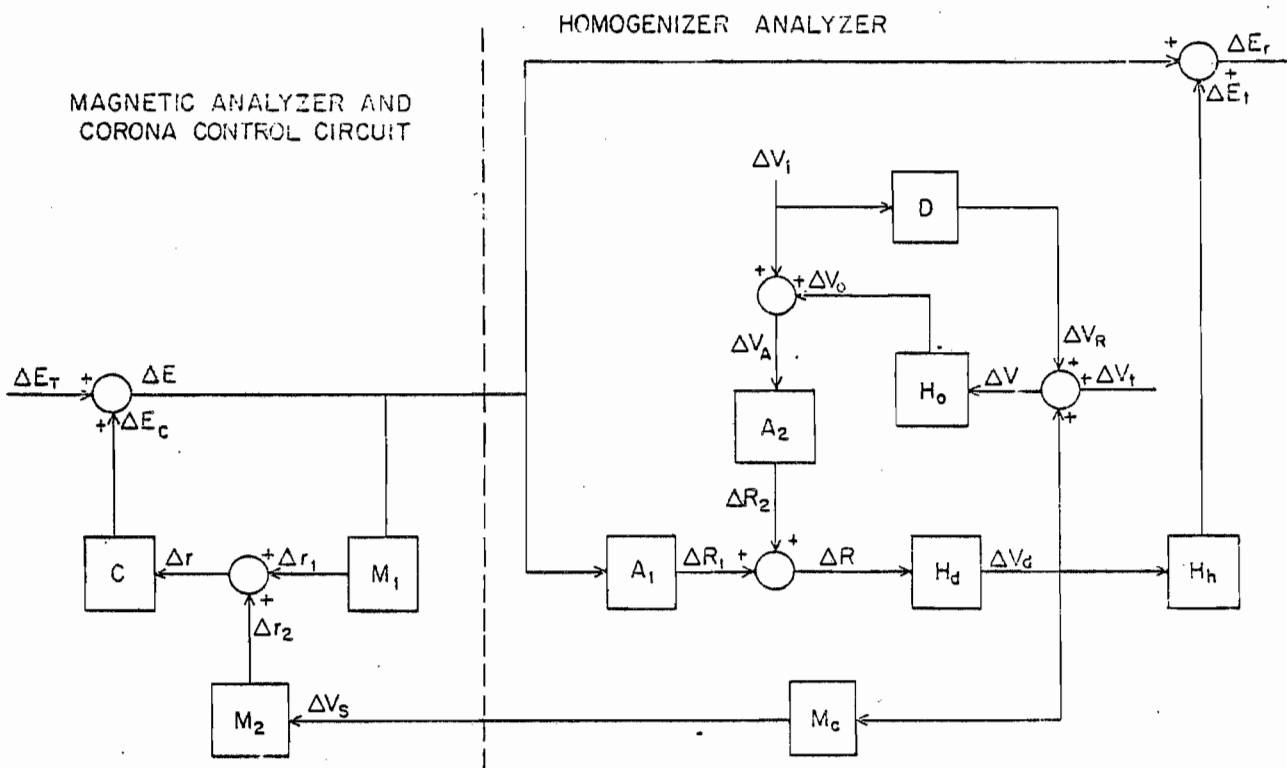
$|A_i(\omega)|$  is the transfer function of the  $i^{\text{th}}$  component and  $\varphi_i(\omega)$  is its phase shift. More complete discussions of servo control systems and conditions for the stability of these systems can be found in books by Kuo (1962) and Thaler and Brown (1960).

Reference to Figure A.7 gives the schematic diagram of the homogenizer row in use in the TUNL 3 MV accelerator laboratory. Boxes represent transfer functions and circles represent summing points. The letters in the boxes are the complex representations of the transfer function as a function of angular frequency. Letters on lines represent signals and the arrows give the direction of signal flow. The definitions of the signals and transfer functions are:

$\Delta V_i$  are the fluctuations in the d.c. high voltage power supply.

$\Delta V_e$  is the output of the inverting amplifier.

Figure A.7 Block Diagram of the Control Systems in the 3 MV Laboratory.



$\Delta V_d$  is the output of the difference amplifier.

$\Delta V_t$  is the test input to the homogenizer (normally zero when the system is operation).

$\Delta V$  is the sum of  $\Delta V_2$ ,  $\Delta V_d$ , and  $\Delta V_t$ .

$\Delta V_s$  is the output of the summing amplifier.

$\Delta V_a$  is the total voltage fluctuation across the analyzer, the sum of  $\Delta V_i$  and  $\Delta V_o$ .

$\Delta V_m$  is the output of the magnet controller.

$\Delta R$  is the total fluctuation in the beam position at the output of the analyzer, the sum of  $\Delta R_1$  and  $\Delta R_2$ .

$\Delta R_1$  is the component of the beam position fluctuation due to changes in input energy.

$\Delta R_2$  is the component of beam position fluctuations due to changes in voltage across the analyzer.

$\Delta r$  is the change in position of the beam at the corona control slits due to energy fluctuations.

$\Delta r_i$  is the change in position of beam at the corona control slits due to signals from the magnet controller.

$\Delta r$  is the sum of  $\Delta r_1$  and  $\Delta r_i$ .

$\Delta E_t$  is the total unregulated energy fluctuations on the Van de Graaff accelerator.

$\Delta E_c$  is the correction signal for energy fluctuations supplied by the corona control circuit.

$\Delta E$  is the residual energy fluctuations remaining after corrections by the corona control circuit.

$\Delta E_t$  is the correction signal for energy fluctuations

supplied by the homogenizer.

$\Delta E_r$  is the residual energy fluctuations remaining after corrections by the homogenizer.

D is the transfer function of the high voltage power supply stabilizer.

$H_o$  is the transfer function of the summing amplifier.

$H_d$  is the transfer function of slits, resistors and difference amplifier (PAR Model 113).

$H_h$  is the transfer function of the high voltage amplifier.

$M_c$  is the transfer function of the magnet controller.

$A_1$  and  $A_2$  are the transfer functions of the electrostatic analyzer defined as

$$A_1 \equiv \left. \frac{\partial R}{\partial E} \right)_{V_A} \quad A_2 \equiv \left. \frac{\partial R}{\partial V_A} \right)_{E}$$

$M_1$  and  $M_2$  are the transfer functions of the analyzing magnet defined as

$$M_1 \equiv \left. \frac{\partial r}{\partial E} \right)_{\Delta V_s} \quad M_2 \equiv \left. \frac{\partial r}{\partial \Delta V_s} \right)_{E}$$

C is the transfer function of the corona amplifier.

With analysis similar to that of section A.2 one can obtain a relation for  $\Delta R / \Delta E$

$$\Delta R = \frac{\Delta E A_1 + \Delta V_i (1 + D H_o A_2) + \Delta V_t H_o A_2}{1 - H_d H_o A_2} \quad (A.4.1)$$

The effects of  $\Delta V_i$  can be eliminated if

$$D = -1/H_0 A_2 \quad (\text{A.4.2})$$

Equation (A.4.2) is the requirement that the inverting and summing amplifier have combined gains so that a 555  $\mu\text{V}$  offset of the differential voltmeter puts 5 volts on the outer plate. Since  $\Delta V_t$  is zero during operation equations (A.4.1) and (A.4.2) give

$$\frac{\Delta R}{\Delta E} = \frac{A_1}{1 - H_d H_0 A_2} \quad (\text{A.4.3})$$

Regulation factors can be defined as

$$R = \frac{\Delta E_r}{\Delta E} \quad (\text{A.4.4})$$

The factor  $R$  is the percentage of the energy fluctuations remaining on the target and should be small if the system is to work correctly. From figure A.7, the value of  $\Delta E_r$  is

$$\Delta E_r = \Delta E - H_n H_d \Delta R \quad (\text{A.4.5})$$

or

$$\frac{\Delta E_r}{\Delta E} = R = 1 - \frac{\Delta R}{\Delta E} H_d H_n$$

Using  $\Delta R/\Delta E$  from equation (A.4.3)

$$R = \frac{1}{1 + H_d H_n A_2} \quad (\text{A.4.6})$$

The gain of the high voltage amplifier must be calibrated so that the voltage applied to the target is  $2/\ln(R_0/R_i)$  times the voltage applied to the analyzer outer plate. Using the approximation for the ratio

$$H_n = -\frac{A_2}{A_1} H_o \quad (A.4.7)$$

From equations (A.4.6) and (A.4.7) the regulation factor is

$$R = \frac{1}{1 + H_d H_n A_2} \quad (A.4.8)$$

If there were no phase lags in the system (all transfer functions are real)  $R$  could be made arbitrarily small. However, since there are phase lags  $R$  could be made extremely large if the denominator of equation (A.4.8) became small. This corresponds to oscillations in the system. A similar analysis can be performed to give the regulation factor for the corona control circuit. One obtains for  $\Delta E$

$$\Delta E = \Delta E_T + \Delta r C \quad (A.4.9)$$

and for  $\Delta r$

$$\Delta r = \Delta E \left( M_1 + \frac{M_2 M_c H_d A_1}{(1 - H_d H_o A_2)} \right) \quad (A.4.10)$$

The regulation factor for the corona control circuit is

$$\frac{\Delta E}{\Delta E_T} \equiv R_c = \frac{1}{1 - M_1 C - \frac{M_2 M_c H_d A_1 C}{(1 - H_d H_o A_2)}} \quad (A.4.11)$$

In equation (A.4.11) for  $R_c$  the term containing  $M_c$ , the transfer function for the magnet controller, couples the



corona control system and the homogenizer.  $|M_c|$  must remain small or instabilities in  $R_c$  will result. In practice this requirement is not difficult to meet as long as the corona system does not change the accelerator energy by more than 30 keV. The coupling is only for low frequencies (less than 0.02 Hz). This system has been used with the outer plate capacitively coupled to the summing amplifier and only the magnet controller supplying the d.c. stability for the system. No resolution degradation was observed. The regulation factor for the corona control system and homogenizer is

$$R_T = R_c R = \frac{1}{\left(1 - M_1 C - \frac{M_2 M_c H_d H_1 C}{1 - H_d H_o A_z}\right) \left(1 + H_d H_k A_z\right)} \quad (\text{A.4.12})$$

### I.5 Conclusions and Recommendations for Improvements

This system is composed of semiconductor integrated circuits except for three transistors and one vacuum tube. It has proven highly reliable. The present system is modular and new ideas for improvements in electronics can be tested without disrupting the system. The current load resistor in the high voltage amplifier needs to have its maximum power dissipation increased. The precision divider in the control room should be placed near the shielded stack to prevent temperature differences from affecting the energy calibration. The environment of the divider should be more

carefully regulated to prevent energy shifts due to temperature changes.

More comprehensively, a control system similar to one described by Bloch (1968) could be added to the system. The Bloch system monitors the beam position after it has been sent through an analysing magnet and regulates the beams position by changing its energy. The energy of the beam is changed by modulating the focus ring of the accelerator with energy information sent to the high voltage terminal encoded on a light beam. This would allow the direct measurement of the resolution of the proton beam by looking at the signals sent to the outer plate of the analyzer by the present system. Any residual fluctuations, which should be small, could be easily removed. The combination of the two types of regulators would give as monoenergetic an ion beam as possible with a Van de Graaff accelerator. This very monoenergetic beam would be very useful in studying target and ion source contributions to resolution. Another advantage of the Bloch type system is that other ion beams with only one ionization state could be used in the high resolution mode of the 3 MV accelerator with the same target chamber facilities.

## Appendix B

This appendix lists the p-wave resonance parameters determined from the analysis of the scattering data from  $^{56}\text{Fe}(p,p')^{56}\text{Fe}$  and  $^{48}\text{Ti}(p,p')^{48}\text{Ti}$ . The parameters determined from elastic scattering are taken from Prochnow (1971). Resonances with no inelastic scattering yield or which had inconsistent mixing ratios as determined from the analysis have no inelastic width entries. Resonances with spin assignments in parenthesis have uncertain assignments. Those spin assignments which are followed by an asterisk have had spin assignments changed. Uncertainties in the elastic and inelastic widths are less than 25%. The procedures used to determine these resonance parameters are discussed in Chapter 4.

Table B.1

Res. No.	$E_p$ (Mev)	$J^\pi$	$\Gamma_p$ (eV)	$\gamma_p^2$ (keV)	$\Gamma_{p'}$ (eV)	$\gamma_{p'}^2$ (keV)
1	2.0776	(1/2-)	20.	2.78		
2	2.4111	1/2-	50.	2.18		
3	2.4357	(1/2-)	12.	0.48		
4	2.4920	(1/2-)	20.	0.68		
5	2.5131	3/2- *	20.	0.63	1.10	1.112
6	2.5340	1/2-	1350.	41.00	0.63	0.570
7	2.5597	3/2-	25.	0.70	4.50	3.506
8	2.5760	1/2-	40.	1.07		
9	2.5976	(1/2-)	20.	0.51		
10	2.6765	(1/2-)	20.	0.41		
11	2.6883	(1/2-)	30.	0.60		
12	2.7146	3/2- *	30.	0.56	2.50	0.885
13	2.7146	1/2-	15.	0.28	10.00	3.253
14	2.7844	3/2-	15.	0.24	8.60	2.208
15	2.7965	3/2-	15.	0.23	8.50	2.068
16	2.8244	3/2- *	15.	0.21	1.60	0.345
17	2.8290	3/2-	55.	0.79		
18	2.8299	3/2- *	12.	0.17	1.20	0.252
19	2.8365	3/2-	10.	0.14	2.80	0.573
20	2.8572	3/2-	10.	0.13	2.80	0.525
21	2.8591	3/2-	10.	0.13	2.10	0.390
22	2.8600	3/2- *	40.	0.53	0.90	0.167
23	2.8763	1/2-	50.	0.64		
24	2.8878	3/2- *	12.	0.15	4.40	0.726
25	2.9054	3/2-	75.	0.90	70.00	10.756
26	2.9297	(1/2-)	15.	0.17		
27	2.9388	3/2- *	45.	0.50	7.00	0.942
28	2.9444	(3/2-)	20.	0.20		
29	2.9791	3/2-	15.	0.15	9.70	1.117

Table B.1

Res. No.	$E_p$ (MeV)	$J^\pi$	$\Gamma_p$ (eV)	$\gamma_p^2$ (keV)	$\Gamma_{p'}$ (eV)	$\gamma_{p'}^2$ (keV)
30	2.9876	3/2- *	15.	0.15	2.70	0.301
31	2.9997	3/2- *	50.	0.49	12.80	1.364
32	3.0098	3/2-	250.	2.42	140.00	14.367
33	3.0120	3/2- *	20.	0.19	12.80	1.303
34	3.0472	(1/2-)	20.	0.18		
35	3.0656	3/2- *	30.	0.26	2.20	0.184
36	3.0673	(1/2-)	70.	0.60		

Table B.2

Res. No.	Exp.	$a_2$	$\delta_{j_1}$	$\delta_{s_1}$	$\phi_{j_1}$	$\phi_{s_1}$
5	GAMM	0.450+OR-0.034	-0.334+ - 0.117	-7.048+ -18.166	-18.5+8.20 -5.80	-81.9+8.20 -5.80
5	PROT	0.479+OR-0.086	-0.500+ - 0.454	99999+ - 0.000	-26.6+0.01 -0.00	-90.0+ 17. -0.00
7	GAMM	0.112+OR-0.036	-1.861+ - 0.501	1.419+ - 0.282	-61.7+4.72 -5.31	54.8+4.72 -5.31
7	PROT	-0.271+OR-0.082	-2.735+ - 0.896	1.059+ - 0.160	-69.9+4.73 -4.69	46.6+4.73 -4.69
12	GAMM	0.256+OR-0.037	0.977+ - 0.135	-0.346+ - 0.085	44.3+4.23 -4.24	-19.1+4.23 -4.24
12	PROT	-0.493+OR-0.069	0.573+ - 0.093	-0.665+ - 0.110	29.8+4.43 -4.16	-33.6+4.43 -4.16
14	GAMM	0.498+OR-0.035	0.056+ - 0.056	-1.750+ - 0.250	3.2+ 12. -3.18	-60.3+ 12. -3.18
14	PROT	-0.074+OR-0.082	0.087+ - 0.098	-1.629+ - 0.426	5.0+5.09 -5.60	-58.5+5.09 -5.60
15	PROT	0.139+OR-0.086	-0.866+ - 0.291	-3.914+ - 99995	-40.9+ 14. - 14.	-75.7+8.27 - 14.
15	GAMM	0.404+OR-0.036	-0.486+ - 0.113	89.90+81.046 - 103.0	-25.9+5.80 - 175	-89.4+5.80 - 175
16	GAMM	0.486+OR-0.036	0.168+ - 0.168	-1.370+ - 0.630	9.6+8.89 -9.56	-53.9+8.89 -9.56
16	PROT	-0.365+OR-0.076	0.408+ - 0.086	-0.877+ - 0.144	22.2+4.44 -4.35	-41.3+4.44 -4.35

Table B.2

Res. No.	Exp.	$a_2$	$\delta_j'$	$\delta_B'$	$\phi_j'$	$\phi_B'$
18	PROT	-0.086+0R-0.076	-1.657+ - 0.353	1.580+ - 0.253	-58.9+5.06 -4.66	57.7+5.06 -4.66
18	GAMM	0.146+0R-0.036	-1.558+ - 0.325	1.682+ - 0.278	-57.3+4.39 -4.72	59.3+4.39 -4.72
19	GAMM	0.135+0R-0.035	-1.644+ - 0.358	1.593+ - 0.260	-58.7+4.38 -4.77	57.9+4.38 -4.77
19	PROT	0.031+0R-0.080	-1.227+ - 0.281	2.220+ - 0.480	-50.8+6.89 -5.64	65.8+6.89 -5.64
20	GAMM	0.105+0R-0.036	-1.936+ - 0.551	1.370+ - 0.241	-62.7+4.76 -5.41	53.9+4.76 -5.41
20	PROT	0.056+0R-0.083	-1.145+ - 0.284	2.439+ - 0.593	-48.9+7.99 -6.15	67.7+7.99 -6.15
21	GAMM	0.495+0R-0.035	0.095+ - 0.095	-1.600+ - 0.400	5.4+ 10. -5.44	-58.0+ 10. -5.44
21	PROT	0.126+0R-0.093	-0.190+ - 0.310	-3.532+ - 99995	-10.8+8.35 - 15.	-74.2+8.35 - 15.
22	GAMM	0.188+0R-0.036	-1.287+ - 0.228	2.089+ - 0.357	-52.1+4.25 -4.42	64.4+4.25 -4.42
22	PROT	-0.246+0R-0.078	-2.536+ - 0.721	1.114+ - 0.161	-68.5+4.53 -4.45	48.1+4.53 -4.45
24	GAMM	0.292+0R-0.035	0.843+ - 0.118	-0.431+ - 0.090	40.1+4.08 -4.19	-23.3+4.08 -4.19
24	PROT	-0.653+0R-0.067	0.866+ - 0.142	-0.415+ - 0.106	40.9+6.07 -4.98	-22.5+6.07 -4.98

Table B.2

Res. No.	Exp.	$a_2$	$\delta_j$	$\delta_s$	$\phi_j$	$\phi_s$
25	GAMM	0.309+0R-0.035	0.787+ - 0.114	-0.471+ - 0.095	38.2+4.12 -4.27	-25.2+4.12 -4.27
25	PROT	-0.604+0R-0.069	0.757+ - 0.122	-0.494+ - 0.106	37.1+5.38 -4.69	-26.3+5.38 -4.69
27	GAMM	0.110+0R-0.036	1.887+ - 0.326	-0.024+ - 0.083	62.1+5.32 -4.72	-1.4+5.32 -4.72
27	PROT	-0.766+0R-0.062	1.321+ - 0.305	-0.187+ - 0.138	52.9+10. -7.41	-10.6+10. -7.41
29	GAMM	0.258+0R-0.036	0.969+ - 0.131	-0.351+ - 0.084	44.1+4.13 -4.15	-19.3+4.13 -4.15
29	PROT	-0.509+0R-0.071	0.595+ - 0.099	-0.641+ - 0.113	30.8+4.70 -4.36	-32.7+4.70 -4.36
30	GAMM	0.441+0R-0.035	-0.366+ - 0.115	-8.843+ -56.974	-20.1+7.39 -5.58	-83.5+7.39 -5.58
30	PROT	0.364+0R-0.082	-0.500+ - 0.441	99999+ - 0.000	-26.6+0.01 -0.00	90.0+16. -0.00
31	GAMM	0.375+0R-0.036	-0.578+ - 0.111	16.481+ -53.749	-30.0+5.01 -174	86.5+4.54 -174
31	PROT	0.264+0R-0.087	-0.500+ - 0.457	99999+ - 0.000	-26.6+0.01 -0.00	90.0+17. -0.00
32	GAMM	0.236+0R-0.036	-1.056+ - 0.168	2.748+ - 0.521	-46.6+4.15 -4.18	70.0+4.15 -4.18
32	PROT	-0.035+0R-0.084	-1.459+ - 0.345	1.803+ - 0.344	-55.6+6.17 -5.42	61.0+6.17 -5.42



Table B.2

Res. No.	Exp.	$a_2$	$\delta_j$	$\delta_s$	$\phi_j$	$\phi_s$
33	GAMM	0.354+OR-0.036	-0.642+ - 0.111	9.286+31.722 - 3.920	-32.7+4.75 -4.41	83.9+4.75 -4.41
33	PROT	0.180+OR-0.085	-0.691+ - 0.324	7.041+ 99991 - 4.116	-34.6+8.08 - 10.	81.9+8.08 - 10.
35	GAMM	0.216+OR-0.037	-1.146+ - 0.190	2.436+ 0.622 - 0.440	-48.9+4.21 -4.30	67.7+4.21 -4.30
35	PROT	-0.139+OR-0.083	-1.896+ - 0.471	1.395+ 0.308 - 0.226	-62.2+5.21 -4.90	54.4+5.21 -4.90

Table B.3

Res. No.	$\delta_{j'}$	$\delta_{s'}$	$\Phi_{j'}$	$\Phi_{s'}$
5	-0.396+ 0.10 - 0.24	-28.832+25.41 -18.16	-21.6+4.9 - 11	-88.0+ 14 -0.8
7	-2.174+ 0.41 - 0.64	1.203+ 0.23 - 0.19	-65.3+4.8 -5.2	50.3+4.8 -5.0
12	0.738+ 0.13 - 0.11	-0.485+ 0.09 - 0.10	36.4+4.4 -4.3	-25.9+4.4 -4.3
14	0.075+ 0.15 - 0.08	-1.682+ 0.45 - 0.35	4.3+8.1 -4.6	-59.3+8.2 -4.5
15	-0.585+ 0.18 - 0.16	-89.745+80.90 - 286.	-30.3+8.5 -6.3	-89.4+5.8 -0.5
16	0.324+ 0.12 - 0.11	-0.983+ 0.18 - 0.25	18.0+5.9 -6.1	-44.5+5.8 -6.4
18	-1.604+ 0.26 - 0.34	1.631+ 0.35 - 0.27	-58.1+4.7 -4.7	58.5+4.7 -4.7
19	-1.423+ 0.26 - 0.32	1.769+ 0.50 - 0.32	-54.9+5.5 -5.2	60.5+5.7 -5.2
20	-1.451+ 0.30 - 0.39	1.581+ 0.51 - 0.31	-55.4+6.5 -6.0	57.7+6.8 -5.9
21	-0.016+ 0.18 - 0.18	-1.600+ 0.52 - 1.32	-0.9+ 10 - 10	-58.0+ 10 - 13
22	-1.602+ 0.26 - 0.35	1.407+ 0.28 - 0.22	-58.0+4.7 -4.9	54.6+4.7 -4.7
24	0.853+ 0.16 - 0.13	-0.424+ 0.10 - 0.10	40.5+4.9 -4.5	-23.0+4.9 -4.5
25	0.774+ 0.14 - 0.12	-0.481+ 0.10 - 0.10	37.7+4.7 -4.5	-25.7+4.7 -4.5
27	1.626+ 0.59 - 0.32	-0.081+ 0.13 - 0.10	58.4+7.3 -5.8	-4.6+7.2 -5.7
29	0.757+ 0.13 - 0.11	-0.473+ 0.09 - 0.10	37.1+4.5 -4.3	-25.3+4.5 -4.3
30	-0.415+ 0.09 - 0.23	52.885+66.50 -56.94	-22.6+4.5 - 10	88.9+0.6 - 16
31	-0.553+ 0.07 - 0.22	79.562+72.46 -53.72	-28.9+3.4 -8.9	89.3+0.3 -1.5
32	-1.188+ 0.19 - 0.23	2.194+ 0.66 - 0.42	-49.9+5.0 -4.8	65.5+5.2 -4.9
33	-0.657+ 0.14 - 0.18	9.285+67.34 - 3.92	-33.3+5.8 -6.6	83.9+5.4 -4.4
35	-1.367+ 0.22 - 0.27	1.743+ 0.41 - 0.30	-53.8+4.8 -4.8	60.2+5.0 -4.8

Table B.4

Res. No.	$\gamma_{j_1}^2$ (keV)	$\gamma_{j_3}^2$ (keV)	$\gamma_{j_1} \gamma_{j_3}$ (keV)	$\gamma_{s_3}^2$ (keV)	$\gamma_{s_5}^2$ (keV)	$\gamma_{s_3} \gamma_{s_5}$ (keV)
5	0.9613	0.1509	-0.3809	0.0013	1.1109	-0.0385
7	0.6121	2.8939	-1.3310	1.4328	2.0733	1.7235
12	0.5730	0.3119	0.4228	0.7167	0.1683	-0.3473
14	2.1957	0.0122	0.1637	0.5765	1.6313	-0.9698
15	1.5401	0.5279	-0.9017	0.0003	2.0678	-0.0230
16	0.3119	0.0327	0.1011	0.1753	0.1693	-0.1723
18	0.0706	0.1818	-0.1133	0.0690	0.1835	0.1125
19	0.1892	0.3834	-0.2693	0.1387	0.4339	0.2453
20	0.1689	0.3557	-0.2451	0.1498	0.3747	0.2370
21	0.3902	0.0001	-0.0062	0.1097	0.2806	-0.1754
22	0.0467	0.1199	-0.0749	0.0559	0.1107	0.0787
24	0.4205	0.3057	0.3585	0.6155	0.1106	-0.2610
25	6.7290	4.0267	5.2053	8.7316	2.0241	-4.2040
27	0.2584	0.6833	0.4202	0.9357	0.0061	-0.0756
29	0.7100	0.4070	0.5376	0.9125	0.2045	-0.4320
30	0.2568	0.0443	-0.1067	0.0001	0.3010	0.0057
31	1.0448	0.3191	-0.5774	0.0002	1.3637	0.0171
32	5.9574	8.4098	-7.0782	2.4710	11.8962	5.4218
33	0.9099	0.3930	-0.5980	0.0149	1.2880	0.1387
35	0.0643	0.1202	-0.0879	0.0457	0.1387	0.0796

Table B.5

Res. No.	$E_p$ (MeV)	$J^\pi$	$\Gamma_p$ (eV)	$\gamma_p^2$ (keV)	$\Gamma_{p'}$ (eV)	$\gamma_{p'}^2$ (keV)
1	1.9019	(3/2-)	15.	1.08		
2	1.9093	(1/2-)	15.	1.05		
3	1.9240	3/2-	30.	1.99		
4	1.9255	(3/2-)	20.	1.32		
5	1.9787	(1/2-)	25.	1.35		
6	2.0323	3/2- *	10.	0.45	0.62	9.793
7	2.0777	3/2- *	130.	5.07	0.36	3.617
8	2.0935	(1/2-)	25.	0.92		
9	2.1014	3/2- *	10.	0.36	0.28	2.312
10	2.1142	(1/2-)	15.	0.52		
11	2.1163	(1/2-)	5.	0.17		
12	2.1496	3/2- *	25.	0.78	0.37	1.941
13	2.1702	1/2-	40.	1.16		
14	2.1805	(1/2-)	20.	0.55		
15	2.1903	1/2-	60.	1.65		
16	2.1936	3/2- *	7.	0.19	0.15	0.561
17	2.2108	(1/2-)	10.	0.26		
18	2.2121	(1/2-)	20.	0.51		
19	2.2296	3/2- *	10.	0.25	0.09	0.243
20	2.2308	1/2-	25.	0.61	0.22	0.505
21	2.2577	(1/2-)	20.	0.45		
22	2.2638	1/2-	90.	2.00	0.12	0.221
23	2.2661	3/2- *	5.	0.11	0.04	0.094
24	2.2806	3/2-	25.	0.53	1.92	3.630
25	2.2912	1/2-	30.	0.62		
26	2.2968	3/2-	25.	0.51	0.78	1.309
27	2.3228	(1/2-)	10.	0.19		
28	2.3401	(1/2-)	15.	0.27		
29	2.3493	1/2-	75.	1.32		

Table B.5

Res. No.	$E_p$ (Mev)	$J^\pi$	$\Gamma_p$ (eV)	$\gamma_p^2$ (keV)	$\Gamma_{p'}$ (eV)	$\gamma_{p'}^2$ (keV)
30	2.3709	3/2- *	70.	1.17	0.07	0.075
31	2.3731	3/2- *	5.	0.08	2.28	2.294
32	2.3780	3/2- *	5.	0.08	0.94	0.916
33	2.3890	3/2- *	15.	0.24	2.45	2.224
34	2.3969	3/2- *	10.	0.16	0.83	0.717
35	2.4008	3/2- *	15.	0.23	0.31	0.257
36	2.4028	3/2- *	5.	0.08	0.23	0.195
37	2.4248	1/2-	50.	0.73		
38	2.4376	3/2-	30.	0.42	0.62	0.415
39	2.4477	1/2-	25.	0.34	1.60	0.918
40	2.4487	3/2- *	25.	0.34	3.89	2.448
41	2.4624	3/2-	30.	0.40	3.41	1.977
42	2.4660	1/2-	225.	2.96		
43	2.4776	3/2-	20.	0.26	2.52	1.337
44	2.4820	3/2-	55.	0.70	0.59	0.303
45	2.4850	1/2-	15.	0.19	2.04	0.932
46	2.5004	3/2- *	15.	0.18	0.18	0.086
47	2.5221	1/2-	75.	0.87	6.75	2.477
48	2.5344	3/2- *	5.	0.06	6.85	2.652
49	2.5380	3/2-	30.	0.33	0.74	0.281
50	2.5657	3/2-	15.	0.16	3.99	1.307
51	2.5734	3/2- *	80.	0.82	1.21	0.380
52	2.5773	1/2-	100.	1.02	4.51	1.275
53	2.5872	3/2- *	150.	1.50	4.91	1.438
54	2.6008	3/2- *	90.	0.87	1.40	0.383
55	2.6081	3/2- *	5.	0.05	5.00	1.318
56	2.6107	3/2-	70.	0.66	9.46	2.462
57	2.6358	3/2-	100.	0.90	13.26	3.047

Table B.5

Res. No.	$E_p$ (MeV)	$J^\pi$	$\Gamma_p$ (eV)	$\gamma_p^2$ (keV)	$\Gamma_{p'}$ (eV)	$\gamma_{p'}^2$ (keV)
58	2.6371	1/2-	25.	0.22	9.00 <sup>9</sup>	1.892
59	2.6525	1/2-	75.	0.65		
60	2.6641	3/2- *	7.	0.06	0.59	0.118
61	2.6915	1/2-	290.	2.32		
62	2.6964	3/2-	50.	0.40	2.59	0.447
63	2.7007	3/2- *	15.	0.12	4.60	0.778
64	2.7035	3/2- *	15.	0.12	1.00	0.167
65	2.7056	3/2-	150.	1.17	12.56 <sup>25</sup>	2.078
66	2.7153	3/2-	30.	0.23	9.69 <sup>2</sup>	1.534
67	2.7184	1/2-	145.	0.55	3.23	0.505
68	2.7198	3/2-	5.	0.01	0.99	0.153
69	2.7235	3/2-	60.	0.45	0.77	0.118
70	2.7295	1/2-	275.	2.04		
71	2.7462	3/2-	150.	1.08	9.27	1.280
72	2.7563	3/2- *	10.	0.07	3.69	0.488
73	2.7596	3/2-	10.	0.07	0.80	0.104
74	2.7699	3/2- *	15.	0.10	6.78 <sup>(25)</sup>	0.845
75	2.7784	1/2-	175.	1.18	1.73	0.388
76	2.7866	3/2- *	15.	0.10	0.57	0.066
77	2.8117	3/2-	55.	0.35	18.39 <sup>26</sup>	1.922
78	2.8175	3/2- *	15.	0.09	2.15	0.220
79	2.8259	3/2-	25.	0.15	7.00 <sup>7</sup>	0.690
80	2.8330	3/2-	30.	0.18	12.00 <sup>12</sup>	1.150
81	2.8355	3/2- *	35.	0.21	1.23	0.117
82	2.8369	3/2- *	25.	0.15	2.53	0.238
83	2.8416	3/2-	110.	0.66	9.95 <sup>9</sup>	0.922
84	2.8468	1/2-	750.	4.46		
85	2.8514	1/2-	250.	1.47		
86	2.8539	3/2-	20.	0.12	6.00 <sup>6</sup>	0.529

Table B.5

Res. No.	$E_p$ (MeV)	$J^\pi$	$\Gamma_p$ (eV)	$\gamma_p^2$ (keV)	$\Gamma_{p'}$ (eV)	$\gamma_{p'}^2$ (keV)
87	2.8553	1/2-	1500.	8.78	40.00 <sup>40</sup>	3.255
88	2.8679	1/2-	900.	5.15		
89	2.8938	(1/2-)	10.	0.05		
90	2.8992	(1/2-)	10.	0.05		
91	2.9007	3/2-	40.	0.22	14.69 <sup>7</sup>	1.080
92	2.9107	3/2- *	7.	0.04	8.08	0.572
93	2.9147	3/2-	100.	0.53	10.53 <sup>13</sup>	0.734
94	2.9336	1/2-	20.	0.10	2.00	0.120
95	2.9393	3/2-	85.	0.43	8.08	0.514
96	2.9443	3/2-	300.	1.50	63.53 <sup>6</sup>	3.971
97	2.9453	3/2-	275.	1.37	14.32 <sup>30</sup>	0.892
98	2.9533	3/2-	2800.	13.81	270.00 <sup>10</sup>	16.333
99	2.9651	3/2-	250.	1.21	6.08	0.353
100	2.9679	3/2-	70.	0.34	23.43 <sup>11</sup>	1.345
101	2.9736	3/2-	40.	0.19	23.01 <sup>12</sup>	1.294
102	2.9740	(1/2-)	15.	0.07		
103	2.9849	1/2-	25.	0.12	4.98	0.251
104	2.9887	(3/2-)	3.	0.01		
105	2.9902	1/2-	35.	0.16		
106	3.0066	1/2-	75.	0.34		
107	3.0145	3/2- *	40.	0.18	0.37	0.018
108	3.0295	3/2-	30.	0.13	8.25 <sup>13</sup>	0.382
109	3.0306	3/2- *	7.	0.03	2.13 <sup>10, 10</sup>	0.098
110	3.0380	3/2-	25.	0.11	3.39 <sup>50</sup>	0.152
111	3.0391	3/2- *	50.	0.21	0.24	0.011
112	3.0497	1/2-	225.	0.95	11.82	0.487
113	3.0633	3/2-	15.	0.06	25	
114	3.0637	1/2-	25.	0.10	65	

Table B.5

Res. No.	$E_p$ (MeV)	$J^\pi$	$\Gamma_p$ (eV)	$\gamma_p^2$ (keV)	$\Gamma_{p'}$ (eV)	$\gamma_{p'}^2$ (keV)
115	3.0674	1/2-	55.	0.23	140	
116	3.0720	3/2-	20.	0.08	20.00	0.804
117	3.0800	1/2-	20.	0.08	25.00	0.905
118	3.0871	3/2-	60.	0.24	25.50	0.976
119	3.0878	3/2- *	15.	0.06	10.00	0.382
120	3.0905	3/2-	15.	0.05	6.00	0.227



Table B.6

Res. No.	Exp.	$a_2$	$\delta_j$	$\delta_s$	$\Phi_j$	$\Phi_s$
6	GAMM	0.178+OR-0.035	-1.344+ - 0.236	1.981+ - 0.323	-53.4+4.13 -4.32	63.2+4.13 -4.32
6	PROT	-0.250+OR-0.067	-2.563+ - 0.610	1.106+ - 0.138	-68.7+3.88 -3.82	47.9+3.88 -3.82
7	GAMM	0.081+OR-0.034	-2.274+ - 0.839	1.204+ - 0.226	-66.3+4.96 -5.93	50.3+4.96 -5.93
7	PROT	-0.274+OR-0.062	-2.759+ - 0.640	1.053+ - 0.122	-70.1+3.55 -3.53	46.5+3.55 -3.53
9	GAMM	0.145+OR-0.036	1.566+ - 0.240	-0.105+ - 0.079	57.4+4.81 -4.46	-6.0+4.81 -4.46
9	PROT	-0.798+OR-0.034	1.812+ - 0.504	-0.041+ - 0.151	61.1+2.33 -8.50	-2.3+2.33 -8.50
12	GAMM	0.083+OR-0.037	-2.248+ - 0.905	1.215+ - 0.244	-66.0+5.28 -6.38	50.5+5.28 -6.38
12	PROT	-0.250+OR-0.077	-2.564+ - 0.733	1.106+ - 0.159	-68.7+4.51 -4.43	47.9+4.51 -4.43
16	GAMM	0.575+OR-0.032	0.000+ - 0.000	-2.000+ - 0.000	0.0+ 14. -0.00	-63.4+ 14. -0.00
16	PROT	-0.211+OR-0.069	0.237+ - 0.075	-1.196+ - 0.191	13.3+4.01 -4.11	-50.1+4.01 -4.11
19	GAMM	0.398+OR-0.036	0.505+ - 0.116	-0.743+ - 0.162	26.8+4.84 -5.54	-36.6+4.84 -5.54
19	PROT	-0.246+OR-0.075	0.275+ - 0.081	-1.114+ - 0.188	15.4+4.31 -4.38	-48.1+4.31 -4.38

Table B.6

Res. No.	Exp.	$a_2$	$\delta_j$	$\delta_B$	$\Phi_j$	$\Phi_B$
23	GAMM	0.246+OR-0.036	1.017+ - 0.136	-0.324+ - 0.081	45.5+4.12 -4.11	-18.0+4.12 -4.11
23	PROT	-0.501+OR-0.060	0.584+ - 0.082	-0.653+ - 0.095	30.3+3.85 -3.63	-33.2+3.85 -3.63
24	GAMM	0.260+OR-0.036	-0.961+ - 0.148	3.212+ - 0.659	-43.9+4.12 -4.10	72.7+4.12 -4.10
24	PROT	0.075+OR-0.078	-1.083+ - 0.260	2.643+ - 0.661	-47.3+8.13 -6.05	69.3+8.13 -6.05
26	GAMM	0.512+OR-0.035	0.000+ - 0.000	-2.000+ - 0.000	0.0+ 15. -0.00	-63.4+ 15. -0.00
26	PROT	0.030+OR-0.076	-0.039+ - 0.114	-2.211+ - 0.894	-2.2+5.38 -6.49	-65.7+5.38 -6.49
30	GAMM	0.073+OR-0.037	-2.415+ - 1.157	1.153+ - 0.246	-67.5+5.48 -6.85	49.1+5.48 -6.85
30	PROT	-0.177+OR-0.072	-2.092+ - 0.468	1.285+ - 0.178	-64.5+4.38 -4.21	52.1+4.38 -4.21
31	GAMM	0.514+OR-0.034	0.000+ - 0.000	-2.000+ - 0.000	0.0+ 15. -0.00	-63.4+ 15. -0.00
31	PROT	-0.136+OR-0.073	0.156+ - 0.081	-1.405+ - 0.267	8.9+4.32 -4.56	-54.6+4.32 -4.56
32	GAMM	0.489+OR-0.035	0.151+ - 0.151	-1.421+ - 0.579	8.6+9.06 -8.57	-54.9+9.06 -8.57
32	PROT	-0.280+OR-0.068	0.311+ - 0.074	-1.041+ - 0.154	17.3+3.91 -3.93	-46.2+3.91 -3.93

Table B.6

Res. No.	Exp.	$a_2$	$\delta_j$	$\delta_s$	$\Phi_j$	$\Phi_s$
33	GAMM	0.329+0R-0.036	-0.722+ - 0.112	6.135+ - 1.963	5.733 -4.22	80.7+4.44 -4.22
33	PROT	0.093+0R-0.077	-1.024+ - 0.255	2.887+ - 0.782	2.785 -6.30	70.9+9.10 -6.30
34	GAMM	0.499+0R-0.035	0.042+ - 0.042	-1.807+ - 0.193	0.697 -2.40	-61.0+13. -2.40
34	PROT	-0.108+0R-0.073	0.126+ - 0.082	-1.498+ - 0.303	0.223 -4.68	-56.3+4.38 -4.68
35	GAMM	0.444+0R-0.035	0.356+ - 0.144	-0.961+ - 0.295	0.174 -7.63	-43.9+5.65 -7.63
35	PROT	-0.142+0R-0.070	0.163+ - 0.077	-1.386+ - 0.246	0.191 -4.32	-54.2+4.11 -4.32
36	GAMM	0.396+0R-0.037	0.513+ - 0.118	-0.735+ - 0.162	0.124 -5.59	-36.3+4.89 -5.59
36	PROT	-0.551+0R-0.052	0.662+ - 0.080	-0.576+ - 0.080	0.080 -3.31	-29.9+3.55 -3.31
38	GAMM	0.151+0R-0.037	-1.521+ - 0.317	1.724+ - 0.290	0.356 -4.77	59.9+4.44 -4.77
38	PROT	-0.239+0R-0.064	-2.481+ - 0.548	1.131+ - 0.137	0.161 -3.68	48.5+3.74 -3.68
40	GAMM	0.472+0R-0.035	0.243+ - 0.243	-1.182+ - 0.818	0.260 -13.	-49.8+7.08 -13.
40	PROT	-0.068+0R-0.073	0.081+ - 0.087	-1.652+ - 0.381	0.264 -5.00	-58.8+4.58 -5.00

Table B.6

Res.	Exp.	$a_2$	$\delta_j$	$\delta_s$	$\Phi_j$	$\Phi_s$	
41	GAMM	0.502+OR-0.034	0.000+ -0.000	0.271 -0.000	-2.000+ 0.879	0.0+ 15. -0.00	-63.4+ 15. -0.00
41	PROT	-0.206+OR-0.069	0.232+ -0.074	0.074 -0.074	-1.208+ 0.158	13.0+3.98 -4.09	-50.4+3.98 -4.09
43	GAMM	0.149+OR-0.036	1.537+ -0.230	0.315 -0.230	-0.114+ 0.082	57.0+4.68 -4.36	-6.5+4.68 -4.36
43	PROT	-0.857+OR-0.029	1.999+ -0.643	0.001 -0.643	0.000+ 0.174	63.4+0.02 -9.85	0.0+0.00 -9.85
44	GAMM	0.414+OR-0.036	0.457+ -0.121	0.111 -0.121	-0.806+ 0.136	24.6+5.04 -5.97	-38.9+5.04 -5.97
44	PROT	-0.190+OR-0.069	0.214+ -0.075	0.075 -0.075	-1.250+ 0.166	12.1+4.03 -4.16	-51.3+4.03 -4.16
46	GAMM	0.239+OR-0.035	-1.045+ -0.972+ 0.564+ 0.601+ 0.401+OR-0.037	0.137 -0.160 0.109 0.110 0.086 -0.076	2.795+ 0.521 3.148+ 5.264 -0.675+ 0.109 -0.635+ 0.083 717.7+ 708.1 729.1	-46.3+4.02 -4.05 -44.2+ 10. -6.68 29.4+4.51 -5.00 31.0+3.50 -3.31 -26.5+5.88 -174	70.3+4.02 -4.05 72.4+ 10. -6.68 -34.0+4.51 -5.00 -32.4+3.50 -3.31 -89.9+5.88 -174
46	PROT	0.108+OR-0.078	-0.972+ -0.257	0.314 -0.257	0.109 -0.110	0.109 -0.110	
48	GAMM	0.379+OR-0.035	0.564+ -0.110	0.109 -0.110	-0.675+ 0.109	29.4+4.51 -5.00	-34.0+4.51 -5.00
48	PROT	-0.513+OR-0.054	0.601+ -0.076	0.086 -0.076	-0.635+ 0.083	31.0+3.50 -3.31	-32.4+3.50 -3.31
49	GAMM	0.401+OR-0.037	-0.498+ -0.116	0.122 -0.116	717.7+ 708.1 729.1	-26.5+5.88 -174	-89.9+5.88 -174
49	PROT	0.126+OR-0.080	-0.190+ -0.310	0.130 -0.310	-3.528+ 1.187 99995	-10.7+7.30 -15.	-74.2+7.30 -15.

Table B.6

Res.	Exp.	$a_2$	$\delta_j'$	$\delta_B'$	$\phi_j'$	$\phi_B'$
50	GAMM	0.240+OR-0.036	1.039+ - 0.139	-0.312+ - 0.081	46.1+4.13 -4.10	-17.3+4.13 -4.10
50	PROT	-0.538+OR-0.053	0.641+ - 0.079	-0.596+ - 0.082	32.7+3.55 -3.33	-30.8+3.55 -3.33
51	GAMM	0.428+OR-0.034	-0.412+ - 0.107	=13.63+ -79.840	-22.4+6.21 - 174	-85.8+6.21 - 174
51	PROT	0.254+OR-0.079	-0.500+ - 0.428	99.999+ - 0.000	-26.6+0.01 -0.00	90.0+ 16. -0.00
53	GAMM	0.550+OR-0.033	0.000+ - 0.000	-2.000+ - 0.000	0.0+ 14. -0.00	-63.4+ 14. -0.00
53	PROT	-0.026+OR-0.073	0.032+ - 0.094	-1.851+ - 0.507	1.8+4.79 -5.40	-61.6+4.79 -5.40
54	GAMM	0.060+OR-0.037	-2.714+ - 1.833	1.065+ - 0.256	-69.8+5.83 -7.82	46.8+5.83 -7.82
54	PROT	-0.175+OR-0.069	-2.083+ - 0.443	1.290+ - 0.173	-64.4+4.20 -4.05	52.2+4.20 -4.05
55	GAMM	0.211+OR-0.036	-1.169+ - 0.192	2.368+ - 0.416	-49.5+4.14 -4.23	67.1+4.14 -4.23
55	PROT	-0.014+OR-0.073	-1.381+ - 0.279	1.919+ - 0.341	-54.1+5.51 -4.84	62.5+5.51 -4.84
56	GAMM	0.384+OR-0.036	-0.551+ - 0.110	25.047+16.788 -45.024	-28.9+5.15 - 174	87.7+4.62 - 174
56	PROT	0.131+OR-0.076	-0.892+ - 0.255	3.687+ - 1.256	-41.7+ 15. -7.19	74.8+ 15. -7.19

Table B.6

Res.	Exp.	$a_2$	$\delta_j$	$\delta_s$	$\Phi_j$	$\Phi_s$
57	GAMM	0.064+OR-0.036	-2.610+ - 1.479	1.092+ - 0.244	-69.0+5.57 -7.22	47.5+5.57 -7.22
57	PROT	-0.300+OR-0.064	-2.998+ - 0.787	1.000+ - 0.120	-71.6+3.65 -3.65	45.0+3.65 -3.65
60	GAMM	0.097+OR-0.036	-2.041+ - 0.639	1.311+ - 0.238	-63.9+4.87 -5.64	52.7+4.87 -5.64
60	PROT	-0.326+OR-0.060	-3.283+ - 0.890	0.949+ - 0.109	-73.1+3.44 -3.47	43.5+3.44 -3.47
62	GAMM	0.431+OR-0.035	-0.400+ - 0.113	11.98+ - 108.1	-21.8+6.76 - 174	-85.2+6.76 - 174
62	PROT	0.121+OR-0.076	-0.181+ - 0.254	-3.424+ -15.452	-10.3+6.86 - 13.	-73.7+6.86 - 13.
63	GAMM	0.178+OR-0.035	-1.347+ - 0.237	1.976+ - 0.323	-53.4+4.14 -4.33	63.2+4.14 -4.33
63	PROT	0.006+OR-0.073	-1.314+ - 0.268	2.036+ - 0.381	-52.7+5.78 -4.98	63.8+5.78 -4.98
64	GAMM	0.567+OR-0.033	0.000+ - 0.000	-2.000+ - 0.000	0.0+ 14. -0.00	-63.4+ 14. -0.00
64	PROT	-0.149+OR-0.071	0.170+ - 0.079	-1.365+ - 0.247	9.7+4.21 -4.42	-53.8+4.21 -4.42
65	GAMM	0.535+OR-0.034	0.000+ - 0.000	-2.000+ - 0.000	0.0+ 15. -0.00	-63.4+ 15. -0.00
65	PROT	-0.085+OR-0.071	0.099+ - 0.083	-1.585+ - 0.334	5.7+4.38 -4.73	-57.8+4.38 -4.73

Table B.6

Res. No.	Exp.	$a_2$	$\delta_j'$	$\delta_{s1}'$	$\Phi_j'$	$\Phi_{s1}'$		
66	GAMM	0.124+0R-0.036	1.744+ - 0.282	0.419 - 0.282	-0.057+ - 0.080	0.088 - 0.080	60.2+5.01 -4.54	-3.3+5.01 -4.54
66	PROT	-0.719+0R-0.039	1.069+ - 0.131	0.194 - 0.131	-0.297+ - 0.072	0.088 - 0.072	46.9+4.71 -3.74	-16.5+4.71 -3.74
68	GAMM	-0.004+0R-0.036	=99999+ - 0.000	99995 - 0.000	0.500+ - 0.000	0.404 - 0.000	-90.0+ 15. -0.00	26.6+ 15. -0.00
68	PROT	-0.539+0R-0.052	=13.81+ -75.564	6.136 -75.564	0.594+ - 0.080	0.080 - 0.080	-85.9+3.28 -3.50	30.7+3.28 -3.50
69	GAMM	0.175+0R-0.036	-1.360+ - 0.250	0.193 - 0.250	1.953+ - 0.328	0.421 - 0.328	-53.7+4.27 -4.48	62.9+4.27 -4.48
69	PROT	-0.283+0R-0.064	-2.839+ - 0.707	0.492 - 0.707	1.035+ - 0.124	0.142 - 0.124	-70.6+3.67 -3.66	46.0+3.67 -3.66
71	GAMM	0.412+0R-0.036	0.462+ - 0.120	0.111 - 0.120	-0.800+ - 0.186	0.135 - 0.186	24.8+5.02 -5.93	-38.6+5.02 -5.93
71	PROT	-0.284+0R-0.067	0.315+ - 0.073	0.076 - 0.073	-1.033+ - 0.151	0.131 - 0.151	17.5+3.87 -3.88	-45.9+3.87 -3.88
72	GAMM	0.154+0R-0.035	1.500+ - 0.219	0.295 - 0.219	-0.125+ - 0.077	0.080 - 0.077	56.3+4.57 -4.28	-7.1+4.57 -4.28
72	PROT	-0.744+0R-0.037	1.179+ - 0.157	0.275 - 0.157	-0.245+ - 0.105	0.105 - 0.105	49.7+5.80 -4.09	-13.7+5.80 -4.09

Table B.6

Res. No.	Exp.	$a_2$	$\delta_j$	$\delta_s$	$\Phi_j$	$\Phi_s$
73	GAMM	0.044+0R-0.035	-3.224+ - 4.293	0.959+ - 0.281	-72.8+6.20 -9.65	43.8+6.20 -9.65
73	PROT	-0.129+0R-0.068	-1.847+ - 0.360	1.428+ - 0.196	-61.6+4.28 -4.06	55.0+4.28 -4.06
74	GAMM	0.075+0R-0.035	-2.374+ - 1.022	1.167+ - 0.235	-67.2+5.24 -6.44	49.4+5.24 -6.44
74	PROT	-0.286+0R-0.065	-2.863+ - 0.732	1.029+ - 0.125	-70.7+3.72 -3.71	45.8+3.72 -3.71
76	GAMM	0.106+0R-0.036	-1.929+ - 0.561	1.375+ - 0.247	-62.6+4.85 -5.52	54.0+4.85 -5.52
76	PROT	-0.174+0R-0.066	-2.074+ - 0.415	1.294+ - 0.166	-64.3+3.99 -3.85	52.3+3.99 -3.85
77	GAMM	0.451+0R-0.035	0.331+ - 0.157	-1.004+ - 0.351	18.3+5.90 -8.46	-45.1+5.90 -8.46
77	PROT	-0.273+0R-0.066	0.304+ - 0.071	-1.056+ - 0.150	16.9+3.76 -3.79	-46.6+3.76 -3.79
78	GAMM	0.243+0R-0.035	1.028+ - 0.136	-0.318+ - 0.080	45.8+4.09 -4.07	-17.6+4.09 -4.07
78	PROT	-0.665+0R-0.043	0.896+ - 0.102	-0.396+ - 0.070	41.8+3.90 -3.40	-21.6+3.90 -3.40
79	GAMM	0.427+0R-0.035	-0.414+ - 0.111	=13.95+ -64.902	-22.5+6.45 - 174	-85.9+6.45 - 174
79	PROT	0.155+0R-0.077	-0.255+ - 0.245	-4.597+ - 99994	-14.3+8.14 - 12.	-77.7+8.14 - 12.



Table B.6

Res.	Exp.	$a_2$	$\delta_j$	$\delta_s$	$\Phi_j$	$\Phi_s$
80	GAMM	0.335+0R-0.036	0.701+ - 0.118	-0.541+ - 0.107	35.0+4.30 -4.55	-28.4+4.30 -4.55
80	PROT	-0.456+0R-0.057	0.521+ - 0.072	-0.724+ - 0.093	27.5+3.49 -3.35	-35.9+3.49 -3.35
81	GAMM	0.197+0R-0.036	-1.238+ - 0.212	2.194+ - 0.378	-51.1+4.20 -4.34	65.5+4.20 -4.34
81	PROT	-0.141+0R-0.066	-1.905+ - 0.366	1.390+ - 0.184	-62.3+4.13 -3.94	54.3+4.13 -3.94
82	GAMM	0.022+0R-0.035	-4.617+ - 99994	0.804+ - 0.304	-77.8+7.65 - 12.	38.8+7.65 - 12.
82	PROT	-0.412+0R-0.058	-4.715+ - 1.955	0.797+ - 0.101	-78.0+3.35 -3.45	38.5+3.35 -3.45
83	GAMM	0.415+0R-0.035	0.453+ - 0.121	-0.812+ - 0.190	24.4+5.03 -5.98	-39.1+5.03 -5.98
83	PROT	-0.323+0R-0.063	0.359+ - 0.070	-0.955+ - 0.128	19.8+3.62 -3.60	-43.7+3.62 -3.60
86	GAMM	0.188+0R-0.036	1.290+ - 0.176	-0.198+ - 0.076	52.2+4.30 -4.14	-11.2+4.30 -4.14
86	PROT	-0.640+0R-0.044	0.835+ - 0.094	-0.436+ - 0.071	39.9+3.71 -3.31	-23.6+3.71 -3.31
91	GAMM	0.379+0R-0.035	0.566+ - 0.110	-0.673+ - 0.135	29.5+4.50 -4.98	-33.9+4.50 -4.98
91	PROT	-0.481+0R-0.054	0.555+ - 0.073	-0.685+ - 0.088	29.0+3.44 -3.28	-34.4+3.44 -3.28

Table B.6

Res. No.	Exp.	$a_2$	$\delta_j$	$\delta_s$	$\phi_j$	$\phi_s$
92	GAMM	0.142+OR-0.035	-1.591+ - 0.335	1.646+ - 0.269	-57.8+4.36 -4.71	58.7+4.36 -4.71
92	PROT	-0.032+OR-0.072	-1.447+ - 0.286	1.820+ - 0.307	-55.3+5.22 -4.67	61.2+5.22 -4.67
93	GAMM	0.005+OR-0.035	10.253+ - 6.856	0.384+ - 0.205	84.4+5.57 - 10.	21.0+5.57 - 10.
93	PROT	-0.764+OR-0.036	3.562+ - 1.562	0.192+ - 0.192	74.3+4.64 - 10.	10.9+4.64 - 10.
95	GAMM	0.450+OR-0.035	0.332+ - 0.156	-1.002+ - 0.348	18.4+5.88 -8.40	-45.1+5.88 -8.40
95	PROT	-0.143+OR-0.070	0.163+ - 0.077	-1.384+ - 0.248	9.3+4.13 -4.34	-54.2+4.13 -4.34
96	GAMM	0.462+OR-0.035	0.288+ - 0.201	-1.086+ - 0.544	16.1+6.38 - 11.	-47.4+6.38 - 11.
96	PROT	-0.202+OR-0.068	0.226+ - 0.073	-1.221+ - 0.193	12.8+3.94 -4.06	-50.7+3.94 -4.06
97	GAMM	0.163+OR-0.036	1.435+ - 0.205	-0.146+ - 0.077	55.1+4.50 -4.25	-8.3+4.50 -4.25
97	PROT	-0.728+OR-0.039	1.105+ - 0.142	-0.279+ - 0.075	47.9+5.14 -3.92	-15.6+5.14 -3.92
98	GAMM	0.192+OR-0.036	-1.269+ - 0.218	2.126+ - 0.359	-51.8+4.16 -4.32	64.8+4.16 -4.32
98	PROT	0.031+OR-0.075	-1.228+ - 0.263	2.217+ - 0.456	-50.8+6.40 -5.31	65.7+6.40 -5.31

Table B.6

Res. No.	Exp.	$a_2$	$\delta_j$	$\delta_s$	$\Phi_j$	$\Phi_s$
99	GAMM	0.161+OR-0.038	-1.454+ - 0.302	1.810+ - 0.398	-55.5+4.55 -4.85	61.1+4.55 -4.85
99	PROT	-0.009+OR-0.075	-1.366+ - 0.252	1.943+ - 0.592	-53.8+5.70 -4.98	62.8+5.70 -4.98
100	GAMM	0.321+OR-0.035	-0.748+ - 0.120	5.539+ - 1.641	-36.8+4.34 -4.15	79.8+4.34 -4.15
100	PROT	0.165+OR-0.077	-0.763+ - 0.277	5.249+ - 2.436	-37.4+ 10. -8.78	79.2+ 10. -8.78
101	GAMM	0.299+OR-0.035	0.819+ - 0.116	-0.448+ - 0.083	39.3+4.10 -4.22	-24.1+4.10 -4.22
101	PROT	-0.667+OR-0.043	0.902+ - 0.103	-0.392+ - 0.078	42.0+3.96 -3.44	-21.4+3.96 -3.44
107	GAMM	0.131+OR-0.036	-1.675+ - 0.381	1.564+ - 0.260	-59.2+4.48 -4.90	57.4+4.48 -4.90
107	PROT	-0.233+OR-0.065	-2.441+ - 0.545	1.144+ - 0.167	-67.7+3.83 -3.76	48.8+3.83 -3.76
108	GAMM	0.411+OR-0.035	0.465+ - 0.118	-0.795+ - 0.181	24.9+4.95 -5.82	-38.5+4.95 -5.82
108	PROT	-0.257+OR-0.064	0.286+ - 0.069	-1.089+ - 0.132	16.0+3.69 -3.73	-47.5+3.69 -3.73
109	GAMM	0.430+OR-0.035	0.405+ - 0.127	-0.882+ - 0.226	22.0+5.23 -6.52	-41.4+5.23 -6.52
109	PROT	-0.078+OR-0.072	0.092+ - 0.084	-1.610+ - 0.349	5.3+4.43 -4.80	-58.2+4.43 -4.80

Table B.6

Res. No.	Exp.	$a_2$	$\delta_{j'}$	$\delta_{B'}$	$\phi_{j'}$	$\phi_{B'}$
110	GAMM	0.209+OR-0.036	-1.181+ - 0.158	2.335+ - 0.404	-49.8+4.09 -4.19	66.8+4.09 -4.19
110	PROT	-0.102+OR-0.069	-1.725+ - 0.333	1.520+ - 0.218	-59.9+4.47 -4.18	56.7+4.47 -4.18
111	GAMM	0.348+OR-0.034	-0.662+ - 0.105	0.201+13.936 - 3.080	-33.5+4.37 -4.10	83.0+4.37 -4.10
111	PROT	0.021+OR-0.072	-1.263+ - 0.257	2.139+ - 0.412	-51.6+5.91 -5.02	64.9+5.91 -5.02
116	GAMM	0.468+OR-0.035	0.261+ - 0.261	-1.142+ - 0.858	14.6+6.78 - 14.	-48.8+6.78 - 14.
116	PROT	-0.134+OR-0.069	0.154+ - 0.076	-1.413+ - 0.253	8.7+4.10 -4.32	-54.7+4.10 -4.32
118	GAMM	0.333+OR-0.035	0.708+ - 0.109	-0.534+ - 0.103	35.3+4.16 -4.39	-28.1+4.16 -4.39
118	PROT	-0.572+OR-0.049	0.698+ - 0.080	-0.544+ - 0.075	34.9+3.46 -3.21	-28.5+3.46 -3.21
119	GAMM	0.259+OR-0.036	-0.965+ - 0.150	3.188+ - 0.654	-44.0+4.14 -4.12	72.6+4.14 -4.12
119	PROT	-0.113+OR-0.068	-1.771+ - 0.342	1.483+ - 0.209	-60.6+4.38 -4.13	56.0+4.38 -4.13
120	GAMM	0.460+OR-0.034	0.296+ - 0.185	-1.071+ - 0.477	16.5+6.21 - 10.	-47.0+6.21 - 10.
120	PROT	-0.284+OR-0.066	0.316+ - 0.071	-1.032+ - 0.146	17.5+3.76 -3.78	-45.9+3.76 -3.78

Table B.7

Res. No.	$\delta_{j'}$	$\delta_{s'}$	$\bar{\Phi}_{j'}$	$\bar{\Phi}_{s'}$
6	-1.693+ 0.26 - 0.34	1.359+ 0.24 - 0.19	-59.4+4.3 -4.4	53.7+4.3 -4.2
7	-2.536+ 0.45 - 0.73	1.108+ 0.18 - 0.16	-68.5+4.1 -4.5	47.9+4.1 -4.5
9	1.678+ 0.27 - 0.36	-0.075+ 0.06 - 0.11	59.2+3.6 -6.4	-4.3+3.7 -6.3
12	-2.414+ 0.48 - 0.81	1.151+ 0.22 - 0.19	-67.5+4.8 -5.3	49.0+4.9 -5.3
16	0.151+ 0.14 - 0.05	-1.428+ 0.36 - 0.14	8.6+7.8 -2.7	-55.0+8.1 -2.4
19	0.371+ 0.09 - 0.10	-0.912+ 0.14 - 0.17	20.4+4.6 -5.0	-42.3+4.6 -5.0
23	0.746+ 0.12 - 0.10	-0.476+ 0.08 - 0.09	36.7+4.1 -4.0	-25.4+4.1 -3.9
24	-1.003+ 0.18 - 0.19	2.980+ 1.38 - 0.66	-45.1+5.6 -4.9	71.4+5.6 -4.8
26	-0.022+ 0.17 - 0.06	-2.083+ 0.72 - 0.35	-1.3+9.8 -3.7	-64.4+ 10 -3.3
30	-2.198+ 0.41 - 0.69	1.226+ 0.24 - 0.21	-65.5+4.8 -5.4	50.8+4.8 -5.3
31	0.099+ 0.15 - 0.05	-1.612+ 0.44 - 0.17	5.6+8.3 -2.9	-58.2+8.6 -2.6
32	0.260+ 0.11 - 0.10	-1.128+ 0.19 - 0.25	14.5+5.5 -5.4	-48.4+5.3 -5.6
33	-0.812+ 0.16 - 0.16	3.916+ 3.72 - 1.16	-39.1+6.1 -5.1	75.7+6.9 -5.6
34	0.095+ 0.14 - 0.07	-1.613+ 0.40 - 0.26	5.4+7.6 -3.8	-58.2+7.7 -3.7
35	0.234+ 0.09 - 0.10	-1.181+ 0.18 - 0.27	13.2+4.8 -5.6	-49.7+4.8 -5.7
36	0.598+ 0.10 - 0.10	-0.632+ 0.10 - 0.11	30.9+4.1 -4.2	-32.3+4.1 -4.3
38	-1.872+ 0.29 - 0.40	1.318+ 0.22 - 0.18	-61.9+4.2 -4.4	52.8+4.2 -4.2
40	0.131+ 0.10 - 0.14	-1.476+ 0.26 - 0.54	7.5+5.4 -7.7	-55.9+5.4 -7.8
41	0.150+ 0.14 - 0.05	-1.434+ 0.36 - 0.14	8.5+7.9 -2.7	-55.1+8.2 -2.4

Table B.7

Res. No.	$\delta_j$	$\delta_s$	$\Phi_j$	$\Phi_s$
43	1.749+ 0.17 - 0.42	-0.059+ 0.04 - 0.12	60.2+2.3 -7.2	-3.4+2.4 -7.0
44	0.309+ 0.09 - 0.09	-1.013+ 0.15 - 0.20	17.2+4.5 -5.0	-45.4+4.6 -5.0
46	-1.020+ 0.20 - 0.19	2.856+ 1.55 - 0.59	-45.6+6.1 -4.9	70.7+6.5 -4.5
48	0.585+ 0.10 - 0.09	-0.651+ 0.09 - 0.10	30.3+3.9 -4.0	-33.1+3.9 -4.0
49	-0.390+ 0.12 - 0.18	-707.593+ 698. - 2135	-21.3+6.5 -8.6	-89.9+5.9 -0.1
50	0.785+ 0.12 - 0.10	-0.452+ 0.08 - 0.08	38.1+3.9 -3.7	-24.3+3.9 -3.7
51	-0.442+ 0.08 - 0.22	74.331+96.13 -79.77	-23.9+3.9 -9.6	89.2+0.4 - 16
53	0.019+ 0.16 - 0.06	-1.924+ 0.59 - 0.26	1.1+8.9 -3.2	-62.5+9.4 -2.9
54	-2.233+ 0.42 - 0.77	1.191+ 0.23 - 0.21	-65.9+4.7 -5.7	50.0+4.9 -5.5
55	-1.254+ 0.19 - 0.23	2.132+ 0.56 - 0.38	-51.4+4.8 -4.5	64.9+4.8 -4.5
56	-0.638+ 0.18 - 0.15	25.034+78.55 -45.00	-32.5+8.1 -5.6	87.7+1.7 - 17
57	-2.847+ 0.56 - 1.06	1.032+ 0.17 - 0.16	-70.6+4.3 -5.0	45.9+4.4 -4.9
60	-2.546+ 0.46 - 0.74	1.063+ 0.17 - 0.15	-68.6+4.2 -4.5	46.8+4.1 -4.3
62	-0.314+ 0.13 - 0.17	-4.498+ 1.84 -27.09	-17.4+6.9 -8.3	-77.5+8.1 - 10
63	-1.332+ 0.21 - 0.25	2.001+ 0.51 - 0.35	-53.1+4.9 -4.6	63.4+4.9 -4.6
64	0.108+ 0.15 - 0.05	-1.578+ 0.42 - 0.16	6.1+8.1 -2.8	-57.6+8.4 -2.5
65	0.062+ 0.15 - 0.05	-1.750+ 0.49 - 0.20	3.6+8.4 -3.0	-60.3+8.7 -2.6
66	1.282+ 0.26 - 0.18	-0.180+ 0.09 - 0.08	52.1+5.1 -4.2	-10.2+4.9 -4.2
68	-95.440+87.76 -75.50	0.567+ 0.17 - 0.06	-89.4+6.8 -0.3	29.6+6.9 -2.5

Table B.7

Res. No.	$\delta_j$	$\delta_s$	$\Phi_j$	$\Phi_s$
69	-1.759+ 0.27 - 0.37	1.276+ 0.22 - 0.18	-60.4+4.3 -4.5	51.9+4.2 -4.2
71	0.373+ 0.09 - 0.09	-0.924+ 0.13 - 0.17	20.4+4.4 -4.7	-42.7+4.4 -4.8
72	1.326+ 0.28 - 0.19	-0.180+ 0.09 - 0.08	53.0+5.2 -4.2	-10.2+5.2 -4.2
73	-2.000+ 0.36 - 0.80	1.209+ 0.24 - 0.24	-63.4+4.8 -6.9	50.4+5.1 -6.2
74	-2.644+ 0.50 - 0.86	1.079+ 0.18 - 0.16	-69.3+4.3 -4.8	47.2+4.3 -4.7
76	-2.009+ 0.33 - 0.48	1.328+ 0.24 - 0.20	-63.5+4.4 -4.6	53.0+4.4 -4.6
77	0.313+ 0.09 - 0.10	-1.038+ 0.15 - 0.22	17.4+4.5 -5.4	-46.1+4.5 -5.4
78	0.954+ 0.14 - 0.12	-0.358+ 0.08 - 0.08	43.6+4.0 -3.7	-19.7+4.0 -3.7
79	-0.354+ 0.13 - 0.16	-13.950+ 8.58 - 138.	-19.5+7.1 -7.8	-85.9+6.5 -3.7
80	0.593+ 0.10 - 0.09	-0.637+ 0.09 - 0.10	30.7+3.9 -3.9	-32.5+3.9 -3.9
81	-1.482+ 0.22 - 0.27	1.648+ 0.32 - 0.25	-56.0+4.3 -4.3	58.8+4.3 -4.3
82	-4.715+ 1.07 - 4.98	0.798+ 0.14 - 0.15	-78.0+3.4 -6.1	38.6+4.5 -5.6
83	0.395+ 0.09 - 0.09	-0.894+ 0.12 - 0.15	21.6+4.2 -4.5	-41.8+4.2 -4.6
86	0.992+ 0.15 - 0.12	-0.320+ 0.08 - 0.07	44.8+4.1 -3.7	-17.8+4.0 -3.7
91	0.559+ 0.09 - 0.09	-0.680+ 0.09 - 0.11	29.2+3.9 -4.0	-34.2+3.9 -4.0
92	-1.516+ 0.24 - 0.31	1.721+ 0.39 - 0.29	-56.6+4.8 -4.7	59.8+4.8 -4.7
93	3.562+ 4.69 - 1.56	0.281+ 0.10 - 0.20	74.3+8.8 - 10	15.7+5.2 - 10
95	0.224+ 0.09 - 0.11	-1.212+ 0.19 - 0.29	12.6+4.8 -5.9	-50.5+4.8 -5.9
96	0.246+ 0.09 - 0.11	-1.178+ 0.18 - 0.30	13.8+4.7 -6.3	-49.7+4.6 -6.3

Table B.7

Res. No.	$\delta_j'$	$\delta_s'$	$\Phi_j'$	$\Phi_s'$
97	1.248+ 0.24 - 0.17	-0.210+ 0.09 - 0.08	51.3+4.9 -4.1	-11.8+4.8 -4.1
98	-1.251+ 0.21 - 0.24	2.161+ 0.63 - 0.40	-51.4+5.1 -4.7	65.2+5.1 -4.7
99	-1.411+ 0.24 - 0.29	1.867+ 0.48 - 0.33	-54.7+5.1 -4.9	61.8+5.1 -4.9
100	-0.753+ 0.16 - 0.17	5.539+ 9.94 - 1.64	-37.0+6.2 -5.6	79.8+6.5 -4.2
101	0.861+ 0.13 - 0.11	-0.417+ 0.08 - 0.08	40.7+4.0 -3.8	-22.7+4.0 -3.8
107	-1.986+ 0.32 - 0.45	1.292+ 0.22 - 0.18	-63.3+4.2 -4.4	52.3+4.2 -4.3
108	0.354+ 0.09 - 0.09	-0.949+ 0.13 - 0.17	19.5+4.2 -4.6	-43.5+4.3 -4.6
109	0.219+ 0.09 - 0.10	-1.164+ 0.19 - 0.27	12.4+4.9 -5.7	-49.3+5.0 -5.8
110	-1.380+ 0.20 - 0.24	1.804+ 0.38 - 0.28	-54.1+4.4 -4.3	61.0+4.4 -4.3
111	-0.843+ 0.14 - 0.15	2.524+ 1.58 - 0.58	-40.1+5.2 -4.7	68.4+7.9 -5.6
116	0.183+ 0.09 - 0.13	-1.334+ 0.21 - 0.43	10.4+4.9 -7.2	-53.2+4.8 -7.3
118	0.702+ 0.10 - 0.09	-0.540+ 0.08 - 0.09	35.1+3.8 -3.7	-28.4+3.8 -3.7
119	-1.216+ 0.18 - 0.21	1.861+ 0.45 - 0.31	-50.6+4.5 -4.4	61.7+4.8 -4.5
120	0.310+ 0.09 - 0.11	-1.043+ 0.15 - 0.24	17.2+4.5 -5.8	-46.2+4.5 -5.9



Table B.8

Res. No.	$\gamma_{j_1}^2$ (keV)	$\gamma_{j_3}^2$ (keV)	$\gamma_{j_1} \gamma_{j_3}$ (keV)	$\gamma_{s_3}^2$ (keV)	$\gamma_{s_5}^2$ (keV)	$\gamma_{s_3} \gamma_{s_5}$ (keV)
7	0.4868	3.1306	-1.2346	1.6238	1.9936	1.7992
9	0.6061	1.7060	1.0169	2.2991	0.0130	-0.1732
12	0.2842	1.6567	-0.6862	0.8351	1.1058	0.9610
16	0.5488	0.0125	0.0828	0.1847	0.3765	-0.2637
19	0.2136	0.0294	0.0793	0.1328	0.1103	-0.1210
23	0.0603	0.0335	0.0449	0.0765	0.0173	-0.0364
24	1.8094	1.8204	-1.8149	0.3674	3.2623	1.0948
26	1.3087	0.0006	-0.0290	0.2451	1.0642	-0.5108
30	0.0128	0.0618	-0.0281	0.0298	0.0448	0.0365
31	2.2721	0.0221	0.2239	0.6375	1.6567	-1.0277
32	0.8579	0.0578	0.2227	0.4030	0.5127	-0.4545
33	1.3399	0.8845	-1.0886	0.1362	2.0882	0.5333
34	0.7101	0.0064	0.0673	0.1990	0.5175	-0.3209
35	0.2438	0.0133	0.0570	0.1074	0.1497	-0.1268
36	0.1434	0.0513	0.0857	0.1390	0.0556	-0.0879
38	0.0921	0.3226	-0.1724	0.1515	0.2632	0.1997
40	2.4063	0.0412	0.3150	0.7702	1.6774	-1.1366
41	1.9333	0.0433	0.2895	0.6468	1.3298	-0.9274
43	0.3294	1.0072	0.5760	1.3319	0.0046	-0.0787
44	0.2769	0.0265	0.0857	0.1497	0.1537	-0.1517
46	0.0421	0.0437	-0.0429	0.0094	0.0764	0.0268
48	1.9748	0.6768	1.1561	1.8621	0.7895	-1.2125
49	0.2440	0.0371	-0.0951	0.0000	0.2811	-0.0004
50	0.8087	0.4980	0.6346	1.0851	0.2215	-0.4903
51	0.3177	0.0622	-0.1406	0.0001	0.3798	0.0051
53	1.4378	0.0005	0.0272	0.3060	1.1324	-0.5886
54	0.0639	0.3188	-0.1427	0.1582	0.2245	0.1885
55	0.5124	0.8055	-0.6424	0.2377	1.0801	0.5067
56	1.7496	0.7124	-1.1164	0.0039	2.4581	0.0982

Table B.8

Res. No.	$\gamma_{j_1}^2$ (keV)	$\gamma_{j_3}^2$ (keV)	$\gamma_{j_1} \gamma_{j_3}$ (keV)	$\gamma_{s_3}^2$ (keV)	$\gamma_{s_5}^2$ (keV)	$\gamma_{s_3} \gamma_{s_5}$ (keV)
57	0.3345	2.7122	-0.9526	1.4750	1.5718	1.5226
60	0.0158	0.1022	-0.0401	0.0553	0.0626	0.0589
62	0.4074	0.0401	-0.1278	0.0211	0.4264	-0.0948
63	0.2804	0.4975	-0.3735	0.1555	0.6224	0.3111
64	0.1655	0.0019	0.0178	0.0480	0.1194	-0.0757
65	2.0695	0.0080	0.1288	0.5115	1.5660	-0.8950
66	0.5802	0.9541	0.7440	1.4863	0.0480	-0.2671
68	0.0000	0.1534	-0.0016	0.1161	0.0373	0.0658
69	0.0288	0.0891	-0.0507	0.0449	0.0730	0.0573
71	1.1237	0.1562	0.4189	0.6906	0.5893	-0.6379
72	0.1770	0.3111	0.2346	0.4727	0.0154	-0.0853
73	0.0208	0.0831	-0.0415	0.0422	0.0616	0.0510
74	0.1058	0.7393	-0.2797	0.3906	0.4545	0.4214
76	0.0131	0.0528	-0.0263	0.0239	0.0421	0.0317
77	1.7506	0.1716	0.5481	0.9254	0.9968	-0.9604
78	0.1151	0.1047	0.1098	0.1948	0.0250	-0.0698
79	0.6137	0.0767	-0.2170	0.0035	0.6869	-0.0492
80	0.8510	0.2990	0.5045	0.8183	0.3318	-0.5210
81	0.0365	0.0803	-0.0542	0.0314	0.0854	0.0518
82	0.0103	0.2280	-0.0484	0.1455	0.0927	0.1162
83	0.7972	0.1244	0.3149	0.5123	0.4093	-0.4579
86	0.2665	0.2624	0.2645	0.4797	0.0492	-0.1536
91	0.8225	0.2574	0.4601	0.7385	0.3414	-0.5021
92	0.1733	0.3985	-0.2628	0.1443	0.4275	0.2484
93	0.0536	0.6807	0.1911	0.6805	0.0538	0.1913
95	0.4899	0.0245	0.1095	0.2083	0.3061	-0.2525
96	3.7453	0.2260	0.9200	1.6631	2.3082	-1.9593
97	0.3487	0.5428	0.4351	0.8540	0.0375	-0.1790

Table B.8

Res. No.	$\gamma_{j_1}^2$ (keV)	$\gamma_{j_3}^2$ (keV)	$\gamma_{j_1} \gamma_{j_3}$ (keV)	$\gamma_{s_3}^2$ (keV)	$\gamma_{s_5}^2$ (keV)	$\gamma_{s_3} \gamma_{s_5}$ (keV)
98	6.3675	9.9654	-7.9659	2.8805	13.4524	6.2249
99	0.1180	0.2348	-0.1664	0.0786	0.2741	0.1468
100	0.8583	0.4862	-0.6460	0.0424	1.3021	0.2351
101	0.7431	0.5508	0.6397	1.1018	0.1920	-0.4600
107	0.0037	0.0144	-0.0073	0.0068	0.0113	0.0087
108	0.3396	0.0427	0.1204	0.2011	0.1812	-0.1909
109	0.0938	0.0045	0.0206	0.0417	0.0565	-0.0486
110	0.0525	0.1000	-0.0724	0.0358	0.1166	0.0646
111	0.0062	0.0044	-0.0052	0.0014	0.0091	0.0036
116	0.7776	0.0262	0.1426	0.2891	0.5147	-0.3857
118	0.6535	0.3224	0.4590	0.7558	0.2201	-0.4078
119	0.1541	0.2277	-0.1873	0.0855	0.2962	0.1592
120	0.2072	0.0199	0.0641	0.1088	0.1183	-0.1134

## Appendix C

This appendix contains two programs useful for evaluating angular correlation formulas. The programs are listed, and at the end of each listing is a set of sample data and the output from that sample data. The program CORR is more complicated to use and has a set of instructions preceeding the listing of the program. The program ANGLE is very simple to use and the comments in the listing are sufficient for its use.

Program CORR consists essentially of ten do loops which allow an angular correlation formula consisting of a sum of products of numbers, angular momentum coupling coefficients and functions to be evaluated. The system has some special constants which are:

```
#E=e, the base of natural logarithms,  
#P=Pi,  
#I= $\sqrt{-1}$ .
```

The program's ten do loops allow ten variables to be summed over in any increments to any final value as long as the control variable is greater than zero. The input is concerned with setting up variable values and ranges. The data is input using PL/1 data strings. These strings consist of the variable to be input set equal to the value the user wants the variable to have. An example is:

```
VARI=3,CAT='CAT',DOG=66.6,T=5;
```

Note that the variables are separated by commas and the data string is terminated by a semicolon. Character string data

(equivalent to Hclorith data in FORTRAN) are enclosed by single quotes as in the example above `CAT='CAT'`.

The first data input string is of the form:

```
TEST=X1,NLOOP=X2,NKW=X3,NKZ=X4,NKC=X5,MAXV=X6;
```

X1 is either 1 or 0. If X1 is 1, then the program outputs the input data and runs the program without evaluating the angular correlation formula. This allows the input to be checked for errors. Since this is a general symbolic manipulation program, incorrect input will give a formula which may look correct. Great care must be taken with the input to avoid costly mistakes. If X1 is 0, then the angular correlation formula is evaluated and the running sum is output for each term which is non-zero. X2 is an integer from 1 to 10. This is the number of variables to be summed over. X3 is a positive integer which gives the number of W-coefficients in the correlation formula. If X3 is zero, then there is no W-coefficient in the formula. X4 is the same as X3 except that it is the delimiter for Z-coefficients. X5 is the same as X3 except that it is the delimiter for Clebsch-Gordan coefficients. X6 is the maximum number of non-integer variables which are to be summed over. To determine X6, count the number of the non-integer variables in each do loop. The maximum number obtained is X6. For example, say there are three do loops with non-integer variables:

```
Loop1: 1/2,7/2,3/2
Loop2: 3/2,9/2,7/2,15/2
Loop3: 5/2,3,2
```

Loop2 has the largest number of variables and the value of MAXV is four.

The second data input string is of the form:

```
NVAR(10)=X1,NVAR(9)=X2,...NVAR(1)=X10;
```

NVAR(I) is the number of non-integer variables in do loop-I. If NVAR(I) is zero, then it may be omitted. There must be at least one NVAR(J)=X in the string even if X=0. This is a peculiarity of the PL/1 GET DATA(XXXX) statement. That is,

a string cannot be blank.

The third data input string is of the form:

```

IB(10)=X1,II(10)=X2,IE(10)=X3,
  IB(9)=Y1, II(9)=Y3, IE(9)=Y3,
      .
      .
      .
IB(2)=Z1, II(2)=Z2, IE(2)=Z3,
IB(1)=W1, II(1)=W2, IE(1)=W3;

```

The index numbers correspond to do loop numbers with an associated control variable. For example:

```
DO I09=IB(9) BY II(9) TO IE(9);
```

is the beginning statement of do loop nine. Thus, I09 starts at IB(9) increments by II(9) and ends at IE(9). If one only uses five do loops, only IB, II, and IE with index from 5 to 1 must be input. The rest may be omitted since they are initialized so that do loops not mentioned in the input are skipped. Note: the index refers to the do loop number. The loops are numbered inner to outer, 1 to 10. If a variable to be summed over is an integer, one can use the names of the control variable in the correlation formula to be evaluated.

The fourth data input string is of the form:

```

CVAR(10,1)='X1',CVAR(10,2)='X2',...,CVAR(10,MAXV)='XMAX',
CVAR(9,1)='Y1',CVAR(9,2)='Y2',...,CVAR(9,MAXV)='YMAX',
      .
      .
      .
CVAR(2,1)='Z1',CVAR(2,2)='Z2',...,CVAR(2,MAXV)='ZMAX',
CVAR(1,1)='W1',CVAR(1,2)='W2',...,CVAR(1,MAXV)='WMAX';

```

These data are the names of variables summed over which are non-integer. CVAR(I,J) is the name of the variable value for the Ith do loop, Jth term. The use of this input will become clear in an example which follows.

The fifth data input string is of the form:

```
CWW(1,2)='X2',CWW(1,3)='X3',...,CWW(1,7)='X7',
CWW(2,2)='Y2',CWW(2,3)='X3',...,CWW(2,7)='Y7',
.
.
.
CWW(NKW,2)='W2',CWW(NKW,3)='W3',...,CWW(NKW,7)='W7';
```

The sixth data input string is of the form:

```
CZZ(1,2)='X2',CZZ(1,3)='X3',...,CZZ(1,7)='X7',
CZZ(2,2)='Y2',CZZ(2,3)='Y3',...,CZZ(2,7)='Y7',
.
.
.
CZZ(NKZ,2)='W2',CZZ(NKZ,3)='W2',...,CZZ(NKZ,7)='W7';
```

The seventh data input string is of the form:

```
CCG(1,2)='X2',CCG(1,3)='X3',...,CCG(1,7)='X7',
CCG(2,2)='Y2',CCG(2,3)='Y3',...,CCG(2,7)='Y7',
.
.
.
CCG(NKC,2)='W2',CCG(NKC,3)='W3',...,CCG(NKC,7)='W7';
```

The fifth, sixth, and seventh data strings are similar. The CWW are the arguments for the W-coefficient, the CZZ are the arguments for the Z-coefficients, and the CCG are the arguments for the Clebsch-Gordan coefficients. The first index, I, in the example below, determines the number of the coefficient which will take on the value W(I)

$$CWW(I,J) = '1/2'$$

The second index J is the index giving the entry into the coefficient subroutine. If any of these are zero they do not have to be read in. If a non-integer value has to be read into the subroutine, one writes an input like the following

$$CWW(2,4) = 'BVAF(2,I)'$$

This third entry into the W-coefficient subroutine (second call) is 'BVAR(2,I)' which is the FORMAC variable equal to the input variable CVAR(2,I). The arguments go into the coefficient generating subroutine in the following way. (Notation is that of Brink and Satchler).

$$W(a \ b \ c \ d ; \ e \ f) = WW(W(I), CWW(I,2), CWW(I,3), \dots, CWW(I,7))$$

That is, for the Ith call or use of the W-coefficient subroutine, the coefficient is equal to W(I) and a=CWW(I,2), b=CWW(I,3), ..., f=CWW(I,7). Similar argument inputs are used for Clebsch-Gordan and Z-coefficients, viz.,

$$\begin{aligned} &CLEBG(C(I), CCG(I,2), CCG(I,3), \dots, CCG(I,7)) \\ &ZZ(Z(I), CZZ(I,2), CZZ(I,3), \dots, CZZ(I,7)) \end{aligned}$$

Where C(I) and Z(I) are the values of the coefficients and the other arguments have the meaning.

$$\begin{aligned} C(I) &= \langle a \ b \ c \ d ; \ e \ f \rangle, \quad a=CCG(I,2), \quad b=CCG(I,3), \dots, \quad f=CCG(I,7) \\ Z(I) &= Z(a \ b \ c \ d ; \ e \ f), \quad a=CZZ(I,2), \quad b=CZZ(I,3), \dots, \quad f=CZZ(I,7). \end{aligned}$$

If any of the above types of coupling coefficients are not used, one must have an input like the following:

$$CCG(0,J) = '0';$$

One must use a similar expression for any other coefficient not used. This is to keep the input ordering correct. The value of the coefficients are assigned the names below:

$$\begin{array}{lll} Z(1) & W(1) & C(1) \\ Z(2) & W(2) & C(2) \\ & \cdot & \\ & \cdot & \\ & \cdot & \\ Z(NKZ) & W(NBW) & C(NKC) \end{array}$$

These values must be used in the correlation formula as it is input.



The eighth data input string is of the form:

CACOR='NUMBERS\*Z(1)\*Z(2)...Z(NKZ)\*W(1)\*W(2)...W(NKW)\*C(1)\*  
C(2)...,C(NKC)\*MATRIX ELEMENTS\*ANGULAR FUNCTIONS';

The equation is enclosed in single quotes. This input is the angular correlation formula to be evaluated.

The following data is an example. The correlation formula to be evaluated is:

$$W(\Theta_{p'}) = \sum_{x} (-1)^{A-2B_2+C-2j_1-2j_1'+l_p+l_{p'}+3K+(l_1-l_2+l_1'-l_2')/2} \\ (\hat{B}_1 \hat{B}_2)^2 (\hat{A} \hat{l}_p \hat{l}_{p'} + \pi)^2 Z(l_1 j_1 l_2 j_2; l_p k) W(j_2 B_2 j_1 B_1; A k) \times \\ Z(l_1' j_1' l_2' j_2'; l_{p'} k) W(j_2' B_2 j_1' B_1; C k) P_k(\Theta_{p'}) \times \\ \langle B_1 C_1 j_1' | O_c | B_1 \rangle \langle B_2 C_2 j_2' | O_c | B_2 \rangle^*$$

$$\text{WITH } A=0, C=2, B_1=B_2=B=3/2, j_1=j_2=3/2, l_p=l_{p'}=1/2, l_1=l_2=1, \\ l_1'=l_2'=1$$

The formula above becomes:

$$W(\Theta_{p'}) = \sum_{k, j_1', j_2'} (-1)^{-3+3K-2j_1'} Z(1 \ 3/2 \ 1 \ 3/2; 1/2 k) W(3/2 \ 3/2 \ 3/2 \ 3/2; 0 k) \times \\ Z(1 \ j_1' \ 1 \ j_2'; 1/2 k) W(j_2' \ 3/2 \ j_1' \ 3/2; 2 k) \times \\ P_k(\Theta_{p'}) \gamma_{j_1'} \gamma_{j_2'}^*$$

First data string:

TEST=0, NLOCP=3, NKW=2, NKZ=2, NKC=0, MAXV=2;

Second data string:

NVAR(3)=0, NVAR(2)=2, NVAR(1)=2;

Third data string:

IB(3)=0, II(3)=2, IF(3)=2,

IB(2)=1,II(2)=1,IE(2)=2,

IB(1)=1,II(1)=1,IE(1)=2;

Fourth data string:

CVAR(2,1)='1/2',CVAR(2,2)='3/2',

CVAR(1,1)='1/2',CVAR(1,2)='3/2';

Fifth data string:

CWW(1,2)='3/2',CWW(1,3)='1/2',CWW(1,4)='3/2',CWW(1,5)='3/2',  
 CWW(1,6)='0',CWW(1,7)='I03',  
 CWW(2,2)='BVAR(1,I01)',CWW(2,3)='3/2',CWW(2,4)='BVAR(2,I02)',  
 CWW(2,5)='3/2',CWW(2,6)='2',CWW(2,7)='I03';

Sixth data string:

CZZ(1,2)='1',CZZ(1,3)='3/2',CZZ(1,4)='1',CZZ(1,5)='3/2',  
 CZZ(1,6)='1/2',CZZ(1,7)='I03',  
 CZZ(2,2)='1',CZZ(2,3)='BVAR(2,I02)',CZZ(2,4)='1',  
 CZZ(2,5)='BVAR(1,I01)',CZZ(2,6)='1/2',CZZ(2,7)='I3';

Seventh data string:

CCG(0,2)='0';

Eighth data string:

CACOR='((-1)\*\*(-3-2\*BVAR(2,I02)+3\*I03))\*(1/4\*\*P)\*\*2\*Z(1)\*  
 W(1)\*Z(2)\*W(2)\*P.(I03,THETA)\*  
 GAM.(BVAR(2,I02))\*GAMC.(BVAR(1,I01))';

Arbitrary user defined functions use the form XXXXX. as in the above function GAM.(BVAR(2,I02)). As many sets of eight data strings may be input for calculation as the user wishes.

```

COFF:PRECEDENCE OPTIONS (MAIN):
FCFMAC_OPTIONS:
/*DEFINE SQUARE OF TRIANGLE FUNCTION-TRISQ */
LET(FNC (TRISQ) =FAC (S (1) +S (2) -S (3)) *FAC (S (1) +S (3) -S (2))
      *FAC (S (2) +S (3) -S (1)) /FAC (S (1) +S (2) +S (3) +1);
ON ENDFILE (SYSTEM) GO TO EXIT;
/* IF TEST=1 THE PROGRAM READS INPUT AND PUTS IT IN THE ARRAYS IT */
/* USES AND PRINTS OUT THE INPUT VARIABLES FOR CHECKING. IT DOES */
/* NOT EVALUATE THE FORMULA. IF TEST=0, IT EVALUATES THE FORMULA. */
/* */
/* INPUT THE NUMBER OF DO LOOPS. NLOOP<=10. */
/* INPUT THE NUMBER OF W-COEFFICIENTS IN THE CORRELATION FORMULA. */
/* VARIABLE=NKW */
/* */
/* INPUT THE NUMBER OF Z-COEFFICIENTS IN THE CORRELATION FORMULA. */
/* VARIABLE=NKZ. */
/* */
/* INPUT THE NUMBER OF CG-COEFFICIENTS IN THE CORRELATION FORMULA. */
/* VARIABLE=NKC. */
/* */
/* DETERMINE THE NUMBER OF NON-INTEGER VARIABLES FOR EACH DO LOOP. */
/* NVAR(L) IS THE NUMBER OF NON-INTEGER VARIABLES IN DO LOOP-L. */
/* DO LOOPS ARE NUMBERED FROM BOTTOM TO TOP */
/* */
/* ALSO DETERMINE THE MAXIMUM NUMBER OF NON-INTEGER VARIABLES ONE */
/* WILL USE IN ANY LOOP-MAXV. */
/* */
START:GET DATA (TEST,NLOOP,NKW,NKZ,NKC,MAXV);
BLCK:BEGIN;
  DECLARE (CVAR (NLOOP,0:MAXV)) CHARACTER (30) VARYING;
  DECLARE (CWW (0:NKW,7)) CHARACTER (30) VARYING;
  DECLARE (CZZ (0:NKZ,7)) CHARACTER (30) VARYING;
  DECLARE (CCG (0:NKC,7)) CHARACTER (30) VARYING;
  DECLARE CACOF CHARACTER (300) VARYING INITIAL ((300)'0');
  DECLARE (IE (10)) FIXED BINARY;
  DECLARE (II (10)) FIXED BINARY;
  DECLARE (IE (10)) FIXED BINARY;
  DECLARE (NVAR (10)) FIXED BINARY;
  DO I=1 TO NLOOP;
    DO J=0 TO MAXV;
      CVAR (I,J) = '0';
    END;
  END;
  DO I=0 TO NKW;
    DO J=1 TO 7;
      CWW (I,J) = '0';
    END;
  END;
  DO I=0 TO NKZ;
    DO J=1 TO 7;
      CZZ (I,J) = '0';
    END;
  END;
  DO I=0 TO NKC;
    DO J=1 TO 7;
      CCG (I,J) = '0';
    END;
  END;
  DO I=1 TO 10;

```

```

IB(I)=0;
II(I)=1;
IE(I)=0;
NVAR(I)=0;
END;
/* READ VALUES OF NVAR */
GET DATA(NVAR);
/* READ IN BEGINNING, INCREMENTING, AND ENDING VALUES FOR THE
/* CCNTFOL VARIABLES FOR THE IO LOGPS. THEY MUST BE INTEGERS.
/* THE SMALLEST ALLOWABLE VALUE IS ZERO.
GET DATA(IB,II,IE);
/* READ IN VALUES FOR NON-INTEGEE VAPIABLES.
GET DATA(CVAR);
/* CONVERT FROM PL/1 CHARACTER VARIABLES TO FORMAC VARIABLES.
DO ILO=1 TO NLOOP; LET(LL0="LLO");
DO KKO=0 TO NVAR(LL0); LET(KKO="KKO");
LET(BVAR(LL0,KKO)="CVAR(LL0,KKO)");
END;
END;
/* INPUT VARIABLE NAMES FOR USE IN W-COEFFICIENT SUBROUTINE.
GET DATA(CWW);
/* INPUT VARIABLE NAMES FOR USE IN Z-COEFFICIENT SUBROUTINE.
GET DATA(CZZ);
/* INPUT VARIABLE NAMES FOR USE IN CG-COEFFICIENT SUBROUTINE.
GET DATA(CCG);
/* READ IN ANGULAR CORRELATION FORMULA.
GET DATA(CACOR);
LET(MT=0);
DO I10=IE(10) BY II(10) TO IE(10); LET(I10="I10");
DO I09=IE(9) BY II(9) TO IE(9); LET(I09="I09");
DO I08=IE(8) BY II(8) TO IE(8); LET(I08="I08");
DO I07=IE(7) BY II(7) TO IE(7); LET(I07="I07");
DO I06=IE(6) BY II(6) TO IE(6); LET(I06="I06");
DO I05=IE(5) BY II(5) TO IE(5); LET(I05="I05");
DO I04=IE(4) BY II(4) TO IE(4); LET(I04="I04");
DO I03=IE(3) BY II(3) TO IE(3); LET(I03="I03");
DO I02=IE(2) BY II(2) TO IE(2); LET(I02="I02");
DO I01=IE(1) BY II(1) TO IE(1); LET(I01="I01");
PUT DATA(I10,I09,I08,I07,I06,I05,I04,I03,I02,I01);
PUT SKIP(2);
/* CONVERT FROM PL/1 CHARACTER VARIABLES TO FORMAC VARIABLES.
DO LL1=1 TO NKW; LET(LL1="LL1");
DO KK1=1 TO 7; LET(KK1="KK1");
LET(WW(LL1,KK1)="CWW(LL1,KK1)");
END;
END;
/* CONVERT FROM PL/1 CHARACTER VARIABLES TO FORMAC VARIABLES.
DO LL2=1 TO NKZ; LET(LL2="LL2");
DO KK2=1 TO 7; LET(KK2="KK2");
LET(ZZ(LL2,KK2)="CZZ(LL2,KK2)");
END;
END;
/* CONVERT FROM PL/1 CHARACTER VARIABLES TO FORMAC VARIABLES.
DO LL3=1 TO NRC; LET(LL3="LL3");
DO KK3=1 TO 7; LET(KK3="KK3");
LET(CG(LL3,KK3)="CCG(LL3,KK3)");
END;
END;
IF TEST=0 THEN
DC;

```

```

DO KW=1 TO NKW; LET (KW="KW");
CALL WW ('WW(KW,1)', 'WW(KW,2)', 'WW(KW,3)', 'WW(KW,4)', 'WW(KW,5)',
        'WW(KW,6)', 'WW(KW,7)');
LET (W(KW)=WW(KW,1));
IF IDENT(WW(KW,1);0) THEN GO TO OVER;
END;
DO KZ=1 TO NKZ; LET (KZ="KZ");
CALL ZZ ('ZZ(KZ,1)', 'ZZ(KZ,2)', 'ZZ(KZ,3)', 'ZZ(KZ,4)', 'ZZ(KZ,5)',
        'ZZ(KZ,6)', 'ZZ(KZ,7)');
LET (Z(KZ)=ZZ(KZ,1));
IF IDENT(ZZ(KZ,1);0) THEN GO TO OVER;
END;
DO KC=1 TO NKC; LET (KC="KC");
CALL CLEBG ('CG(KC,1)', 'CG(KC,2)', 'CG(KC,3)', 'CG(KC,4)', 'CG(KC,5)',
          'CG(KC,6)', 'CG(KC,7)');
LET (C(KZ)=CG(KC,1));
IF IDENT(CG(KC,1);0) THEN GO TO OVER;
END;
LET (ICACOP="CACOP";
    ACCFF=ICACOP);
CALL PRETSYN ('ACOPR', PFLAG);
CPTSET (PFINT);
LET (MT=MT+ACOPR);
OPTSET (NOPRINT);
PUT SKIP (4);
END;
OVER: ENC;
      ENC;
      ENC;
      ENC;
      ENC;
      ENC;
      ENC;
      ENC;
      ENC;
      ENC;
      ENC;
      ENC;
      ENC;
      PUT PAGE;
      PFINT_CUT (MT);
      PUT PAGE;
      IF TEST=1 THEN
      DC;
      PUT DATA (TEST, NLOOP, NKW, NKZ, NKC, MAXV) SKIP (2);
      PUT DATA (IB, II, IE, NVAR) SKIP (2);
      PUT DATA (CVAP) SKIP (2);
      PUT DATA (CWW) SKIP (2);
      PUT DATA (CZZ) SKIP (2);
      PUT DATA (CCG) SKIP (2);
      PUT DATA (CACOP) SKIP (2);
      GO TO SKIP;
      END;
      END BLOCK;
SKIP: GC TO START;
/*
/*
/*-----CLEBG-CLEBG-CLEBG-CLEBG-CLEBG-CLEBG-CLEBG-CLEBG-CLEBG-----*/
/*
/*
/*
/* PROCEDURE CLEBG WRITTEN BY W. K. WELLS MAY 1978 TO EVALUATE
/* CLEBSCH-GORDAN COEFFICIENTS. IT IS WRITTEN IN FORTRAN, AN
/* UNOFFICIAL IBM LANGUAGE WHICH ALLOWS FOR COMPLEX SYMBOLIC
*/

```

```

/* MANIPULATIONS. THE FOLLOWING CAPD GIVES A STANDARD CALL FOR THE */
/* ROUTINE. NOTE THAT THE ARGUMENTS ARE IN SINGLE QUOTES AND ARE */
/* FORMAC VARIABLES, ONE CAN ONLY CALL THIS ROUTINE FROM A FORMAC */
/* PROCEDURE. */
/* CALL CLEBG('CG','J1','J2','MJ1','MJ2','J3','MJ3'); */
/* */
/* THE USER DEFINED FUNCTION SHOWN BELOW NEEDS PLACING IN MAIN */
/* FORMAC PROCEDURE. IT DEFINES THE TRIANGLE COEFFICIENT AND SHOULD */
/* BE THE FIRST EXECUTABLE STATEMENT IN THE MAIN PROCEDURE. */
/* LET (FNC (TRISQ)=FAC ($ (1)+$ (2)-$ (3)) *FAC ($ (1)+$ (3)-$ (2)) */
/* *FAC ($ (2)+$ (3)-$ (1)) /FAC ($ (1)+$ (2)+$ (3)+1)); */
/* */
/* MAIN PROCEDURE ALSO NEEDS PROCEDURES VALFA AND VALID FOR USE */
/* IN THIS PROCEDURE. */
/* FOR DISCUSSION OF CLEBSCH-GORDAN COEFFICIENTS SEE BRINK AND */
/* SATCHLER ANGULAR MOMENTUM, SECOND EDITION, P. 34 */
/* */
/*-----CLEBG-CLEBG-CLEBG-CLEBG-CLEBG-CLEBG-CLEBG-CLEBG-CLEBG-----*/
/* */
/* */
/* */
CLEBG:PROCEDURE (CG,CA,CB,CALPH,CBETA,CC,CGAMA);
  DECLARE (CC,CA,CB,CG,CALPH,CBETA,CGAMA) CHARACTER (10) VARYING;
/* */
/* INITIALIZE CG-COEFFICIENT AND REDEFINE FOR USE IN SPECIAL FORMAC */
/* FUNCTIONS */
/* */
/* CQ SHOULD BE ZERO FOR NON-ZERO CG-COEFFICIENT */
/* */
  LET ("CG"=1;
      CA1="CA";
      CB1="CB";
      CC1="CC";
      CQ="CALPH"+"CBETA"+"CGAMA");
/* */
/* CHECK FOR CONSERVATION OF MAGNETIC PROJECTION */
/* */
  IF ~(IDENT(CQ;0)) THEN
    EC;
    LET ("CG"=0);
    RETURN;
  FND;
/* */
/* INITIALIZE FOLLOWING VALUES FOR SUM */
/* */
  LET (CNU=0;
      CAA=0;
      CIA (1)="CA"+"CALPH";
      CIA (2)="CC"+"CB"+"CALPH";
      CIA (3)="CB"+"CBETA";
      CIA (4)="CC"+"CA"+"CBETA";
      CIA (6)="CA"+"CB"+"CC";
      CIB (1)=1;
      CIB (3)=1;
      CIB (6)=1);
/* */
/* SUM OVER ALL CNU WHICH LEAD TO NON-NEGATIVE FACTORIALS */
/* */
  DO WHILE (INTEGER (CIB (1)) > 0 & INTEGER (CIB (3)) > 0 & INTEGER (CIB (6)) > 0);
    LET (CIB (0) = (-1) ** CNU;
        CIB (1) = CIA (1) - CNU;

```

```

CIB (2)=CIA (2)+CNU;
CIB (3)=CIA (3)-CNU;
CIB (4)=CIA (4)+CNU;
CIB (5)=CNU;
CIB (6)=CIA (6)-CNU;
CNU=CNU+1);

/*
/* CHECK TO SEE IF TERMS ARE POSITIVE INTEGERS. ONLY USE POSITIVE
/* INTEGER TERMS IN SUM.
/*
/*      LET (CNEG=1);
/*
/* THE FOLLOWING TRAP FOR THE INDEX IN THE DO LOOP IS NECESSARY
/* SINCE ALL FORNAC VARIABLES ARE GLOBAL TO ALL PROCEDURES. IF
/* ONE DOES NOT USE DIFFERENT NAMES FOR THE DUMMY VARIABLES OF
/* DOES NOT TRAP OUT THE DUMMY VARIABLE IN DO LOOPS, OTHER DO LOOPS
/* IN THE PROGRAM WILL USE THE LAST VALUE OF THE VARIABLE IF THEY
/* HAVE THE SAME NAME. ONE MUST RESUME USING THE CORRECT VALUE
/* OF THE DUMMY INDEX AFTER EXITING THE DO LOOP .
/*
/*      LET (CSVTP (1)=CJ);
/*      DO CJ=1 TO 6; LET (CJ="CJ");
/*      CALL VALFA ('CIB (CJ)', 'CU (CJ) ');
/*      LET (CNEG=CNEG*CU (CJ));
/*      END;
/*      LET (CJ=CSVTP (1));
/*      IF IDENT (CNEG;0) THEN GO TO NEG;
/*      LET (CAA=CAA+CIB (0) / (FAC (CIB (1)) *FAC (CIB (2)) *FAC (CIB (3))
/*          *FAC (CIB (4)) *FAC (CIB (5)) *FAC (CIB (6))));
NEG:END;
/*
/* IF CAA = 0 THEN COEFFICIENT IS ZERO..
/*
/*      IF IDENT (CAA;0) THEN
/*      DC;
/*      LET ("CG"=0);
/*      SETUPN;
/*      END;
/*
/* CHECK FOR TERMS IN STATEMENT SUM1 TO MAKE SURE ALL ARGUMENTS GIVE
/* RISE TO POSITIVE INTEGERS.
/*
/*      LET (CFACS=0;
/*      CAF (0)=2*"CC"+1;
/*      CAF (1)="CA"+"CALPH";
/*      CAF (2)="CA"- "CALPH";
/*      CAF (3)="CB"+"CBETA";
/*      CAF (4)="CB"- "CBETA";
/*      CAF (5)="CC"+"CGAMA";
/*      CAF (6)="CC"- "CGAMA");
/*      LET (CNULL=1);
/*
/*          DUMMY UP INDEX
/*
/*      LET (CSVTP (1)=CI);
/*      DO CI=0 TO 6; LET (CI="CI");
/*      CALL VALFA ('CAF (CI)', 'CV (CI) ');
/*      LET (CNULL=CNULL*CV (CI));
/*      END;
/*      LET (CI=CSVTP (1));

```





```

WW:PROCEDURE (W,WA,WB,WC,WD,WE,WF);
  DECLARE (W,WA,WE,WC,WD,WE,WF) CHARACTER (10) VARYING;
/*
/* CONVERT INPUT VARIABLES TO ONES WITHOUT QUOTES.
/*
  LET (WA2="WA";
      WB2="WB";
      WC2="WC";
      WD2="WD";
      WE2="WE";
      WF2="WF");
/*
/* INITIALIZE FOLLOWING VALUES FOR SUM
/*
  LET (SW=1;
      WAA=0;
      WZ=0;
      WIA (1)=WA2+WB2+WC2+WD2+1;
      WIA (3)=WE2+WF2-WA2-WD2;
      WIA (4)=WE2+WF2-WB2-WC2;
      WIA (5)=WA2+WB2-WE2;
      WIA (6)=WC2+WD2-WZ2;
      WIA (7)=WA2+WC2-WF2;
      WIA (8)=WB2+WD2-WF2;
      WIB (1)=1;
      WIB (5)=1;
      WIB (6)=1;
      WIB (7)=1;
      WIB (8)=1);
/*
/* SUM OVER ALL Z2 WHICH LEAD TO NON-NEGATIVE INTEGERS
/*
/*
  DO WHILE (INTEGER (WIB (1)) > 0 & INTEGER (WIB (5)) > 0 & INTEGER (WIB (6)) > 0 &
  INTEGER (WIB (7)) > 0 & INTEGER (WIB (8)) > 0);
  LET (WIB (0) = (-1) ** WZ;
      WIB (1) = WIA (1) - WZ;
      WIB (2) = WZ;
      WIB (3) = WIA (3) + WZ;
      WIB (4) = WIA (4) + WZ;
      WIB (5) = WIA (5) - WZ;
      WIB (6) = WIA (6) - WZ;
      WIB (7) = WIA (7) - WZ;
      WIB (8) = WIA (8) - WZ;
      WZ = WZ + 1);
/*
/* CHECK TO SEE IF TERMS ARE POSITIVE INTEGERS. ONLY USE POSITIVE
/* INTEGER TERMS IN SW.
/*
  LET (WNEG=1);
/*
/* THE FOLLOWING TRAP FOR THE INDEX IN THE DO LOOP IS NECESSARY
/* SINCE ALL FORNAC VARIABLES ARE GLOBAL TO ALL PROCEDURES. IF
/* ONE DOES NOT USE DIFFERENT NAMES FOR THE DUMMY VARIABLES OF
/* DOES NOT TRAP OUT THE DUMMY VARIABLE IN DO LOOPS, OTHER DO LOOPS
/* IN THE PROGRAM WILL USE THE LAST VALUE OF THE VARIABLE IF THEY
/* HAVE THE SAME NAME. ONE MUST RESUME USING THE CORRECT VALUE
/* OF THE DUMMY INDEX AFTER EXITING THE DO LOOP.
/*
  LET (WSVTE (1) = WJ);
  DO WJ = 1 TO 8; LET (WJ = "WJ");

```

```

CALL VALFA('WIB(WJ)', 'W'(WJ)');
LET(WNEG=WNEG*WJ(WJ));
END;
LET(WJ=WSVTP(1));
IF IDENT(WNEG;0) THEN GO TO NEG;
LET(WAA=WAA+WIB(0)*FAC(WIB(1))/(FAC(WIB(2))*FAC(WIB(3))*
FAC(WIB(4))*FAC(WIB(5))*FAC(WIB(6))*FAC(WIB(7))*
FAC(WIB(8))));
NEG:END;
/*
/* DETERMINE SIGN OF W COEFFICIENT.
/*
WAI=AFITH(WAA);
WPHAS=SIGN(WAI);
LET(WPHAS="WPHAS");
/*
/* IF WPHAS = 0 THEN COEFFICIENT IS ZERO
/*
IF IDENT(WPHAS;0) THEN
DC;
LET("W"=0);
RETURN;
END;
/*
/* CHECK ARGUMENTS OF TRISQ.
/*
CALL VALID('WA2','WB2','WE2','WP1');
CALL VALID('WA2','WC2','WF2','WP2');
CALL VALID('WB2','WE2','WF2','WP3');
CALL VALID('WC2','WD2','WE2','WP4');
LET(WPHAS=WPHAS*WP1*WP2*WP3*WP4);
/*
/* IF WPHAS = 0 THEN COEFFICIENT IS ZERO
/*
IF IDENT(WPHAS;0) THEN
DC;
LET("W"=0);
RETURN;
END;
LET("W"=WPHAS*FCOT.(TRISQ(WA2,WR2,WE2)*TRISQ(WA2,WC2,WF2)
*TRISQ(WB2,WD2,WE2)*TRISQ(WC2,WD2,WE2)*WAA**2));
RETURN;
END WR;
/*
/*
/*-----ZZ-ZZ-ZZ-ZZ-ZZ-ZZ-ZZ-ZZ-ZZ-ZZ-ZZ-ZZ-ZZ-ZZ-ZZ-ZZ-----*/
/* PROCEDURE ZZ WRITTEN BY W. K. WELLS MAY 1978 TO EVALUATE Z
/* COEFFICIENTS. IT IS WRITTEN IN FORMAC, AN UNOFFICIAL IBM LANGUAGE
/* WHICH ALLOWS COMPLEX SYMBOLIC MANIPULATIONS. THE STANDARD CALL
/* FOR THE ROUTINE IS GIVEN BELOW. NOTE THE ARGUMENTS ARE IN
/* SINGLE QUOTES AND ARE FORMAC VARIABLES. ONE CAN CALL THIS
/* ROUTINE ONLY FROM FORMAC PROCEDURES.
/* CALL ZZ('Z','L1','J1','L2','J2','S','L');
/*
/* THE MAIN PROCEDURE NEEDS THE PROCEDURES CLEBG AND WW, WHICH
/* THIS ROUTINE CALLS.
/*-----ZZ-ZZ-ZZ-ZZ-ZZ-ZZ-ZZ-ZZ-ZZ-ZZ-ZZ-ZZ-ZZ-ZZ-ZZ-ZZ-----*/
/*
/*
ZZ:PROCEDURE(Z,ZL1,ZJ1,ZL2,ZJ2,ZS,ZI);

```

```

DECLARE (Z,ZL1,ZJ1,ZL2,ZJ2,ZS,ZI) CHARACTER (10) VARYING;
LET (ZAA=0;ZBB=0;ZCC=0;
      ZL12="ZL1";
      ZJ12="ZJ1";
      ZL22="ZL2";
      ZJ22="ZJ2";
      ZS2="ZS";
      ZL2="ZL";
      ZAA=(2*ZL12+1)*(2*ZL22+1)*(2*ZJ12+1)*(2*ZJ22+1));
CALL NW ('ZBB','ZL12','ZJ12','ZL22','ZJ22','ZS2','ZL2');
IF IDENT (ZBB;0) THEN
DO;
LET ("Z"=0);
RETURN;
END;
CALL CIEG ('ZCC','ZL12','ZL22','0','0','ZL2','0');
IF IDENT (ZCC;0) THEN
DO;
LET ("Z"=0);
RETURN;
END;
LET (ZB=EVAL (ZBB,ROOT. ($),$(1));
      ZC=EVAL (ZCC,ROOT. ($),$(1));
      ZINT=ZC*ZB);
ZAI=ARITH (ZINT);
ZPHAS=SIGN (ZAI);
ZASS=ABS (ZAI);
IF (ZAI=-ZASS) THEN LET (ZINT=-ZINT);
LET (ZPHAS="ZPHAS";
      "Z"=ZPHAS*(#I** (ZL2-ZI12+ZL22)) *ROOT. (ZINT*ZAA));
RETURN;
END ZZ;
/*
/*
/*---VALID-VALID-VALID-VALID-VALID-VALID-VALID-VALID-VALID-VALID---*/
/*
/* VALID CHECKS TRIANGLE FUNCTION ARGUMENTS FOR VALIDITY. RETURNS */
/* V=1 FOR VALID ARGUMENTS,V=0 OTHERWISE. */
/*
/*---VALID-VALID-VALID-VALID-VALID-VALID-VALID-VALID-VALID-VALID---*/
/*
/*
VALID:PROCEDURE (VP,VQ,VR,V);
DECLARE (VE,VQ,VR,V) CHARACTER (10) VARYING;
LET ("V"=1;
      VCHK1="VP"+"VQ"+"VR";
      VCHK2="VP"+"VQ"- "VR";
      VCHK3="VP"+"VR"- "VQ";
      VCHK4="VQ"+"VR"- "VP");
VA1=ARITH (VCHK1);
VA2=ARITH (VCHK2);
VA3=ARITH (VCHK3);
VA4=ARITH (VCHK4);
VE1=INTEGER (VCHK1);
VE2=INTEGER (VCHK2);
VE3=INTEGER (VCHK3);
VE4=INTEGER (VCHK4);
VC1=VE1-VA1;
VC2=VE2-VA2;
VC3=VE3-VA3;

```

```

VC4=VB4-VA4;
IF (VA1<0|VA2<0|VA3<0|VA4<0) THEN
DC;
LET ("V"=0);
RETURN;
END;
IF (VC1<0|VC2<0|VC3<0|VC4<0) THEN
DC;
LET ("V"=0);
RETURN;
END;
RETURN;
END VALID;

/*
/*
/*---VALFA-VALFA-VALFA-VALFA-VALFA-VALFA-VALFA-VALFA-VALFA-VALFA---*/
/*
/* VALFA-CHECKS ARGUMENT S TO SEE IF IT IS A POSITIVE INTEGER.
/* FOR USE IN TESTING ARGUMENTS OF FAC. W=1 FOR INTEGER>=0,W=0
/* OTHERWISE.
/*
/*
/*---VALFA-VALFA-VALFA-VALFA-VALFA-VALFA-VALFA-VALFA-VALFA-VALFA---*/
/*
/*
VALFA:PROCEDURE (US,U);
  DECLARE (US,U) CHARACTER (10) VARYING;
  LET ("U"=1;
      USS="US");
  UCK1=ARITH (USS);
  UCK2=INTEGER (USS);
  UCK3=UCK2-UCK1;
  IF UCK1<0 THEN
  DC;
  LET ("U"=0);
  RETURN;
  END;
  IF UCK3<0 THEN
  DC;
  LET ("U"=0);
  RETURN;
  END;
  RETURN;
  END VALFA;

/*
/*
/*
/*
/* PERTSYM IS A SUBROUTINE WHICH SIMPLIFIES AN EXPRESSION WHICH
/* CONTAINS PRODUCTS OF THE ROOT FUNCTIONS INTO ONE ROOT FUNCTION
/*
/*
/*
/*
PERTSYM:PROCEDURE (PPING,PFLAG);
  DECLARE PINTPOT CHARACTER (30) VARYING;
  DECLARE PPING CHARACTER (30) VARYING;
  DECLARE (PN,PM,PINT,PSPT,PJ,PFLAG) FIXED BINARY;
  PFLAG=0;
  LET (PINT=1;
      JFLAG=1;

```

```

        PRRING="PRRING");
/* DETERMINE THE LEAD OPERATOR. */
    FN=LOP(FPRRING);
    IF (FN=25;FN=24) THEN
    DC;
    II=NARGS(FPRRING);
    IF II=1 THEN
    EC;
    IF FN=25 THEN
    DC;
    LET (JFLAG=-1);
    END;
    LET (PRRING=ARG (1,PRRING);
        "PRRING"=PRRING);
    END;
    END;
    FN=LOP(FPRRING);
/* IF LEAD OPERATOR IS * THEN SIMPLIFY ROOT. PRODUCTS */
    IF FN=26 THEN
    DC;
    PFLAG=1;
/* PM= NUMBER OF OPERATORS UNDER * */
    FN=NARGS(PRRING);
    BLCK:BEGIN;
        DECLARE PWHICH(PM) FIXED BINARY;
        DO I=1 TO PM;
            PWHICH(I)=0;
        END;
/* LOCATE ROOT. FUNCTION AND DETERMINE PRODUCT OF SQUARES OF ROOT. */
        DO PI=1 TO PM; LET (PI="PI");
            LET (PARG(PI)=ARG (PI,PRRING);
                POT=EVAL (PARG (PI),ROOT. ($),$(1)*0));
            IF IDENT (POT;0) THEN
            DC;
            LET (PR=EVAL (PARG (PI),ROOT. ($),$(1));
                PINT=PINT*PR);
            PWHICH (PI)=1;
            END;
        END;
/* RECONSTRUCT PRRING WITH SIMPLIFIED ROOT. FUNCTION */
        LET (PING=1);
        DO PJ=1 TO PM; LET (PJ="PJ");
            IF PWHICH (PJ)=1 THEN
            DC;
            LET (PARG (PJ)=1);
            END;
            LET (PING=PING*PARG (PJ));
            END;
            LET ("PRRING"=PING*ROOT. (PINT)*JFLAG);
        RETURN;
    END BLCK;
    END;
    RETURN;
    END PRFISYM;
EXIT:END CORR;

```

```

//TEST JOB DU.020.AA3152,'J-3 WELLS',T=4,P=90,M=1,R=300K,0=DUKE,
//      FORMS=111A
// *PW=NUKETUNL
//      EXEC          PGM=COBH
//STEPLIR DD DSN=DU.020.AA3152.WELLS.MAT,DISP=SHR
//SYSPRINT DD SYSOUT=A
//SYSIN DD *
TEST=0,NL00P=5,NKW=2,NKZ=2,NKC=0,MAXV=4;
NVAR(5)=0,NVAR(4)=0,NVAR(3)=0,NVAR(2)=4,NVAR(1)=4;
IR(5)=0,II(5)=2,IE(5)=2;
IR(4)=1,II(4)=2,IE(4)=3;
IR(3)=1,II(3)=2,IE(3)=3;
IR(2)=1,II(2)=1,IE(2)=4;
IR(1)=1,II(1)=1,IE(1)=4;
CVAR(1,1)='1/2',CVAR(1,2)='3/2',CVAR(1,3)='5/2',CVAR(1,4)='7/2';
CVAR(2,1)='1/2',CVAR(2,2)='3/2',CVAR(2,3)='5/2',CVAR(2,4)='7/2';
CWW(1,5)='3/2',CWW(1,6)='0',CWW(1,7)='I05';
CWW(2,2)='RVAR(1,I01)',CWW(2,3)='3/2',CWW(2,4)=
'RVAR(2,I02)',CWW(2,5)='3/2',CWW(2,6)='2',CWW(2,7)='I05';
CZZ(1,2)='1',CZZ(1,3)='3/2',CZZ(1,4)='1';
CZZ(1,5)='3/2',CZZ(1,6)='1/2',CZZ(1,7)='I05';
CZZ(2,2)='I04',CZZ(2,3)='RVAR(2,I02)',CZZ(2,4)='I03';
CZZ(2,5)='RVAR(1,I01)',CZZ(2,6)='1/2',CZZ(2,7)='I05';
CCG(0,2)='0';
CACOR='((-1)*(-3-2*RVAR(2,I02)+3*I05+(I04-I03)/2))*Z(1)*W(1)*Z(2)*W(2)*
GAM.(RVAR(2,I02))*GAMC.(RVAR(1,I01))*P.(I05,THETA)';
/*
//

```

```

TEST= 1.00000E+00
MAXV= 4;
NLOOP= 5
MKW= 2
MKZ= 2
MK= 0
IB(1)= 1
IB(2)= 1
IB(3)= 1
IB(4)= 1
IB(5)= 0
IB(6)= 0
IB(7)= 0
IB(8)= 0
IB(9)= 0
IB(10)= 0
II(1)= 1
II(2)= 1
II(3)= 2
II(4)= 2
II(5)= 2
II(6)= 1
II(7)= 1
II(8)= 1
II(9)= 1
II(10)= 2
IE(1)= 4
IE(2)= 4
IE(3)= 3
IE(4)= 3
IE(5)= 2
IE(6)= 0
IE(7)= 0
IE(8)= 0
IE(9)= 0
IE(10)= 0
NVAR(1)= 4
NVAR(2)= 4
NVAR(3)= 0
NVAR(4)= 0
NVAR(5)= 0
NVAR(6)= 0
NVAR(7)= 0
NVAR(8)= 0
NVAR(9)= 0
NVAR(10)= 0
CVAR(1,0)=0.0
CVAR(2,0)=0.0
CVAR(3,0)=0.0
CVAR(4,0)=0.0
CVAR(5,0)=0.0
CWH(0,1)=0.0
CWH(0,2)=0.0
CWH(0,3)=0.0
CWH(0,4)=0.0
CWH(0,5)=0.0
CWH(0,6)=0.0
CWH(0,7)=0.0
CWH(1,4)=3/2
CWH(1,5)=3/2
CWH(2,2)=BVAR(1,101)
CWH(2,3)=3/2
CWH(2,7)=I05
CZZ(0,1)=0.0
CZZ(0,2)=0.0
CZZ(0,3)=0.0
CZZ(0,4)=0.0
CZZ(0,5)=0.0
CZZ(0,6)=0.0
CZZ(0,7)=0.0
CZZ(1,4)=1
CZZ(1,5)=3/2
CZZ(2,2)=I04
CZZ(2,7)=I05
CCG(0,1)=0.0
CCG(0,2)=0.0
CCG(0,3)=0.0
CCG(0,4)=0.0
CCG(0,5)=0.0
CACOR=((-1)**(-3-2*BVAR(2,102)+3*I05+(I04-I03)/2))*Z(1)*W(1)*Z(2)*W(2)*
I05,THETA);
GAM=(BVAR(2,102))*GANC-(BVAR(1,101))*P-

```

DEN1001 DENDNT UNABLE TO OPEN SYSUT1

I10= 0 I09= 0 I08= 0 I07= 0 I06= 0  
 I05= 0 I04= 1 I03= 1 I02= 1 I01= 1

NT = ROOT. ( 1/16 ) GAMC. ( 1/2 ) GAM. ( 1/2 ) P. ( 0, THETA )

I10= 0 I09= 0 I08= 0 I07= 0 I06= 0  
 I05= 0 I04= 1 I03= 1 I02= 1 I01= 2;  
 I10= 0 I09= 0 I08= 0 I07= 0 I06= 0  
 I05= 0 I04= 1 I03= 1 I02= 1 I01= 3;  
 I10= 0 I09= 0 I08= 0 I07= 0 I06= 0  
 I05= 0 I04= 1 I03= 1 I02= 1 I01= 4;  
 I10= 0 I09= 0 I08= 0 I07= 0 I06= 0  
 I05= 0 I04= 1 I03= 1 I02= 2 I01= 1;  
 I10= 0 I09= 0 I08= 0 I07= 0 I06= 0  
 I05= 0 I04= 1 I03= 1 I02= 2 I01= 2;

NT = ROOT. ( 1/16 ) GAMC. ( 1/2 ) GAM. ( 1/2 ) P. ( 0, THETA ) + ROOT. ( 1/16 ) GAMC. ( 3/2 ) GAM. ( 3/2 ) P. ( 0, THETA )

I10= 0 I09= 0 I08= 0 I07= 0 I06= 0  
 I05= 0 I04= 1 I03= 1 I02= 2 I01= 3;  
 I10= 0 I09= 0 I08= 0 I07= 0 I06= 0  
 I05= 0 I04= 1 I03= 1 I02= 2 I01= 4;  
 I10= 0 I09= 0 I08= 0 I07= 0 I06= 0  
 I05= 0 I04= 1 I03= 1 I02= 3 I01= 1;  
 I10= 0 I09= 0 I08= 0 I07= 0 I06= 0  
 I05= 0 I04= 1 I03= 1 I02= 3 I01= 2;  
 I10= 0 I09= 0 I08= 0 I07= 0 I06= 0  
 I05= 0 I04= 1 I03= 1 I02= 3 I01= 3;  
 I10= 0 I09= 0 I08= 0 I07= 0 I06= 0  
 I05= 0 I04= 1 I03= 1 I02= 3 I01= 4;  
 I10= 0 I09= 0 I08= 0 I07= 0 I06= 0  
 I05= 0 I04= 1 I03= 1 I02= 4 I01= 1;  
 I10= 0 I09= 0 I08= 0 I07= 0 I06= 0  
 I05= 0 I04= 1 I03= 1 I02= 4 I01= 2;  
 I10= 0 I09= 0 I08= 0 I07= 0 I06= 0  
 I05= 0 I04= 1 I03= 1 I02= 4 I01= 3;



I10=	C	0	I09=	0	I08=	0	I07=	0	I06=	0
I05=	0	1	I04=	1	I03=	1	I02=	4	I01=	4;
I10=	0	0	I09=	0	I08=	0	I07=	0	I06=	0
I05=	0	1	I04=	1	I03=	3	I02=	1	I01=	1;
I10=	0	0	I09=	0	I08=	0	I07=	0	I06=	0
I05=	0	1	I04=	1	I03=	3	I02=	1	I01=	2;
I10=	0	0	I09=	0	I08=	0	I07=	0	I06=	0
I05=	0	1	I04=	1	I03=	3	I02=	1	I01=	3;
I10=	0	0	I09=	0	I08=	0	I07=	0	I06=	0
I05=	0	1	I04=	1	I03=	3	I02=	1	I01=	4;
I10=	0	0	I09=	0	I08=	0	I07=	0	I06=	0
I05=	0	1	I04=	1	I03=	3	I02=	2	I01=	1;
I10=	0	0	I09=	0	I08=	0	I07=	0	I06=	0
I05=	0	1	I04=	1	I03=	3	I02=	2	I01=	2;
I10=	0	0	I09=	0	I08=	0	I07=	0	I06=	0
I05=	0	1	I04=	1	I03=	3	I02=	2	I01=	3;
I10=	0	0	I09=	0	I08=	0	I07=	0	I06=	0
I05=	0	1	I04=	1	I03=	3	I02=	3	I01=	4;
I10=	0	0	I09=	0	I08=	0	I07=	0	I06=	0
I05=	0	1	I04=	1	I03=	3	I02=	3	I01=	1;
I10=	0	0	I09=	0	I08=	0	I07=	0	I06=	0
I05=	0	1	I04=	1	I03=	3	I02=	3	I01=	2;
I10=	0	0	I09=	0	I08=	0	I07=	0	I06=	0
I05=	0	1	I04=	1	I03=	3	I02=	4	I01=	1;
I10=	0	0	I09=	0	I08=	0	I07=	0	I06=	0
I05=	0	1	I04=	1	I03=	3	I02=	4	I01=	2;
I10=	0	0	I09=	0	I08=	0	I07=	0	I06=	0
I05=	0	1	I04=	1	I03=	3	I02=	4	I01=	3;
I10=	0	0	I09=	0	I08=	0	I07=	0	I06=	0
I05=	0	1	I04=	1	I03=	3	I02=	4	I01=	4;
I10=	0	0	I09=	0	I08=	0	I07=	0	I06=	0
I05=	0	3	I04=	3	I03=	1	I02=	1	I01=	1;
I10=	0	0	I09=	0	I08=	0	I07=	0	I06=	0
I05=	0	3	I04=	3	I03=	1	I02=	1	I01=	2;
I10=	0	0	I09=	0	I08=	0	I07=	0	I06=	0
I05=	0	3	I04=	3	I03=	1	I02=	1	I01=	3;
I10=	0	0	I09=	0	I08=	0	I07=	0	I06=	0
I05=	0	3	I04=	3	I03=	1	I02=	1	I01=	3;



I10=	0	I09=	0	I08=	0	I07=	0	I06=	0
I05=	0	I04=	3	I03=	3	I02=	2	I01=	4;
I10=	0	I09=	0	I08=	0	I07=	0	I06=	0
I05=	0	I04=	3	I03=	3	I02=	3	I01=	1;
I10=	0	I09=	0	I08=	0	I07=	0	I06=	0
I05=	0	I04=	3	I03=	3	I02=	3	I01=	2;
I10=	0	I09=	0	I08=	0	I07=	0	I06=	0
I05=	0	I04=	3	I03=	3	I02=	3	I01=	3;

MT = ROOT.( 1/16 ) GAMC.( 1/2 ) GAM.( 1/2 ) P.( 0, THETA ) + ROOT.( 1/16 ) GAMC.( 3/2 ) GAM.( 3/2 ) P.( 0, THETA ) +  
 ROOT.( 1/16 ) GAMC.( 5/2 ) GAM.( 5/2 ) P.( 0, THETA )

I10=	0	I09=	0	I08=	0	I07=	0	I06=	0
I05=	0	I04=	3	I03=	3	I02=	3	I01=	4;
I10=	0	I09=	0	I08=	0	I07=	0	I06=	0
I05=	0	I04=	3	I03=	3	I02=	4	I01=	1;
I10=	0	I09=	0	I08=	0	I07=	0	I06=	0
I05=	0	I04=	3	I03=	3	I02=	4	I01=	2;
I10=	0	I09=	0	I08=	0	I07=	0	I06=	0
I05=	0	I04=	3	I03=	3	I02=	4	I01=	3;
I10=	0	I09=	0	I08=	0	I07=	0	I06=	0
I05=	0	I04=	3	I03=	3	I02=	4	I01=	4;

MT = ROOT.( 1/16 ) GAMC.( 1/2 ) GAM.( 1/2 ) P.( 0, THETA ) + ROOT.( 1/16 ) GAMC.( 3/2 ) GAM.( 3/2 ) P.( 0, THETA ) +  
 ROOT.( 1/16 ) GAMC.( 5/2 ) GAM.( 5/2 ) P.( 0, THETA ) + ROOT.( 1/16 ) GAMC.( 7/2 ) GAM.( 7/2 ) P.( 0, THETA )

I10=	0	I09=	0	I08=	0	I07=	0	I06=	0
I05=	2	I04=	1	I03=	1	I02=	1	I01=	1;
I10=	0	I09=	0	I08=	0	I07=	0	I06=	0
I05=	2	I04=	1	I03=	1	I02=	1	I01=	2;

MT = ROOT.( 1/16 ) GAMC.( 1/2 ) GAM.( 1/2 ) P.( 0, THETA ) + ROOT.( 1/16 ) GAMC.( 3/2 ) GAM.( 3/2 ) P.( 0, THETA ) +  
 ROOT.( 1/16 ) GAMC.( 5/2 ) GAM.( 5/2 ) P.( 0, THETA ) + ROOT.( 1/16 ) GAMC.( 7/2 ) GAM.( 7/2 ) P.( 0, THETA ) - FOOT.(  
 1/100 ) GAMC.( 3/2 ) GAM.( 1/2 ) P.( 2, THETA )

I10=	0	I09=	0	I08=	0	I07=	0	I06=	0
------	---	------	---	------	---	------	---	------	---

I05= 2 I04= 1 I03= 1 I02= 1 I01= 3;  
 I10= 0 I09= 0 I08= 0 I07= 0 I06= 0  
 I05= 2 I04= 1 I03= 1 I02= 1 I01= 4;  
 I10= 0 I09= 0 I08= 0 I07= 0 I06= 0  
 I05= 2 I04= 1 I03= 1 I02= 2 I01= 1;  
 MT = ROOT. ( 1/16 ) GAMC. ( 1/2 ) P. ( 0, THETA ) + ROOT. ( 1/16 ) GAMC. ( 3/2 ) P. ( 0, THETA ) +  
 ROOT. ( 1/16 ) GAMC. ( 5/2 ) P. ( 0, THETA ) + ROOT. ( 1/16 ) GAMC. ( 7/2 ) P. ( 0, THETA ) - ROOT. ( 1/100 ) GAMC. ( 3/2 ) P. ( 2, THETA ) - ROOT. ( 1/100 ) GAMC. ( 1/2 ) P. ( 2, THETA )

I10= 0 I09= 0 I08= 0 I07= 0 I06= 0  
 I05= 2 I04= 1 I03= 1 I02= 2 I01= 2;  
 HT = ROOT. ( 1/16 ) GAMC. ( 1/2 ) P. ( 0, THETA ) + ROOT. ( 1/16 ) GAMC. ( 3/2 ) P. ( 0, THETA ) +  
 ROOT. ( 1/16 ) GAMC. ( 5/2 ) P. ( 0, THETA ) + ROOT. ( 1/16 ) GAMC. ( 7/2 ) P. ( 0, THETA ) - ROOT. ( 1/100 ) GAMC. ( 3/2 ) P. ( 2, THETA ) - ROOT. ( 1/100 ) GAMC. ( 1/2 ) P. ( 2, THETA )  
 ) GAMC. ( 3/2 ) P. ( 2, THETA )

I10= 0 I09= 0 I08= 0 I07= 0 I06= 0  
 I05= 2 I04= 1 I03= 1 I02= 2 I01= 3;  
 I10= 0 I09= 0 I08= 0 I07= 0 I06= 0  
 I05= 2 I04= 1 I03= 1 I02= 2 I01= 4;  
 I10= 0 I09= 0 I08= 0 I07= 0 I06= 0  
 I05= 2 I04= 1 I03= 1 I02= 3 I01= 1;  
 I10= 0 I09= 0 I08= 0 I07= 0 I06= 0  
 I05= 2 I04= 1 I03= 1 I02= 3 I01= 2;  
 I10= 0 I09= 0 I08= 0 I07= 0 I06= 0  
 I05= 2 I04= 1 I03= 1 I02= 3 I01= 3;  
 I10= 0 I09= 0 I08= 0 I07= 0 I06= 0  
 I05= 2 I04= 1 I03= 1 I02= 3 I01= 4;  
 I10= 0 I09= 0 I08= 0 I07= 0 I06= 0  
 I05= 2 I04= 1 I03= 1 I02= 4 I01= 1;  
 I10= 0 I09= 0 I08= 0 I07= 0 I06= 0  
 I05= 2 I04= 1 I03= 1 I02= 4 I01= 2;  
 I10= 0 I09= 0 I08= 0 I07= 0 I06= 0  
 I05= 2 I04= 1 I03= 1 I02= 4 I01= 3;  
 I10= 0 I09= 0 I08= 0 I07= 0 I06= 0  
 I05= 2 I04= 1 I03= 1 I02= 4 I01= 3;

I10= 0 I09= 0 I08= 0 I07= 0 I06= 0  
 I05= 2 I04= 1 I03= 1 I02= 4 I01= 4;  
  
 I10= 0 I09= 0 I08= 0 I07= 0 I06= 0  
 I05= 2 I04= 1 I03= 3 I02= 1 I01= 1;  
  
 I10= 0 I09= 0 I08= 0 I07= 0 I06= 0  
 I05= 2 I04= 1 I03= 3 I02= 1 I01= 2;  
  
 I10= 0 I09= 0 I08= 0 I07= 0 I06= 0  
 I05= 2 I04= 1 I03= 3 I02= 1 I01= 3;  
  
 NT = FOOT.( 1/16 ) GAMC.( 1/2 ) GAM.( 1/2 ) P.( 0, THETA ) + ROOT.( 1/16 ) GAMC.( 3/2 ) GAM.( 3/2 ) P.( 0, THETA ) +  
 ROOT.( 1/16 ) GAMC.( 5/2 ) GAM.( 5/2 ) P.( 0, THETA ) + ROOT.( 1/16 ) GAMC.( 7/2 ) GAM.( 7/2 ) P.( 0, THETA ) - ROOT.(  
 1/100 ) GAMC.( 3/2 ) GAM.( 1/2 ) P.( 2, THETA ) - ROOT.( 21/400 ) GAMC.( 5/2 ) GAM.( 1/2 ) P.( 2, THETA ) - ROOT.( 1/  
 100 ) GAMC.( 1/2 ) GAM.( 3/2 ) P.( 2, THETA ) - ROOT.( 9/400 ) GAMC.( 3/2 ) GAM.( 3/2 ) P.( 2, THETA )

I10= 0 I09= 0 I08= 0 I07= 0 I06= 0  
 I05= 2 I04= 1 I03= 3 I02= 1 I01= 4;  
  
 I10= 0 I09= 0 I08= 0 I07= 0 I06= 0  
 I05= 2 I04= 1 I03= 3 I02= 2 I01= 1;  
  
 I10= 0 I09= 0 I08= 0 I07= 0 I06= 0  
 I05= 2 I04= 1 I03= 3 I02= 2 I01= 2;  
  
 I10= 0 I09= 0 I08= 0 I07= 0 I06= 0  
 I05= 2 I04= 1 I03= 3 I02= 2 I01= 3;  
  
 NT = ROOT.( 1/16 ) GAMC.( 1/2 ) GAM.( 1/2 ) P.( 0, THETA ) + ROOT.( 1/16 ) GAMC.( 3/2 ) GAM.( 3/2 ) P.( 0, THETA ) +  
 ROOT.( 1/16 ) GAMC.( 5/2 ) GAM.( 5/2 ) P.( 0, THETA ) + ROOT.( 1/16 ) GAMC.( 7/2 ) GAM.( 7/2 ) P.( 0, THETA ) - ROOT.(  
 1/100 ) GAMC.( 3/2 ) GAM.( 1/2 ) P.( 2, THETA ) - ROOT.( 21/400 ) GAMC.( 5/2 ) GAM.( 1/2 ) P.( 2, THETA ) - ROOT.( 1/  
 100 ) GAMC.( 1/2 ) GAM.( 3/2 ) P.( 2, THETA ) - ROOT.( 9/400 ) GAMC.( 3/2 ) GAM.( 3/2 ) P.( 2, THETA ) + ROOT.( 3/700 )  
 GAMC.( 5/2 ) GAM.( 3/2 ) P.( 2, THETA )

I10= 0 I09= 0 I08= 0 I07= 0 I06= 0  
 I05= 2 I04= 1 I03= 3 I02= 2 I01= 4;  
  
 I10= 0 I09= 0 I08= 0 I07= 0 I06= 0  
 I05= 2 I04= 1 I03= 3 I02= 2 I01= 4;  
  
 NT = ROOT.( 1/16 ) GAMC.( 1/2 ) GAM.( 1/2 ) P.( 0, THETA ) + ROOT.( 1/16 ) GAMC.( 3/2 ) GAM.( 3/2 ) P.( 0, THETA ) +  
 ROOT.( 1/16 ) GAMC.( 5/2 ) GAM.( 5/2 ) P.( 0, THETA ) + ROOT.( 1/16 ) GAMC.( 7/2 ) GAM.( 7/2 ) P.( 0, THETA ) - ROOT.(  
 1/100 ) GAMC.( 3/2 ) GAM.( 1/2 ) P.( 2, THETA ) - ROOT.( 21/400 ) GAMC.( 5/2 ) GAM.( 1/2 ) P.( 2, THETA ) - ROOT.( 1/  
 100 ) GAMC.( 1/2 ) GAM.( 3/2 ) P.( 2, THETA ) - ROOT.( 9/400 ) GAMC.( 3/2 ) GAM.( 3/2 ) P.( 2, THETA ) + ROOT.( 3/700 )

GAMC. ( 5/2 ) GAM. ( 3/2 ) P. ( 2, THETA ) - ROOT. ( 9/350 ) GAMC. ( 7/2 ) GAM. ( 3/2 ) P. ( 2, THETA )

I10=	0	I09=	0	I08=	0	I07=	0	I06=	0
I05=	2	I04=	1	I03=	3	I02=	3	I01=	1;
I10=	0	I09=	0	I08=	0	I07=	0	I06=	0
I05=	2	I04=	1	I03=	3	I02=	3	I01=	2;
I10=	0	I09=	0	I08=	0	I07=	0	I06=	0
I05=	2	I04=	1	I03=	3	I02=	3	I01=	3;
I10=	0	I09=	0	I08=	0	I07=	0	I06=	0
I05=	2	I04=	1	I03=	3	I02=	3	I01=	4;
I10=	0	I09=	0	I08=	0	I07=	0	I06=	0
I05=	2	I04=	1	I03=	3	I02=	4	I01=	1;
I10=	0	I09=	0	I08=	0	I07=	0	I06=	0
I05=	2	I04=	1	I03=	3	I02=	4	I01=	2;
I10=	0	I09=	0	I08=	0	I07=	0	I06=	0
I05=	2	I04=	1	I03=	3	I02=	4	I01=	3;
I10=	0	I09=	0	I08=	0	I07=	0	I06=	0
I05=	2	I04=	1	I03=	3	I02=	4	I01=	4;
I10=	0	I09=	0	I08=	0	I07=	0	I06=	0
I05=	2	I04=	3	I03=	1	I02=	1	I01=	1;
I10=	0	I09=	0	I08=	0	I07=	0	I06=	0
I05=	2	I04=	3	I03=	1	I02=	1	I01=	2;
I10=	0	I09=	0	I08=	0	I07=	0	I06=	0
I05=	2	I04=	3	I03=	1	I02=	1	I01=	3;
I10=	0	I09=	0	I08=	0	I07=	0	I06=	0
I05=	2	I04=	3	I03=	1	I02=	1	I01=	4;
I10=	0	I09=	0	I08=	0	I07=	0	I06=	0
I05=	2	I04=	3	I03=	1	I02=	2	I01=	1;
I10=	0	I09=	0	I08=	0	I07=	0	I06=	0
I05=	2	I04=	3	I03=	1	I02=	2	I01=	2;
I10=	0	I09=	0	I08=	0	I07=	0	I06=	0
I05=	2	I04=	3	I03=	1	I02=	2	I01=	3;
I10=	0	I09=	0	I08=	0	I07=	0	I06=	0
I05=	2	I04=	3	I03=	1	I02=	2	I01=	4;
I10=	0	I09=	0	I08=	0	I07=	0	I06=	0
I05=	2	I04=	3	I03=	1	I02=	3	I01=	1;

HT = ROOT. ( 1/16 ) GAMC. ( 1/2 ) GAM. ( 1/2 ) P. ( 0, THETA ) + ROOT. ( 1/16 ) GAMC. ( 3/2 ) GAM. ( 3/2 ) P. ( 0, THETA ) +

ROOT.( 1/16 ) GAMC.( 5/2 ) GAM.( 5/2 ) P.( 0, THETA ) + ROOT.( 1/16 ) GAMC.( 7/2 ) GAM.( 7/2 ) P.( 0, THETA ) - ROOT.( 1/100 ) GAMC.( 3/2 ) GAM.( 1/2 ) P.( 2, THETA ) - ROOT.( 21/400 ) GAMC.( 5/2 ) GAM.( 1/2 ) P.( 2, THETA ) - ROOT.( 1/100 ) GAMC.( 1/2 ) GAM.( 3/2 ) P.( 2, THETA ) - ROOT.( 9/400 ) GAMC.( 3/2 ) GAM.( 3/2 ) P.( 2, THETA ) + ROOT.( 3/700 ) GAMC.( 5/2 ) GAM.( 3/2 ) P.( 2, THETA ) - ROOT.( 9/350 ) GAMC.( 7/2 ) GAM.( 3/2 ) P.( 2, THETA ) - ROOT.( 21/400 ) GAMC.( 1/2 ) GAM.( 5/2 ) P.( 2, THETA )

I10= 0 I09= 0 I08= 0 I07= 0 I06= 0  
 I05= 2 I04= 3 I03= 1 I02= 3 I01= 2;

NT = ROOT.( 1/16 ) GAMC.( 1/2 ) GAM.( 1/2 ) P.( 0, THETA ) + ROOT.( 1/16 ) GAMC.( 3/2 ) GAM.( 3/2 ) P.( 0, THETA ) + ROOT.( 1/16 ) GAMC.( 5/2 ) GAM.( 5/2 ) P.( 0, THETA ) + ROOT.( 1/16 ) GAMC.( 7/2 ) GAM.( 7/2 ) P.( 0, THETA ) - ROOT.( 1/100 ) GAMC.( 3/2 ) GAM.( 1/2 ) P.( 2, THETA ) - ROOT.( 21/400 ) GAMC.( 5/2 ) GAM.( 1/2 ) P.( 2, THETA ) - ROOT.( 1/100 ) GAMC.( 1/2 ) GAM.( 3/2 ) P.( 2, THETA ) - ROOT.( 9/400 ) GAMC.( 3/2 ) GAM.( 3/2 ) P.( 2, THETA ) + ROOT.( 3/700 ) GAMC.( 5/2 ) GAM.( 3/2 ) P.( 2, THETA ) - ROOT.( 9/350 ) GAMC.( 7/2 ) GAM.( 3/2 ) P.( 2, THETA ) - ROOT.( 21/400 ) GAMC.( 1/2 ) GAM.( 5/2 ) P.( 2, THETA ) + ROOT.( 3/700 ) GAMC.( 3/2 ) P.( 2, THETA )

I10= 0 I09= 0 I08= 0 I07= 0 I06= 0  
 I05= 2 I04= 3 I03= 1 I02= 3 I01= 3;  
 I10= 0 I09= 0 I08= 0 I07= 0 I06= 0  
 I05= 2 I04= 3 I03= 1 I02= 4 I01= 4;  
 I10= 0 I09= 0 I08= 0 I07= 0 I06= 0  
 I05= 2 I04= 3 I03= 1 I02= 4 I01= 1;  
 I10= 0 I09= 0 I08= 0 I07= 0 I06= 0  
 I05= 2 I04= 3 I03= 1 I02= 4 I01= 2;

NT = ROOT.( 1/16 ) GAMC.( 1/2 ) GAM.( 1/2 ) P.( 0, THETA ) + ROOT.( 1/16 ) GAMC.( 3/2 ) GAM.( 3/2 ) P.( 0, THETA ) + ROOT.( 1/16 ) GAMC.( 5/2 ) GAM.( 5/2 ) P.( 0, THETA ) + ROOT.( 1/16 ) GAMC.( 7/2 ) GAM.( 7/2 ) P.( 0, THETA ) - ROOT.( 1/100 ) GAMC.( 3/2 ) GAM.( 1/2 ) P.( 2, THETA ) - ROOT.( 21/400 ) GAMC.( 5/2 ) GAM.( 1/2 ) P.( 2, THETA ) - ROOT.( 1/100 ) GAMC.( 1/2 ) GAM.( 3/2 ) P.( 2, THETA ) - ROOT.( 9/400 ) GAMC.( 3/2 ) GAM.( 3/2 ) P.( 2, THETA ) + ROOT.( 3/700 ) GAMC.( 5/2 ) GAM.( 3/2 ) P.( 2, THETA ) - ROOT.( 9/350 ) GAMC.( 7/2 ) GAM.( 3/2 ) P.( 2, THETA ) - ROOT.( 21/400 ) GAMC.( 1/2 ) GAM.( 5/2 ) P.( 2, THETA ) - ROOT.( 9/350 ) GAMC.( 3/2 ) P.( 2, THETA )

I10=	0	I09=	0	I08=	0	I07=	0	I06=	0
I05=	2	I04=	3	I03=	1	I02=	4	I01=	3;
I10=	0	I09=	0	I08=	0	I07=	0	I06=	0
I05=	2	I04=	3	I03=	1	I02=	4	I01=	4;
I10=	0	I09=	0	I08=	0	I07=	0	I06=	0
I05=	2	I04=	3	I03=	3	I02=	1	I01=	1;
I10=	0	I09=	0	I08=	0	I07=	0	I06=	0
I05=	2	I04=	3	I03=	3	I02=	1	I01=	2;
I10=	0	I09=	0	I08=	0	I07=	0	I06=	0
I05=	2	I04=	3	I03=	3	I02=	1	I01=	4;
I10=	0	I09=	0	I08=	0	I07=	0	I06=	0
I05=	2	I04=	3	I03=	3	I02=	2	I01=	1;
I10=	0	I09=	0	I08=	0	I07=	0	I06=	0
I05=	2	I04=	3	I03=	3	I02=	2	I01=	2;
I10=	0	I09=	0	I08=	0	I07=	0	I06=	0
I05=	2	I04=	3	I03=	3	I02=	2	I01=	3;
I10=	0	I09=	0	I08=	0	I07=	0	I06=	0
I05=	2	I04=	3	I03=	3	I02=	2	I01=	4;
I10=	0	I09=	0	I08=	0	I07=	0	I06=	0
I05=	2	I04=	3	I03=	3	I02=	3	I01=	1;
I10=	0	I09=	0	I08=	0	I07=	0	I06=	0
I05=	2	I04=	3	I03=	3	I02=	3	I01=	2;
I10=	0	I09=	0	I08=	0	I07=	0	I06=	0
I05=	2	I04=	3	I03=	3	I02=	3	I01=	3;

$HT = \text{ROOT} \left( \frac{1}{16} \right) \text{GAMC} \left( \frac{1}{2} \right) \text{GAM} \left( \frac{1}{2} \right) P \left( 0, \text{THETA} \right) + \text{ROOT} \left( \frac{1}{16} \right) \text{GAMC} \left( \frac{3}{2} \right) \text{GAM} \left( \frac{3}{2} \right) P \left( 0, \text{THETA} \right) +$   
 $\text{ROOT} \left( \frac{1}{16} \right) \text{GAMC} \left( \frac{5}{2} \right) \text{GAM} \left( \frac{5}{2} \right) P \left( 0, \text{THETA} \right) + \text{ROOT} \left( \frac{1}{16} \right) \text{GAMC} \left( \frac{7}{2} \right) \text{GAM} \left( \frac{7}{2} \right) P \left( 0, \text{THETA} \right) - \text{ROOT} \left( \frac{1}{100} \right) \text{GAMC} \left( \frac{3}{2} \right) \text{GAM} \left( \frac{1}{2} \right) P \left( 2, \text{THETA} \right) - \text{ROOT} \left( \frac{21}{400} \right) \text{GAMC} \left( \frac{5}{2} \right) \text{GAM} \left( \frac{1}{2} \right) P \left( 2, \text{THETA} \right) - \text{ROOT} \left( \frac{1}{100} \right) \text{GAMC} \left( \frac{1}{2} \right) \text{GAM} \left( \frac{3}{2} \right) P \left( 2, \text{THETA} \right) - \text{ROOT} \left( \frac{9}{400} \right) \text{GAMC} \left( \frac{3}{2} \right) \text{GAM} \left( \frac{3}{2} \right) P \left( 2, \text{THETA} \right) + \text{ROOT} \left( \frac{3}{700} \right) \text{GAMC} \left( \frac{5}{2} \right) \text{GAM} \left( \frac{3}{2} \right) P \left( 2, \text{THETA} \right) - \text{ROOT} \left( \frac{9}{350} \right) \text{GAMC} \left( \frac{7}{2} \right) \text{GAM} \left( \frac{3}{2} \right) P \left( 2, \text{THETA} \right) - \text{ROOT} \left( \frac{21}{400} \right) \text{GAMC} \left( \frac{1}{2} \right) \text{GAM} \left( 5/2 \right) P \left( 2, \text{THETA} \right) + \text{ROOT} \left( \frac{3}{700} \right) \text{GAMC} \left( \frac{3}{2} \right) \text{GAM} \left( 5/2 \right) P \left( 2, \text{THETA} \right) - \text{ROOT} \left( \frac{1}{1225} \right) \text{GAMC} \left( \frac{5}{2} \right) \text{GAM} \left( 5/2 \right) P \left( 2, \text{THETA} \right) - \text{ROOT} \left( \frac{9}{350} \right) \text{GAMC} \left( \frac{3}{2} \right) \text{GAM} \left( 7/2 \right) P \left( 2, \text{THETA} \right)$

I10=	0	I09=	0	I08=	0	I07=	0	I06=	0
I05=	2	I04=	3	I03=	3	I02=	3	I01=	4;





GAMC. ( 5/2 ) GAM. ( 3/2 ) P. ( 2, THETA ) - ROOT. ( 9/350 ) GAMC. ( 7/2 ) GAM. ( 3/2 ) P. ( 2, THETA ) - ROOT. ( 21/400 )  
 -----  
 GAMC. ( 1/2 ) GAM. ( 5/2 ) P. ( 2, THETA ) + ROOT. ( 3/700 ) GAMC. ( 3/2 ) GAM. ( 5/2 ) P. ( 2, THETA ) - ROOT. ( 1/1225 ) GAMC  
 -----  
 . ( 5/2 ) GAM. ( 5/2 ) P. ( 2, THETA ) + ROOT. ( 6/1225 ) GAMC. ( 7/2 ) GAM. ( 5/2 ) P. ( 2, THETA ) - ROOT. ( 9/350 ) GAMC. ( 3  
 /2 ) GAM. ( 7/2 ) P. ( 2, THETA ) + ROOT. ( 6/1225 ) GAMC. ( 5/2 ) GAM. ( 7/2 ) P. ( 2, THETA ) + ROOT. ( 25/784 ) GAMC. ( 7/2  
 ) GAM. ( 7/2 ) P. ( 2, THETA )  
 -----



```

/*
/*
/*---ANGLE-ANGLE-ANGLE-ANGLE-ANGLE-ANGLE-ANGLE-ANGLE-ANGLE-ANGLE---*/
/* ANGLE WRITTEN BY W. K. WELLS TO EVALUATE CLEBSCH-GORDAN, W AND Z*/
/* COEFFICIENTS. IT GIVES THEM IN A FORM--SIGN TIMES FOOT. (A/B), */
/* WHERE A AND B ARE INTEGERS. THE SUBROUTINES AND MAIN PROCEDURE */
/* ARE WRITTEN IN FORMAC, A SYMBOLIC MANIPULATION LANGUAGE WRITTEN */
/* BY IEM. THE FOLLOWING CARDS GIVE INPUT FORMAT. */
/*
/*
  'Z', '0', '1/2', '0', '1/2', '1/2', '0'
  'W', '0', '1/2', '0', '1/2', '1/2', '0'
  'C', '4', '4', '0', '0', '6', '0'
/*
/* NOTICE THAT THE DATA IS SEPARATED BY COMMAS AND IS ENCLOSED IN */
/* SINGLE QUOTES. THE FIRST PARAMETER, EITHER 'C', 'W', OR 'Z' */
/* SPECIFIES THE COEFFICIENT TO BE CALCULATED. THE NEXT SIX */
/* PARAMETERS ARE THE STANDARD ENTRIES FOR THE COEFFICIENT */
/* SPECIFIED. THE OUTPUT ALSO GIVES THE FLOATING POINT VALUE OF */
/* THE COEFFICIENTS. */
/* FOR THE ORDER OF ARGUMENTS USED IN THIS PROGRAM SEE BRINK AND */
/* AND SATCHLER ANGULAR MOMENTUM, SECOND EDITION. */
/*---ANGLE-ANGLE-ANGLE-ANGLE-ANGLE-ANGLE-ANGLE-ANGLE-ANGLE-ANGLE---*/
/*
/*
ANGLE:PROCEDURE OPTIONS (MAIN):
  FCPRAC_OPTIONS;
  DECLAR (OP,AG1,AG2,AG3,AG4,AG5,AG6) CHARACTER(5) VARYING;
/*DEFINE SQUARE OF TRIANGLE FUNCTION-TRISQ
  LET (FNC (TRISQ)=FAC (3 (1)+3 (2)-3 (3))*FAC (3 (1)+3 (3)-3 (2))
      *FAC (3 (2)+3 (3)-3 (1))/FAC (3 (1)+3 (2)+3 (3)+1));
  ON ENDFILE (SYSIN) GO TO QUIT;
NEXT:GET LIST (OP,AG1,AG2,AG3,AG4,AG5,AG6);
IF (OP='C') THEN GO TO CS;
IF (OP='W') THEN GO TO WS;
IF (OP='Z') THEN GO TO ZS;
PUT LIST ('EFFOR IN INPUT-CHECK CARD WITH PARAMETERS',OP,AG1,AG2,
AG3,AG4,AG5,AG6);
GO TO NEXT;
CS: PUT LIST ('C(',AG1,AG2,AG3,AG4,',',AG5,AG6,')=');
LET (J1="AG1";
    J2="AG2";
    J3="AG5";
    MJ1="AG3";
    MJ2="AG4";
    MJ3="AG6");
CALL CLIEG ('CG',J1,J2,'MJ1','MJ2','J3','MJ3');
PRINT_OUT (CG);
/*
/* GIVE FLOATING POINT VALUE FOR CG-COEFFICIENT
/*
LET (CGF=CG;
    FCG=EVAL (CGF,FOOT. (5),SQRT (3 (1))));
PRINT_OUT (FCG);
GO TO NEXT;
WS: PUT LIST ('W(',AG1,AG2,AG3,AG4,',',AG5,AG6,')=');
LET (L1="AG1";
    J1="AG2";
    L2="AG3";

```

```

        J2="AG4";
        S="AG5";
        L="AG6";
        CALL WW('W','L1','J1','L2','J2','S','L');
        PRINT_OUT(W);
/*
/* GIVE FLOATING POINT VALUE FOR W-COEFFICIENT
/*
        LET(WF=W;
            FW=EVAL(WF,ROOT.(S),SQRT(S(1)));
        PRINT_OUT(FW);
        GC TO NEXT;
ZS:PUT LIST('Z','AG1,AG2,AG3,AG4',' ','AG5,AG6,')='');
        LET(L1="AG1";
            J1="AG2";
            L2="AG3";
            J2="AG4";
            S="AG5";
            L="AG6");
        CALL ZZ('Z','L1','J1','L2','J2','S','L');
        PRINT_OUT(Z);
/*
/* GIVE FLOATING POINT VALUE FOR Z-COEFFICIENT
/*
        LET(ZF=Z;
            FZ=EVAL(ZF,ROOT.(S),SQRT(S(1)));
        PRINT_OUT(FZ);
        GO TO NEXT;
QUIT:PUT LIST('END OF JOB') PAGE;
/*
/*
/*---CLEBG-CLEBG-CLEBG-CLEBG-CLEBG-CLEBG-CLEBG-CLEBG-CLEBG---*/
/*
/*
/* PROCEDURE CLEBG WRITTEN BY W. K. WELLS MAY 1978 TO EVALUATE
/* CLEBSCH-GORDAN COEFFICIENTS. IT IS WRITTEN IN FORMAC, AN
/* UNOFFICIAL IBM LANGUAGE WHICH ALLOWS FOR COMPLEX SYMBOLIC
/* MANIPULATIONS. THE FOLLOWING CARD GIVES A STANDARD CALL FOR THE
/* ROUTINE. NOTE THAT THE ARGUMENTS ARE IN SINGLE QUOTES AND ARE
/* FORMAC VARIABLES, ONE CAN ONLY CALL THIS ROUTINE FROM A FORMAC
/* PROCEDURE.
/* CALL CLEBG('CG','J1','J2','MJ1','MJ2','J3','MJ3');
/*
/* THE USER DEFINED FUNCTION SHOWN BELOW NEEDS PLACING IN MAIN
/* FORMAC PROCEDURE. IT DEFINES THE TRIANGLE COEFFICIENT AND SHOULD
/* BE THE FIRST EXECUTABLE STATEMENT IN THE MAIN PROCEDURE.
/* LET(FNC(TRISO)=FAC(S(1)+S(2)-S(3))*FAC(S(1)+S(3)-S(2))
/* *FAC(S(2)+S(3)-S(1))/FAC(S(1)+S(2)+S(3)+1));
/*
/* MAIN PROCEDURE ALSO NEEDS PROCEDURES VALPA AND VALID FOR USE
/* IN THIS PROCEDURE.
/* FOR DISCUSSION OF CLEBSCH-GORDAN COEFFICIENTS SEE BRINK AND
/* SATCELER ANGULAR MOMENTUM, SECOND EDITION, P. 34
/*
/*---CLEBG-CLEBG-CLEBG-CLEBG-CLEBG-CLEBG-CLEBG-CLEBG-CLEBG---*/
/*
/*
CLEBG:PROCEDURE(CG,CA,CB,CALPH,CBETA,CC,CGAMA);
        DECLAE(CC,CA,CB,CG,CALPH,CBETA,CGAMA) CHARACTER(10) VARYING;
/*

```

```

/* INITIALIZE CG-COEFFICIENT AND REDEFINE FOR USE IN SPECIAL FORMAC*/
/*                                     FUNCTIONS                                     */
/*                                     */
/* CQ SHOULD BE ZERO FOR NON-ZERO CG-COEFFICIENT                                */
/*                                     */
    LET ("CG"=1;
        CA1="CA";
        CB1="CB";
        CC1="CC";
        CQ="CALPH"+"CBETA"+"CGAMA");
/*                                     */
/* CHECK FOR CONSERVATION OF MAGNETIC PROJECTION                                */
/*                                     */
    IF -(IDENT(CQ;0)) THEN
    DC;
    LET ("CG"=0);
    RETURN;
    END;
/*                                     */
/*                                     */
/* INITIALIZE FOLLOWING VALUES FOR SUM                                         */
/*                                     */
    LET (CNU=0;
        CAA=0;
        CIA (1)="CA"- "CALPH";
        CIA (2)="CC"- "CB"+ "CALPH";
        CIA (3)="CB"+ "CBETA";
        CIA (4)="CC"- "CA"- "CBETA";
        CIA (6)="CA"+ "CB"- "CC";
        CIB (1)=1;
        CIB (3)=1;
        CIB (6)=1);
/*                                     */
/* SUM OVER ALL CNU WHICH LEAD TO NON-NEGATIVE FACTORIALS                     */
/*                                     */
    DO WHILE (INTEGER (CIB (1)) > 0 & INTEGER (CIB (3)) > 0 & INTEGER (CIB (6)) > 0);
    LET (CIB (0)=(-1)**CNU;
        CIB (1)=CIA (1)-CNU;
        CIB (2)=CIA (2)+CNU;
        CIB (3)=CIA (3)-CNU;
        CIB (4)=CIA (4)+CNU;
        CIB (5)=CNU;
        CIB (6)=CIA (6)-CNU;
        CNU=CNU+1);
/*                                     */
/* CHECK TO SEE IF TERMS ARE POSITIVE INTEGERS. ONLY USE POSITIVE             */
/* INTEGER TERMS IN SUM.                                                         */
/*                                     */
    LET (CNEG=1);
/*                                     */
/* THE FOLLOWING TRAP FOR THE INDEX IN THE DO LOOP IS NECESSARY                */
/* SINCE ALL FORMAC VARIABLES ARE GLOBAL TO ALL PROCEDURES. IF                */
/* ONE DOES NOT USE DIFFERENT NAMES FOR THE DUMMY VARIABLES OR                */
/* DOES NOT TRAP OUT THE DUMMY VARIABLE IN DO LOOPS, OTHER DO LOOPS          */
/* IN THE PROGRAM WILL USE THE LAST VALUE OF THE VARIABLE IF THEY            */
/* HAVE THE SAME NAME. ONE MUST RESUME USING THE CORRECT VALUE                */
/* OF THE DUMMY INDEX AFTER EXITING THE DO LOOP.                                */
/*                                     */
    LET (CSVIP (1)=CJ);
    DC CJ=1 TO 6; LET (CJ="CJ");
    CALL VALFA ('CIB (CJ)', 'CV (CJ)');

```

```

LET (CNEG=CNEG*CU (CJ));
END;
LET (CJ=CSVTP (1));
IF IDENT (CNEG;0) THEN GO TO NEG;
LET (CAA=CAA+CIB (0) / (FAC (CIB (1)) *FAC (CIB (2)) *FAC (CIB (3))
    *FAC (CIB (4)) *FAC (CIB (5)) *FAC (CIB (6))));
NEG:END;
/*
/* IF CAA = 0 THEN COEFFICIENT IS ZERO..
/*
/*
IF IDENT (CAA;0) THEN
DO;
LET ("CG"=0);
RETURN;
END;
/*
/* CHECK FOR TERMS IN STATEMENT SUM1 TO MAKE SURE ALL ARGUMENTS GIVE
/* RISE TO POSITIVE INTEGERS.
/*
/*
LET (CFACS=0;
    CAP (0)=2*"CC"+1;
    CAF (1)="CA"+"CALPH";
    CAP (2)="CA"- "CALPH";
    CAR (3)="CB"+"CBETA";
    CAP (4)="CB"- "CBETA";
    CAR (5)="CC"+"CGAMA";
    CAR (6)="CC"- "CGAMA");
LET (CUALL=1);
/*
/*          DUMMY UP INDEX
/*
/*
LET (CSVTP (1)=CI);
DO CI=0 TO 6; LET (CI="CI");
CALL VALFA ('CAP (CI)', 'CV (CI)');
LET (CUALL=CUALL*CV (CI));
END;
LET (CI=CSVTP (1));
IF IDENT (CUALL;0) THEN
DO;
LET ("CG"=0);
RETURN;
END;
SUM1:LET (CFACS=CAR (0) *FAC (CAR (1)) *FAC (CAR (2)) *FAC (CAR (3))
    *FAC (CAR (4)) *FAC (CAR (5)) *FAC (CAR (6)));
/*
/* ROOT. IS AN ARBITRARY FUNCTION WHICH IS TO BE READ AS A SQUARE
/* FOOT. IT IS A DEVICE TO KEEP ANGULAR COUPLING COEFFICIENTS
/* AS RATIONAL NUMBERS. IT DOES NOT ACTUALLY TAKE THE SQUARE ROOT.
/* ONE CAN USE THE FORMAC ROUTINE EVAL TO MAKE FOOT. TAKE ON THE
/* FUNCTION OF SQUARE ROOT AT ANY LATER TIME IN THE PROGRAM
/*
/*
    CAI=ARITH (CAA);
    CPHAS=SIGN (CAI);
    LET (CPHAS="CPHAS");
/*
/* CHECK ARGUMENTS OF TRISQ.
/*
/*
    CALL VALID ('CA1', 'CB1', 'CC1', 'CPC');
    LET (CPHAS=CPHAS*CPC);
/*

```

```

/* IF CPHAS = 0 THEN COEFFICIENT=0. */
/*
  IF IDENT(CPHAS;0) THEN
    DC;
    LET("CG"=0);
    RETURN;
  END;
  LET("CG"=CPHAS*FOOT.(CFACS*TRISQ(CA1,CB1,CC1)*CAA**2));
  RETURN;
  END CLEEG;
*/
/*
  ---WW-WW-WW-WW-WW-WW-WW-WW-WW-WW-WW-WW-WW-WW-WW-WW-WW-WW-WW-WW-WW-WW---
*/
/*
  PROCEDURE WW WRITTEN BY W. K. WELLS MAY 1978 TO EVALUATE W
  COEFFICIENTS. IT IS WRITTEN IN FORMAC, AN UNOFFICIAL IBM
  LANGUAGE, WHICH ALLOWS COMPLEX SYMBOLIC MANIPULATIONS. THE
  FOLLOWING CARD GIVES A STANDARD CALL FOR THE ROUTINE. NOTE
  THAT THE ARGUMENTS ARE IN SINGLE QUOTES AND ARE FORMAC VARIABLES.
  ONE CAN ONLY CALL THIS ROUTINE FROM A FORMAC PROCEDURE.
  CALL WW('W','L1','J1','L2','J2','S','L');
*/
/*
  THE USER DEFINED FUNCTION SHOWN BELOW NEEDS PLACING IN MAIN
  FORMAC PROCEDURE. IT DEFINES THE TRIANGLE COEFFICIENT AND SHOULD
  BE THE FIRST EXECUTABLE STATEMENT IN THE MAIN PROCEDURE.
  LET(FNC(TRISQ)=FAC(S(1)+S(2)-S(3))*FAC(S(1)+S(3)-S(2))
    *FAC(S(2)+S(3)-S(1))/FAC(S(1)+S(2)+S(3)+1));
*/
/*
  MAIN PROCEDURE ALSO NEEDS PROCEDURES VALFA AND VALID FOR USE
  IN THIS PROCEDURE.
  FOR DISCUSSION OF W COEFFICIENTS SEE BRINK AND SATCHLER
  ANGULAR MOMENTUM, SECOND EDITION, P. 43
*/
/*
  ---WW-WW-WW-WW-WW-WW-WW-WW-WW-WW-WW-WW-WW-WW-WW-WW-WW-WW-WW-WW-WW-WW---
*/
/*
  WW:PROCEDURE(W,WA,WB,WC,WD,WE,WF);
  DECLARE(W,WA,WB,WC,WD,WE,WF) CHARACTER(10) VARYING;
*/
/*
  CONVERT INPUT VARIABLES TO ONES WITHOUT QUOTES.
*/
/*
  LET(WA2="WA";
    WB2="WB";
    WC2="WC";
    WD2="WD";
    WE2="WE";
    WF2="WF");
*/
/*
  INITIALIZE FOLLOWING VALUES FOR SUM
*/
/*
  LET("W"=1;
    WAA=0;
    WZ=0;
    WIA(1)=WA2+WB2+WC2+WD2+1;
    WIA(3)=WE2+WF2-WA2-WD2;
    WIA(4)=WE2+WF2-WB2-WC2;
    WIA(5)=WA2+WB2-WE2;
    WIA(6)=WC2+WD2-WE2;
    WIA(7)=WA2+WC2-WF2;
*/

```



```

WIA (8) =WB2+WD2-WF2;
WIB (1) =1;
WIB (5) =1;
WIB (6) =1;
WIB (7) =1;
WIB (8) =1);

/*
/* SUM OVER ALL Z2 WHICH LEAD TO NON-NEGATIVE INTEGERS
/*
DO WHILE (INTEGER (WIB (1)) >0&INTEGER (WIB (5)) >0&INTEGER (WIB (6)) >0&
INTEGER (WIB (7)) >0&INTEGER (WIB (8)) >0);
LET (WIB (0) = (-1) **WZ;
WIB (1) =WIA (1) -WZ;
WIB (2) =WZ;
WIB (3) =WIA (3) +WZ;
WIB (4) =WIA (4) +WZ;
WIB (5) =WIA (5) -WZ;
WIB (6) =WIA (6) -WZ;
WIB (7) =WIA (7) -WZ;
WIB (8) =WIA (8) -WZ;
WZ =WZ+1);

/*
/* CHECK TO SEE IF TERMS ARE POSITIVE INTEGERS. ONLY USE POSITIVE
/* INTEGER TERMS IN SUM.
/*
LET (WNEG=1);

/*
/* THE FOLLOWING TRAP FOR THE INDEX IN THE DO LOOP IS NECESSARY
/* SINCE ALL FORMAC VARIABLES ARE GLOBAL TO ALL PROCEDURES. IF
/* ONE DOES NOT USE DIFFERENT NAMES FOR THE DUMMY VARIABLES OR
/* DOES NOT TRAP OUT THE DUMMY VARIABLE IN DO LOOPS, OTHER DO LOOPS
/* IN THE PROGRAM WILL USE THE LAST VALUE OF THE VARIABLE IF THEY
/* HAVE THE SAME NAME. ONE MUST RESUME USING THE CORRECT VALUE
/* OF THE DUMMY INDEX AFTER EXITING THE DO LOOP .
/*
LET (WSVTP (1) =WJ);
DO WJ=1 TO 8; LET (WJ="WJ");
CALL VALFA ('WIB{WJ}', 'WU (WJ)');
LET (WNEG=WNEG*WU (WJ));
END;
LET (WJ=WSVTP (1));
IF IDENT (WNEG;0) THEN GO TO NEG;
LET (WAA=WAA+WIB (0) *FAC (WIB (1)) / (FAC (WIB (2)) *FAC (WIB (3)) *
FAC (WIB (4)) *FAC (WIB (5)) *FAC (WIB (6)) *FAC (WIB (7)) *
FAC (WIB (8))));
NEG:END;

/*
/* DETERMINE SIGN OF W COEFFICIENT.
/*
WAI=APIIH (WAA);
WPHAS=SIGN (WAI);
LET (WPHAS="WPHAS");

/*
/* IF WPHAS = 0 THEN COEFFICIENT IS ZERO
/*
IF IDENT (WPHAS;0) THEN
DO;
LET ("W"=0);
RETURN;
END;

```

```

/*
/* CHECK ARGUMENTS OF TRISQ.
/*
CALL VALID('WA2','WB2','WE2','WP1');
CALL VALID('WA2','WC2','WF2','WP2');
CALL VALID('WB2','WE2','WF2','WP3');
CALL VALID('WC2','WE2','WF2','WP4');
LET (WPHAS=WPHAS*WP1*WP2*WF3*WP4);

/*
/* IF WPHAS = 0 THEN COEFFICIENT IS ZERO
/*
IF IDENT(WPHAS;0) THEN
DC:
LET ("W"=0);
RETURN;
END;
LET ("W"=WPHAS*ROOT. (TRISQ (WA2,WB2,WE2)*TRISQ (WA2,WC2,WF2)
*TRISQ (WB2,WD2,WF2)*TRISQ (WC2,WD2,WE2)*WAA**2));
RETURN;
END WW;

/*
/*
/*---ZZ-ZZ-ZZ-ZZ-ZZ-ZZ-ZZ-ZZ-ZZ-ZZ-ZZ-ZZ-ZZ-ZZ-ZZ-ZZ---*/
/* PROCEDURE ZZ WRITTEN BY W. K. WELLS MAY 1978 TO EVALUATE Z
/* COEFFICIENTS. IT IS WRITTEN IN FORMAC, AN UNOFFICIAL IBM LANGUAGE*
/* WHICH ALLOWS COMPLEX SYNDOLIC MANIPULATIONS. THE STANDARD CALL
/* FOR THE ROUTINE IS GIVEN BELOW. NOTE THE ARGUMENTS ARE IN
/* SINGLE QUOTES AND ARE FORMAC VARIABLES. ONE CAN CALL THIS
/* ROUTINE ONLY FROM FORMAC PROCEDURES.
/* CALL ZZ ('Z','L1','J1','L2','J2','S','L');
/*
/* THE MAIN PROCEDURE NEEDS THE PROCEDURES CLEBG AND WW, WHICH
/* THIS ROUTINE CALLS.
/*---ZZ-ZZ-ZZ-ZZ-ZZ-ZZ-ZZ-ZZ-ZZ-ZZ-ZZ-ZZ-ZZ-ZZ-ZZ-ZZ---*/
/*
/*
ZZ: PROCEDURE (Z,ZL1,ZJ1,ZL2,ZJ2,ZS,ZL);
DECLAR F(Z,ZL1,ZJ1,ZL2,ZJ2,ZS,ZL) CHARACTER (10) VARYING;
LET (ZAA=0;ZBB=0;ZCC=0;
ZL12="ZL1";
ZJ12="ZJ1";
ZL22="ZL2";
ZJ22="ZJ2";
ZS2="ZS";
ZL2="ZL";
ZAA=(2*ZL12+1)*(2*ZL22+1)*(2*ZJ12+1)*(2*ZJ22+1));
CALL WW ('ZBB','ZL12','ZJ12','ZL22','ZJ22','ZS2','ZL2');
IF IDENT (ZBB;0) THEN
DO:
LET ("Z"=0);
RETURN;
END;
CALL CLEBG ('ZCC','ZL12','ZL22','0','0','ZL2','0');
IF IDENT (ZCC;0) THEN
DC:
LET ("Z"=0);
RETURN;
END;
LET (ZB=EVAL (ZBB, ROOT. (S), 3 (1));
ZC=EVAL (ZCC, ROOT. (S), 3 (1));

```

```

        ZINT=ZC*ZB);
ZAI=ARITH(ZINT);
ZPHAS=SIGN(ZAI);
ZASS=ABS(ZAI);
IF (ZAI/=ZASS) THEN LET (ZIFT=-ZINT);
LET (ZPHAS="ZPHAS";
     "Z"=ZPHAS*(#I** (ZL2-ZL12+ZL22)) *ROOT. (ZINT*ZAA));
RETURN;
END ZZ;

/*
/*
/*---VALID-VALID-VALID-VALID-VALID-VALID-VALID-VALID-VALID-VALID---*/
/*
/*
/* VALID CHECKS TRIANGLE FUNCTION ARGUMENTS FOR VALIDITY. RETURNS
/* V=1 FOR VALID ARGUMENTS, V=0 OTHERWISE.
/*
/*
/*---VALID-VALID-VALID-VALID-VALID-VALID-VALID-VALID-VALID-VALID---*/
/*
/*
/*
VALID: PROCEDURE (VP, VQ, VR, V);
DECLARE (VP, VQ, VR, V) CHARACTER(10) VARYING;
LET ("V"=1;
     VCHK1="VP"+"VQ"+"VR";
     VCHK2="VP"+"VQ"-"VR";
     VCHK3="VP"+"VR"-"VQ";
     VCHK4="VQ"+"VR"-"VP");
VA1=ARITH(VCHK1);
VA2=ARITH(VCHK2);
VA3=ARITH(VCHK3);
VA4=ARITH(VCHK4);
VB1=INTEGER(VCHK1);
VB2=INTEGER(VCHK2);
VB3=INTEGER(VCHK3);
VB4=INTEGER(VCHK4);
VC1=VB1-VA1;
VC2=VB2-VA2;
VC3=VB3-VA3;
VC4=VB4-VA4;
IF (VA1<0|VA2<0|VA3<0|VA4<0) THEN
DO;
LET ("V"=0);
RETURN;
END;
IF (VC1<0|VC2<0|VC3<0|VC4<0) THEN
DO;
LET ("V"=0);
RETURN;
END;
RETURN;
END VALID;

/*
/*
/*---VALFA-VALFA-VALFA-VALFA-VALFA-VALFA-VALFA-VALFA-VALFA-VALFA---*/
/*
/*
/* VALFA-CHECKS ARGUMENTS TO SEE IF IT IS A POSITIVE INTEGER.
/* FOR USE IN TESTING ARGUMENTS OF FAC. W=1 FOR INTEGER>=0, W=0
/* OTHERWISE.
/*
/*
/*---VALFA-VALFA-VALFA-VALFA-VALFA-VALFA-VALFA-VALFA-VALFA-VALFA---*/
/*
/*

```

```
/*
VALFA: PFOCEDURE (US, U);
DECLAPE (US, U) CHAPACTER (10) VAPYING;
LET ("U"=1;
    USS="US");
UCK1=ARITH (USS);
UCK2=INTEGER (USS);
UCK3=UCK2-UCK1;
IF UCK1<0 THEN
DO;
LET ("U"=0);
RETURN;
END;
IF UCK3<0 THEN
DO;
LET ("U"=0);
RETURN;
END;
RETURN;
END VALFA;
END ANGLE;
*/
```



```

W(
0
) =
-----
W = ROOT.( 1/25 )
FW = .2
-----
W(
3/2
) =
-----
W = ROOT.( 1/20 )
FW = .22360679
-----
W(
3/2
) =
-----
W = - ROOT.( 1/16 )
FW = - .25
-----
W(
2
) =
-----
W = 0
FW = 0
-----
W(
0
) =
-----
W = 0
FW = 0
-----
W(
1
) =
-----
W = ROOT.( 1/16 )
FW = .25
-----
W(
1
) =
-----
W = 0
FW = 0
-----
W(
2
) =
-----
W = 0
FW = 0
-----
W(
4
) =
-----
W = 0
FW = 0
-----
W(
1/2
) =
-----
W = - ROOT.( 7/200 )
FW = - .18768296
-----

```

```

W(
 1/2
W = ROOT.( 1/100 )
FW = .1
-----
W(
 1
W = - FCOT.( 7/300 )
FW = -.15275252
-----
W(
 1/2
W = 0
FW = 0
-----
W(
 2
W = 0
FW = 0
-----
W(
 2
W = ROOT.( 1/24 )
FW = .20412414
-----
W(
 2
W = 0
FW = 0
-----
W(
 1/2
W = ROOT.( 1/90 )
FW = .10540925
-----
W(
 1
W = 0
FW = 0
-----
W(
 2
W = 0
FW = 0
-----
W(
 3
W = 0
FW = 0
-----

```

W(	W =	FW =	W(	W =	FW =	W(	W =	FW =
1/2	ROOT.( 1/100 )	.1	1	- FCOT.( 7/300 )	-.15275252	1/2	0	0
1	- FCOT.( 7/300 )	-.15275252	1/2	0	0	2	0	0
1/2	0	0	2	0	0	2	ROOT.( 1/24 )	.20412414
2	0	0	2	0	0	1/2	ROOT.( 1/90 )	.10540925
1	0	0	1	0	0	2	0	0
2	0	0	3	0	0	3	0	0

```

W(      1
3      0
) = 0
FW = 0
-----
W(      1
2      0
) = 0
FW = 0
-----
W(      1
3      0
) = 0
FW = 0
-----
W(      1
1      0
) = 0
FW = 0
-----
W(      1
2      0
) = 0
FW = 0
-----
C(      1
2      0
) = 0
CG = 0
-----
C(      1
2      0
) = 0
CG = - ROOT.( 3/7 )
-----
C(      1
2      0
) = 0
CG = - .65465367
-----
C(      1
2      0
) = 0
CG = ROOT.( 1/14 )
-----
C(      1
2      0
) = 0
CG = .26726124
-----
C(      1
2      0
) = 0
CG = - ROOT.( 2/7 )
-----
C(      1
3      0
) = 0
CG = 0
-----
C(      1
2      0
) = 0
CG = 0
-----

```



```

C(          2 1 1 1 1
2          2 )=
CG = - ROOT.( 1/3 )
-----
FCG = - .57735026
-----
C(          2 1 1 1 1
2          2 )=
3          2
CG = 0
-----
FCG = 0
-----
C(          2 1 1 1 1
2          2 )=
-2          0
CG = - ROOT.( 2/3 )
-----
FCG = - .81649658
-----
C(          2 1 1 1 1
2          2 )=
0          1
CG = - ROOT.( 1/2 )
-----
FCG = - .70710678
-----
C(          1 2 1 1 1
2          2 )=
CG = ROOT.( 1/3 )
-----
FCG = .57735026
-----
C(          1 2 1 1 1
2          2 )=
0          1
CG = - ROOT.( 1/2 )
-----
FCG = - .70710678
-----
C(          1 2 1 1 1
2          2 )=
-3          -2
CG = 0
-----
FCG = 0
-----
C(          1 2 1 1 1
2          2 )=
-2          -1
CG = - ROOT.( 1/3 )
-----
FCG = - .57735026
-----
C(          1 1 1 1 1
2          2 )=
1          0
CG = ROOT.( 1/2 )
-----
FCG = .70710678
-----
C(          1 2 1 1 1
2          2 )=
1          1
CG = FOOT.( 1 )
-----
FCG = 1
-----

```

C(	1	1	1	0	:
2	1	)=			
CG = FOOT. ( 1/2 )					
-----					
FCG = .70710678					
C(	1	0	0	-1	:
2	-1	)=			
CG = FOOT. ( 1/2 )					
-----					
FCG = .70710678					
C(	1	-1	-1	-1	:
2	-2	)=			
CG = FOOT. ( 1 )					
-----					
FCG = 1					
C(	1	1	1	0	:
2	1	)=			
CG = FOOT. ( 1/2 )					
-----					
FCG = .70710678					
C(	0	0	0	-1	:
2	-1	)=			
CG = 0					
-----					
FCG = 0					
C(	0	0	0	1	:
2	1	)=			
CG = 0					
-----					
FCG = 0					
C(	0	-1	-1	0	:
2	-1	)=			
CG = 0					
-----					
FCG = 0					
C(	0	0	0	-1	:
2	-1	)=			
CG = 0					
-----					
FCG = 0					
C(	2	1	1	1	:
0	2	)=			
CG = 0					
-----					
FCG = 0					
C(	2	1	1	-1	:
0	2	)=			
CG = - FOOT. ( 1/5 )					
-----					
FCG = -.44721359					

```

C(      2      2      0      ;
0      2      0      ;
CG = 0
-----
FCG = 0
-----
C(      2      1      -1      ;
0      2      -1      ;
CG = - ROOT.( 1/5 )
-----
FCG = - .44721359
-----
C(      2      -1      -1      ;
0      2      -1      ;
CG = 0
-----
FCG = 0
-----
C(      2      1      -1      ;
0      2      -1      ;
CG = ROOT.( 1/14 )
-----
FCG = .26726124
-----
C(      1      0      0      ;
0      1      0      ;
CG = - ROOT.( 1/3 )
-----
FCG = - .57735026
-----
C(      2      1      -1      ;
0      2      -1      ;
CG = ROOT.( P/35 )
-----
FCG = .47809144
-----
C(      2      1      -1      ;
0      2      -1      ;
CG = - ROOT.( 1/5 )
-----
FCG = - .44721359
-----
C(      3      0      0      ;
0      3      0      ;
CG = ROOT.( 4/21 )
-----
FCG = .43643578
-----
C(      3      0      0      ;
0      3      0      ;
CG = - ROOT.( 1/7 )
-----
FCG = - .37796447
-----
C(      1      0      0      ;
0      1      0      ;
CG = ROOT.( 2/3 )
-----
FCG = .81649658
-----

```

C( 3  
 4 0  
 CG = - ROOT. ( 18/77 )  
 -----  
 FCG = - .48349377  
 -----  
 C( 3  
 2 0  
 CG = ROOT. ( 4/21 )  
 -----  
 FCG = .43643578  
 -----

3  
 )= 0  
 0  
 0  
 0  
 3  
 )= 0  
 0  
 0

## BIBLIOGRAPHY

- V. Baudinet-Robinet, Nucl. Phys. A222 (1974) 525.
- F. Becvar, R.E. Chrien, and O.A. Wasson, Nucl. Phys. A236 (1974) 198.
- L. C. Biedenharn and M.E. Rose, Rev. Mod. Phys. 25 (1953) 729.
- E. G. Bilpuch, A. M. Lane, G. E. Mitchell, and J.D. Moses, Phys. Rep. 28C (1976) 149.
- M. E. Bleck, unpublished Ph.D. dissertation, Duke University (1978).
- J. M. Blatt and V. F. Weisskopf, Theoretical Nuclear Physics, John Wiley and Sons, New York, New York (1952).
- R. Bloch, E. E. Pixley, W. Reichart, and F. Zamboni, Nucl. Instr. and Meth. 59 (1968) 325.
- Aage Bohr and Ben R. Mottelson, Nuclear Structure, W. A. Benjamin, New York, New York (1969).
- R. O. Bondelid and C. A. Kennedy, A Two Meter Positive-Ion Beam Electrostatic Analyzer, NREL Report 5083 (1958).
- J. C. Browne, unpublished Ph.D. dissertation, Duke University (1969).
- R. E. Chrien, M. F. Bhat, and G. N. Cole, Phys. Rev. C8 (1973) 336.
- J. R. Chandler, unpublished Ph. D. dissertation N. C. State University (1978).

- F. Coester and J. M. Jauch, *Helv. Phys. Acta*, 26 (1953) 3.
- S. Devons and L. J. B. Goldfarb, *Handbuch der Physik*, Vol. 42 (1957) 362.
- T. R. Dittrich, C. R. Gould, G. E. Mitchell, E. G. Bilpuch, and K. Stelzer, *Phys. Lett.* 59B (1975) 230.
- T. R. Dittrich, unpublished Ph.D. dissertation, N. C. State University (1976).
- Freeman J. Dyson, *J. Math. Phys.* 3 (1962) 1199.
- U. Fano, *Phys. Rev.* 90 (1953) 577.
- A. J. Ferguson, *Angular Correlation Methods in Gamma-Ray Spectroscopy*, North Holland, Amsterdam (1965).
- H. E. Gove, *Nuclear Reactions*, vol. 1, edited by P. M. Endt and M. Demeur, North Holland, Amsterdam (1959) 259.
- H. L. Harney, *Nucl. Phys.* A119 (1968) 591.
- R. Herzog, *Z. Physik* 89 (1934) 447.
- A. A. Kraus, J. P. Schiffer, F. W. Prosser, Jr., and L. C. Biedenharn, *Phys. Rev.* 104 (1956) 1667.
- T. J. Krieger and C. E. Porter, *J. Math. Phys.* 4 (1963) 1272.
- B. C. Kuo, *Automatic Control Systems*, Prentice-Hall Inc. (1962).
- A. M. Lane and F. G. Thomas, *Rev. Mod. Phys.* 30 (1958) 257.
- A. M. Lane *Ann. Phys.* 63 (1971) 171.

- A. M. Lane, T. R. Dittrich, G. E. Mitchell, and E. G. Bilpuch, Phys. Rev. Lett. 41 (1978) 454.
- C. M. Lederer, J. M. Hollander, and I. Perlman, Tables of Isotopes, John Wiley and Sons (1967).
- D. P. Lindstrom, unpublished Ph.D. dissertation, Duke University (1970).
- H. I. Liou, H. S. Camarda, S. Wynchank, M. Slagowitz, G. Hacken, F. Rahn, and J. Rainwater, Phys. Rev. C5 (1972) 974.
- M. L. Mehta, Nucl. Phys. 18 (1960) 395.
- G. E. Mitchell, T. R. Ditterich, and E. G. Bilpuch, to be published, Z. Physik, (1978).
- P. B. Parks, H. W. Newson, and R. M. Williamson, Rev. Sci. Instr. 29 (1958) 834.
- C. E. Porter and F. G. Thomas, Phys. Rev. 104 (1956) 483.
- C. E. Porter and N. Rosenzweig, Ann. Acad. Sci. Fennicae AVI 44 (1960) 5.
- C. E. Porter, ed. Statistical Theories of Spectra: Fluctuations, Academic Press, New York (1965).
- M. J. Posakony, Rev. Sci. Instr. 43 (1972) 270.
- H. H. Prochnow, unpublished Ph.D. dissertation, Duke University (1970).
- G. R. Satchler, Thesis, Oxford University (1955).
- D. L. Sellin, unpublished Ph. D. dissertation, Duke University (1969).

Thaler and Brown, Analysis and Design of Feedback Control Systems, McGraw-Hill (1960).

W. J. Thompson and W. I. van Rij, Notes on Applied Angular Correlation Theory, (1968).

W. J. Thompson, J. L. Adams, and D. Robson, Phys. Rev. 173 (1968) 975.

A. Louis Toller, unpublished Ph.D. dissertation, Duke University (1954).

W. Ullah, J. Math. Phys. 4 (1963) 1229.

R. E. Warren, J. I. Powell, and R. G. Herb, Rev. Sci. Instr. 18 (1947) 559.

William Watson, private communication (1978).

C. R. Westerfeldt, unpublished masters thesis, N. C. State University (1978).

E. P. Wigner ORNL-2309 (1956).

W. M. Wilson, E. G. Bilpuch, and G. E. Mitchell, Nucl. Phys. A245 (1975) 285.

J. F. Wimpey, unpublished Ph.D. dissertation, N. C. State University (1974).

H. Wollnik, Focusing of Charged Particles ed. by Albert Septier, Vol. II Academic Press (1967) 163.

C. N. Yang, Phys. Rev. 74 (1948) 764.

S. A. A. Zaidi and S. Darmodjo, Phys. Rev. Lett. 19 (1967) 1446.



## BIOGRAPHY

William Kent Wells

**Birthdate:**

May 14, 1949

**Birthplace:**

Starkville, Mississippi

**Citizenship:**

United States

**Personal:**

Married December 27, 1975 to Lisa Kaufmann

**Education:**

Mississippi State University, B.S. (Physics), 1971

**Employment:**

Research Assistant, Duke University, 1971-1972, 1974-present  
Teaching Assistant, Duke University, 1972-1974

**Society Memberships:**

Sigma Xi

**References:**

**Abstracts:**

High Resolution Proton Inelastic Scattering on  $^{56}\text{Fe}$ . W.K. Wells, D.A. Outlaw, E.G. Bilpuch, and G.E. Mitchell, B.A.P.S. Vol. 21 (1976), p. 662.

A Three Loop Regulator For The TUNL Tandem Van de Graaff Accelerator. M.E. Bleck, W.K. Wells, D.A. Outlaw, F.O. Purser, and E.G. Bilpuch, B.A.P.S., Vol. 22 (1977), p. 578.

High Resolution Proton Inelastic Scattering on  $^{48}\text{Ti}$ . W.K. Wells, E.G. Bilpuch, and G.E. Mitchell, B.A.P.S., Vol. 23 (1978), p. 521.

A High Resolution Study of the Lowest  $1/2^+$  Analogue State in  $^{91}\text{Ni}$ . M.E. Bleck, W.K. Wells, D.A. Outlaw, C.R. Westerfeldt, E.G. Bilpuch, and G.E. Mitchell. B.A.P.S., Vol. 23 (1978), p. 554.